



**A chemical approach to regenerating the
performance of thermally damaged glass fibres**

A thesis in fulfilment of the requirements for the degree of Doctor
of Philosophy

By

Sairah Tahir Bashir

Department of Mechanical and Aerospace Engineering
University of Strathclyde
Glasgow
UK
2019

Declaration of Authenticity and Author's Rights

This thesis is the result of the author's original research. It has been composed by the author and has not been previously submitted for examination which has led to the award of a degree.

The copyright of this thesis belongs to the author under the terms of the United Kingdom Copyright Acts as qualified by University of Strathclyde Regulation 3.50. Due acknowledgement must always be made of the use of any material contained in, or derived from, this thesis.

Signed: 

Date: 23/09/19

Acknowledgements

I would like to start by thanking my main supervisor Dr Liu Yang for giving me the opportunity to pursue this research project. His advice and guidance has been integral to my studies, and he helped me grow as a researcher. I also would like to acknowledge my second supervisor Dr John Liggat for his continued support throughout my PhD. Gratitude is extended to past and present members of the Advanced Composites Group for their help and friendship. The departmental technicians and staff at the Advanced Materials Research Laboratory have also been of great assistance during my research. In addition, the work carried out by my undergraduate research students has been very instrumental in my studies. I would like to express thanks to the Royal Society of Chemistry (RSC), Society of Chemical Industry (SCI) and the University of Strathclyde for awarding me various travel bursaries to help cover conference expenses over the course of my PhD. Further gratitude is given to the University of Strathclyde for funding my research. Finally, I would like to thank friends and family for their support over the years.

Publications

A significant part of the experimental results in this thesis has already been published over the course of the PhD, in the form of journal articles and conference proceedings.

ST Bashir, L Yang, R Anderson, PL Tang, JJ Liggat, JL Thomason (2017) Composites Part A: Applied Science and Manufacturing 102: 76.
Doi:<http://dx.doi.org/10.1016/j.compositesa.2017.07.023>

ST Bashir, L Yang, JJ Liggat, JL Thomason (2018) Journal of Materials Science 53: 1710. Doi:10.1007/s10853-017-1627-z

ST Bashir, L Yang (2019) Journal of Materials Science (under review)

S Bashir, L Yang, R Anderson, et al. (2016) 17th European Conference on Composite Materials, Munich, Germany

S Bashir, L Yang, J Liggat, J Thomason (2018) 18th European Conference on Composite Materials, Athens, Greece

Abstract

Glass fibre reinforced thermosetting polymers (GRP) have been used in a wide range of applications over the past decades, such as in the production of wind turbine blades. Once these materials reach the end of their life cycle, they are often deposited in landfill sites, a disposal option that is becoming more expensive and environmentally-unfriendly. The glass fibres can be recycled from the composite waste by degrading the polymer matrix at elevated temperatures, however this leads to fibres with drastically low mechanical strength. The main objective of this research project was to develop chemical treatments to regenerate the strength of such fibres, to allow their reuse in second-life composite materials.

In this work, glass fibres were heated in a furnace to mimic thermal recycling conditions, before chemical treatments were applied to regenerate their strength. It was discovered that a short treatment of fibres in hot and concentrated sodium hydroxide (NaOH) or potassium hydroxide (KOH) solution significantly increased their strength, likely due to etching of fibre surface flaws. Interestingly, these treatments had a detrimental effect on the strength of virgin fibres. A kinetic investigation was carried out to determine the etching rate of glass fibres in alkaline solutions. This was achieved by accurately measuring the diameter of individual glass fibres before and after alkaline treatment using a scanning electron microscope. It was found that NaOH solution was more corrosive towards the glass fibres than KOH solution, and that increasing the concentration and temperature of the alkaline solution led to an increase in etching rate.

Later in the study, glass fibres were thermally recycled from an end-of-life wind turbine blade. The recycling procedure involved feeding the downsized blade section into an in-house fluidised bed. Fluidised bed recycling is a common thermal

recycling technique where elevated temperatures and oxygen lead to degradation of the composite matrix and recovery of the fibrous components. It was found that a short treatment of the recycled fibres in concentrated NaOH solution managed to considerably regenerate their strength. An effort was made in recovering the strength of the fibres under milder alkaline conditions, though the reported strength increase was not as significant. A case study was conducted to determine the industrial feasibility of treating recycled glass fibre in alkaline solution. It was discovered that the costs of solution preparation and processing conditions can be partially offset through charging businesses for collecting their composite waste, and selling the regenerated glass fibres as chopped fibre products.

Contents

Declaration of Authenticity and Author's Rights	i
Acknowledgements	ii
Publications	iii
Abstract	iv
List of symbols.....	xi
List of figures	xiv
List of tables	xxix
1 Introduction	1
1.1 Background.....	1
1.2 Objectives	3
1.3 Outline of thesis	4
2 Glass fibres – a review.....	5
2.1 Introduction to glass fibres	5
2.2 Glass fibre formulation	6
2.3 Glass fibre sizing.....	9
2.3.1 Film former.....	10
2.3.2 Silane coupling agent	11
2.3.3 Auxiliary components.....	14
2.4 Glass fibre strength loss	16
2.5 Conclusions of literature review	20
3 Regenerating the strength of thermally conditioned glass fibres through hot alkaline treatments	22
3.1 Introduction	22
3.2 Literature review	24
3.2.1 Effect of chemical treatments on virgin glass fibre strength	24

3.2.2	Properties of thermally treated glass fibres	28
3.2.3	Use of chemical treatments to regenerate strength of thermally treated glass fibres	33
3.2.4	Conclusions of literature review	37
3.3	Experimental	38
3.3.1	Materials	38
3.3.2	Thermal treatment.....	39
3.3.3	Alkaline treatment	40
3.3.4	Single fibre tensile testing	42
3.3.5	Scanning electron microscopy (SEM).....	45
3.3.6	Atomic force microscopy (AFM).....	47
3.3.7	Fourier transform infrared spectroscopy (FTIR).....	50
3.3.8	Mass loss and diameter reduction of fibres after alkaline treatment...	52
3.4	Results and discussion	53
3.4.1	Strength regeneration by alkaline treatment.....	53
3.4.2	Etching effect of alkaline solutions on glass fibres	65
3.4.3	Elemental analysis of alkali treated fibres.....	74
3.4.4	Surface roughness and phase imaging of alkali treated fibres	77
3.4.5	FTIR spectroscopic analysis of alkali treated fibres.....	85
3.4.6	Fracture surface analysis of alkali treated fibres	94
3.4.7	Effect of alkaline treatments on virgin and thermally treated glass fibres	98
3.5	Conclusions	117
4	Kinetics of dissolution of glass fibre in hot alkaline solution	119
4.1	Introduction	119
4.2	Literature review	121
4.2.1	Dissolution studies of glass in alkaline solution	121
4.2.2	Solid-state kinetic models for glass dissolution in alkaline solution ..	126

4.2.3	Kinetic parameters determined from dissolution studies of glass in alkaline solution.....	131
4.2.4	Conclusions of literature review.....	133
4.3	Experimental.....	134
4.3.1	Materials.....	134
4.3.2	Single fibre treatment in alkaline solution.....	134
4.3.3	Scanning electron microscopy (SEM).....	137
4.4	Results and discussion.....	138
4.4.1	Effect of alkaline solution concentration on diameter reduction of glass fibres	138
4.4.2	Effect of alkaline solution temperature on diameter reduction of glass fibres	142
4.4.3	Modelling of glass fibre dissolution in alkaline solution.....	146
4.4.4	Determination of reaction order and activation energy.....	150
4.4.5	Correlating fibre diameter reduction with strength.....	158
4.5	Conclusions.....	161
5	Regenerating the performance of thermally recycled glass fibres.....	163
5.1	Introduction.....	163
5.2	Literature review.....	165
5.2.1	Methods of recycling glass fibres from end-of-life composites.....	166
5.2.2	Properties of thermally recycled glass fibres.....	169
5.2.3	Regenerating strength and interface of thermally recycled glass fibres	175
5.2.4	Conclusions of literature review.....	183
5.3	Experimental.....	184
5.3.1	Materials.....	184
5.3.2	Thermal recycling of end-of-life composite.....	185
5.3.3	Concentrated alkaline treatment.....	186
5.3.4	Mild alkaline treatment (pH-scale).....	186

5.3.5	Silane treatment.....	188
5.3.6	Single fibre tensile testing.....	189
5.3.7	Microbond testing	190
5.3.8	Atomic force microscopy (AFM).....	195
5.4	Results and discussion	196
5.4.1	Effect of alkaline treatments on recycled glass fibre strength.....	196
5.4.2	Effect of pH-scale alkaline treatments on recycled glass fibre strength 197	
5.4.3	Effect of hot APS treatment on strength and surface functionality of recycled glass fibres.....	204
5.4.4	Examination of surface flaws of recycled glass fibre by AFM.....	213
5.4.5	Case study into the costs of industrial-scale alkaline treatment of recycled glass fibres.....	219
5.5	Conclusions	223
6	Conclusions.....	225
6.1	Regenerating the strength of thermally conditioned glass fibres through hot alkaline treatments (Chapter 3)	225
6.2	Kinetics of dissolution of glass fibre in hot alkaline solution (Chapter 4) .	227
6.3	Regenerating the performance of thermally recycled glass fibres (Chapter 5)	228
7	Future work	230
7.1	Regenerating the strength of thermally conditioned glass fibres through hot alkaline treatments (Chapter 3)	230
7.2	Kinetics of dissolution of glass fibre in hot alkaline solution (Chapter 4) .	232
7.3	Regenerating the performance of thermally recycled glass fibres (Chapter 5)	233
8	References.....	235
A	Appendix	A-1
A.1	AFM theory.....	A-1
A.1.1	Introduction	A-1
A.1.2	Interaction of AFM probe with sample surface	A-1

A.1.3	Principles of intermittent contact AFM	A-2
A.2	FTIR theory	A-4
A.2.1	Introduction	A-4
A.2.2	Parameters in IR spectroscopic analysis	A-4
A.2.3	General setup of an FTIR	A-6

List of symbols

AFM	Atomic force microscope
Al ₂ O ₃	Aluminium oxide
APS	γ-aminopropyltriethoxysilane
ATR	Attenuated total internal reflectance
c	Flaw depth
CaO	Calcium oxide
D ₀	Initial fibre diameter (t = 0)
D _t	Fibre diameter after time t
DR	Diffuse reflectance
E _a	Activation energy
EDS	Energy dispersive X-ray spectrometer
F	Load at failure
F _{db}	Force at droplet de-bond
FIB	Focused ion beam
FTIR	Fourier transform infrared spectroscopy
GMT	Glass mat thermoplastic
GPa	Gigapascal
GRP	Glass fibre reinforced thermosetting polymers
HCl	Hydrochloric acid
HF	Hydrofluoric acid
HT	Heat treated
IFSS	Interfacial shear strength
k	Rate constant
K _{1c}	Fracture toughness
KOH	Potassium hydroxide

l_d	Droplet embedded length
LiOH	Lithium hydroxide
M	Moles per litre (also abbreviated to mol/L)
M_0	Initial mass of solid ($t = 0$)
M_t	Mass of remaining solid after time t
MAPP	Maleic anhydride grafted polypropylene
MgO	Magnesium oxide
MPa	Megapascal
n	Reaction order with respect to OH^-
N	Newton
NaOH	Sodium hydroxide
NaCl	Sodium chloride
OC	Owens Corning
OH^-	Hydroxide
pH	Potential hydrogen
PP	Polypropylene
r	Reaction rate
R_q	Root mean square roughness
S	Initial glass surface area
SEM	Scanning electron microscope
SiO_2	Silica
SiOH	Silanol
SR	Specular reflectance
t	Reaction time
Y	Geometry factor
α	Conversion

ΔD	Fibre diameter reduction
σ	Tensile strength
$[\text{OH}^-]$	Initial concentration of hydroxide (alkaline solution)

List of figures

Figure 2.1 – Amorphous network structure of silica with network modifiers and formers. Reproduced from [33]	6
Figure 2.2 – Schematic showing the glass fibre forming process. Reproduced from [40]	8
Figure 2.3 – Chemical structure of APS	11
Figure 2.4 – Hydrolysis and condensation process of silane coupling agents. Reproduced from [25].....	12
Figure 2.5 – Bonding of self-condensed silane coupling agent with substrate surface (such as glass). Reproduced from [25]	13
Figure 2.6 – Schematic of 3-D network structure of hydrolysed APS on glass fibre surface. Reproduced from [46].....	14
Figure 2.7 – Schematic showing the fracture surface of a fibre where the flaw originated from the surface. Reproduced from [7].....	17
Figure 2.8 – Scanning electron microscopy (SEM) images of the fracture surface of glass fibres (a) untreated, and (b) thermally treated in air. Reproduced from [7].....	18
Figure 2.9 – Schematic showing the surface flaws on a glass fibre. Reproduced from [20]	20
Figure 3.1 – Mass loss (%) and strength maintenance (%) of E-glass and basalt fibres after treatment in boiling 2 M NaOH solution. Reproduced from [21].....	25

Figure 3.2 – SEM image of E-glass fibre after treatment in boiling 2 M NaOH solution. Reproduced from [21]	26
Figure 3.3 – Schematic diagram of the corrosion process of glass fibres in (a) NaOH solution, and (b) cement solution. Reproduced from [20].....	27
Figure 3.4 – Strength loss (%) of 1) quartz glass, 2) silica, 3) non-alkaline aluminoborosilicate, and 4) soda-calcia-silicate glass fibre after thermal treatment at different temperatures. Reproduced from [79]	29
Figure 3.5 – SEM image showing a 240.2 nm deep crack in an E-glass fibre created by FIB milling. Reproduced from [51]	30
Figure 3.6 – SEM image showing fracture origin of a glass fibre heat treated at 450 °C under vacuum, strength 1.2 GPa. Reproduced from [25].....	31
Figure 3.7 - Tensile strength of bare and APS-sized fibres after being thermally treated at 200, 300, 450, 500 and 600 °C for 25 min as bundles and single fibres. Reproduced from [8].....	32
Figure 3.8 – SEM images of the cross-section of a soda lime silicate glass after HF treatment for (a) 2 minutes, showing severe surface cracks, and (b) 30 minutes, showing U-shaped structures. Reproduced from [12].....	34
Figure 3.9 – Tensile strength of glass fibres heat treated at 450, 500 and 600 °C, and then treated in 1 vol% HF solution for different times. Reproduced from [11]...	35
Figure 3.10 – Tensile strength of glass fibres thermally conditioned at 450, 500 and 600 °C, and treated in NaOH, APS and HF solution [11]. Reproduced from [14]	36
Figure 3.11 – Image of an OC APS-sized E-glass fibre roving	39

Figure 3.12 – Schematic diagram showing the steel rig used for thermal treatment of glass fibre bundles. Reproduced from [25].....	40
Figure 3.13 – Schematic of a fibre tensile test card	42
Figure 3.14 – Image of the Leitz Ergolux optical microscope used for measuring fibre diameters before tensile testing	43
Figure 3.15 – Digital image of a glass fibre captured by the optical microscope, being measured for diameter	43
Figure 3.16 – Image of a tensile test card clamped to the Testometric and cut in half before testing.....	44
Figure 3.17 – Schematic of an SEM plate with mounted glass fibres	46
Figure 3.18 – Schematic of an SEM plate with glass fibres mounted upright	46
Figure 3.19 – Image of the HITACHI SU-6600 FE-SEM	47
Figure 3.20 – Image of the Bruker Innova AFM	48
Figure 3.21 – Schematic of an AFM plate with mounted fibres	49
Figure 3.22 – AFM 3-D height image of an NaOH-treated glass fibre (a) before flattening, (b) after flattening, to remove curvature.....	49
Figure 3.23 – Image of the Agilent Technologies 4100 FTIR.....	50
Figure 3.24 – FTIR analysis of a glass fibre bundle using DR interface	52
Figure 3.25 - Average strength of fibres thermally conditioned at 450 °C and treated in various concentrations of alkaline solutions for 10 minutes	54

Figure 3.26 - Average strength of fibres thermally conditioned at 450 °C and treated in various concentrations of KOH solution for 10 minutes, either with acid or hot water rinse	56
Figure 3.27 – SEM images of glass fibres thermally conditioned at 450 °C and treated in 3 M KOH solution for 10 mins with (a) acid rinse, or (b) hot water rinse ..	57
Figure 3.28 – Average strength of fibres thermally conditioned at 450 or 500 °C, and treated in KOH solution for 10 minutes at different concentrations	58
Figure 3.29 – Average strength of fibres prewashed then thermally conditioned at 450, 500, 550 or 600 °C, and treated with either NaOH [13] or KOH.....	60
Figure 3.30 – Average strength of fibres thermally conditioned at 450 °C and treated in KOH solution at different concentrations and times	61
Figure 3.31 - Average strength of fibres thermally conditioned at 450 °C and treated in different KOH solution concentrations, at each treatment time	62
Figure 3.32 - Average strength of fibres thermally conditioned at 450 °C and treated in NaOH solution at different concentrations and times	63
Figure 3.33 - Average strength of fibres thermally conditioned at 450 °C and treated in different NaOH solution concentrations, at each treatment time	64
Figure 3.34 – Average diameters of fibres thermally conditioned at 450 °C and treated in 5 M KOH or NaOH for various times, measured by optical microscopy...	66
Figure 3.35 – Average strength and load at failure of fibres thermally conditioned at 450 °C and treated in 5 M NaOH for various times	68

Figure 3.36 - Mass loss (%) of glass fibre bundles thermally conditioned at 450 °C and treated in 3 M NaOH and KOH solution at different times.....	70
Figure 3.37 - SEM images of glass fibre bundles thermally conditioned at 450 °C and treated in 3 M KOH solution at (a) 0.5 hours, (b) 1 hour, (c) 2 hours and (d) 5 hours, without rinsing	71
Figure 3.38 - SEM images of glass fibre bundles thermally conditioned at 450 °C and treated in 3 M NaOH solution at (a) 0.5 hours, (b) 1 hour, (c) 2 hours and (d) 5 hours, without rinsing	72
Figure 3.39 - Fibre diameter reduction (%) and calculated mass loss (%) of single glass fibre after treatment in 3 M NaOH and KOH solution at different times	73
Figure 3.40 - AFM height and tapping phase images of (a) untreated fibre, and fibre treated in 3 M KOH solution for (b) 5 minutes, (c) 10 minutes, (d) 20 minutes and (e) 30 minutes.....	79
Figure 3.41 - AFM height and tapping phase images of (a) untreated fibre, and fibre treated in 3 M NaOH solution for (b) 5 minutes, (c) 10 minutes, (d) 20 minutes and (e) 30 minutes	81
Figure 3.42 - Roughness (R_q) values for untreated fibres and fibres treated in 3 M KOH and NaOH solution at different times.....	82
Figure 3.43 – Strength of fibres thermally conditioned at 450 °C and treated in 3 M KOH or NaOH solution at various times, plotted against their surface roughness...	84
Figure 3.44 - Stacked view of FTIR diffuse reflectance spectra of glass fibres (a) as received, (b) after HT, and then treatment in 5 M KOH solution for (c) 5 minutes, (d) 10 minutes, (e) 20 minutes, (f) 30 minutes and (g) 120 minutes, with rinsing.....	86

Figure 3.45 - Stacked view of FTIR diffuse reflectance spectra of glass fibres (a) as received, (b) after HT, and then treatment in 5 M NaOH solution for (c) 5 minutes, (d) 10 minutes, (e) 20 minutes, (f) 30 minutes and (g) 120 minutes, with rinsing 88

Figure 3.46 - Stacked view of FTIR specular reflectance spectra of glass fibres (a) as received, (b) after HT, and then treatment in 5 M NaOH solution for (c) 5 minutes, (d) 10 minutes, (e) 20 minutes, (f) 30 minutes and (g) 120 minutes, with rinsing 90

Figure 3.47 – Image of the clamp used to apply pressure to the sample in diamond ATR 91

Figure 3.48 - Stacked view of FTIR attenuated total internal reflectance spectra of glass fibres (a) as received, (b) after HT, and then treatment in 5 M NaOH solution for (c) 5 minutes, (d) 10 minutes, (e) 20 minutes, (f) 30 minutes and (g) 120 minutes, with rinsing 92

Figure 3.49 – Images of glass fibres (a) as received, (b) after HT, and then treatment in 5 M NaOH solution for (c) 5 minutes, (d) 10 minutes, (e) 20 minutes, (f) 30 minutes and (g) 120 minutes, with rinsing, after FTIR analysis with ATR interface 93

Figure 3.50 - SEM images of fracture surfaces of fibres HT and treated in (a) 5 M KOH solution for 120 minutes and (b) 5 M NaOH solution for 120 minutes 95

Figure 3.51 - Schematic showing strength regeneration mechanism of glass fibre by alkaline solution 96

Figure 3.52 - SEM images of the cross-section of (a) untreated glass fibre, and (b) glass fibre treated in 5 M NaOH solution for 120 minutes 97

Figure 3.53 – Average strength of APS-sized, HT and bare glass fibres after treatment in 3 M NaOH solution at various times	99
Figure 3.54 – Mass loss (%) of APS-sized, HT and bare glass fibres after treatment in 3 M NaOH solution at various times	101
Figure 3.55 – Average strength of APS-sized, HT and bare glass fibres after treatment in 3 M NaOH solution as a function of diameter reduction (%)	102
Figure 3.56 – Average strength of APS-sized, HT and bare glass fibres after treatment in 1.5 M NaOH solution for various times.....	103
Figure 3.57 – Mass loss (%) of fibre bundles after treatment in 1.5 M NaOH solution at various times	105
Figure 3.58 – Mass gain (%) of fibre bundles after treatment in 1.5 M NaOH solution at various times, without rinsing	106
Figure 3.59 – Average strength of APS-sized, HT and bare glass fibres against their diameter reduction after treatment in 1.5 M NaOH solution at various times.....	107
Figure 3.60 – SEM images of APS-sized glass fibres after 1.5 M NaOH treatment for (a) 30 minutes (without rinsing), (b) 30 minutes (with rinsing), (c) 120 minutes (without rinsing), and (d) 120 minutes (with rinsing).....	108
Figure 3.61 - SEM images of HT glass fibres after 1.5 M NaOH treatment for (a) 30 minutes (without rinsing), (b) 30 minutes (with rinsing), (c) 120 minutes (without rinsing), and (d) 120 minutes (with rinsing)	109

Figure 3.62 - SEM images of bare glass fibres after 1.5 M NaOH treatment for (a) 30 minutes (without rinsing), (b) 30 minutes (with rinsing), (c) 120 minutes (without rinsing), and (d) 120 minutes (with rinsing)	110
Figure 3.63 – Weight (%) of elements present on APS-sized glass fibres before and after alkaline treatment.....	111
Figure 3.64 - Weight (%) of elements present on HT glass fibres before and after alkaline treatment	112
Figure 3.65 – Weight (%) of elements present on bare glass fibres before and after alkaline treatment	113
Figure 3.66 - Stacked view of FTIR diffuse reflectance spectra of glass fibres (a) APS-sized only, then after 1.5 M NaOH treatment for (b) 30 minutes (with rinsing), (c) 120 minutes (with rinsing), (d) 30 minutes (without rinsing), and (e) 120 minutes (without rinsing)	114
Figure 3.67 - Stacked view of FTIR diffuse reflectance spectra of glass fibres (a) APS-sized + HT only, then after 1.5 M NaOH treatment for (b) 30 minutes (with rinsing), (c) 120 minutes (with rinsing), (d) 30 minutes (without rinsing), and (e) 120 minutes (without rinsing)	115
Figure 3.68 - Stacked view of FTIR diffuse reflectance spectra of glass fibres (a) bare only, then after 1.5 M NaOH treatment for (b) 30 minutes (with rinsing), (c) 120 minutes (with rinsing), (d) 30 minutes (without rinsing), and (e) 120 minutes (without rinsing).....	116
Figure 4.1 – Initial dissolution rate of vitreous silica glass in various alkaline solutions and concentrations at 80 °C. Reproduced from [96]	123

Figure 4.2 – Mass loss fraction (α) of glass fibres after treatment in saturated $\text{Ca}(\text{OH})_2$ solution at 25 °C for several days. Reproduced from [118]	125
Figure 4.3 – Schematic diagram of the shrinking core model. Reproduced from [129]	130
Figure 4.4 – Schematic showing the fibre sample preparation for alkaline treatment	135
Figure 4.5 – SEM image of a fibre being measured for its diameter	137
Figure 4.6 - Diameter reduction in glass fibres after treatment in KOH solution at various concentrations and times	139
Figure 4.7 - Diameter reduction in glass fibres after treatment in NaOH solution at various concentrations and times	140
Figure 4.8 - Rate of diameter reduction in glass fibres after treatment in KOH and NaOH solution at various concentrations	141
Figure 4.9 - SEM images of glass fibre (a) untreated (16.5 μm), (b) treated in 3 mol/L KOH at 95 °C for 5 hours (9.7 μm) and (c) treated in 3 mol/L NaOH at 95 °C for 5 hours (3.5 μm).....	142
Figure 4.10 - Diameter reduction in glass fibres after treatment in KOH solution at various temperatures and times	143
Figure 4.11 - Diameter reduction in glass fibres after treatment in NaOH solution at various temperatures and times	144
Figure 4.12 - Rate of diameter reduction in glass fibres after treatment in KOH and NaOH solution at various temperatures	145

Figure 4.13 - Fitting of kinetic data for 3 mol/L KOH and NaOH treatment of glass fibres at 75 °C in (a) zero order model, (b) shrinking cylinder model, (c) 2-D diffusion model (KOH), (d) 2-D diffusion model (NaOH).....	147
Figure 4.14 - Fitting of kinetic data for 3 mol/L KOH and NaOH treatment of glass fibre bundles at 95 °C in (a) zero order model, (b) shrinking cylinder model, (c) 2-D diffusion model (KOH), (d) 2-D diffusion model (NaOH)	149
Figure 4.15 - Plot to determine reaction order with respect to KOH through curve fitting.....	151
Figure 4.16 - Plot to determine reaction order with respect to NaOH through curve fitting.....	152
Figure 4.17 - Plot to determine activation energy for glass fibre reaction with KOH through curve fitting.....	155
Figure 4.18 - Plot to determine activation energy for glass fibre reaction with NaOH through curve fitting.....	156
Figure 4.19 - Plot of strength recovery (%) of HT fibre bundles against conversion (shrinking cylinder model) of single fibres after KOH treatment at various conditions	159
Figure 4.20 - Plot of strength recovery (%) of HT fibre bundles against conversion (shrinking cylinder model) of single fibres after NaOH treatment at various conditions	160
Figure 5.1 – Recycling techniques developed for composite waste.....	166

Figure 5.2 – Schematic showing the fluidised bed recycling process. Reproduced from [5]	168
Figure 5.3 – Image of glass fibres recovered from SMC feed using the fluidised bed. Reproduced from [141].....	170
Figure 5.4 – Strength of glass fibres recycled from SMC feed at different fluidised bed recycling temperatures. Reproduced from [141]	171
Figure 5.5 – Images of the in-house developed fluidised bed. Reproduced from [66]	172
Figure 5.6 - Glass fibres recycled in the fluidised bed at a temperature of a) 400 °C, b) 450 °C, c) 500 °C, d) 550 °C and e) 500 °C + thermal cleaning. Reproduced from [66]	172
Figure 5.7 - Tensile strength of glass fibres recycled at various fluidised bed temperatures. Reproduced from [66]	173
Figure 5.8 - SEM images showing scratches on the surface of glass fibres recycled in the fluidised bed at 500 °C. Reproduced from [66].....	174
Figure 5.9 – Tensile strength of glass fibres thermally treated and thermally ‘recycled’ out of a composite at 600 °C, before and after treatment in NaOH and APS solution. Reproduced from [14]	176
Figure 5.10 – Effect of treatments on IFSS of glass fibre with PP matrix. Reproduced from [14]	177
Figure 5.11 – Tensile strength of GMT with the glass fibres receiving different treatments. Reproduced from [14].....	178

Figure 5.12 - SEM image of fluidised bed recycled glass fibre treated in 5 M NaOH solution for 20 minutes, showing possible surface pitting.	179
Figure 5.13 – Tensile strength of glass fibres recycled from model epoxy composite in fluidised bed and treated in hot NaOH solution at various concentrations and times. Reproduced from [66]	180
Figure 5.14 - Tensile strength of glass fibres recycled from model epoxy composite in fluidised bed and treated in hot water at various times. Reproduced from [66]..	181
Figure 5.15 – Tensile strength of glass fibres recycled from model epoxy composite (in-house recycle) and end-of-life wind turbine blade, before and after treatment in hot alkaline solution (7 M NaOH for 2 hours) and hot water (4 days). Reproduced from [66]	182
Figure 5.16 – Image of wind turbine blade aerofoil (a) before downsizing, and (b) after downsizing for thermal recycling. Reproduced from [66]	184
Figure 5.17 – Image of glass fibres thermally recycled from wind turbine blade in the fluidised bed	185
Figure 5.18 – Schematic of fibre tensile test card at 5 mm gauge length	189
Figure 5.19 – Schematic showing sample preparation for microbond test. Reproduced from [66].....	191
Figure 5.20 – Vacuum oven temperature profile for preparing microbond samples. Reproduced from [66].....	192
Figure 5.21 – Image of a polymer droplet formed on a glass fibre, being measured using ImageJ. Reproduced from [66]	192

Figure 5.22 – Image of the microbond test setup on the Instron. Reproduced from [66]	193
Figure 5.23 – Schematic of droplet during microbond test.....	194
Figure 5.24 - Example of a typical load-extension plot output from Instron Bluehill 2 software. Reproduced from [66].....	194
Figure 5.25 – Tensile strength of thermally recycled glass fibres after treatment in hot NaOH solution for 2 hours at various concentrations.....	196
Figure 5.26 – Tensile strength of thermally recycled glass fibres after treatment in pH 7, 10 and 14 solutions at various times	198
Figure 5.27 – Average diameters of thermally recycled glass fibres after treatment in pH 7, 10 and 14 solutions at various times	200
Figure 5.28 – Images of thermally recycled glass fibres after treatment in solution for 2 days at (a) pH 7, (b) pH 10, and (c) pH 14	201
Figure 5.29 - Images of solutions after treating thermally recycled glass fibres for 2 days at (a) pH 7, (b) pH 10, and (c) pH 14	202
Figure 5.30 – Measured pH of solutions (25 °C) prepared at different theoretical pH values, before and after treatment of thermally recycled glass fibres at various times	203
Figure 5.31 – Tensile strength of thermally recycled glass fibres after treatment in hot 1 vol% APS solution (hydrolysed hot or ambient) or pH 10 NaOH solution for various times	206

Figure 5.32 – Tensile strength of thermally recycled glass fibres after treatment in hot APS solution (hot hydrolysis) for 5 days at various concentrations.....	207
Figure 5.33 - Measured pH of APS solutions (25 °C) prepared at different concentrations, before and after treatment of thermally recycled glass fibres at various times	208
Figure 5.34 – IFSS of thermally recycled glass fibres after treatment in hot 1 vol% APS solution (ambient hydrolysis) for various times, with PP as matrix	209
Figure 5.35 – IFSS of thermally recycled glass fibres after treatment in hot 1 vol% APS solution (ambient and hot hydrolysis) for various times, with PP as matrix ...	210
Figure 5.36 – IFSS of thermally recycled glass fibres after treatment in various APS solutions, with PP and PP/MAPP as matrices.....	211
Figure 5.37 – 3-D AFM (a) height image, and (b) phase image of the surface of a glass fibre thermally recycled from an end-of-life wind turbine blade using the fluidised bed	215
Figure 5.38 – Screenshot of NanoScope Analysis software being used to measure the depth of potential surface flaws on a glass fibre thermally recycled from an end-of-life wind turbine blade in the fluidised bed	216
Figure 5.39 - 3-D AFM (a) height image, and (b) phase image of the surface of a glass fibre thermally recycled from a model epoxy composite using the fluidised bed, and treated in 90 °C 5 M NaOH solution for 20 minutes	217
Figure 5.40 - Screenshot of NanoScope Analysis software being used to measure the depth of potential surface flaws on a glass fibre thermally recycled from a model	

epoxy composite using the fluidised bed, and treated in 90 °C 5 M NaOH solution for 20 minutes	218
Figure A.1 – Schematic diagram of an AFM probe showing the cantilever and tip. Reproduced from [25].....	A-2
Figure A.2 – Schematic diagram showing the feedback loop electronics for AFM in intermittent contact mode. Reproduced from [25]	A-3
Figure A.3 - Basic components of an FTIR spectrometer	A-6
Figure A.4 – Schematic showing the IR beam paths in (a) ATR, (b) SR, and (c) DR	A-7

List of tables

Table 2.1 – Typical wt% of various oxides in E-glass, taken from [25, 39]	8
Table 3.1 – Interfaces available with the Agilent Technologies 4100 FTIR and their attributes.....	51
Table 3.2 - Weight (%) of each element present in residue on 3 M KOH treated fibres at different times, determined by EDS.....	75
Table 3.3 - Weight (%) of each element present in residue on 3 M NaOH treated fibres at different times, determined by EDS.....	76
Table 4.1 – Summary of kinetic parameters obtained from various glass dissolution studies in the literature	132
Table 4.2 - Alkaline treatment conditions employed for kinetic study of glass fibre dissolution	136
Table 4.3 - Rate of reaction (r) of glass fibre with KOH and NaOH solution at various concentrations and constant temperature (95 °C).....	151
Table 4.4 - Rate constant (k) of glass fibre reaction with KOH and NaOH solutions at various temperatures and constant concentration (3 mol/L)	155
Table 5.1 - Predicted strength of glass fibre thermally recycled from an end-of-life wind turbine blade using the fluidised bed, based on crater depths from the AFM 216	
Table 5.2 – Predicted strength of glass fibre thermally recycled from a model epoxy composite using the fluidised bed, and treated in 90 °C 5 M NaOH solution for 20 minutes, based on crater depths from the AFM	219

Table 5.3 – Estimate of quantities and costs of chemicals for large-scale alkaline treatment of recycled glass fibres.....222

1 Introduction

1.1 Background

There is growing concern for the negative effect current disposal methods of composite waste are having on the environment. It is estimated that by 2020 the composites market will reach almost £80 billion globally, and as a result, there will be a high volume of waste once these materials reach the end of their life cycle [1]. Glass fibre is currently used as reinforcement in over 90% of all fibre-reinforced composites produced, and production waste represents 5 – 10% of composites production [2]. The high rigidity and chemical resistance of these composites, particularly glass fibre reinforced thermosetting polymers (GRP), are required for optimum performance but unfortunately result in poor recyclability; when such materials are no longer fit for purpose, they are deposited frequently in landfill sites. The rising costs associated with landfill together with increasingly stringent legislation means this disposal route is becoming ever more undesirable. Consequently, alternative methods for dealing with GRP manufacturing waste are needed [3]. In addition, the accelerating growth in use of GRP materials such as in the production of wind turbine blades means it is imperative that a long-term, cost-effective, recycling solution be developed for end-of-life composites [4].

In an effort to reduce the environmental damage caused by disposal of end-of-life composite materials, a range of recycling techniques have been investigated, some of which are now exploited on an industrial scale [5, 6]. Thermal treatment is one of the most widespread recycling technologies; by subjecting the composite to elevated temperatures, degradation of the polymeric matrix is achieved, facilitating subsequent extraction of any fibrous reinforcement [6]. Due to the harsh conditions employed in this procedure the glass fibres suffer from a severe loss in strength,

and therefore cannot be reused in many forms of composite applications [7-10]. These damaged filaments can however be reused as reinforcements if their strength is restored by means of chemical treatment. Such an example has recently been given where the strength of glass fibres heat conditioned at 450 – 600 °C can almost triple after a few minutes of immersion in dilute hydrofluoric acid (HF) [11]. HF is proven to be an effective chemical etchant, and is thought to strengthen glass by smoothing out sharp, severe surface flaws [12]. However, as HF is highly toxic in nature, its commercial use for regenerating strength of thermally weakened glass fibres is problematic. Consequently, there is a need to find less challenging chemical routes to enable a solution to the problem of cost-effective recycling and reuse of the glass fibres in GRP waste.

More recently, it was discovered that sodium hydroxide (NaOH) solution, prepared at high temperatures and at concentrations of 1.5 M and above, can significantly improve the strength of thermally treated glass fibre [13, 14]. The dissolution of glass in alkali is well documented in literature [15-17], however the use of these corrosive substances for strengthening thermally conditioned glass fibres is a novel concept, given that alkaline treatments are shown to have a detrimental effect on virgin glass fibre strength [18-22]. It is believed that the reduction in strength of fibres after heat treatment can be attributed to the creation of new flaws on the surface and/or the growth of pre-existing flaws [23, 24]. The mechanism by which these flaws develop is not yet fully understood; it has been postulated that it could involve the interaction of water with the fibre surface during the heat treatment process [23, 24]. However, it was found that when fibres were heat treated under vacuum they experienced a similar degree of tensile strength loss, suggesting that the presence of water has no effect on the development of fibre surface flaws [25]. It can be hypothesised that the reaction of silica (SiO_2) in the glass fibre with

hydroxide ions (OH^-) from the alkaline solution leads to the smoothing of the sharp, severe surface flaws, and thus increases the tensile strength of the fibre [20]. The modification of surface flaws has been reported previously on bulk glass with HF as the corrosive medium [12].

1.2 Objectives

As mentioned in the previous section, the application of hot alkaline treatments to thermally conditioned glass fibres can be an effective approach to regenerate their strength, and is relatively safer than using HF. This thesis presents the results of an in-depth investigation into the use of hot alkaline solutions to improve the strength of thermally treated E-glass fibres. To further the understanding of the reaction of glass with alkaline solutions, hydroxides based on other alkali metals were also surveyed: lithium hydroxide (LiOH) and potassium hydroxide (KOH). It is thought the nature of the alkaline solution, temperature, molarity and treatment duration influence the etching rate of the glass surface. Parameters related to the glass fibre itself, such as its diameter and the presence of sizing, can also influence the reaction rate. In this research study, the effects of various alkaline solution conditions on fibre properties were explored. The influence of alkaline treatments on virgin glass fibres was also examined. In addition, the kinetics of the reaction between glass fibres and alkaline solutions were investigated to learn more about the etching mechanism. Finally, a study into the effects of various chemical treatments on the properties of glass fibres thermally recycled out of an end-of-life wind turbine blade was conducted.

The ultimate aim of this research project was to develop chemical treatments to regenerate the performance of thermally conditioned or recycled glass fibres. This can offer a potential cost-effective route to GRP recycling, and ultimately reduce the

negative environmental impact from landfill disposal. Additional objectives include generating further understanding of the etching mechanism and how differences in chemical properties of alkali metal hydroxides affect their reaction with glass fibre.

1.3 Outline of thesis

This chapter is an introduction to the background, objectives and outline of the thesis. The next chapter (Chapter 2) gives a general literature review on the manufacture, applications and properties of glass fibres. Presentation of research work carried out to address the project objectives is shown in Chapters 3 to 5. Each of these chapters includes a more specific literature review and experimental section. Chapter 3 discusses the use of alkaline treatments to improve the strength of glass fibres thermally treated in a furnace to mimic recycling conditions. Being the most significant chapter in terms of content, it also reports detailed investigations into the etching effect of alkaline solutions on glass fibres, and examination of the alkali treated fibre surfaces from a range of analytical techniques. Chapter 4 explores in more depth the kinetics of the reaction of glass fibres with alkaline solutions. Finally, Chapter 5 investigates the effect of alkaline as well as other chemical treatments to regenerate the performance of glass fibres that were thermally recycled out of an end-of-life wind turbine blade using an in-house fluidised bed. Focus of this chapter is more on developing chemical treatments that are cost-effective and hence industrially-feasible. Conclusions of the work reported in this thesis are given in Chapter 6, and areas for future work described in Chapter 7. There is also an Appendix which provides more information on the theory behind some of the analytical techniques employed in this research project to examine the fibre surface after alkaline treatment.

2 Glass fibres – a review

This chapter gives a general review of the literature concerning the development, properties and applications of glass fibres. Chapters 3 to 5 contain separate literature reviews that look specifically into the strength loss of glass fibres from thermal recycling and how glass can be altered from chemical treatment such as alkaline solution to regenerate strength.

2.1 Introduction to glass fibres

In the 1940s, Slayter of Owens Corning filed the first patents on manufacturing glass fibres [26-29]. Despite the recent development of these materials, they were in fact used hundreds of years ago by the Venetians for decoration [25, 30]. Since the mass production by Owens Corning, glass fibres have been used commercially in various applications, from composite materials to printed circuit boards (PCBs) [25, 31]. Glass fibres, usually E (electric) grade, are used in over 90% of fibre reinforced composites manufactured today [14]. When also taking yarns into account, it is estimated that the total consumption of E-glass could already be above 7 Mton [14].

Glass fibres have numerous beneficial properties which allow them to be used in a wide range of applications. As glass fibres possess a high surface to volume ratio there is a decrease in the population of critical flaws on the surface according to Griffith's theory [32]; because of this, glass fibres have an excellent tensile strength, which can range from 2 to 4.7 GPa. Glass fibres can however lose tensile strength following exposure to highly corrosive environments and elevated temperatures, as described later in this thesis.

The rest of this chapter focuses particularly on how glass fibres are produced industrially, their chemical composition, and how they can lose strength through processes such as thermal recycling from composite waste.

2.2 Glass fibre formulation

The manufacture of glass fibres involves mixing certain naturally occurring minerals in various ratios according to the grade of fibre that needs to be produced. Many types of glass fibres, such as E-glass fibres, are composed mainly of silica (SiO_2). Although one might consider silica as a discrete molecule, in reality it forms an amorphous network structure in glass fibres as shown in Figure 2.1 [33]. The glass structure also incorporates network formers and modifiers, and their definitions are explained later.

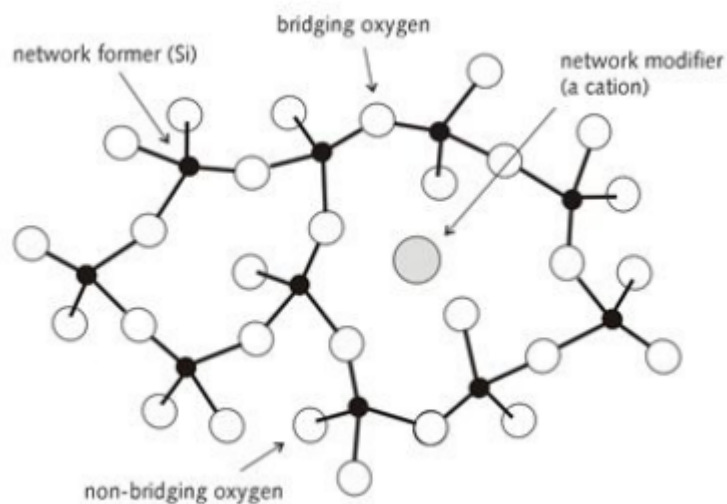


Figure 2.1 – Amorphous network structure of silica with network modifiers and formers.
Reproduced from [33]

The non-bridging oxygens in the glass network can bond to hydrogen atoms to form silanol groups (SiOH); in fact, many studies in the past involved measuring the silanol group concentration on the surface of bulk and fibrous silica glass [34-38].

The production of glass fibres relies on the glass mixture to be liquid so that filaments can be drawn out. Amorphous silica softens at a very high temperature of 1650 °C, but does not have a true melting point. Other minerals are added to the glass mixture to make fibre production easier. These minerals form oxides in the glass melt and affect the properties of the resulting fibre. Among these are aluminium oxide (Al_2O_3) and boron oxide (B_2O_3), which are classified as network formers as they become part of the silica structure. The incorporation of these network formers results in a decrease in the temperature required to process the glass melt. Network modifiers also exist in the glass mixture, such as calcium oxide (CaO) and magnesium oxide (MgO). These additives create gaps in the silica structure and balance the excess negative charge from oxygen ions in the network. Some oxides like Al_2O_3 are also categorised as intermediate oxides, meaning they can function both as network modifiers and formers in the glass. Other metal oxides can be present in the glass mixture, but usually in trace amounts.

E-glass is the most popular grade employed in glass fibre production, and was used in this research study. The typical composition of E-glass fibre (boron containing or boron free) is presented in Table 2.1. The concentration of each oxide is given as a range as there can be slight variation amongst different glass fibre manufacturers. In recent years, work has been done with removing boron and fluorine from glass fibre formulations because of health concerns.

Table 2.1 – Typical wt% of various oxides in E-glass, taken from [25, 39]

Component	Typical composition (wt%)								
	SiO ₂	Al ₂ O ₃	B ₂ O ₃	CaO	MgO	Na ₂ O + K ₂ O	TiO ₂	Fe ₂ O ₃	F ₂
Boron containing E-glass	52 – 56	12 – 16	4 – 10	16 – 25	0 – 6	0 – 2	0 – 0.5	0 – 0.4	0 – 0.7
Boron free E-glass	59 – 60.1	12.1 – 13.2	–	22.1 – 22.6	3 – 3.4	0 – 0.9	0.5 – 1.5	0.2	0 – 0.1

In industry, all the components of the glass mixture are melted in a furnace and fibres are drawn out as shown in the schematic in Figure 2.2 [40].

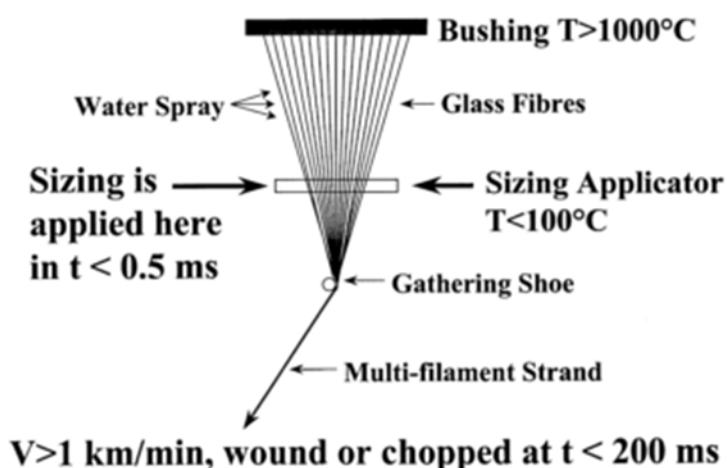


Figure 2.2 – Schematic showing the glass fibre forming process. Reproduced from [40]

Fibres are drawn out individually from the molten glass through a bushing, before being cooled with water spray. Because of the nature of the drawing process, the diameters of the fibres can vary, from 3 to 24 μm [40]. Also, the composition of the various oxides shown in Table 2.1 can differ slightly with each fibre [40]. As soon as the glass fibres are formed and quenched, their surfaces are coated with a ‘sizing’

usually via an applicator roll as shown in Figure 2.2. The sizing is an aqueous mixture containing a myriad of ingredients such as film former, silane coupling agent and lubricant. More information on the purpose of some of these sizing components is given in the following section. In general, the sizing is applied to the fibre to protect the surface from damage and to improve its bonding to the polymer matrix in the composite. Once fibres are coated in a sizing, they are gathered together into a strand and move to the next stage of processing. The handling of the fibre bundles at this stage depends on their intended use; they could be chopped into short strands, or wound into a roving. Some of the components in the sizing are designed to aid winding or chopping of the fibre strands. The next section goes into more detail on the various ingredients usually present in commercial sizings, and their functions.

2.3 Glass fibre sizing

Thomason and Adzima state that sizing is probably the main component that affects the quality of glass reinforcement products [40]. Sizings are water-based solutions with 0.05 to 10% solid content. These solids require water as a medium for coating the glass fibres during manufacturing. Each of the components of the sizing performs a particular function for the fibre, as described in this section. The nature of the constituents in glass fibre sizings and their composition are generally kept proprietary by the glass fibre manufacturer, however the most commonly used ingredients are known and mentioned here.

2.3.1 Film former

The polymer film former is generally the main component of the glass fibre sizing by weight. This is essentially an emulsion of a polymer or a combination of polymers; because of their immiscibility in water, the polymers require an emulsifying agent. The nature of the polymer or polymers in the film former usually depends on the matrix the fibres will bond to in the composite material. For example, if the glass fibres are intended for use in an epoxy-based composite, then it is likely the film former in the glass fibre sizing would be an epoxy emulsion. When this polymer emulsion is applied to glass fibres as part of a sizing and dried, a film is formed around the surface. The purpose of this film former is to hold the fibres together in a bundle during processing and protect the surface from damage. Because the nature of the polymer will closely match that of the composite matrix, the film former can also improve the interfacial adhesion of the glass fibres.

Zinck et al. [41, 42] examined the effect of sizing (including film former alone) on the properties of glass fibres. They report that the film former can affect the healing of flaws already present on the unsized glass fibre surface, and the probability of new flaws being formed [42]. In addition, the authors found that the tensile strength of fibres increased after coating with a mixture of film former and silane coupling agent, and to a greater extent than coating fibres with only one of these sizing components; because of this, they assumed a synergistic effect of the film former with the silane coupling agent. Details on the functions of silane coupling agents in glass fibre sizings are given in the following section.

2.3.2 Silane coupling agent

Despite being the second most significant constituent in terms of weight, the silane coupling agent is thought to be the most crucial ingredient in glass fibre sizings. The silane coupling agent is essentially a bridging material that improves the bonding of glass fibres to the polymer matrix in the composite [43, 44]. The general structure of a silane coupling agent is $[X-Si(OR)_3]$, where X is usually an organic functional group that can bond to the polymer matrix material. OR tends to be a methoxy or ethoxy group, of which the alkyl group hydrolyses and thus can react with the hydroxyl groups on the glass surface.

Aminosilanes are the most widely used silane coupling agents as they can be compatible with both thermoplastic and thermoset polymer matrix materials [25]. The coupling agent used for the experimental work reported in this thesis is γ -aminopropyltriethoxysilane (APS) (see the chemical structure in Figure 2.3), which is also the most widely used coupling agent in commercial glass fibre sizings.

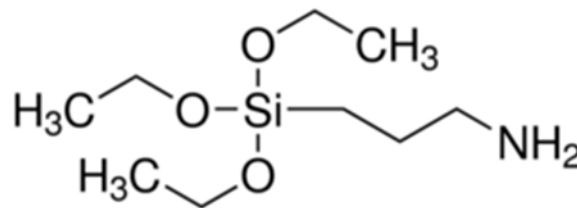


Figure 2.3 – Chemical structure of APS

The hydrolysable components of APS (R) are the ethyl groups (CH_3CH_2-). The organic functional group (X) is a propyl chain that terminates with a primary amine (NH_2).

To hydrolyse the APS, it is made into an aqueous solution. The water from the solution detaches the ethyl groups from the APS, and is eliminated in the form of ethanol. The ethyl groups are substituted with hydrogen atoms; these resulting silanol groups (SiOH) from the APS molecules react with each other through a condensation step to form a siloxane structure as shown in Figure 2.4.

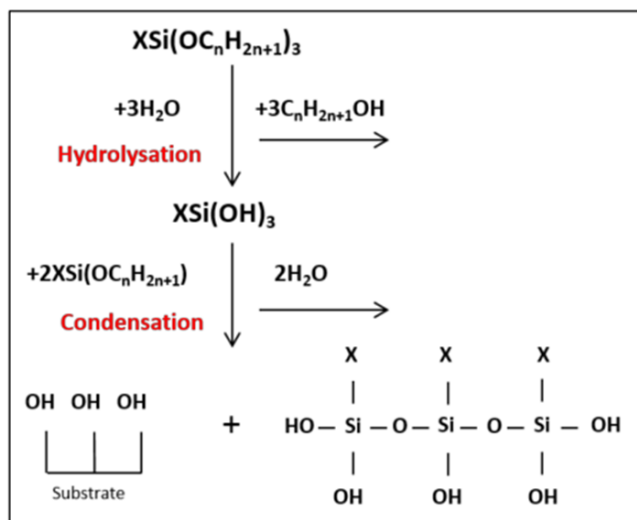


Figure 2.4 – Hydrolysatation and condensation process of silane coupling agents. Reproduced from [25]

The hydroxyl groups left in the siloxane structure then react with the hydroxyl groups on the glass fibre surface leading to covalent bonding upon drying as presented in Figure 2.5.

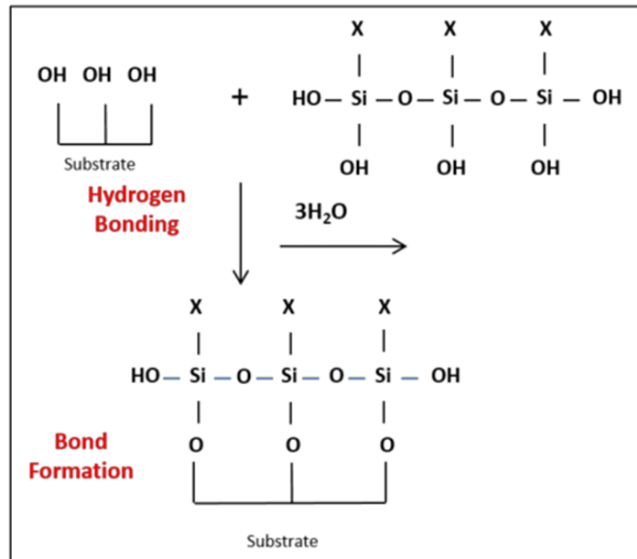


Figure 2.5 – Bonding of self-condensed silane coupling agent with substrate surface (such as glass). Reproduced from [25]

Although the reaction scheme in Figure 2.5 suggests a monolayer of coupling agent bonds to the glass surface, in reality there could be a 3-D network structure comprised of: APS chemically bonded to the glass surface at the interface, APS molecules self-condensed to form a complex polysiloxane network, and short chained self-condensed APS (oligomers) loosely bonded at the surface (see Figure 2.6) [25, 45, 46].

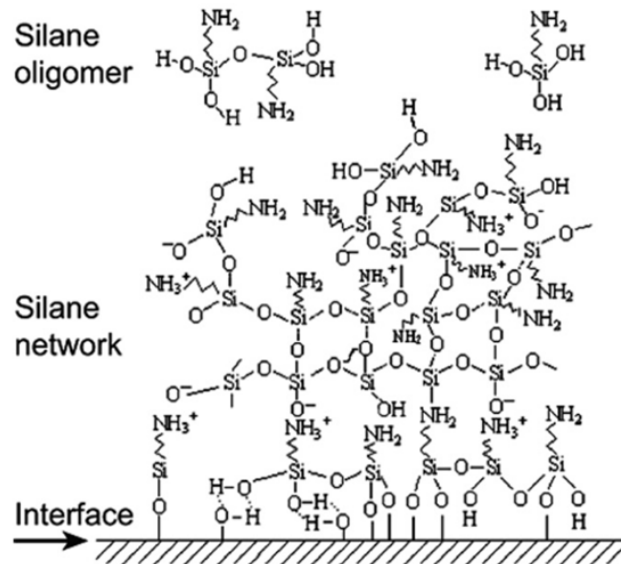


Figure 2.6 – Schematic of 3-D network structure of hydrolysed APS on glass fibre surface. Reproduced from [46]

As well as promoting the adhesion of glass fibres with the polymer matrix, silane coupling agents, whether applied alone or as part of a sizing, can improve the strength of bare fibres; this can be through a flaw healing mechanism as proposed by Zinck et al. [41, 42] or, most likely, by protecting the fibre surface from damage in the first place [47, 48].

Other ingredients aside from film formers and silane coupling agents are included in commercial glass fibre sizings. A brief description of some of these components is presented in the next section.

2.3.3 Auxiliary components

The previous sections summarise the functions of the two main constituents of commercial glass fibre sizings: the film former, and the silane coupling agent. Other

components can be found in sizings, though they are usually present in lower concentrations. Auxiliary ingredients in glass fibre sizings could include: lubricants, anti-static agents, emulsifiers, chopping aids, wetting agents and antioxidants [40]. Lubricants are added to sizings to reduce fibre-fibre abrasion. Anti-static agents keep static electricity from building up on the non-conductive fibres as they are being produced and converted at high speeds. Emulsifiers, although identified as additives, are generally incorporated into the film former to allow the polymer to disperse in water. They also improve the dispersion of other sizing components that would otherwise be immiscible in water. Chopping aids are included in sizings to, like the name suggests, make it easier to chop the fibre strands during the manufacturing stage. Wetting agents reduce the surface tension of the sizing so that it can wet the fibre surface more easily. Finally, antioxidants slow down the degradation of the sizing thereby increasing its lifetime.

To summarise, sizing aids the processing of glass fibres when they are being manufactured, as well as acting as a protective coating during usage and promoting fibre adhesion to the polymer matrix in the composite material. Despite the protective capability of the sizing, glass fibres can still lose strength during service, for instance through exposure to corrosive environments and during mechanical handling. In particular, the reduction of strength is severe when recycling fibres out of composite waste through thermal treatment. The following section looks into what causes the decrease in strength of glass fibres and methods in which fibre strength can potentially be recovered.

2.4 Glass fibre strength loss

The ability of the sizing to protect the glass fibre surface from damage is discussed in the previous section. Glass fibres can still suffer strength loss from processes such as mechanical handling (fibre-fibre rubbing and abrasion), chemical corrosion, and thermal recycling. Understanding the mechanism of strength loss of glass fibres, especially when they are recycled out of composite waste, can help to develop an approach to regenerate their strength and allow their reuse in second-life composite materials. A more in-depth literature review on the strength loss of virgin glass fibres from chemical and thermal treatments is given in Chapter 3. Here, more focus is given on the factors that govern the strength loss of glass fibres in general.

Fibres with no flaws on the surface or in the bulk are referred to as pristine. The strength of pristine fibres is denoted as the 'intrinsic' strength; it is controlled by the structure and composition of the glass [49, 50]. The strength of non-pristine fibres is usually discussed in the literature ('extrinsic' strength). The extrinsic strength is influenced by 2-D flaws or cracks, which are of nanometre scale. Because the surface of the fibre is the first point of contact, one might assume that these cracks are usually present on the surface rather than in the bulk. Feih et al. [7, 24, 51] examined the fracture surface (cross-section) of glass fibres before and after thermal treatment to determine the source of the flaw. A schematic diagram of what a fibre fracture surface would look like if the flaw originated at the surface is displayed in Figure 2.7.

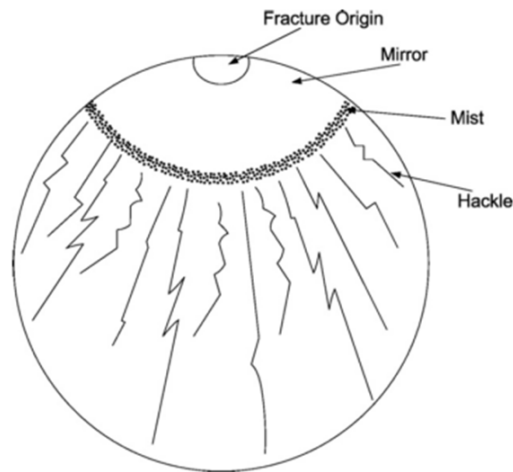


Figure 2.7 – Schematic showing the fracture surface of a fibre where the flaw originated from the surface. Reproduced from [7]

The three main features of the fracture surface shown in Figure 2.7 are the mirror, mist and hackle [7]. Close to the fracture origin is the mirror zone, which is smooth and is inversely related to the fibre tensile strength; the larger the mirror zone, the more severe the surface crack, and hence the lower the strength of the fibre. At the edge of the mirror zone is a speckled region known as the mist, and protruding from this region are branches which are referred to as hackle. Feih et al. observed these features for untreated and thermally treated glass fibres (see Figure 2.8), suggesting that strength loss in both cases was due to critical flaws at the surface [7].

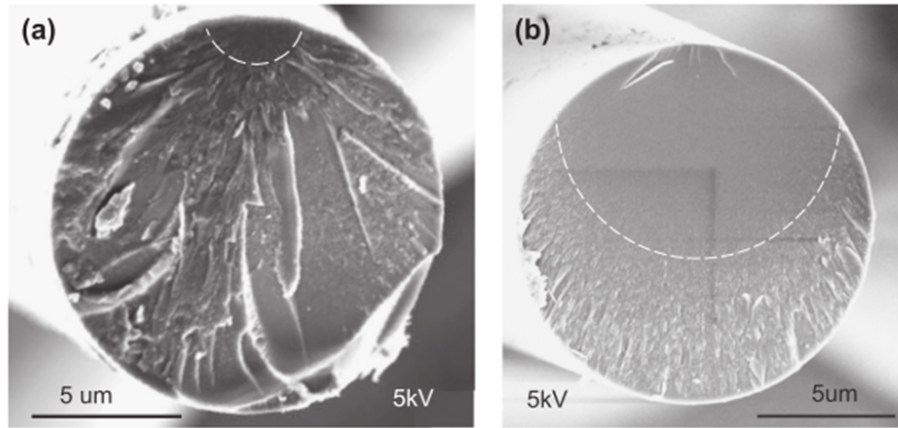


Figure 2.8 – Scanning electron microscopy (SEM) images of the fracture surface of glass fibres (a) untreated, and (b) thermally treated in air. Reproduced from [7]

The idea that the strength of glass fibres is controlled by superficial flaws is well documented in the literature [7, 8, 23-25, 51-60]. Korwin-Edson et al. [59] state that mechanical and/or chemical damage can cause the development of the surface flaws. These surface flaws are focal points for stresses applied on the glass; eventually, under stress, the critical surface crack propagates leading to failure of the glass article. In the 1920s, Griffith et al. [32] expressed the following relationship between the strength and crack depth in brittle materials (Equation 2.1):

$$\sigma_f = \sqrt{\frac{2E\gamma}{\pi c^*}}$$

Equation 2.1

σ_f refers to the failure stress of the specimen (strength), E the Young's modulus, γ the fracture surface energy, and c^* the critical crack depth for crack growth [32].

There is a stress concentration on the critical crack tip; the strained bonds at this tip eventually break and the crack proliferates under stress, resulting in failure of the glass [59]. It is thought that water molecules can react with siloxane bonds on the glass surface, resulting in increased severity of cracks and consequently a lower tensile strength of the glass fibre; Feih et al. postulate that this could be a mechanism of strength loss of glass fibres after thermal treatment, where the elevated temperature accelerates the corrosion of the glass by adsorbed surface water [7, 24, 51]. The adverse effect of water on glass strength has been investigated decades earlier [61-63]. The loss in strength of virgin glass fibres after treatment in alkaline solutions and hydrofluoric acid (HF) is also thought to be due to the breakdown of siloxane bonds, and is explored further in Chapter 3. The strength reduction of fibres after treatment in acids other than HF (such as hydrochloric acid, HCl) is believed to involve leaching of ions from the glass rather than degradation of the silicate network [64, 65].

From reviewing the literature, it is clear that the strength of glass fibres is generally controlled by cracks on the surface; the mechanism of crack growth is not fully understood, but is thought to involve the interaction of the glass surface with water or other chemical species if damage is mainly inflicted by chemical treatment. Examining a surface flaw on a fibre before and after thermal or chemical treatment could provide further insight into how strength loss occurs, however because of the nanometre scale of the flaws they cannot be easily probed even with a powerful microscope. As a result, surface flaws on glass fibres are usually schematically represented in the literature like in Figure 2.9.

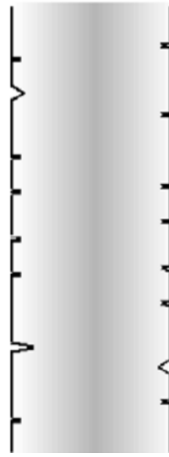


Figure 2.9 – Schematic showing the surface flaws on a glass fibre. Reproduced from [20]

More recently, cracks have been observed on thermally recycled glass fibres using an SEM [66] and further investigated using other techniques like atomic force microscopy (AFM) in this thesis. Assuming that surface cracks mainly control the strength of glass fibres, it can be said that improving the strength of glass fibres thermally recycled out of composite waste can potentially be achieved by altering these cracks through chemical treatment. This may seem counter-intuitive given that chemical treatments such as alkaline solution are shown to decrease virgin fibre strength possibly by creating and propagating surface flaws in the first place [18-22], however work by previous authors [13, 14] and the results presented in this thesis show the potential of alkaline solution to regenerate strength of thermally treated glass fibres through the very same chemical mechanism.

2.5 Conclusions of literature review

Glass fibres have been used since ancient times, but the application of these materials in composites has only been prevalent in the past decades. Glass fibres,

particularly E-glass fibres, are the most widely used reinforcement materials in composites today, owing to their excellent strength and chemical resistance. Commercial glass fibres tend to be produced from a blend of silica and various metal oxides, the purpose of the latter being to make the fibre manufacturing stage easier. Individual filaments are drawn out of the molten glass, cooled, and coated with a sizing to protect the glass fibre surface and improve adhesion to the polymer matrix in the composite. The sizing is an aqueous solution containing a variety of ingredients, each with a specific function or functions for the fibre. Arguably the most vital component of the sizing, the silane coupling agent, promotes the adhesion of the glass fibres with the composite matrix and protects the fibre surface.

Despite the excellent thermal and chemical resistance of the sizing, it can unfortunately degrade during processes such as thermal recycling of the composite or through chemical corrosion, thus exposing the fibre surface to physical and chemical damage. The main factor controlling the strength of the glass fibre is believed to be the surface flaws, which become more severe by thermal/chemical treatment and mechanical handling. The strength loss of fibres subjected to thermal treatment is said to involve the degradation of the glass network by surface water, a process believed to be accelerated by the elevated temperature. A similar procedure is said to be followed when fibres are chemically treated, for example in alkaline solution. The breakdown of the network is thought to result in the propagation of surface cracks on the glass fibre, leading to poor tensile strength. Due to the nanometre scale of these cracks they are difficult to detect even microscopically. The feasibility of certain chemical treatments to modify the severe surface cracks of thermally treated or recycled glass fibres and hence improve tensile strength is explored in this thesis.

3 Regenerating the strength of thermally conditioned glass fibres through hot alkaline treatments

3.1 Introduction

As discussed previously in Chapter 2, glass fibres suffer from a severe loss in tensile strength after being thermally recycled from GRP waste; this renders them unfeasible for reuse in various composite applications [7-10, 25, 67]. To address this issue, fibres can be treated in a chemical solution to regenerate their strength. Such an example is given in [11] where the strength of glass fibres heat conditioned at 450 – 600 °C can almost triple after a few minutes of immersion in dilute hydrofluoric acid (HF). HF is proven to be an effective chemical etchant, and is thought to strengthen glass by smoothing out sharp, severe surface flaws [12]. However, as HF is highly toxic in nature, its commercial use for regenerating strength of thermally recycled glass fibres is problematic. It was recently discovered that strength regeneration of thermally conditioned glass fibres can also be achieved by treating them in alkaline solution at elevated temperature and at concentrations of 1.5 M and above [13, 14]. Despite the aggressive conditions employed in this treatment, alkaline solution is still relatively safer than HF and hence more practical for treating recycled glass fibres on an industrial scale. A more detailed investigation into the cost-effectiveness of using alkaline solution on a commercial scale to treat recycled fibres is described in Chapter 5.

This chapter presents the results of an investigation of the use of hot alkaline solutions in regenerating the strength of E-glass fibres that were thermally treated in a furnace to simulate recycling conditions. Firstly, a literature review was carried out

into the effect of chemical treatments on the properties of virgin glass fibres; this research has been conducted extensively as there is a need to assess the durability of commercial glass fibres in various chemical environments. The influence of thermal treatment on the mechanical properties of glass fibres was also examined in the literature, as well as the effect of chemical treatments in regenerating their strength.

The work carried out in [13, 14] involved the use of sodium hydroxide (NaOH) as the alkaline medium to regenerate fibre strength. It is thought the reaction of glass fibre with alkaline solution, and therefore the extent to which fibre strength is recovered, is strongly dependent on various conditions; this can include the nature of alkali, temperature, molarity and treatment duration. In this research study, the feasibility of alkali metal hydroxides as well as NaOH was surveyed: lithium hydroxide (LiOH) and potassium hydroxide (KOH). Once fibre bundles were thermally conditioned in the furnace to mimic recycling conditions, they were treated in these alkaline solutions at various concentrations and times. The tensile strength of these fibres was then measured to establish whether the treatment was successful. In addition, the effect of these alkaline treatments on the strength of virgin glass fibres was examined.

As well as characterising the fibre strength, the resulting deposit formed on the fibre surface after alkaline treatment and the glass surface topography were both analysed through various techniques. Although the research presented in [13, 14] show how alkaline treatment can recover a significant amount of strength in damaged fibres, the mechanism of this strength regeneration has not yet been investigated. It is thought that the strength recovery could involve the etching of the damaged surface layer of the fibre by the alkaline solution; the validity of this theory is investigated in this chapter. The main aim of the research study presented in the

chapter is to validate the hypothesis that alkaline treatment can regenerate the strength of thermally recycled glass fibres, offer a potential cost-effective route to GRP recycling, and ultimately reduce the negative environmental impact from landfill disposal. Additional objectives include generating fundamental understanding of the etching mechanism and how differences in chemical properties of alkali metal hydroxides affect their reaction with glass fibre. The key results given in this chapter have recently been published in a journal article [2] and in conference proceedings [68, 69].

3.2 Literature review

3.2.1 Effect of chemical treatments on virgin glass fibre strength

It is important for glass fibres to exhibit excellent chemical resistance in order for them to be used in composites manufacturing. Studies on the resistance of glass fibre reinforced composites in various chemical environments have been carried out according to the literature [70-72]. Previous research shows that the component of glass fibre reinforced composites responsible for their failure in corrosive environments is the fibre rather than the resin [73-75]. Significant chemical corrosion of glass fibres is shown to have an adverse effect on the mechanical performance of glass fibre reinforced composites [71, 72, 76]. Although the resin is generally critical to the chemical durability of the composite, the fibre also plays an important role and is the primary focus of this literature review.

The performance of virgin glass fibres following exposure to acidic and alkaline solutions have been explored comprehensively according to the literature. Friedrich et al. [18] examined the durability of both E-glass and basalt fibres in alkaline

environments by treating the fibres in hot NaOH solution and then measuring their tensile strength and mass loss; they found that although the basalt fibres dissolved in the alkaline solution at a faster rate than the E-glass, they retained more of their strength. A similar investigation was carried out by Wei et al. [21] where both fibres were also treated in hydrochloric acid (HCl). The authors discovered that the basalt fibres displayed superior acid resistance and preserved more of its mass after alkaline treatment, but in contrast to the results in [18], suffered from more severe strength loss than the E-glass fibre [21]. These results also contradict those presented in [77], where basalt fibres were shown to have poor resistance to acids and exceptional durability in alkaline environments. For both glass and basalt fibres, the strength and mass typically drops precipitously after exposure to alkaline solution and then levels off with time, as indicated in Figure 3.1 [21].

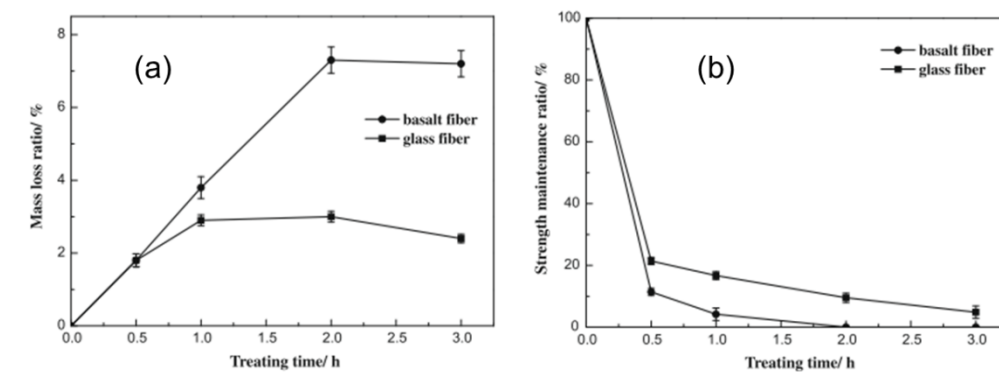


Figure 3.1 – Mass loss (%) and strength maintenance (%) of E-glass and basalt fibres after treatment in boiling 2 M NaOH solution. Reproduced from [21]

The fibres (all unsized) lose their mass linearly with treatment time in the NaOH solution, then remain constant after 2 hours for the glass fibre, and 1 hour for the basalt fibre; this is probably due to the build-up of a product layer on the fibre

surface which impedes the dissolution process [21]. The strength of the fibres drops dramatically after just half an hour of alkaline treatment, and then decreases more gradually with time, as does the mass. Analysis of the fibre surface with a scanning electron microscope (SEM) proved the existence of a product layer (image shown in Figure 3.2) [21].

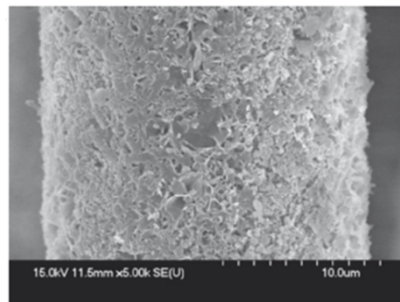


Figure 3.2 – SEM image of E-glass fibre after treatment in boiling 2 M NaOH solution. Reproduced from [21]

In another article the authors assess the chemical resistance of ECR (electrical and chemical resistant) and S (high strength) glass fibres in alkaline solution [22]. The S-glass fibre showed marginally better strength retention though its dissolution in the hot NaOH solution was significantly greater than that of ECR-glass fibre [22].

Velpari et al. [78] explored the stability of E-glass fibre in cement extract solution to assess whether it was feasible as a reinforcement material in Portland cement. Although the alkaline conditions of the cement solution was not as corrosive as in other studies (pH 12 to 13), the fibres suffered from a drastic loss of tensile strength after being immersed [78]. The behaviour of AR (alkali resistant) glass fibres in both cement and NaOH solution has been investigated by Scheffler et al. [20]. In this article, the alkaline resistance of sized and unsized fibres was studied; in other

reports the sizing was always removed from the fibre surface with acetone treatment to avoid its influence on mass loss measurements [18, 21, 22]. The authors found that although the sizing initially protected the fibre from alkaline attack, it was eventually removed thus resulting in a similar strength loss of the fibre to when it was unsized [20]. It was also proposed that the NaOH and cement solution, though both alkaline in nature, reacted with the fibre surface through different mechanisms; Figure 3.3 shows schematic diagrams of the hypothesised corrosion process of glass fibres in NaOH and cement solution [20].

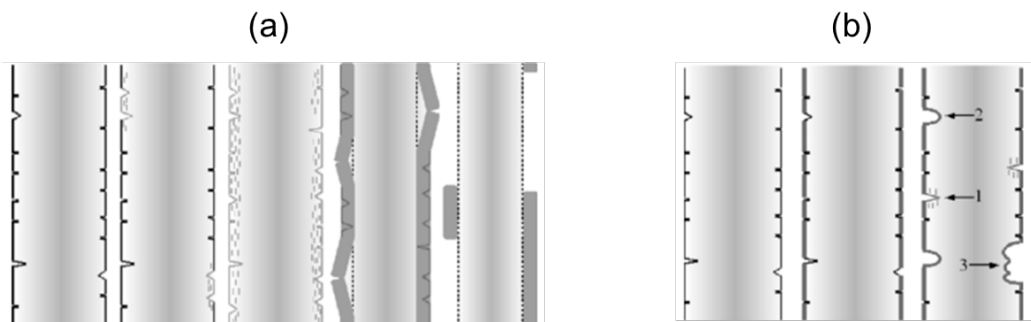


Figure 3.3 – Schematic diagram of the corrosion process of glass fibres in (a) NaOH solution, and (b) cement solution. Reproduced from [20]

Figure 3.3a initially shows the fibre with flaws on the surface, which reacts with the NaOH solution to form a corrosion layer that eventually peels off to reveal an apparently smoother fibre surface underneath; the authors believed that this stage of the corrosion process explained the occasional increase in failure stress of NaOH treated fibres [20]. They assumed that with the new fibre surface the corrosion process would start from the beginning again, and this cycle would be repeated as the fibres remain in the solution. Figure 3.3b conversely demonstrates that cement solution has a limited, local attack on the fibre surface which leads to defects that

increase in size to eventually form holes; SEM images of these features are presented in [20]. In-depth investigations into the mechanism of glass corrosion in alkaline solution are well documented in the literature [15-17] and explored further in Chapter 4. The subsequent section looks into the damaging effect of thermal treatment on glass fibres, and how alkaline solution can potentially regenerate their performance.

3.2.2 Properties of thermally treated glass fibres

This section explores the damaging effect of chemical treatments on virgin glass fibres. This similar degradation of mechanical properties can be experienced when fibres are subjected to elevated temperatures. In order to recover glass fibres from GRP waste, it typically requires thermal treatment at 450 to 600 °C to degrade the polymeric matrix. The drastic loss in tensile strength of glass fibres from thermal treatment is a major issue, as this limits their reuse in second-life composite materials. This section looks into how thermal treatment reduces glass fibre strength, and in what way certain chemical solutions can potentially regenerate the strength of these filaments.

It has been discussed previously in Chapter 2 how the strength of glass fibres is normally governed by surface flaws. Although it is well-established that thermal treatment leads to a reduction in strength of glass fibres, the mechanism of strength loss is not yet understood, except for the fact that new flaws on the surface are created and pre-existing flaws become more severe in some way [23, 24]. It is postulated that the mechanism of flaw development could involve the interaction of water with the fibre surface during the heat treatment process [23, 24].

Studies on the influence of thermal treatment on glass fibre strength were conducted several decades ago [79-82]. Aslanova [79] reported up to 70% strength loss of glass fibres when heated at 400 – 600 °C. It was also discovered that the chemical composition of the fibres had a significant impact on the extent of strength degradation, as demonstrated in Figure 3.4 [79].

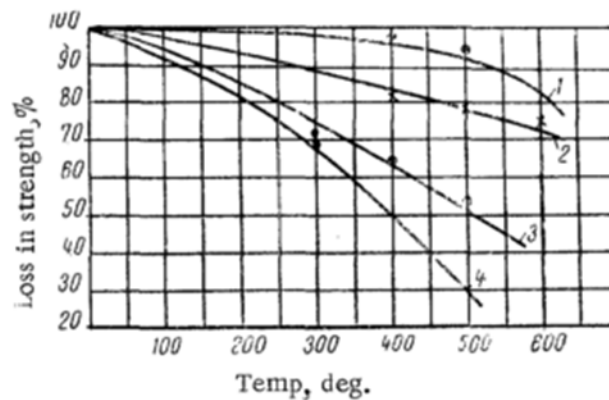


Figure 3.4 – Strength loss (%) of 1) quartz glass, 2) silica, 3) non-alkaline aluminoborosilicate, and 4) soda-calcia-silicate glass fibre after thermal treatment at different temperatures. Reproduced from [79]

Figure 3.4 shows that the strength loss of fibres of alkaline composition (curve 4) occurs more rapidly and at lower temperatures, with quartz fibre (curve 1) being the most thermally resistant. Aslanova found that the more acute strength reduction of the fibres correlated with a higher rate of crystallisation, implying that crystallisation leads to strength loss [79]. Crystalline structures have been observed through SEM imaging of the fibres [79, 83], and it is suggested that this crystallisation process leads to the formation of superficial cracks, which is the key reason for fibres losing their strength [83].

Research into the strength loss of thermally treated E-glass fibres was carried out many decades ago [53, 84, 85]; these studies showed that strength loss became more severe with increasing temperature. More recently Feih et al. [7, 24] replicated this work using sized fibres and observed a dependence of strength loss on the treatment temperature and time. From fracture surface analysis of the fibres the authors suggested that the strength loss was due to defects on the surface as opposed to internal damage; in addition, the mechanism of surface flaw growth was assumed to involve the interaction of the fibre surface with water during the heat treatment [7, 24]. Feih et al. [51] also employed focussed ion beam (FIB) milling to artificially create nano-sized cracks in the fibre surface (example given in Figure 3.5). They discovered that the strength loss and other fracture parameters for nano-notched and thermally treated fibres were the same, concluding that the development of surface flaws is the main cause of strength degradation of glass fibres after thermal treatment [51].

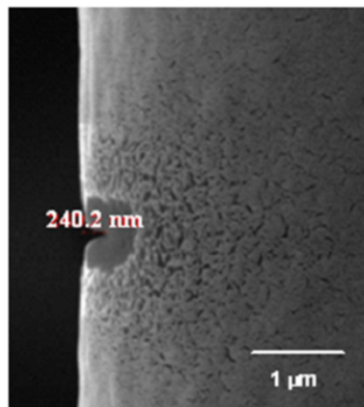


Figure 3.5 – SEM image showing a 240.2 nm deep crack in an E-glass fibre created by FIB milling. Reproduced from [51]

Jenkins [25] detected a possible surface flaw of a heat treated glass fibre when examining its fracture surface with SEM; the predicted flaw depth for this fibre (measured strength 1.2 GPa) was 0.11 μm , close to the measured value shown in Figure 3.6 (0.12 μm).

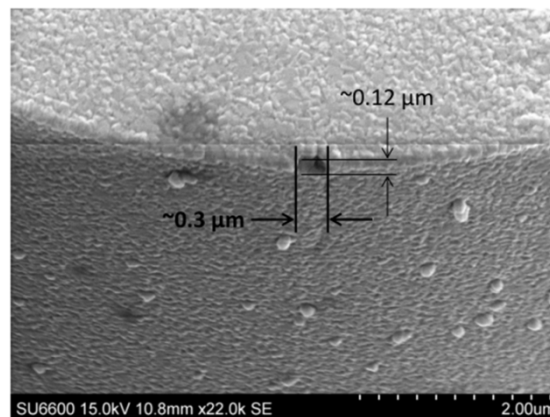


Figure 3.6 – SEM image showing fracture origin of a glass fibre heat treated at 450 °C under vacuum, strength 1.2 GPa. Reproduced from [25]

Jenkins et al. [8] found that in addition to thermal treatment, mechanical damage imposed on glass fibres can also have an effect on strength. Figure 3.7 displays the tensile strength of both sized and bare E-glass fibres after being thermally treated as a bundle and as individual fibres [8].

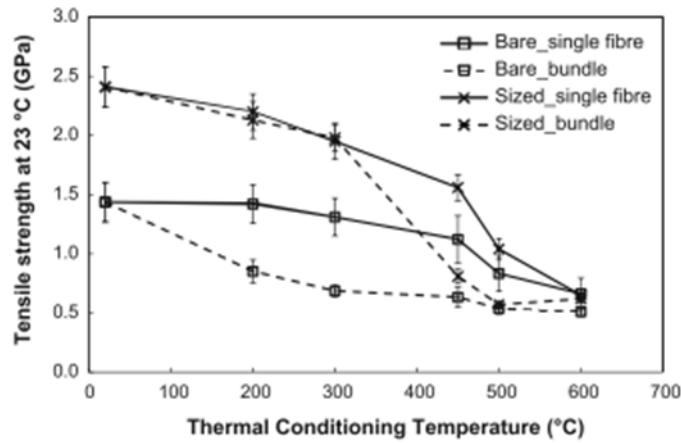


Figure 3.7 - Tensile strength of bare and APS-sized fibres after being thermally treated at 200, 300, 450, 500 and 600 °C for 25 min as bundles and single fibres. Reproduced from [8]

The bare glass fibres are initially weaker than the sized fibre as the sizing protects the fibre surface from physical and chemical damage. The sizing remains an effective barrier until after 300 °C, where there is a precipitous drop in tensile strength of the fibres treated as a bundle. The bare fibres, whether heated as a bundle or individually, exhibit a fairly steady decrease in strength with treatment temperature. Significant strength retention up to 450 °C is observed when sized fibres are treated individually. Fibres can be difficult to separate from bundles after thermal conditioning; the purpose of the single fibre treatment procedure was to remove these mechanical effects. The fact that fibres retain more strength when heated individually implies that mechanical handling can have an adverse effect on fibre strength as well as the thermal conditioning process itself.

3.2.3 Use of chemical treatments to regenerate strength of thermally treated glass fibres

It is assumed that thermal treatment leads to strength loss of glass fibres by the growth of new and pre-existing surface flaws. From reviewing the literature it also seems clear that corrosive treatments, such as alkaline solution, can have a detrimental effect on virgin fibre strength. The mechanism involving the reaction of glass fibre and alkaline solution is thought to involve the etching of the fibre surface. Whilst this proves to have a negative effect on the strength of virgin glass fibres, the influence on thermally treated fibres can potentially differ; it can be hypothesised that the reaction of silica (SiO_2) in the glass fibre with hydroxide ions (OH^-) from the alkaline solution [20] leads to the smoothing of the sharp, severe surface flaws, leading to an increase in the tensile strength of the thermally conditioned fibre.

Other chemical solutions, like HF, exhibit an etching effect on glass fibre. Numerous studies have been conducted in the past regarding the etching of bulk glass by HF [12, 86-91]. The etching of glass by HF is evidenced by SEM imaging, which show the increased roughness of the glass surface [12, 86]. Spierings [12] presents SEM images showing severe surface cracks on the bulk glass, which are then transformed into smooth U-shaped structures with extended HF treatment as indicated in Figure 3.8.

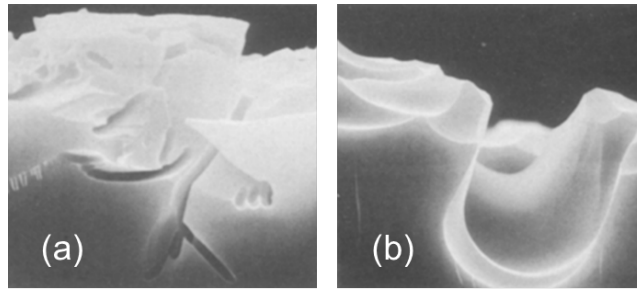


Figure 3.8 – SEM images of the cross-section of a soda lime silicate glass after HF treatment for (a) 2 minutes, showing severe surface cracks, and (b) 30 minutes, showing U-shaped structures. Reproduced from [12]

Spierings commented that etching away surface cracks on glass using a corrosive solution like HF is an effective method to increase its strength [12]. This concept had been demonstrated several decades ago; Sakka [82] and Aslanova [79] found that HF treatment significantly enhanced the strength of thermally conditioned fibres, and they stress how much of an effect the presence of surface defects has on fibre strength. Due to the nanoscale of surface cracks present on glass fibres, they would be challenging to probe before and after chemical treatment for any change in depth or shape; this is an area where work is yet to be done [25].

The research carried out in [79, 82] was recently replicated by Yang et al. [11]. The aim of this study was to develop a treatment that can regenerate enough strength in thermally recycled glass fibres to allow their reprocessing in second-life composite materials. E-glass fibres were heated in a furnace at 450 to 600 °C to mimic thermal recycling conditions, before being treated for a few minutes in dilute HF solution. Figure 3.9 [11] shows the extent of strength recovery achieved in these fibres.

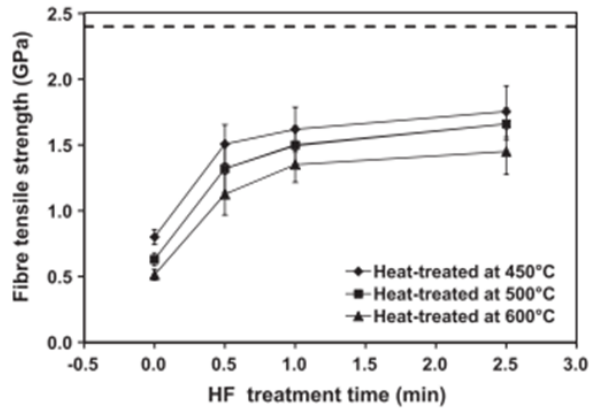


Figure 3.9 – Tensile strength of glass fibres heat treated at 450, 500 and 600 °C, and then treated in 1 vol% HF solution for different times. Reproduced from [11]

Clearly HF treatments can almost triple the strength of glass fibres thermally conditioned even at 600 °C, which is at the upper end of the thermal recycling temperature range. It was also found that the fibre diameter reduction (%) increased as a function of HF treatment time, confirming that HF etches away the glass surface and that this is likely the process by which the fibre strength is improved [11].

Despite the positive impact of HF treatments on the strength of thermally conditioned glass fibres, it is apparent that the extreme toxicity of HF will render it unfeasible for treating fibres on an industrial scale. Silane and hydrochloric acid (HCl) treatments were shown to be ineffective at regenerating fibre strength [92] as they cannot etch away glass like HF. Fortunately hot alkaline solution, which does etch glass, was discovered to be a safer alternative to HF for recovering the strength of thermally conditioned fibres [13, 14, 67]. Saez [13] investigated the efficacy of NaOH treatments in improving the strength of thermally conditioned glass fibre bundles, and Nagel [67] went on to apply this treatment to chopped glass fibres to assess their effect on composite performance. Thomason et al. [14] reports on the

influence of NaOH treatment on the strength of fibres conditioned at different temperatures within the thermal recycling range (450, 500 and 600 °C), as shown in Figure 3.10.

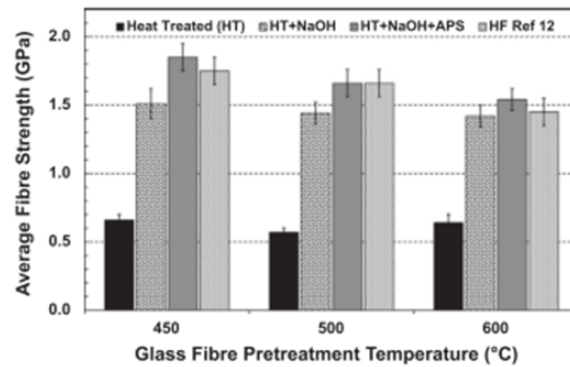


Figure 3.10 – Tensile strength of glass fibres thermally conditioned at 450, 500 and 600 °C, and treated in NaOH, APS and HF solution [11]. Reproduced from [14]

The strength of the fibres is enhanced considerably after NaOH treatment, reaching up to 1.5 GPa with 450 °C thermal conditioning temperature; this is considered to be an important target strength for recycled fibres to reach to allow them to compete with chopped glass fibre products [14]. Although the strength recovery is marginally lower than for HF treated fibres, NaOH solution appears to be an effective and more viable chemical treatment to regenerate fibre strength. Figure 3.10 shows that application of a silane (APS) to the NaOH treated fibres can further increase their strength to above the values presented for fibres treated in HF; this can be due to the silane protecting the fibres during handling after NaOH treatment. In spite of the fact that fibre diameter reduction was not apparent following NaOH treatment, it is widely accepted that alkaline solutions can etch bulk and fibrous glass. Furthermore,

the fact that NaOH solution does not etch glass fibres as much as HF is advantageous as it would lead to reduced material loss during the treatment.

3.2.4 Conclusions of literature review

It is widely accepted that alkaline solution has an adverse effect on the properties of virgin glass fibres. Studies have mainly been carried out using fibres with the sizing removed, as it can have an influence on the mass loss measurements. However, this is not representative of how fibres will be exposed to various chemical environments; in all applications, glass fibres require the application of a sizing. Investigation has been carried out into the alkaline resistance of sized glass fibres; the presence of sizing does suspend the dissolution and hence strength loss of glass fibres, however once this is removed the fibres undergo a considerable decrease in mass and strength like unsized fibres. Reaction of glass fibre with alkali results in the formation of a corrosion layer which begins to retard the mass and strength loss.

The strength loss of glass fibres after thermal treatment can stem from a combination of effects, such as mechanical handling and the chemical composition of the fibre. Although more research needs to be done into the mechanism of strength degradation of these fibres, it is widely accepted that the presence of severe surface cracks is the main cause of strength loss. Taking this into account, along with the fact that certain chemical treatments can etch away the glass fibre surface, it seems that treating thermally conditioned fibres in a corrosive solution is a feasible route to regenerating their strength. Work that has been done in this research area so far is also reviewed in the literature.

HF solution is shown to be an effective chemical solution to regenerate the strength of thermally treated glass fibres; it has been theorised decades earlier that a corrosive agent like HF can improve the strength of glass by smoothing out surface defects. More recently work has been done with developing relatively safer chemical treatments to regenerate strength of thermally conditioned glass fibres. Hot and concentrated NaOH solution can significantly increase the strength of thermally treated fibres, and the strength can be improved further with the application of a silane such as APS. The use of NaOH solution for strengthening thermally conditioned glass fibres is a novel concept, given that it is shown to have a detrimental effect on virgin glass fibre strength. The rest of this chapter will focus on experimental work carried out to further understand the effect of alkaline treatments on thermally treated glass fibres. Other alkaline solutions such as KOH were investigated and the influence of alkali concentration and treatment time on fibre strength recovery was examined. The behaviour of alkaline solution towards bare and APS-sized glass fibres without any thermal treatment (virgin fibres) is also reported.

3.3 Experimental

3.3.1 Materials

Boron-free E-glass fibres supplied by Owens Corning (OC) were used in this study. These OC fibre rovings (one of them shown in Figure 3.11) were manufactured on a pilot scale bushing and received as 20 kg continuous single end square edge packages. Each roving had a nominal tex of 1200 and a nominal fibre diameter of 17 μm . During production, fibres were coated with a 1% volume γ -

aminopropyltriethoxysilane (APS) hydrolysed solution in deionised water. The purpose of this APS sizing is to functionalise and protect the fibre surface.



Figure 3.11 – Image of an OC APS-sized E-glass fibre roving

Unsize (bare) glass fibres were also used in this research study; APS solution was not applied to these fibres and they were water sprayed only. Mechanical properties of these bare and APS-sized glass fibres at room temperature are reported in Figure 3.7 and elsewhere [47]. The chemicals used in this project were purchased from Sigma Aldrich and included NaOH pellets, LiOH powder, KOH flakes (all at commercial grade), and standard 37% concentrated hydrochloric acid (HCl).

3.3.2 Thermal treatment

APS-sized fibre bundles were cut from the roving shown in Figure 3.11 and fixed to a steel rig using a bolt and washer (schematic diagram of the rig is displayed in Figure 3.12) [25].

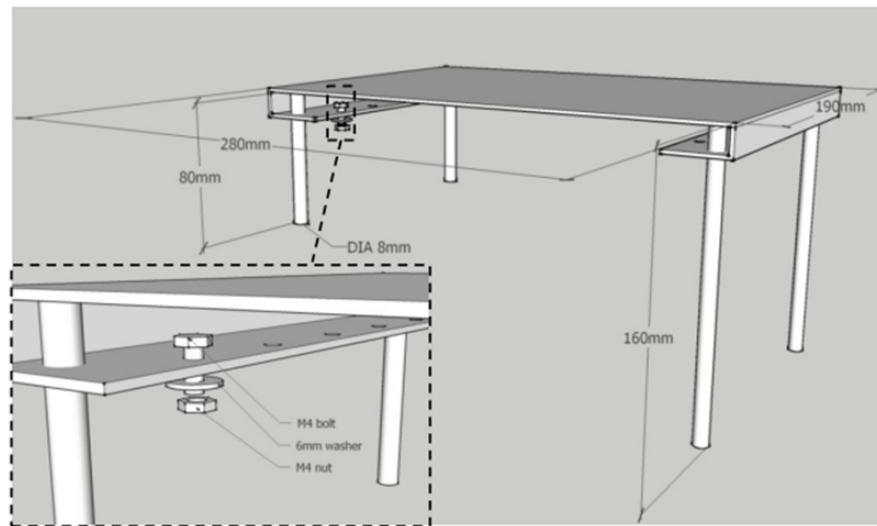


Figure 3.12 – Schematic diagram showing the steel rig used for thermal treatment of glass fibre bundles. Reproduced from [25]

The rig was placed in a Carbolite furnace, which was preheated to 450 °C. The fibres were left for 25 minutes in the furnace to thermally condition under air. In some experiments the thermal treatment temperature was increased to 500, 550 and 600 °C. After the thermal conditioning procedure, the rig was extracted from the furnace and left to cool at room temperature, before fibre bundles were removed and treated in various alkaline solutions.

3.3.3 Alkaline treatment

NaOH, LiOH and KOH solutions were prepared in 500 ml volumetric flasks according to the following molarities: 1.5, 2, 3 and 5 M. The mass of alkali required to make a 500 ml solution at a specific molarity can be calculated from Equation 3.1.

$$\text{Mass (g)} = \text{Molarity} \left(\frac{\text{mol}}{\text{L}} \text{ or } M \right) \times \text{Molecular mass} \left(\frac{\text{g}}{\text{mol}} \right) \times \text{Volume (L)}$$

Equation 3.1

Once the desired mass of alkali was measured and added to the volumetric flask, deionised water was poured in slowly up to the mark. The dissolution of alkali in water is an exothermic process, so heat is given off; because of this, care had to be taken when adding the water to the volumetric flask. A stopper was then placed on top of the flask and inverted a few times to ensure the alkali thoroughly dissolved. The alkaline solution was then transferred to a polypropylene (PP) container, sealed with a lid, and placed in a preheated oven at 95 °C for 2 hours which was sufficient time to heat 500 ml solution to the desired temperature. Fibre bundles were then immersed in the solution for a particular time. The standard treatment duration was 10 minutes, however this was varied in subsequent experiments (at 2, 5, 20, 30 and 120 minutes) to investigate time effect on fibre properties. The container was sealed and remained in the oven over the course of the fibre treatment. Once the treatment was complete, the fibres were removed from the container and rinsed in 10 vol% HCl solution for 10 minutes followed by rinsing with deionised water for 1 minute. The purpose of this rinsing procedure was to ensure the effective removal of residual deposits which developed on the fibre surface as a result of interaction with alkaline solution [21]. In addition, previous experimentation did not show any significant change in mechanical properties of glass fibres after a short period of acid rinsing alone. Once the fibres were rinsed after alkaline treatment, they were dried out in an oven at 110 °C for 15 minutes.

3.3.4 Single fibre tensile testing

Single fibre tensile testing was performed following the standard ASTM C1557-03. After heat and chemical treatment, glass filaments were carefully separated from the bundle and mounted on card tabs with the central window matching the desired gauge length of 20 mm (a schematic of a tensile test card is presented in Figure 3.13).

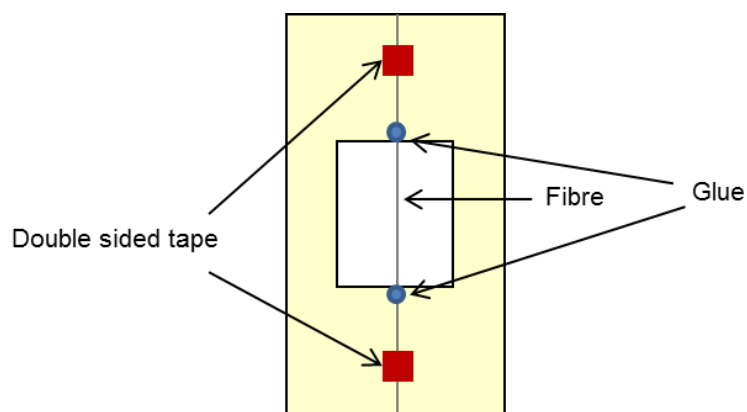


Figure 3.13 – Schematic of a fibre tensile test card

Double sided tape was initially used to position the fibre as vertically as possible on the card, before being secured with superglue. The samples were then left for at least 24 hours to allow the glue to fully set. A total of 30 samples were prepared for each treatment condition.

Before testing the strength of the fibres, their diameters had to be measured with an optical microscope (Leitz Ergolux microscope, image shown in Figure 3.14).



Figure 3.14 – Image of the Leitz Ergolux optical microscope used for measuring fibre diameters before tensile testing

Digital images were captured of each individual fibre at x500 magnification using ToupView software. To measure the diameter, the images were opened in ImageJ (open source image analysis software). Using a calibration scale marker, the diameter of each fibre was measured and recorded in μm . Figure 3.15 shows an image of a fibre being measured for diameter.

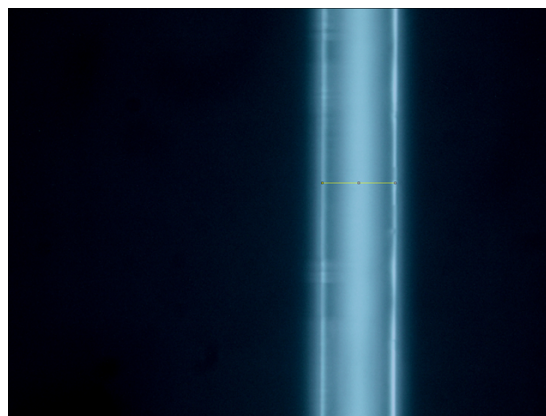


Figure 3.15 – Digital image of a glass fibre captured by the optical microscope, being measured for diameter

Once the diameters were measured of the fibres, they were tested for tensile strength using a Testometric tensile testing machine equipped with a 5 N load cell. A tensile card sample was clamped onto the instrument and a small pair of scissors used to carefully cut the card in half as shown in Figure 3.16.

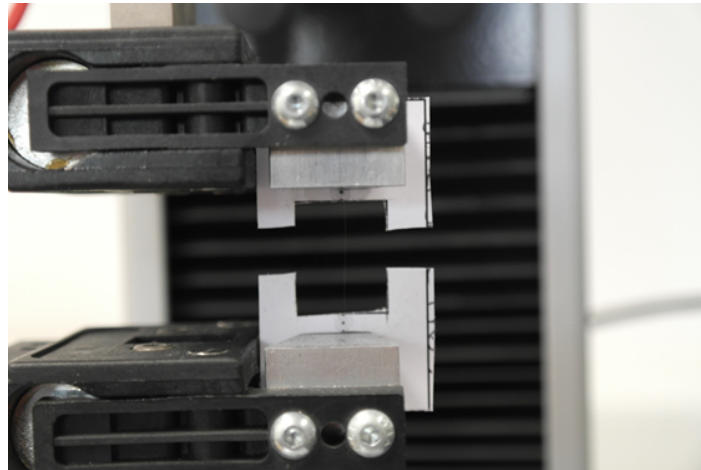


Figure 3.16 – Image of a tensile test card clamped to the Testometric and cut in half before testing

Once inputting the diameter of the fibre into the software (winTest Analysis) the tensile test was commenced. A 1.5% strain rate was applied to the fibre sample (0.3 mm/min) and the force required to break the fibre (load at failure, N) was measured. This was converted to tensile strength (GPa) by the software using the cross-sectional area of the fibre (calculated from diameter) according to Equation 3.2.

$$\sigma = \frac{F}{A}$$

Equation 3.2

where σ is the tensile strength, F the load at failure and A the cross-sectional area of the fibre. The tensile strength was measured of the 30 fibre samples at ambient environment and then averaged to get the average strength for that specific treatment condition. Occasionally fibres would break prematurely (before tensile testing) or break at the glue after the tensile test was completed; these measurements were always discounted from the dataset.

Error bars associated with the strength measurements in this thesis represent 95% confidence limits (C.L.); this was calculated from Equation 3.3.

$$95\% \text{ C.L.} = 1.96 \left(\frac{s}{\sqrt{n}} \right)$$

Equation 3.3

In Equation 3.3, s stands for the standard deviation, and n is the sample size.

3.3.5 Scanning electron microscopy (SEM)

To prepare fibre samples for SEM analysis, a layer of sticky carbon tape was placed on an SEM metal plate. Fibres were then mounted on the tape as vertically as possible as indicated in the schematic in Figure 3.17. In some cases, bundles of fibres were mounted together on the carbon tape.

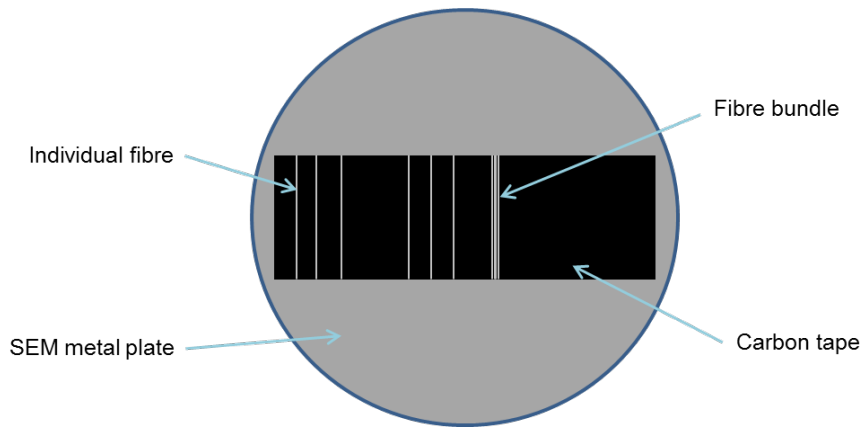


Figure 3.17 – Schematic of an SEM plate with mounted glass fibres

To analyse the fracture surface, fibres were mounted in a way so that the SEM was able to look directly above their cross-sections. This was achieved by placing folded copper tape on the carbon tape of the SEM stud, and mounting fibres in an upright position as shown in Figure 3.18.

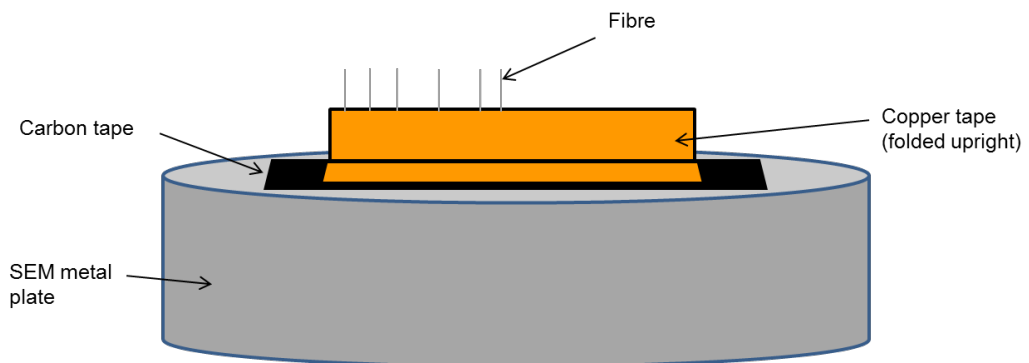


Figure 3.18 – Schematic of an SEM plate with glass fibres mounted upright

As well as mounting fibres in this position, the tilt and rotation functions of the SEM stage were also used to help get a clear view of the fibre cross-section [25]. All the

mounted glass fibre samples were coated in gold using an Edwards S150 sputter coater in order to prevent charge build-up since glass fibres are non-conductive.

A HITACHI SU-6600 field emission scanning electron microscope (FE-SEM) (see Figure 3.19), equipped with an energy dispersive X-ray spectrometer (EDS), was used for surface morphology and compositional analysis of the fibre samples. Images were captured at an accelerating voltage of 15 kV and extraction voltage of 1.8 kV.

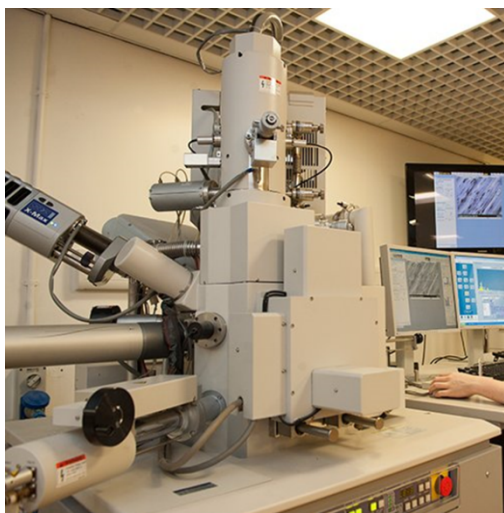


Figure 3.19 – Image of the HITACHI SU-6600 FE-SEM

3.3.6 Atomic force microscopy (AFM)

A Bruker Innova atomic force microscope (see Figure 3.20) was used for analysing the surface roughness of fibres following alkaline treatment.



Figure 3.20 – Image of the Bruker Innova AFM

Tapping mode was used with a visible apex Si tip that had a mean resonance frequency of 70 kHz and a low spring constant (2 N/m) ideal for fibrous samples. AFM images were acquired at 128 x 128 pixel resolution and a low scan rate (0.1 Hz).

For each treatment condition, three individual fibres were selected at random and mounted on a metal plate (see the schematic in Figure 3.21). Two randomly selected areas of each fibre were scanned in a 3 x 3 μm region.

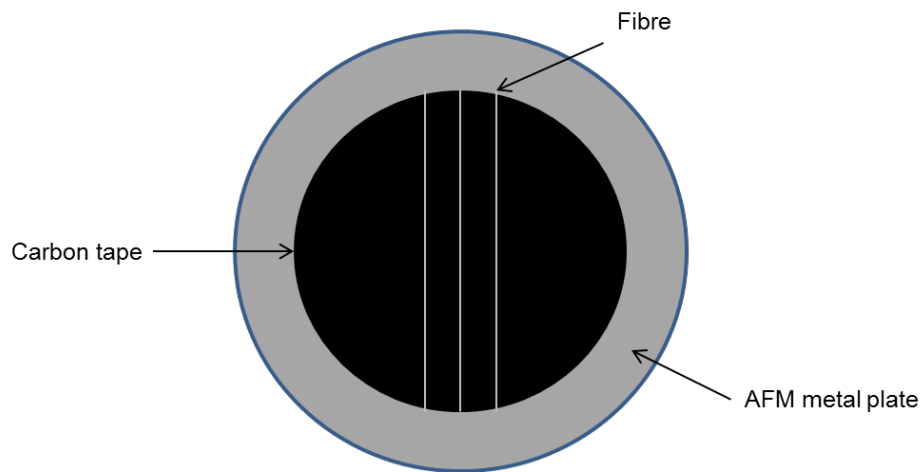


Figure 3.21 – Schematic of an AFM plate with mounted fibres

Height and tapping phase images were flattened to remove curvature by using the ‘Flatten’ function in NanoScope Analysis at 2nd order; an example of this is given in Figure 3.22.

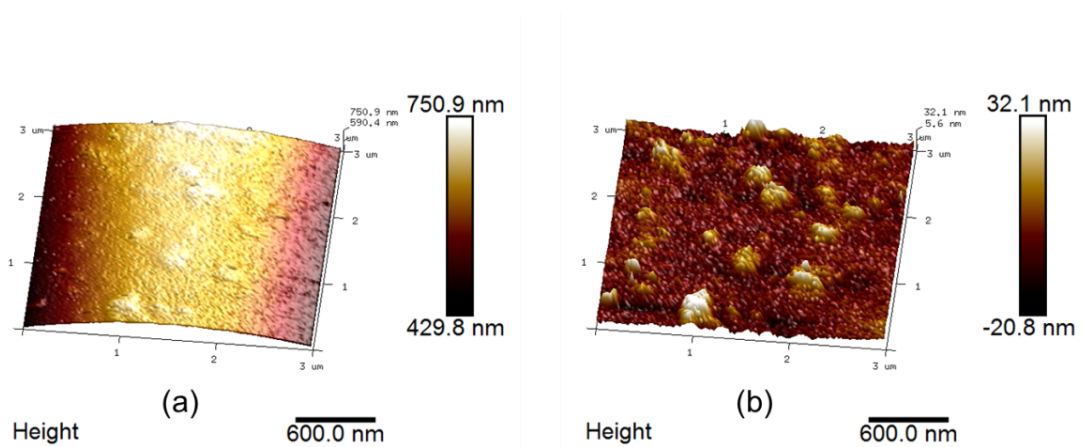


Figure 3.22 – AFM 3-D height image of an NaOH-treated glass fibre (a) before flattening, (b) after flattening, to remove curvature

The roughness of the fibre surfaces was also measured using the NanoScope Analysis software, and plotted in terms of R_q (root mean square roughness, in nm)

as a function of alkaline treatment time. Details of the theory of AFM are given in the Appendix.

3.3.7 Fourier transform infrared spectroscopy (FTIR)





Examination of the observable mid-infrared chemical vibrational modes in the alkali treated fibres was achieved using an Agilent Technologies 4100 FTIR (see Figure 3.23).



Figure 3.23 – Image of the Agilent Technologies 4100 FTIR

This instrument can be used with any one of the following interfaces listed in Table 3.1, depending on the nature of the sample and spectral data required.

Table 3.1 – Interfaces available with the Agilent Technologies 4100 FTIR and their attributes

Interface	Diffuse reflectance (DR)	Specular reflectance (SR)	Grazing angle (GA)	Attenuated total internal reflectance (ATR)
Image				
Typical DOP (depth of penetration)	>200 μm - ~500 μm	~50 – 200 μm	~50 – 200 μm	~2 μm (at 1,000 cm^{-1})
Typical LOD (limit of detection)	~0.01% ~10 – 100 ppm	~0.1 $\mu\text{g}/\text{cm}^2$ (weight/area)	~0.1 $\mu\text{g}/\text{cm}^2$ (weight/area)	~0.5 - 1.0%
Examples of applications	GRP, coatings	Contamination on metals, weathering of coatings	Contamination on metals, weathering of coatings	Coatings, plastics

For analysing the glass fibre bundles, the DR, SR and ATR interfaces were employed. Further information on these interfaces in terms of how the IR beam interacts with the sample and the difference in penetration depth can be found in the Appendix. The DR and SR interfaces allowed collection of spectral data in a preparation-free manner and force-free manner leaving the sample completely intact. With the ATR interface, pressure had to be applied to the sample via a clamp, which resulted in occasional breakage of the fibres as discussed later in this chapter. FTIR spectra were acquired of 128 scans at 8 cm^{-1} resolution resulting in a data collection time of 40 seconds. The bundled glass fibre samples were examined throughout their whole length (as shown in Figure 3.24) and then analysed and averaged per treatment using data processing software (OriginPro).

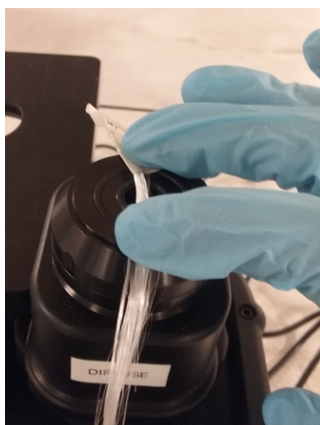


Figure 3.24 – FTIR analysis of a glass fibre bundle using DR interface

Further information concerning the theory of FTIR is presented in the Appendix.

3.3.8 Mass loss and diameter reduction of fibres after alkaline treatment

To understand the etching effect of hot alkaline solution on glass fibre, two separate experiments were conducted; firstly, three heat conditioned glass fibre bundles were treated in 3 M KOH or NaOH for each treatment duration (1, 2, 3 and 5 hours) and thoroughly rinsed in acid and water to remove as much residue as possible. The mass of these bundles was measured before and after alkaline treatment using a microbalance and the loss (%) calculated. The second experiment involved monitoring the same single fibre before and after treatment and measuring the diameter change using an SEM. When sized glass fibres are heat treated, they are difficult to separate as the fibres bond to each other from the cross-linking of the silane. For that reason, unsized glass fibres were used in this experiment, though it was not believed that this had an impact on the results obtained. Each fibre was cut into three portions (1- untreated, 2- treated in 3 M KOH and 3- treated in 3 M NaOH). Portions 2 and 3 were treated in the respective alkaline solution for 1, 2, 3

and 5 hours, rinsed in acid and water, and dried. Five fibres were treated in alkaline solution at each treatment time. Diameters were then measured under the SEM, and by comparing values before and after treatment, the fibre diameter reduction (%) was determined. More information on the single fibre treatment procedure can be found in Chapter 4. The error bars used for mass loss and diameter reduction measurements show the standard deviation.

A separate study on the corrosion of bare and APS-sized glass fibres in alkaline solution was also carried out. Here the mass loss of fibre bundles before and after alkaline treatment was examined, following the same method described in this section.

3.4 Results and discussion

3.4.1 Strength regeneration by alkaline treatment

Figure 3.25 shows tensile test results for heat treated (HT) glass fibres treated with KOH, NaOH, and LiOH solution for 10 minutes in a wide range of molarities.

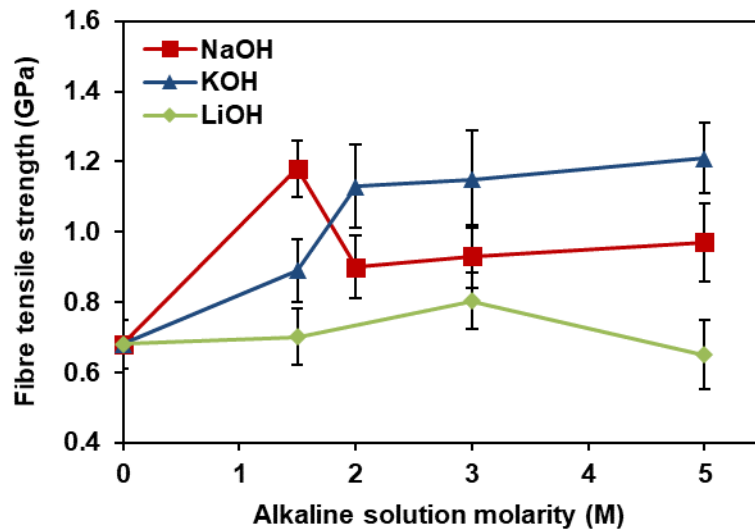


Figure 3.25 - Average strength of fibres thermally conditioned at 450 °C and treated in various concentrations of alkaline solutions for 10 minutes

The average strength of HT fibres is shown to be reduced drastically, from approximately 2.3 GPa (untreated reference value) to as low as 0.68 GPa. Despite the precipitous drop in performance of HT fibres, a significant amount of strength can be restored through a tailored alkaline treatment as shown in Figure 3.25. A major increase in HT fibre strength is observed following immersion in 1.5 M NaOH. As the molarity of NaOH increases, the treatment does not significantly improve the strength of the fibres. KOH enhances fibre strength at 1.5 M, although to a lesser extent than NaOH at the same molarity. Treatment of fibres in KOH from 2 M onwards results in an increase in fibre strength to values similar to what NaOH can achieve at a lower molarity of 1.5 M. LiOH appears to have little effect on HT fibre properties for the molarity range investigated.

Studies show NaOH dissolves glass at a faster rate than any other alkali metal hydroxide, with KOH slightly less reactive and LiOH the least [93]. Assuming these alkaline solutions improve fibre strength through an interaction with the damaged

glass surface, we would assume NaOH to be the most efficient treatment option overall. This is supported by results in Figure 3.25, which indicates NaOH treatment can significantly improve HT fibre strength at a molarity of 1.5 M, whereas for KOH to have a similar effect a more concentrated solution is required. LiOH, NaOH and KOH are considered to be strong bases as they completely dissociate into the metal cations and hydroxide anions in water. Some early studies suggest, however, that LiOH and NaOH do not completely dissociate; the dissociation constant (which indicates how well the base dissociates) was found to vary between 0.5 and 1.2 for LiOH, and 3.1 to 8.1 for NaOH (at 25 °C) [93-95]. The difference in the dissociation constant for these alkalis could be due to the atomic size of the metal cation. Li, Na and K belong to the same group in the periodic table (the group 1 alkali metals) and the atomic size of the element increases down a group. Li, being at the top of group 1, has a smaller atomic size and has a stronger affinity for the OH⁻ in LiOH; this could explain why the dissociation constant was measured to be lower. It is believed that the OH⁻ ions are responsible for the modification of the surface of HT glass fibre; consequently the fewer OH⁻ ions present from LiOH leads to a reduced rate of attack, and therefore a low tensile strength recovery. Conversely, Na and K possess a larger atomic size and are more willing to liberate hydroxide ions. Since K has a greater atomic size than Na, one might assume KOH to be a stronger base; early studies show KOH completely dissociates unlike NaOH [93-95]. However, research conducted by numerous authors [17, 93, 96] show that NaOH is the most corrosive alkali towards glass. The reason for this is seldom explained, though it is suggested it could be due to the reaction products from NaOH and glass being formed more readily and more exothermally [93]. Another possible theory is that the smaller Na⁺ ions have a stronger attraction to OH⁻ ions in solution, which reduces the likelihood of OH⁻ ions to interact with neighbouring water molecules and as a result they will

travel to the glass surface more easily to react [97]. One of the experiments discussed in this chapter involved treating glass fibres in NaOH and KOH and examining their degree of reactivity through mass loss and fibre diameter reduction. What can be accepted is that NaOH and KOH, both being very corrosive alkaline reagents, can restore HT fibre strength to a significant degree through a modification of surface defects. Likewise, poor strength recovery for HT fibres treated in LiOH is attributable to its lower reactivity with glass.

After glass fibres were treated in alkaline solution, they were always rinsed in acid and water to remove residue. To show the effect of rinsing on fibre strength, HT fibres were treated in KOH solution for 10 minutes at different concentrations, but rinsed in hot water instead of acid. Tensile test results are displayed in Figure 3.26.

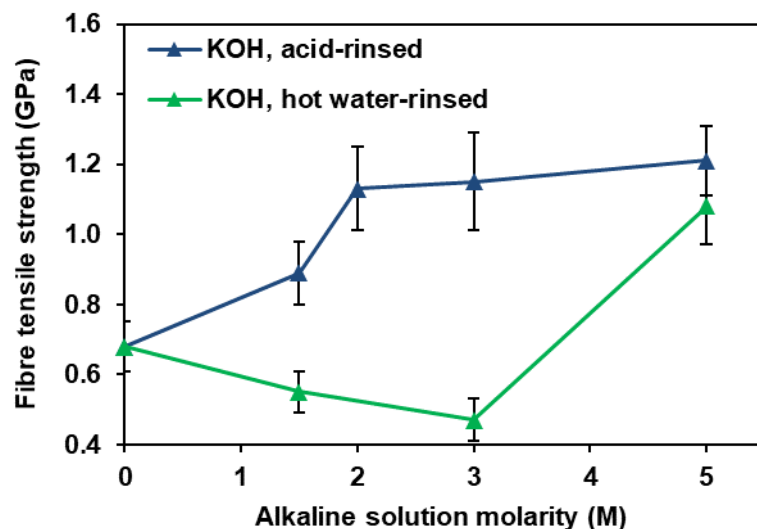


Figure 3.26 - Average strength of fibres thermally conditioned at 450 °C and treated in various concentrations of KOH solution for 10 minutes, either with acid or hot water rinse

It is interesting to observe that at 3 M KOH, where there is a significant increase in HT fibre strength when acid-rinsed, the hot water rinse results in a poor tensile strength of the fibres. At 5 M KOH, the strength of fibres is similar regardless of rinsing method. SEM imaging in Figure 3.27 indicate that the hot water-rinsed fibres generally have more residue on the surface compared to the acid-rinsed fibres.

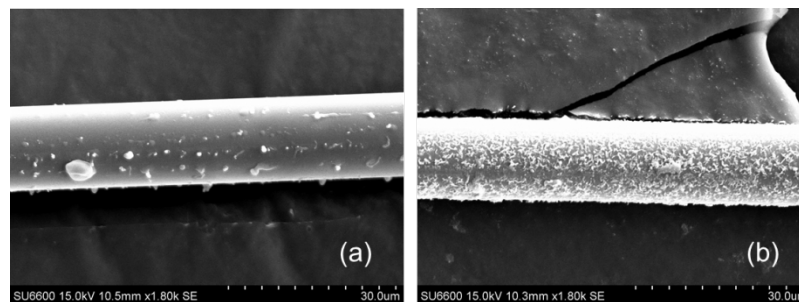


Figure 3.27 – SEM images of glass fibres thermally conditioned at 450 °C and treated in 3 M KOH solution for 10 mins with (a) acid rinse, or (b) hot water rinse

The presence of residue can lead to difficulty in separating fibres for single fibre tensile testing; this might explain why the hot water-rinsed fibres had lower measured strength, and further proves that mechanical handling can have an adverse influence on the strength of fibres. It can also be suggested that the reported strengths for the hot water-rinsed fibres might be higher than the true strength as the difficulty in fibre handling could have resulted in bias towards stronger fibres in the data pool. One might argue that the increased residue on hot water-rinsed fibres might have led to an increased diameter measurement and hence a lower tensile strength. This factor can however be disregarded as care was taken not to incorporate the residual layer in the fibre diameter measurement; moreover, only a grossly overestimated fibre diameter measurement would have

had a significant impact on the tensile strength. Given that treatment of fibres in increased alkaline solution concentration leads to more surface residue, it is unusual to find that 5 M KOH treated fibres rinsed in hot water possess enhanced strength like acid-rinsed fibres; this could be due to the strength recovery finally offsetting the mechanical damage introduced to the fibres during separation. As discussed earlier, the higher tensile strength can also be from bias towards stronger fibres in the dataset.

Although results presented in Figure 3.25 show the positive impact of NaOH and KOH treatments, it is worth bearing in mind that the fibres were HT at 450 °C – the lower end of the thermal recycling range. In a separate study fibres were HT at 500 °C and treated in KOH solution for 10 minutes at various concentrations to see whether any considerable improvement in tensile strength was observed. The tensile test data from this experiment are plotted in Figure 3.28, along with the corresponding results from fibres HT at 450 °C.

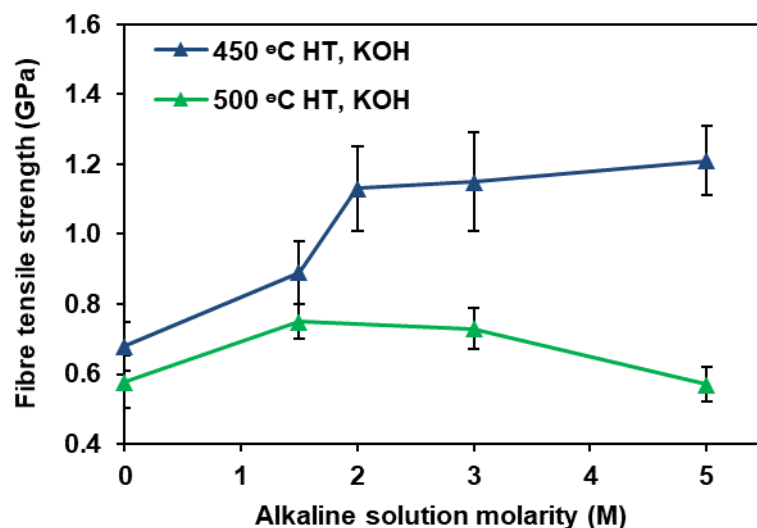


Figure 3.28 – Average strength of fibres thermally conditioned at 450 or 500 °C, and treated in KOH solution for 10 minutes at different concentrations

It is evident that increasing the HT temperature by even 50 °C causes the KOH treatment to be ineffective at improving fibre strength; this is consistent with data reported by Saez [13] where NaOH was employed as the treating solution. Saez also hypothesised that the poorer strength of fibres HT at higher temperatures was due to more significant cross-linking of original silane coupling agent on the fibre surface, and found that washing fibres in hot water before HT facilitated their separation for single fibre testing and led to higher measured fibre strength; furthermore, these fibres exhibited significant strength recovery by NaOH treatment even with higher HT temperatures [13].

Figure 3.29 presents results of an investigation into the effect of prewash on fibre strength. Similar to the procedure outlined in [13], fibres were immersed in 90 °C water for 4 hours, dried, then HT at various temperatures before being treated in alkaline solution. In this study, 5 M KOH treatment was applied to the fibres after HT. The tensile test results are compared with those obtained by Saez using 3 M NaOH (which was found to be the optimal concentration in his study) [13].

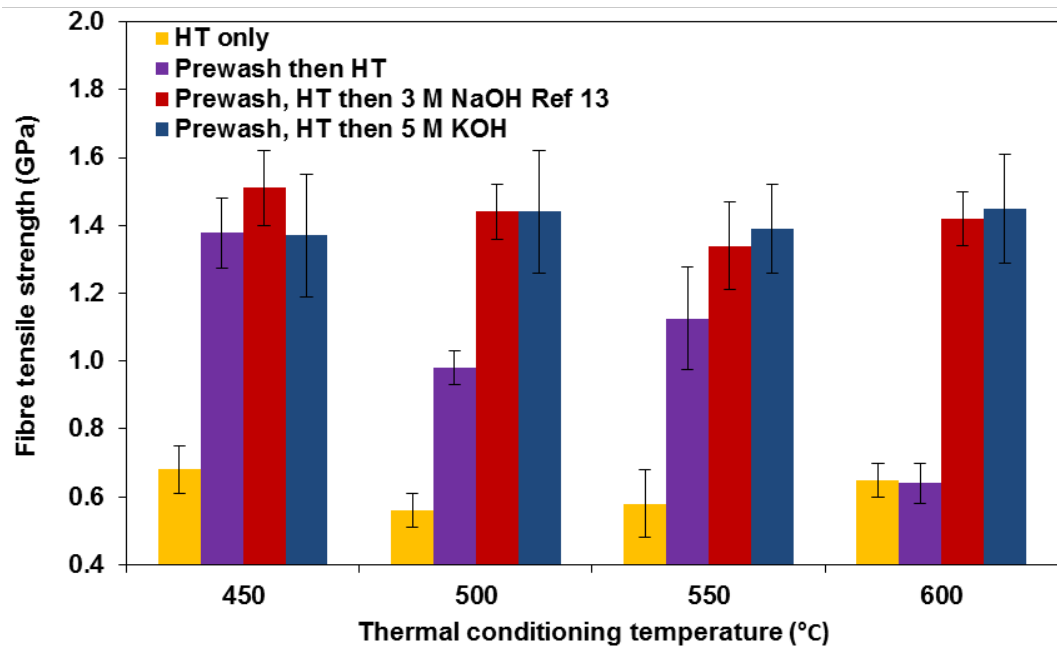


Figure 3.29 – Average strength of fibres prewashed then thermally conditioned at 450, 500, 550 or 600 °C, and treated with either NaOH [13] or KOH

There appears to be a substantial improvement in strength of fibres that were prewashed then HT (apart from 600 °C); this suggests that the prewashing procedure led to increased separation of fibres making them easier to handle during sample preparation thus resulting in higher measured tensile strength. The application of either NaOH or KOH treatment further enhances the strength of the fibres; the strength of alkali-treated fibres is similar with each HT temperature. The fact that prewashing does not affect the strength of fibres after HT at 600 °C but still causes a significant increase with alkaline treatment is interesting; despite this positive impact, the effect of prewashing on fibre strength is unusual and it is unclear whether increased fibre separation is the only cause of strength increase. Though further work in this area can be done, it might not be of any practical use because in reality fibres cannot undergo a prewashing procedure whilst in a composite. Since KOH and NaOH treatments are shown to be successful in regenerating strength of HT 450 °C fibres without prewash (Figure 3.25), it seems worthwhile to continue this

work using 450 °C as the HT temperature, despite it being at the lower end of the thermal recycling temperature range.

Figure 3.30 shows the effect of varying the treatment time of HT 450 °C fibres in KOH solution at different concentrations.

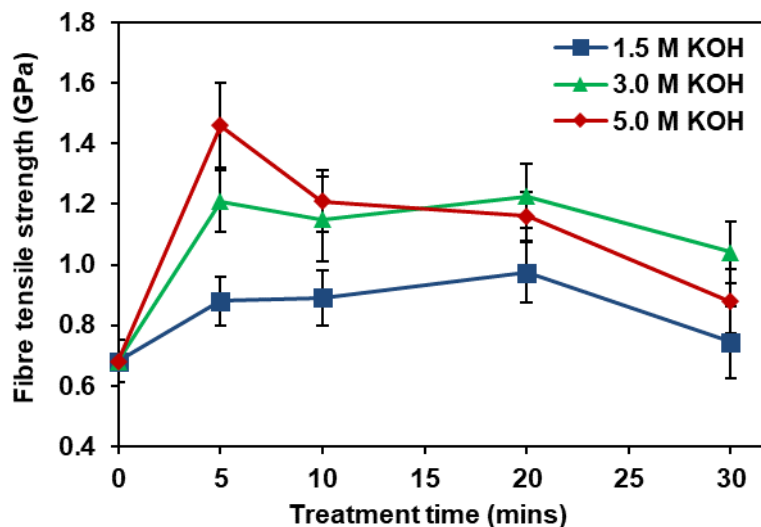


Figure 3.30 – Average strength of fibres thermally conditioned at 450 °C and treated in KOH solution at different concentrations and times

For 1.5 - 5 M KOH, fibre strength increases significantly as the length of treatment time increases up to 5 minutes. The rate of strength regeneration is clearly affected by the concentration of the solution with higher molarity giving higher rate of strength increase. Extended treatment with 1.5 and 3 M KOH after 5 minutes shows little improvement in fibre strength. In fact, prolonged treatment appears to start adversely affecting fibre strength and causes its reduction as indicated by the results after 20 minutes in Figure 3.30. Such behaviour becomes more evident when it comes to 5 M KOH, which shows a sharp increase in fibre strength after a short

period of KOH treatment followed by a more significant reverse effect on strength regeneration at an earlier stage compared to 1.5 M and 3 M.

The results presented in Figure 3.30 can also be interpreted in terms of how the KOH solution molarity affects HT fibre strength at different treatment times as shown in Figure 3.31.

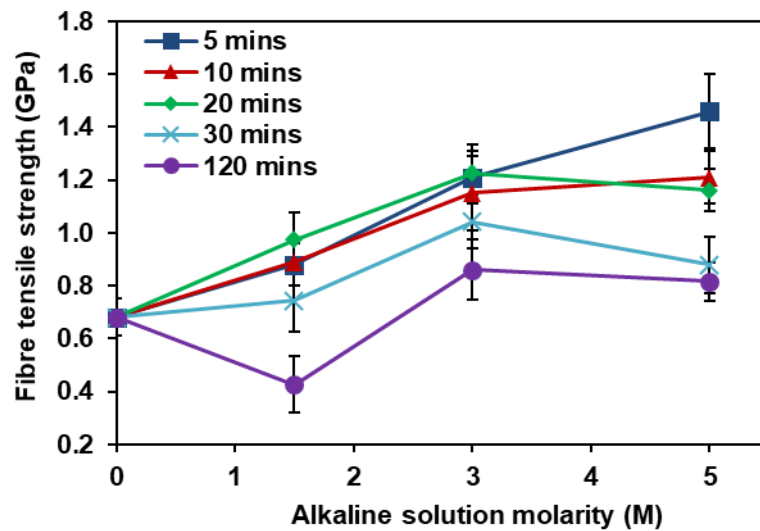


Figure 3.31 - Average strength of fibres thermally conditioned at 450 °C and treated in different KOH solution concentrations, at each treatment time

At the shortest treatment time of 5 minutes, the strength of HT fibres increases as a function of molarity. As the treatment duration becomes longer, the higher concentration of KOH solution does not have as beneficial an effect on strength; at 20 and 30 minutes the strength begins to decrease after 5 M KOH treatment. At the longest treatment time of 120 minutes, the overall strength recovery of HT fibres in KOH solution is poor.

Figure 3.32 shows how variations in treatment time affect HT 450 °C fibres treated in NaOH solution at different concentrations.

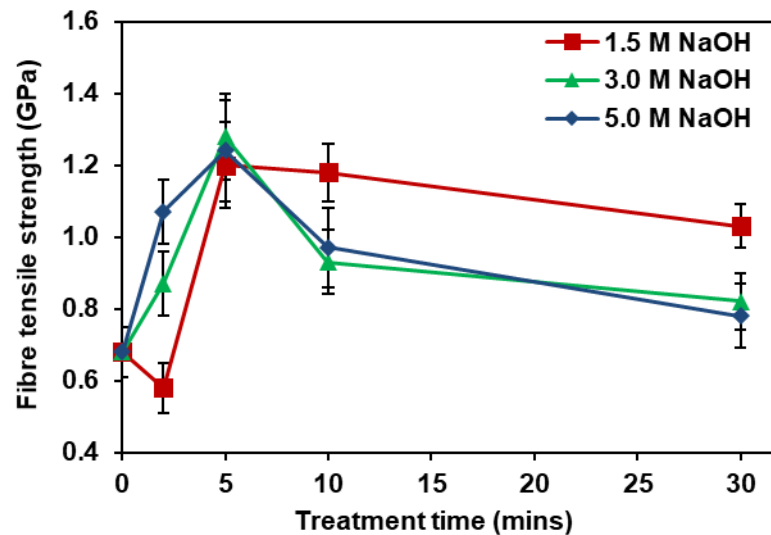


Figure 3.32 - Average strength of fibres thermally conditioned at 450 °C and treated in NaOH solution at different concentrations and times

Figure 3.32 presents overall a similar trend to that in Figure 3.30 for the influence of treatment concentration and time on the strength of HT glass fibres; considerable strength recovery (100% increase) is observed after the first 5 minutes followed by no improvement at low concentration or subsequent strength loss at high concentration. In addition, the strength values presented for all three molarities overlap at 5 minutes; it was initially thought that these data points intersected because the optimum treatment duration of fibres in NaOH had already passed. At a shorter treatment time of 2 minutes we clearly see the strength is molarity dependent; it improves as NaOH solution molarity increases. Despite this observation 5 minutes is yet considered to be overall the optimum treatment

duration regardless of NaOH solution concentration, and HT fibre strength begins to decrease from 10 to 30 minutes.

As with the KOH treatment results, the effect of NaOH molarity on HT fibre strength at each treatment time was also examined as shown in Figure 3.33.

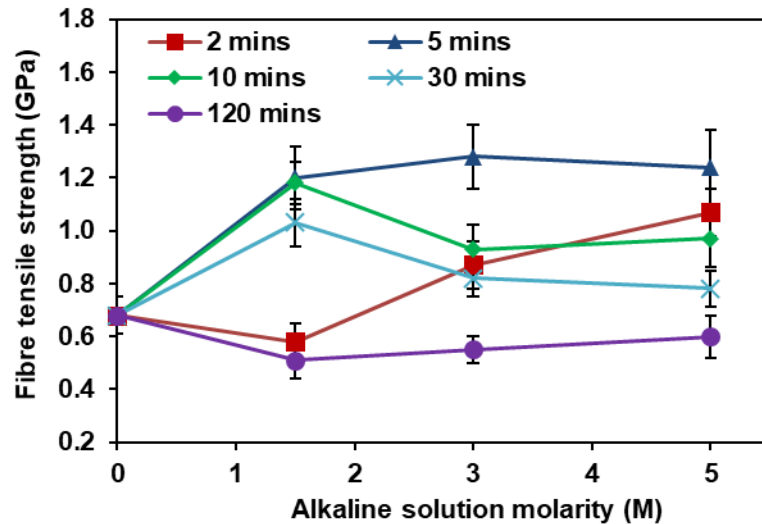


Figure 3.33 - Average strength of fibres thermally conditioned at 450 °C and treated in different NaOH solution concentrations, at each treatment time

An increase in HT fibre strength with NaOH molarity is observed at a short treatment time of 2 minutes. At 5 minutes, the HT fibre strength recovery is similar regardless of NaOH solution molarity. As the treatment time increases, the HT fibre strength begins to decrease after more concentrated NaOH treatments. At the longest duration of 120 minutes, the NaOH treatments have a detrimental effect on HT fibre strength (data was not presented in Figure 3.30 and Figure 3.32 for clarity). The cause of the eventual strength decrease of HT fibres from excessive alkaline treatment is explored later in this chapter.

The results presented in this section clearly demonstrate that both KOH and NaOH treatments can recover a considerable amount of strength in HT (450 °C) fibres. The extent of strength regeneration is determined by the nature of alkaline solution as well as concentration and treatment duration. Other factors such as HT temperature and rinsing method of fibres after alkaline treatment can also impact the strength. The following section focuses specifically on the etching effect of these solutions on glass fibre and whether it can be associated with strength increase.

3.4.2 Etching effect of alkaline solutions on glass fibres

It is generally agreed that the tensile strength of a brittle material such as glass fibre is practically determined by surface flaws of critical size [14]. Therefore, it is reasonable to consider correlating the strength of alkaline treated fibres with flaw geometry through a linear elastic fracture mechanics approach. However, this proves somewhat troublesome since these theoretical defects of submicron scale cannot be readily probed in an experiment. Alternatively, a grossly simplified approach may relate the crack size reduction to glass dissolution caused by the hot alkaline solution. Figure 3.34 presents the average diameters of fibres after treatment in 5 M KOH and NaOH solution for various times, measured by optical microscopy of the tensile test samples.

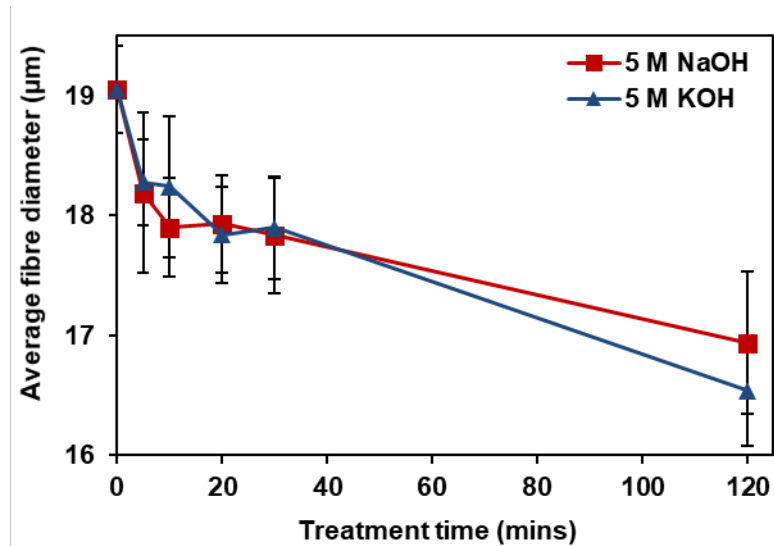


Figure 3.34 – Average diameters of fibres thermally conditioned at 450 °C and treated in 5 M KOH or NaOH for various times, measured by optical microscopy

Figure 3.34 indicates a reduction of a few micrometres in the average diameter of fibres after alkaline treatment up to 2 hours. There appears to be no disparity in etching behaviour of the fibres with KOH and NaOH, which is unusual considering both alkaline solutions affect the fibre strength differently under the same molarity and treatment time. Although Figure 3.34 shows a slight decrease in fibre diameter after alkaline treatment, there is error associated with the use of optical microscopy. Additionally, there is the issue with only 30 fibre diameters being measured for each permutation, and the fact that the same fibres cannot be monitored before and after alkaline treatment.

In spite of the difficulties relating to measuring glass fibre dissolution in alkaline solution, one can foresee that this approach to predicting surface crack size reduction is unlikely to be fruitful as the fracture mechanics model will predict a monotonic increase in fibre strength. Figure 3.25, Figure 3.30 and Figure 3.32 clearly show that there exists an optimal condition for the maximum strength

regeneration, which tends to appear at an early stage of the treatment with both hot concentrated NaOH and KOH solutions. This however should be beneficial from a recycling point of view as the strength of thermally treated glass fibres can be effectively recovered at little expense of removing surface materials.

It has been hypothesised that hot alkaline treatments recover HT fibre strength by smoothing out surface defects; this can translate to a reduced fibre diameter as indicated in Figure 3.34. Even though optical microscopy of the tensile test samples is not an accurate method of measuring fibre diameter reduction as discussed earlier, it appears that alkaline treatment at 5 M for 2 hours can potentially remove over 2 micrometres from the fibre diameter. The cross sectional area of a fibre (which is calculated from the diameter) is inversely related to the strength, meaning fibres with smaller diameters typically possess higher tensile strength. One might argue that the increase of HT fibre strength after alkaline treatment can be due to the reduced diameter from etching. This is unlikely as HT fibres excessively treated in alkaline solution, which should theoretically have smaller diameters, are shown to gradually decrease in strength according to Figure 3.25, Figure 3.30 and Figure 3.32. In addition, a small change in diameter as what is presented in Figure 3.34 should not have a significant impact on the fibre strength. Eliminating the influence of diameter on fibre strength can be possible by analysing only the load at failure, as shown in Figure 3.35.

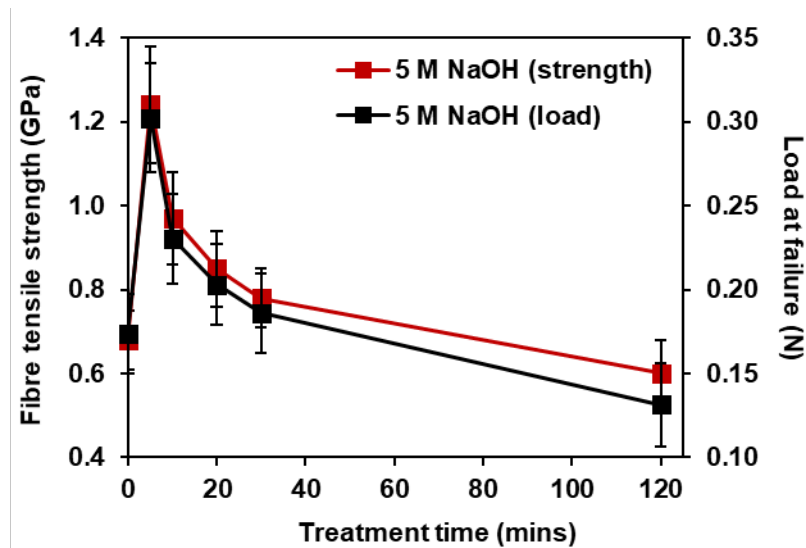
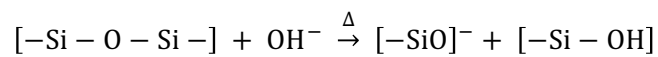


Figure 3.35 – Average strength and load at failure of fibres thermally conditioned at 450 °C and treated in 5 M NaOH for various times

The trend of the load at failure of HT fibres treated in 5 M NaOH at various times matches that of the strength; this proves that any change in diameter of fibres due to the etching effect by alkaline solution does not directly affect the strength. Any improvement in strength of HT fibres with alkaline treatment is likely due to the blunting of surface cracks, and the viability of this theory is surveyed later in the chapter. In addition, the cause of the subsequent decline in HT fibre strength with prolonged alkaline treatment will also be evaluated.

Even though measuring the dissolution behaviour of HT fibres in alkaline solution will not be beneficial in terms of predicting the degree of crack size reduction, it can still reveal useful information on the effects of reaction parameters such as nature of alkali and treatment time. The rest of this section presents results on the etching effect of glass fibres by alkaline solution using a more accurate approach than simply measuring the diameter of tensile test samples via an optical microscope.

SiO₂ is the major component in virtually all types of glass fibre, with a small percentage of various metal oxides such as Al₂O₃, CaO and MgO included. For simplicity silica glass can be referred to as SiO₂, but in reality the SiO₂ exists as a complex network. In addition, Al₂O₃, classed as an intermediate oxide, can function both as a network former or modifier in the glass. CaO and MgO are included in glass as network modifiers only; unlike Al₂O₃ they cannot form part of the network structure with SiO₂. When glass is in contact with hot, concentrated alkaline solution, the hydroxyl ions attack the SiO₂ framework [20-22] according to Equation 3.4:



Equation 3.4

E-glass fibre is composed mainly of SiO₂; it is therefore believed the breakdown of the silicate network in Equation 3.4 is the key process in the dissolution of E-glass fibre by alkaline solutions. Al₂O₃, which is present in small quantities in E-glass fibre, can react with OH⁻ from NaOH or KOH solution in a similar fashion to SiO₂. Due to their basic nature, CaO and MgO may not react directly with KOH or NaOH but they are soluble in the alkaline solution, resulting in further disruption of the glass network structure. All the above mentioned processes should occur in theory, though an EDS analysis of the residue can provide further insight into how alkaline solution interacts with E-glass fibre. The reaction of alkaline solution with glass fibre components establishes the theoretical basis for the etching process, and the results displayed in this sub-chapter validate the concept of alkaline solutions exhibiting an etching effect on E-glass fibre.

A mass loss study of fibre bundles was performed following treatment in NaOH and KOH at 3 M concentration. Extensive treatment durations were selected in order to observe clearly the etching effect of glass fibres, and it is believed that all the fibres in the bundle were in contact with the solution during the treatment. Figure 3.36 gives the mass loss (%) of HT fibre bundles after treatment in alkaline solution for various times (1, 2, 3 and 5 hours).

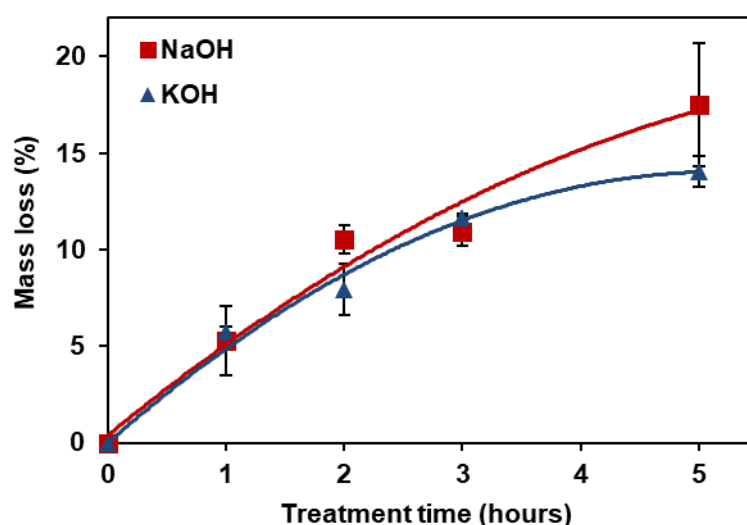


Figure 3.36 - Mass loss (%) of glass fibre bundles thermally conditioned at 450 °C and treated in 3 M NaOH and KOH solution at different times

The fibre mass loss (%) increases after NaOH and KOH treatment, suggesting both alkaline solutions can dissolve the glass fibres. However, it appears the rate of mass loss of glass fibres decreases with treatment time. The data obtained from both treatments can be fitted by a logarithmic function. The decay of glass conversion rate can be attributed to a combination of precipitation of an incrustation of hydrated silicates and zeolites and local contamination of alkaline solution during a static treatment [98-100].

SEM images presented in Figure 3.37 and Figure 3.38 show the gradual build-up of residue on glass fibres after KOH and NaOH treatment respectively.

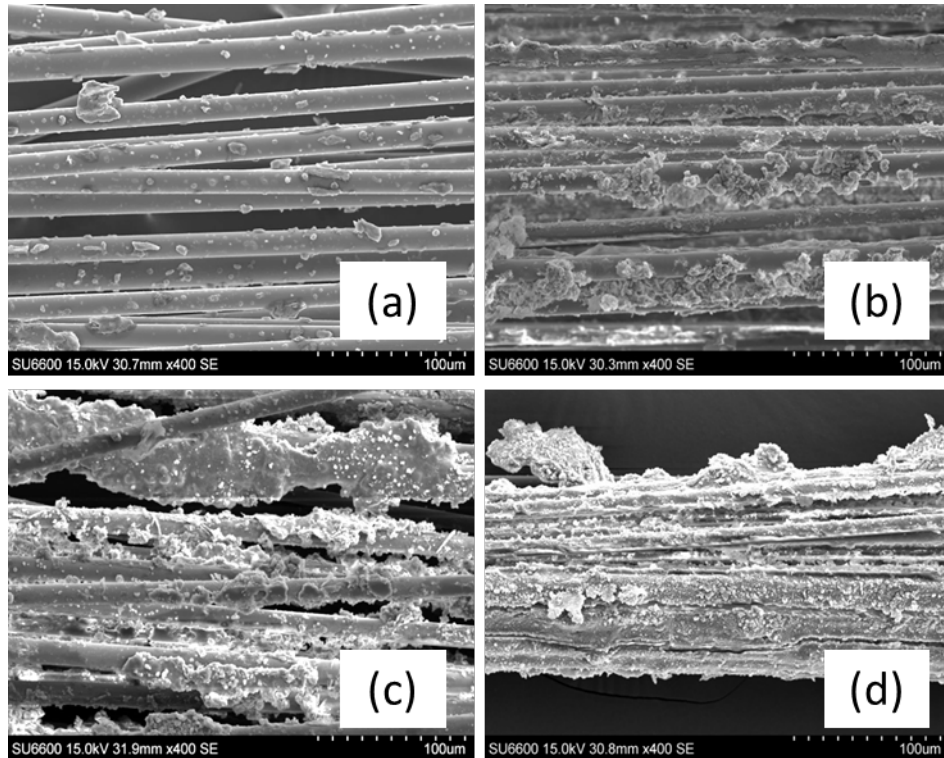


Figure 3.37 - SEM images of glass fibre bundles thermally conditioned at 450 °C and treated in 3 M KOH solution at (a) 0.5 hours, (b) 1 hour, (c) 2 hours and (d) 5 hours, without rinsing

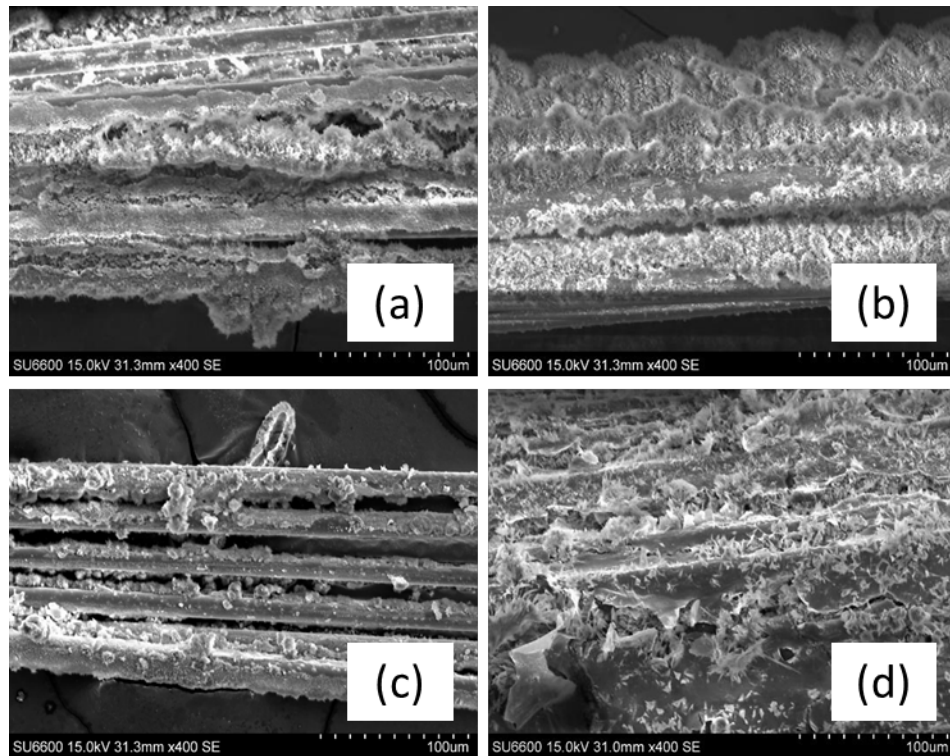


Figure 3.38 - SEM images of glass fibre bundles thermally conditioned at 450 °C and treated in 3 M NaOH solution at (a) 0.5 hours, (b) 1 hour, (c) 2 hours and (d) 5 hours, without rinsing

It is noticed from Figure 3.37 and Figure 3.38 that precipitation of reaction products on the glass surface tends to be more severe after NaOH treatment compared to KOH treatment under the same condition. Despite this observation, the mass loss of the fibres treated in KOH and NaOH solution was fairly similar over the course of the treatment as indicated in Figure 3.36. At 5 hours, however, it becomes clear that NaOH is more corrosive than KOH towards the glass fibres. The acid rinse might not have removed the NaOH-based residual deposits as effectively, which could explain why the measured mass loss was not as high as that shown for KOH-treated fibres. The results at 5 hours in Figure 3.36 and the SEM images shown in Figure 3.37 and Figure 3.38 suggest that NaOH is more corrosive to glass fibre than KOH and this agrees well with the studies of silicate bulk glass in [17, 93].

As mentioned above, the glass dissolution process can be retarded by precipitation of reaction products and local contamination of alkaline solution. Such an effect is likely to be more significant with NaOH than KOH as illustrated in Figure 3.37 and Figure 3.38. Consequently, it obscures fundamental understanding of reactivity of NaOH and KOH with glass fibre. In order to minimise this self-damping factor, individual glass fibres, rather than the fibre strands, were treated with the hot alkaline solutions. Figure 3.39 shows the diameter reduction (%) of individual unsized fibres treated in NaOH and KOH solution and corresponding mass loss calculated from the diameter reduction based on SEM measurement.

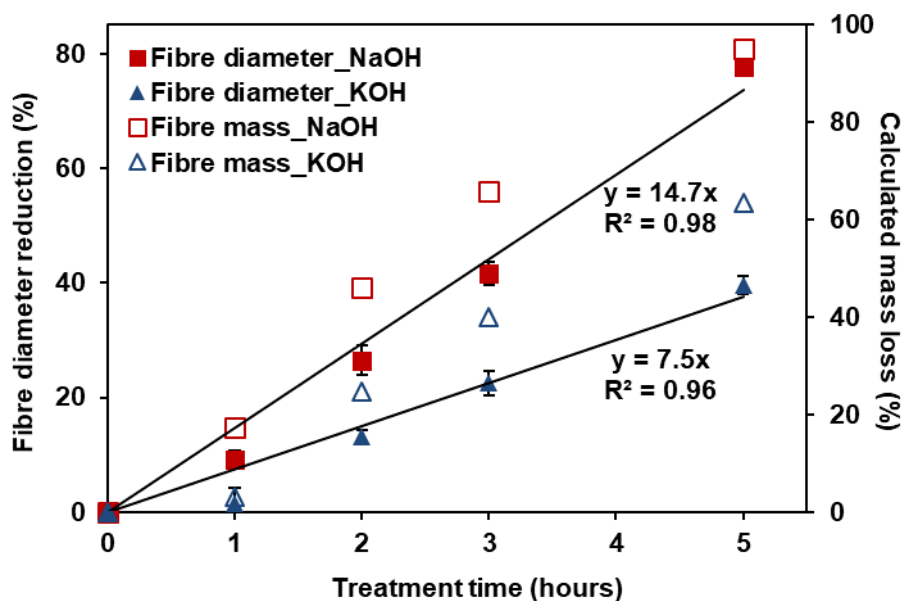


Figure 3.39 - Fibre diameter reduction (%) and calculated mass loss (%) of single glass fibre after treatment in 3 M NaOH and KOH solution at different times

It can be found that without the damping factor glass dissolution apparently proceeds in a linear fashion and at a higher conversion rate compared to the

dissolution behaviour observed in Figure 3.36. This behaviour sustains until fibres are almost fully dissolved as in the case of the fibres treated with NaOH. Furthermore, the results in Figure 3.39 clearly indicate that the hot concentrated NaOH solution is much more reactive with E-glass fibre than KOH and gives rise to nearly twice as much of glass dissolution as that caused by the KOH solution. The results from Figure 3.39 also prove that the method of alkaline treatment to single fibres is a more accurate and effective way of analysing reaction kinetics. A detailed investigation into the kinetics of dissolution of glass fibres in hot alkaline solutions is reported in Chapter 4.

3.4.3 Elemental analysis of alkali treated fibres

Figure 3.37 and Figure 3.38 clearly show the amount of residue that can build up on the HT fibre surface after alkaline treatment. Although acid rinsing can help remove these residual deposits as seen in Figure 3.27, some can still remain on the surface, potentially leading to poor bonding with the polymer matrix if these fibres were to be reprocessed into a composite.

The products formed between HT E-glass fibre and alkaline solution was examined with the objective of developing a more effective rinsing method. The investigation of the nature of these products and the enhancement of the rinsing procedure to remove these materials will improve the bonding of alkali treated fibres to the polymer matrix in the composite. In this experiment HT fibre bundles were treated in 3 M NaOH/KOH solution for extended periods of time (0.5, 1, 2 and 5 hours) and dried without rinsing. An EDS analysis was conducted of the residue to investigate its composition. The results are compared to that of fibres HT at 450 °C alone, referred to as untreated. Taking into account the accelerating voltage (15 kV), the

EDS penetration depth was around 1 μm . So, it is worth bearing in mind that although the residue was analysed through EDS, there was a possibility of some fibres underneath to contribute to the elemental composition. Nevertheless, in the following discussion the compositional analysis is denoted as being of the residue only, except for the untreated fibres.

Table 3.2 gives the weight (%) of each element of the residue after increasing treatment time of fibres in 3 M KOH (error values represent 95% confidence limits).

Table 3.2 - Weight (%) of each element present in residue on 3 M KOH treated fibres at different times, determined by EDS

Element	O	Na	Mg	Al	Si	K	Ca
untreated	52.2 \pm 1.39	0.5 \pm 0.09	1.6 \pm 0.13	5.9 \pm 0.32	23.9 \pm 2.20	0.1 \pm 0.08	15.3 \pm 1.54
0.5 h	50.2 \pm 4.23	0.6 \pm 0.14	1.3 \pm 0.14	6.6 \pm 1.20	17.5 \pm 1.79	12.7 \pm 4.54	9.5 \pm 0.96
1 h	49.8 \pm 2.74	0.1 \pm 0.11	0.9 \pm 0.29	6.3 \pm 2.43	13.2 \pm 3.95	21.2 \pm 8.09	7.9 \pm 2.76
2 h	42.2 \pm 4.55	0.1 \pm 0.06	0.1 \pm 0.10	5.3 \pm 2.16	2.2 \pm 2.08	48.9 \pm 7.19	0.8 \pm 0.69
5 h	41.4 \pm 4.14	0.4 \pm 0.22	0.7 \pm 0.46	2.0 \pm 0.96	8.3 \pm 4.11	40.5 \pm 9.78	6.2 \pm 2.87

Overall as treatment time in KOH increases, the percentage of Si and Ca becomes less significant, and Al at 5 hours. The concentration of O also decreases, as is the case for Na and Mg (which are naturally present in E-glass fibres in trace amounts). Interestingly, the percentage of K increases with time as the concentration of other elements (apart from O) becomes less substantial. This suggests the residue was composed mainly of KOH that precipitated after the fibres were dried. In fact, at 2 and 5 hours treatment time the amount of KOH in the residue was just over 80%. One might consider that the increasing concentration of KOH with time was due to the increase in thickness of the KOH residual material layer; in other words, less of the actual fibre contributed to the EDS results and more of the residue was analysed.

Table 3.3 gives the composition of different elements in residue on fibres treated in 3 M NaOH at 0.5 – 5 hours.

Table 3.3 - Weight (%) of each element present in residue on 3 M NaOH treated fibres at different times, determined by EDS

Element	O	Na	Mg	Al	Si	K	Ca
untreated	52.2 ±1.39	0.5 ±0.09	1.6 ±0.13	5.9 ±0.32	23.9 ±2.20	0.1 ±0.08	15.3 ±1.54
0.5 h	41.2 ±3.34	45.5 ±11.90	-	1.0 ±0.43	3.9 ±2.71	-	7.9 ±7.49
1 h	39.6 ±0.98	58.1 ±1.08	-	0.6 ±0.11	1.2 ±0.16	0.1 ±0.14	0.3 ±0.27
2 h	41.5 ±1.59	51.3 ±4.75	0.2 ±0.25	1.0 ±0.61	3.7 ±2.29	0.2 ±0.18	2.1 ±0.98
5 h	42.0 ±2.76	29.3 ±9.01	-	24.3 ±8.45	2.1 ±1.45	-	2.1 ±1.54

Overall, the percentage of Mg and K is negligible, and O decreases with treatment time. The concentration of Al, Si and Ca decreases with time, and there is a rapid increase in percentage of Na; already at 0.5 hours there is around 85% NaOH present. This composition remains until 2 hours. Unexpectedly, the percentage of Na decreases and Al increases considerably (around 24%) after 5 hours NaOH treatment; this suggests there was possibly a mixture of NaOH and Al₂O₃ in the residue, or perhaps they reacted to form a complex sodium aluminate. It is also shown through SEM imaging in Figure 3.38 that a thick film covers the fibres after 5 hours of NaOH treatment.

So, KOH treated fibres show a gradual increase in concentration of K as treatment time is extended; however for NaOH treated fibres the percentage of Na increases more abruptly, which is consistent with SEM observations in Figure 3.38 of a rapid residue build-up and higher reaction rate shown in Figure 3.39. It is understood that as soon as glass fibre is immersed in alkaline solution, the OH⁻ ions travel to the glass surface and begin to react with the silicate groups. As these ions move toward

the fibre surface, so does the counter-ion (Na^+ or K^+). Eventually these ions congregate around the glass fibre surface, which explains why, when the fibres were removed from solution and dried without rinsing, there was a substantial amount of residual material that was characterised as being mainly precipitated NaOH/KOH from EDS analysis. It is evident in some cases that the EDS registered an overwhelming concentration of KOH and NaOH, which consequently masked the reaction products. The idea of NaOH residue build-up being more severe than KOH is supported by SEM imaging and EDS analysis. This reinforces the observation that NaOH is a more effective E-glass fibre etchant than KOH.

3.4.4 Surface roughness and phase imaging of alkali treated fibres

SEM imaging, EDS analysis and mass loss/diameter reduction measurements indicate that NaOH is more reactive with E-glass fibre than KOH. Here, HT glass fibres were treated in 3 M NaOH and KOH solution and analysed with an AFM for further surface topographic examination.

It was discovered that large amounts of residue on fibres can lead to contamination of the AFM tip and consequently a poor image resolution. From SEM images, it is clear the amount of residue present is significant and would have resulted in difficulty in noticing both the residue phase and the glass phase through phase imaging using an AFM. In tapping mode AFM is able to differentiate between various materials according to their adhesion force and viscoelastic property, and these variances give rise to phase shifts marked by different colours in the phase image. It is worth bearing in mind that if two materials have the same viscoelastic behaviour then there would be no phase difference, and conversely if exactly the

same material is present in different forms (such as amorphous and crystalline) these regions would appear as different phases.

In order to prevent debris pick-up by the tip of the AFM probe and allow both the glass and residue phase to be visible, fibres treated in alkaline solution for a short period of time (5 – 30 minutes) were rinsed in acid before they were examined using AFM. Figure 3.40 shows the height and tapping phase images of untreated glass fibre and after treatment in 3 M KOH solution at 5, 10, 20 and 30 minutes.

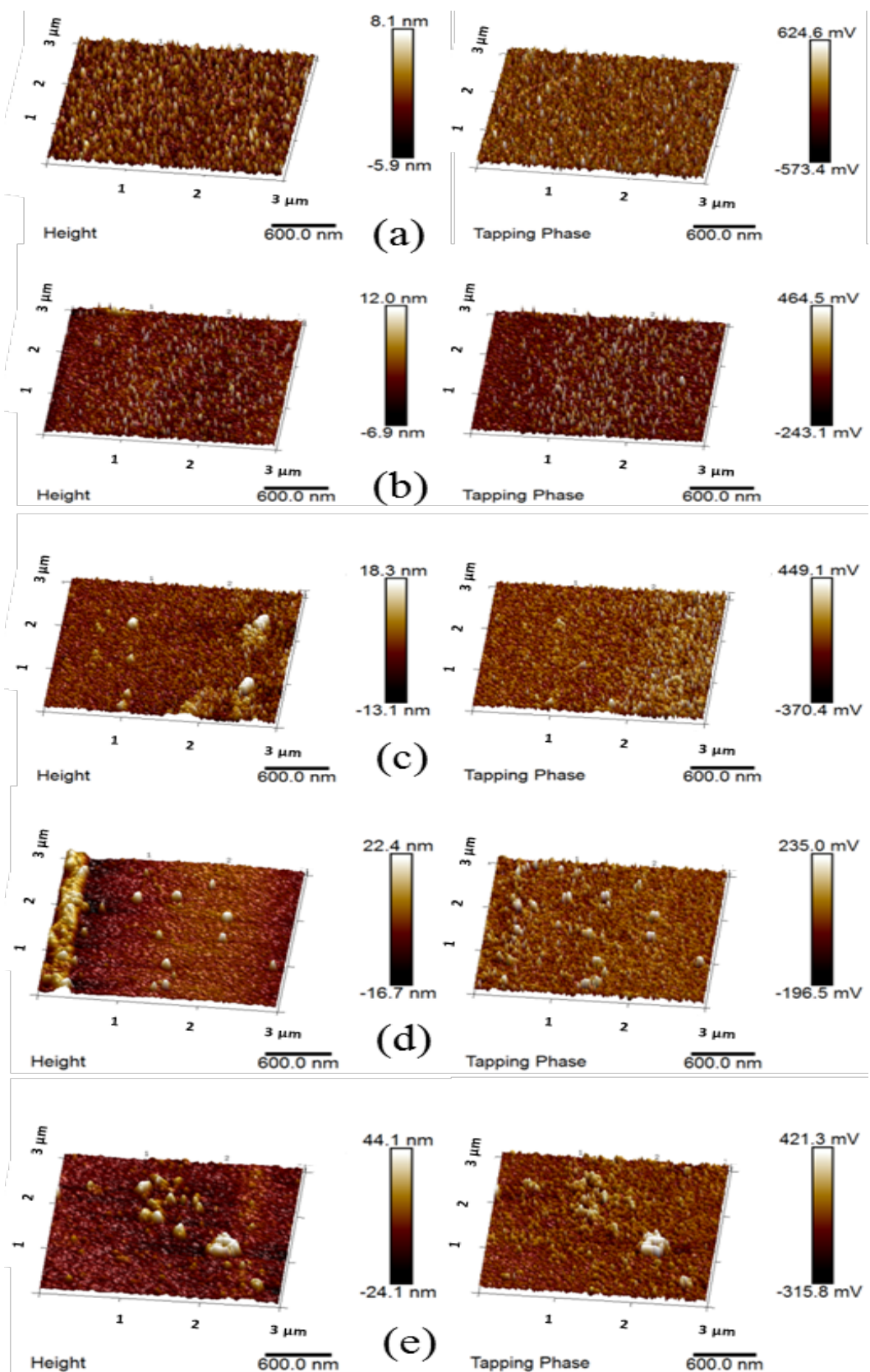


Figure 3.40 - AFM height and tapping phase images of (a) untreated fibre, and fibre treated in 3 M KOH solution for (b) 5 minutes, (c) 10 minutes, (d) 20 minutes and (e) 30 minutes

It is clear that untreated fibres possess a fairly smooth surface as indicated by the 3-D height image. The corresponding phase image shows very little change in terms of phase shifts, suggesting the bulk of the sample was composed of the same material; any regions that may have been indicative of a different material being present on the glass surface was likely as a result of contamination. After treatment of fibres for 5 minutes in KOH solution, numerous spikes begin to appear in the height image that also appear as phase shifts, indicating they belong to a different material from the bulk glass; in other words, they are present as a result of interaction between the fibre and the alkaline solution. These residual spots appear to eventually coalesce and become a common feature on the fibre surface up to 30 minutes. There are occasions where these elevated regions do not translate to phase shifts, implying that the topography of the glass itself was being affected by etching from the alkaline solution.

Figure 3.41 shows both the height and phase images of fibres untreated and after 3 M NaOH treatment from 5 to 30 minutes.

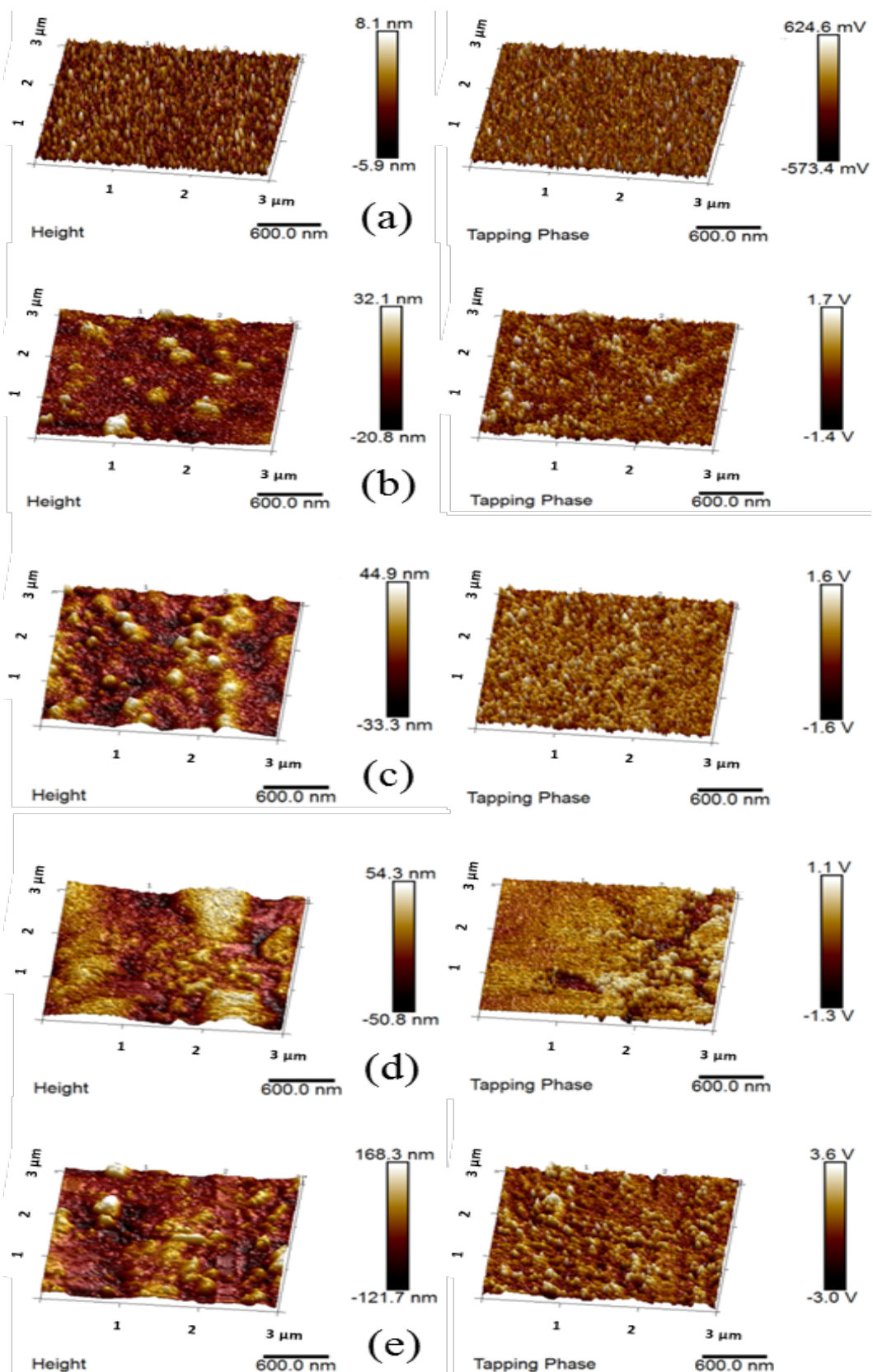


Figure 3.41 - AFM height and tapping phase images of (a) untreated fibre, and fibre treated in 3 M NaOH solution for (b) 5 minutes, (c) 10 minutes, (d) 20 minutes and (e) 30 minutes

There is a substantial amount of elevated spots in the height images already at 5 minutes, which continues to build up with time. It is interesting to find changes in height do not necessarily emerge as changes in material phase; this could be due to the glass surface itself becoming rough after being etched by NaOH. Nevertheless, phase shifts do appear commonly, particularly with longer NaOH treatment times. It could be assumed that both the presence of residue and the changes in glass surface topography contributed significantly to the overall roughness of the fibre. Both of these features are very pronounced for NaOH treated surfaces, which further supports the notion that NaOH is a more corrosive alkaline reagent than KOH towards E-glass fibre.

Figure 3.42 gives the R_q values (root mean square roughness, in nm) of these fibre samples. The error bars represent 95% confidence limits.

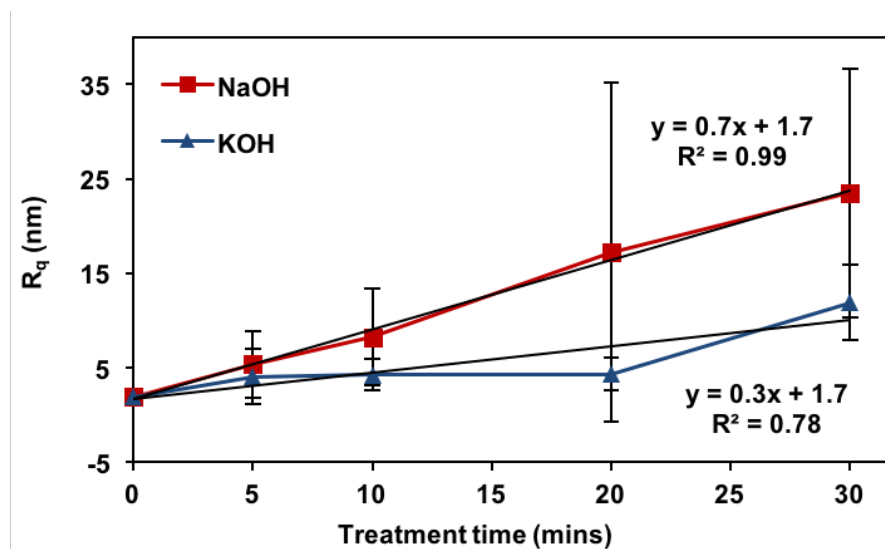


Figure 3.42 - Roughness (R_q) values for untreated fibres and fibres treated in 3 M KOH and NaOH solution at different times

It is evident that the increased presence of residual deposits and topographic changes on the fibre surface leads to greater roughness following alkaline treatment. Although the error bars for both the KOH and NaOH data overlap over the course of the treatment, the R_q values presented for NaOH treated fibres are significantly higher than from fibres treated in KOH, more than twice the magnitude. Also, the increase in roughness of the fibre surface is generally linear with alkaline treatment time, especially for NaOH (though with longer treatment there is greater variation of R_q hence the large error bars). The greater roughness could have been partly due to the increased amount of residual deposits on the fibre surface which appeared for two possible reasons; the acid might have removed Na-based residual deposits less effectively than K-based deposits, and/or there was a more significant build-up of residue after NaOH treatment which could not have been removed by acid very well compared to residue from KOH treatment. It is also understood from phase imaging that changes in glass surface topography from alkaline treatment contribute to roughness, especially with NaOH.

The roughness of the HT fibres after alkaline treatment can also be related to the tensile strength, as shown in Figure 3.43.

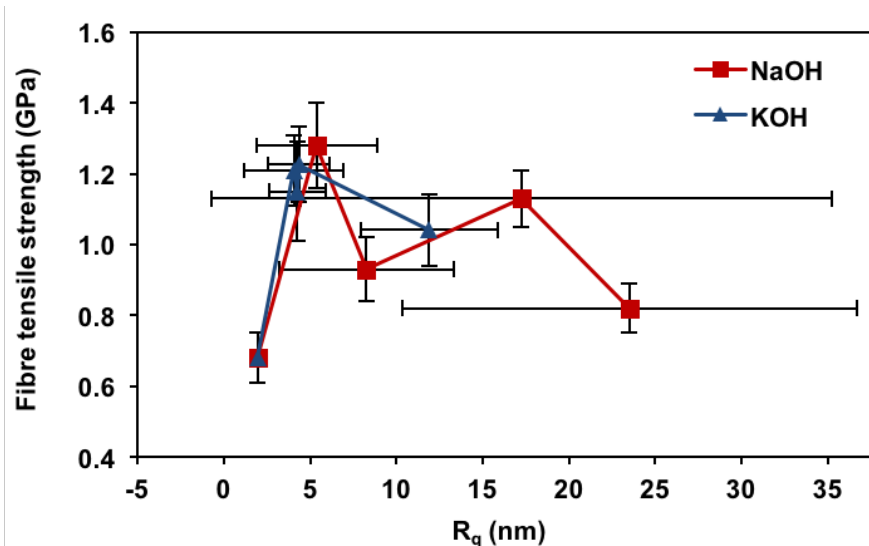


Figure 3.43 – Strength of fibres thermally conditioned at 450 °C and treated in 3 M KOH or NaOH solution at various times, plotted against their surface roughness

It seems that an R_q value of around 5 nm for HT fibres treated in either KOH or NaOH solution correlates to optimum strength recovery. A greater roughness of the fibres relates to declined strength. With KOH treated fibres, the roughness remains at around 5 nm even up to a treatment time of 20 minutes, according to Figure 3.42; this corresponds to consistent fibre strength of approximately 1.2 GPa as shown in Figure 3.43. The R_q then increases considerably to above 10 nm at 30 minutes KOH treatment, which correlates with a lower tensile strength recovery. For NaOH treated fibres, the R_q increases continuously with time, already surpassing 5 nm at 10 minutes; Figure 3.43 shows a relationship between lower fibre strength and increased roughness, particularly above 5 nm. It is assumed that fibre strength regeneration by alkaline treatment is caused by blunting of surface cracks, which theoretically should result in a smoother surface and hence a reduced R_q . The fact that alkali treated fibres show improved tensile strength correlating with rougher fibre surfaces suggests that other factors, such as presence of residue, might have contributed more to the R_q of the fibres than the etching of the glass surface.

It can be concluded that AFM supports previous results from SEM investigations and etching experiments which show NaOH to be more reactive with E-glass than KOH. In addition, the eventual decline of HT fibre strength with prolonged alkaline treatment can be correlated with increased dissolution of the glass, more residual build-up on the fibre surface, and greater roughness. The next section looks deeply into the chemical structure of the glass fibres with FTIR spectroscopy, to establish the cause of this degradation in strength.

3.4.5 FTIR spectroscopic analysis of alkali treated fibres

At the extreme treatment scenarios both NaOH and KOH show a decline in HT fibre strength with time, which is particularly clear from the 5 M KOH and 5 M NaOH data in Figure 3.30 and Figure 3.32 respectively. In an attempt to relate this strength decrease with possible bulk structural change of the glass fibres, an FTIR examination was conducted of the samples. Analysis was carried out using DR, SR and ATR interface.

At this point a possible explanation of the strength decrease of HT fibres after excessive alkaline treatment is as follows: it is believed that similar to HF, NaOH and KOH improved the strength of HT glass fibres by reacting with the surface silicate groups, thereby blunting crack radius and modifying the damaged surface layer. The reduction of surface flaw severity initially improved the fibre strength, but if conditions were too aggressive or long with respect to time, in other words if the alkali was at a high molarity and/or the fibres were immersed in the alkaline solution for an extended period of time, the hydroxide ions would have eventually diffused into the bulk glass structure and cause network breakdown. KOH, being a milder corrosive agent, could have therefore reduced the severity of bulk attack even at

higher molarities and increasing treatment times before it became detrimental to HT fibre properties. NaOH, a more aggressive glass etchant, was optimal at lower molarities and shorter application times; more corrosive alkaline conditions may well have resulted in more extensive glass network damage than KOH.

Figure 3.44 provides a stacked view of the diffuse reflectance spectra of glass fibres as received (APS-sized), after HT, and treatment in 5 M KOH solution for 5 – 120 minutes with rinsing.

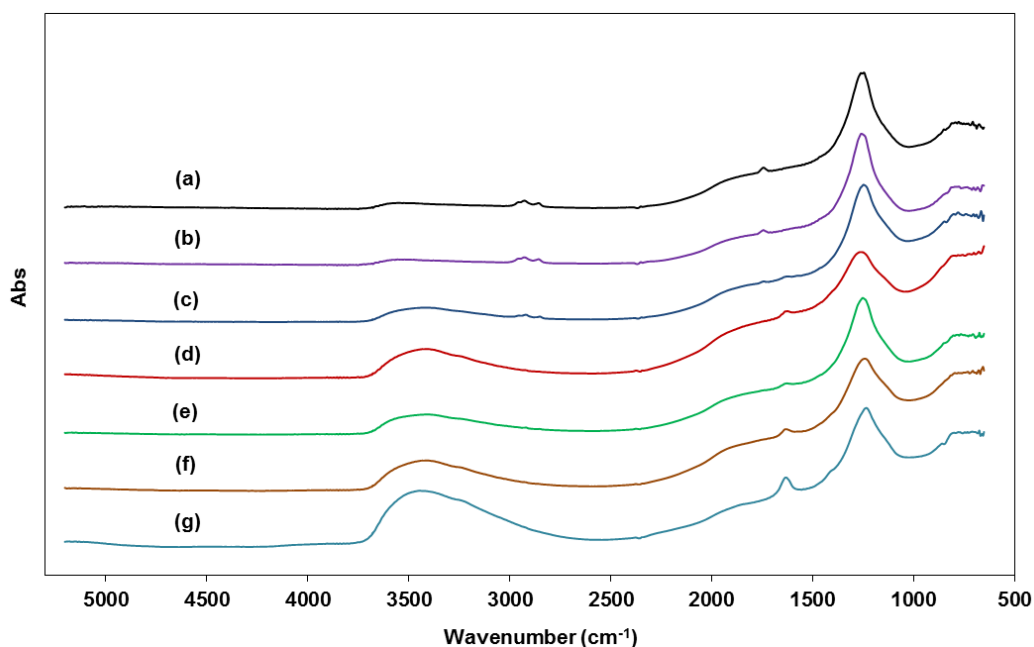


Figure 3.44 - Stacked view of FTIR diffuse reflectance spectra of glass fibres (a) as received, (b) after HT, and then treatment in 5 M KOH solution for (c) 5 minutes, (d) 10 minutes, (e) 20 minutes, (f) 30 minutes and (g) 120 minutes, with rinsing

There seems to be no significant bulk structural change in as received fibres after HT. After KOH treatment, the Si-OH vibration band centred around 3400 cm⁻¹ [101] (which exists as a result of the reaction of the silicate in the glass fibre with OH⁻ from

the alkaline solution) steadily increases with time; the spectral collection was performed on oven dried samples so it was unlikely that residual water from the treatments led to this band. Also present in the spectra is the reduction of the reststrahlen Si-O-Si peak centred at 900 – 1100 cm^{-1} [101]. What appears as a large peak at 1250 cm^{-1} for each spectrum is in fact a point of inflection as a consequence of the reststrahlen effect [102] where features at lower wavenumbers from this point are all negative primarily due to concomitant changes in refractive index with IR absorbance. The initially small peak related to the Si-OH deformation vibrational mode becomes more significant at longer treatment times; this vibrational mode is normally only seen in more open silica structures. The stacking of the spectra enables the visualisation and clarification of peak changes in size or shape changes but also compresses the Y-axis hiding another spectral relationship with the degree and severity of treatment. The raw diffuse reflectance mid-infrared spectral data also displays decrease in reflectivity that is directly related to the degree and extent of the KOH treatment.

Figure 3.45 shows diffuse reflectance spectra of fibres treated in 5 M NaOH solution at 5 – 120 minutes.

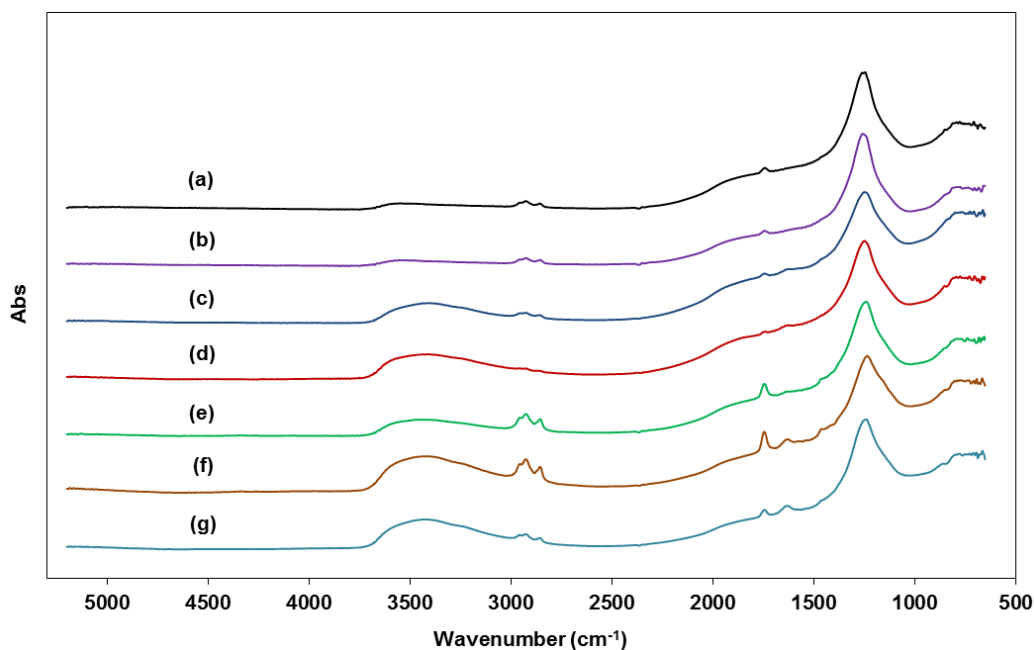


Figure 3.45 - Stacked view of FTIR diffuse reflectance spectra of glass fibres (a) as received, (b) after HT, and then treatment in 5 M NaOH solution for (c) 5 minutes, (d) 10 minutes, (e) 20 minutes, (f) 30 minutes and (g) 120 minutes, with rinsing

The key features described in the spectra for KOH treated fibres again appear here, however one of the key differences is in the appearance of the Si-OH vibration band at various treatment conditions. As expected, there is a gradual increase of this Si-OH band as treatment duration in NaOH lengthens, although the intensity varies with that of KOH treated fibres. For example, after 5 minutes of treatment in NaOH the Si-OH peak is more apparent than in the corresponding spectrum for KOH. On a similar note, the Si-OH signal at 30 minutes NaOH treatment is more intense than for KOH under the same conditions. The observation of the Si-OH band being very strong after 120 minutes of KOH treatment is unusual; however, the OH absorbance could have been due to traces of KOH on the fibres that remained after alkaline treatment and rinsing.

In Figure 3.45 there are additional peaks at around 2900 cm^{-1} (which also appear in Figure 3.44 for a few spectra) that are variable and could be from residual APS [103, 104]. Given that APS should have been removed from the fibres after HT, it was most likely that this absorbance appeared due to organic contaminants on the glass from handling or the atmosphere. Moreover, there is a peak at around 1750 cm^{-1} which is characteristic of a carbonyl (C=O) functional group that is not present in APS [105]. This peak could be as a result of interaction between organic contaminants and alkali to form a halogenated ketone or carboxylic species; Culler et al. [103, 104] observed a range of peaks in their FTIR diffuse reflectance spectra at 1650 to 1300 cm^{-1} corresponding to the bicarbonate salt structure formed between APS and carbon dioxide, and these are absent as is the carbonate absorbance near 2500 cm^{-1} . The carbonyl peaks in our FTIR spectra appear at a high wavenumber of 1750 cm^{-1} which suggests that carboxylic or halogenated ketone groups were present in the fibre samples.

From the FTIR diffuse reflectance spectra it can be shown that immersion of HT E-glass fibres in sub-optimal alkaline solution resulted in the breakdown of the silicate network as indicated by the increase in intensity of the Si-OH bands and the correlated decrease in Si-O-Si peaks. Taking into account the presence of surface flaws in HT fibre, it is believed the alkaline solution initially improved fibre strength by modifying these defects. However, as fibres were treated for a lengthy period, we begin to see clearly from the FTIR diffuse reflectance spectra that the degradation of the glass network became significant and offers a spectral explanation as to why there was an eventual drop in fibre strength. Furthermore, the rapid increase in intensity of the Si-OH band after NaOH treatment is complementary with previous experimentation indicating it is a more corrosive alkali towards E-glass than KOH. The variety and presence of several FTIR markers that correlate to the fibre strength

offers a possible non-destructive method to pre-validate that the optimal conditions have been applied to the recycled and heat treated glass fibres.

The NaOH-treated fibres were also analysed using the SR interface; spectral information is given in Figure 3.46.

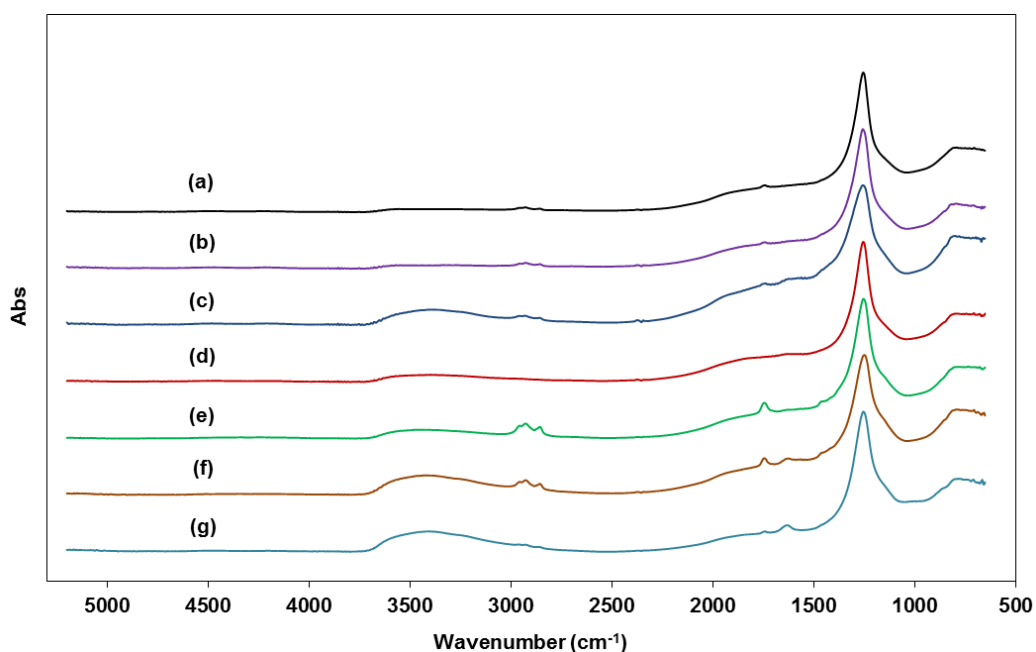


Figure 3.46 - Stacked view of FTIR specular reflectance spectra of glass fibres (a) as received, (b) after HT, and then treatment in 5 M NaOH solution for (c) 5 minutes, (d) 10 minutes, (e) 20 minutes, (f) 30 minutes and (g) 120 minutes, with rinsing

The IR absorbance peaks previously shown for DR spectra again appear here; there is an overall increase in the intensity of the Si-OH band with NaOH treatment time, though there is no clear corresponding decrease in the Si-O-Si absorbance to indicate glass fibre dissolution. Absorbance from residual APS also emerge for some SR spectral data along with C=O peaks at 1750 cm⁻¹ from possible carboxylic species on the fibre. The reststrahlen effect is apparent in the SR data due to the

fact that both SR and DR are reflectance techniques. Overall, the SR data for NaOH treated fibres in Figure 3.46 show a similar pattern to the corresponding DR spectra in Figure 3.45, though the trend in Si-OH and Si-O-Si absorbance with treatment time is not as clear; this could be due to the slightly lower sample penetration depth for SR (penetration depths for all interfaces are listed in Table 3.1).

Lastly, the NaOH treated fibres were examined with the ATR interface; unlike the DR and SR, the analysis involved the application of pressure to the glass fibre sample with a clamp to allow full contact with the diamond ATR crystal, as shown in Figure 3.47.

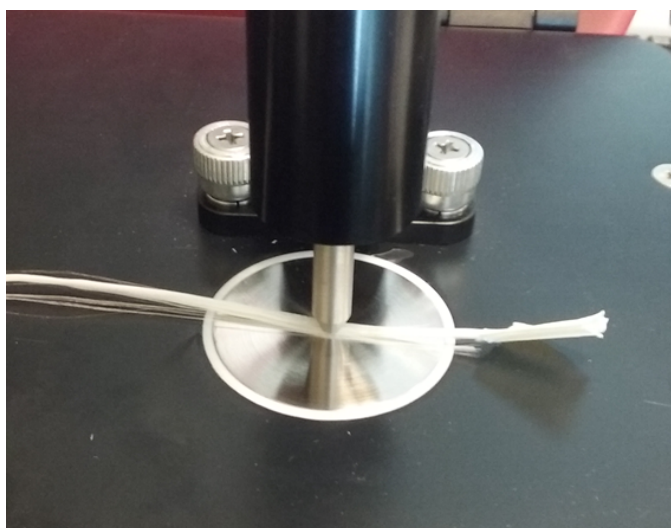


Figure 3.47 – Image of the clamp used to apply pressure to the sample in diamond ATR

Figure 3.48 shows ATR spectra of fibres HT and after treatment in NaOH solution at various times.

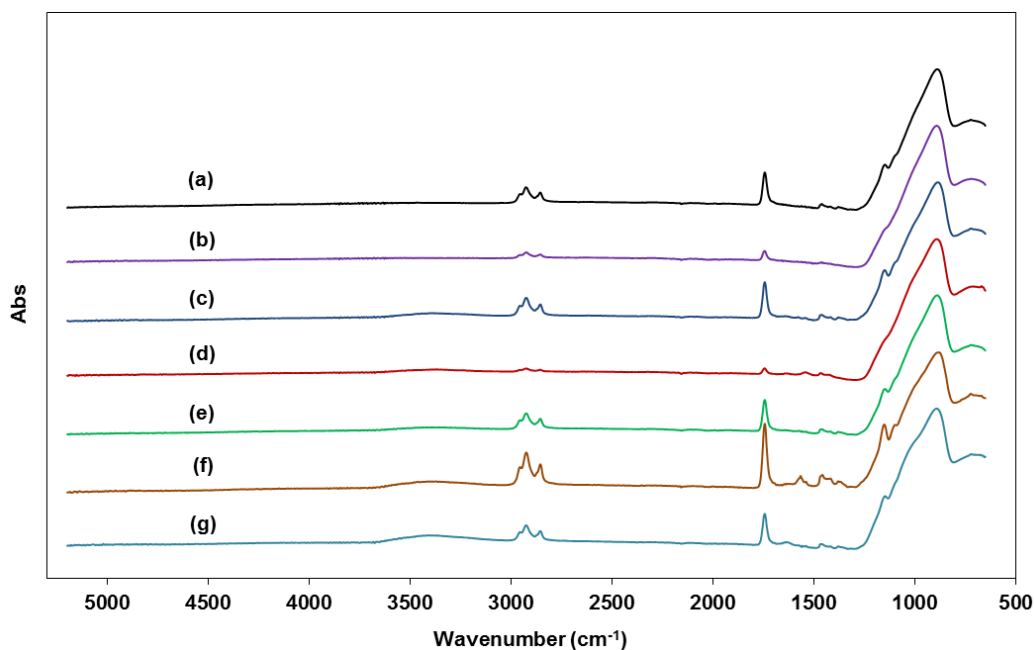


Figure 3.48 - Stacked view of FTIR attenuated total internal reflectance spectra of glass fibres (a) as received, (b) after HT, and then treatment in 5 M NaOH solution for (c) 5 minutes, (d) 10 minutes, (e) 20 minutes, (f) 30 minutes and (g) 120 minutes, with rinsing

There appears to be no significant increase in intensity of the Si-OH band with NaOH treatment time. In addition, the Si-O-Si absorbance peaks (which are not reststrahlen as this phenomenon does not usually occur in ATR [106]) are fairly unaffected by alkaline treatment of the glass fibres. There is a sharp decrease in intensity of the suspected APS absorbance peak at 2900 cm^{-1} after HT, which complements the fact heating as received fibres to very high temperatures results in removal of the APS coating. In spite of this observation, the peak appears again in the NaOH treated fibres, at times more prominently than in as received fibres; this suggests the peak could be present due to contamination rather than residual APS. Once again, the hydrocarbon absorbance at 2900 cm^{-1} corresponds to a strong carbonyl absorbance at 1750 cm^{-1} , indicating the possible presence of carboxylic species on the glass fibres.

One of the major drawbacks of using ATR in this study is that it can be destructive to the sample. Figure 3.49 shows the glass fibre bundles after being used for FTIR analysis with the ATR interface.

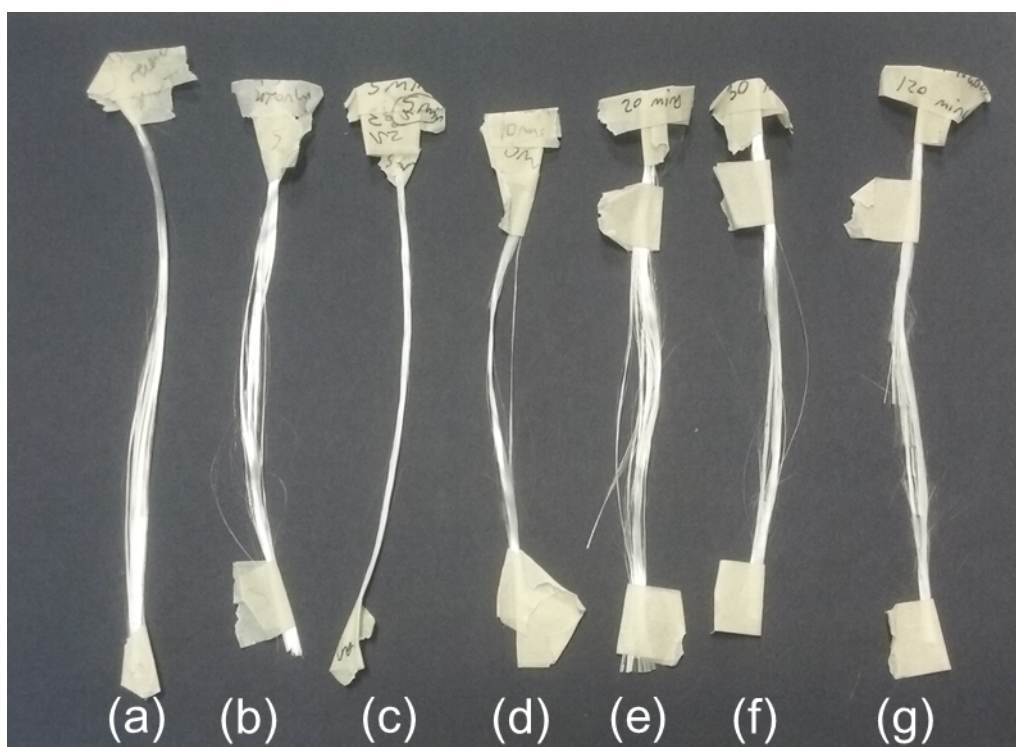


Figure 3.49 – Images of glass fibres (a) as received, (b) after HT, and then treatment in 5 M NaOH solution for (c) 5 minutes, (d) 10 minutes, (e) 20 minutes, (f) 30 minutes and (g) 120 minutes, with rinsing, after FTIR analysis with ATR interface

It seems that the weakest fibre samples in the set (HT only and HT with excessive NaOH treatment) were more prone to breakage after being clamped for ATR analysis; the damage is particularly clear for the fibres treated in NaOH solution at 120 minutes (Figure 3.49g). Another issue with using ATR is that it penetrates only a couple of micrometres into the sample, meaning only the outer surface of fibres can be analysed. This could explain why some of the data is inconsistent at times. An

advantage with using DR, which penetrates hundreds of microns into the sample coupled with a spot size of around 3 mm, is that analysis can be done deep within the fibres of the bundle, leading to more consistent and representative FTIR diffuse reflectance spectra for each treatment condition. An additional benefit of the diffuse reflectance technique employed here (and specular reflectance) is completely non-destructive sample interface interaction as well as no need for any sample preparation.

3.4.6 Fracture surface analysis of alkali treated fibres

FTIR spectra in the previous section indicate probable bulk glass network damage when glass fibres are treated in alkaline solution for an extended period of time (120 minutes). To determine whether the origin of failure of these fibres was internal or superficial, the fracture surface was analysed through SEM. HT glass fibres treated in 5 M KOH and NaOH solution for 120 minutes were tested for tensile strength, which were measured to be 0.82 and 0.60 GPa respectively. The fracture surfaces of some of these fibres were examined under the SEM after tensile testing, with representative images (both for KOH and NaOH treated fibres) displayed in Figure 3.50.

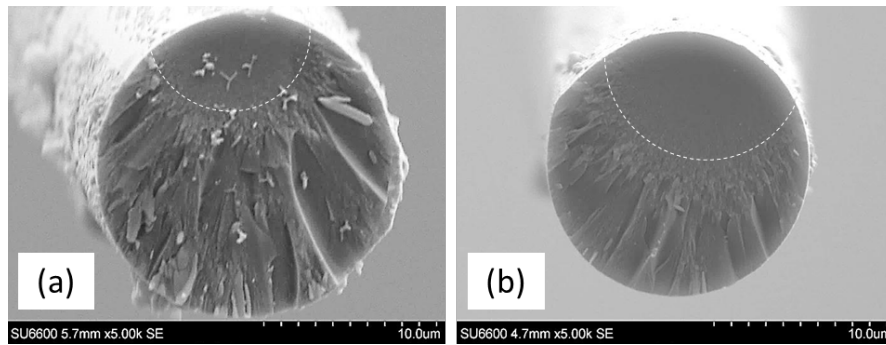


Figure 3.50 - SEM images of fracture surfaces of fibres HT and treated in (a) 5 M KOH solution for 120 minutes and (b) 5 M NaOH solution for 120 minutes

Three distinct regions are generally present in the majority of fibre fracture surfaces- mirror, mist and hackle [7]. The smooth and featureless mirror zone surrounds the original crack that is located at the surface of the fibre. At the edge of the mirror zone there is a pitted surface which is the mist region, and the branches that appear are referred to as hackle. The hackles normally go back to the locus of the failure area of the fibre. The features present in both images in Figure 3.50 suggests the origin of failure was at the surface, even if the bulk glass network was damaged by the severe alkaline treatment; there was no indication from any of the fibre fracture surfaces that failure initiated internally. It is suggested that although the bulk glass structure was damaged with excessive treatment in both NaOH and KOH solution as indicated by the FTIR results, the source of fibre failure was still most likely to have been at the surface. Indeed, for there to have been significant internal damage the glass fibre surface would have had to react first with the alkaline solution and consequently remain the weakest region.

The main difference between the fracture surfaces of KOH and NaOH treated fibres is the size of the mirror region, which is inversely related to tensile strength; the larger the mirror zone, the deeper the surface crack, and consequently the lower the

strength of the fibre. The measured strength of fibres treated in 5 M NaOH solution for 120 minutes was lower than in KOH solution under the same conditions, and it can clearly be seen in Figure 3.50 that the mirror region is larger for NaOH treated fibre.

It is widely accepted that HF and alkaline solutions can etch glass under particular reaction conditions [2, 11, 12, 14, 17]. The etching process involves the breakdown of the silicate network in the glass by the anions of the chemical solution; in alkaline treatments, these would be the hydroxide ions. When glass is in its fibrous form, the corroding effect of HF and alkaline solution can be seen through a reduction in fibre diameter [11, 107]. The thought of HF etching resulting in the removal or alteration in surface cracks has been articulated several decades ago with bulk glass [12] and recently Yang et al. adopted this methodology to recover strength of thermally treated glass fibres [11]. The HF etching of deep, V-shaped surface flaws into smoother, U-shaped structures is reported on bulk glass [12] and it is believed that this is the mechanism by which alkaline solution regenerates the strength of thermally treated glass fibre (see Figure 3.51).

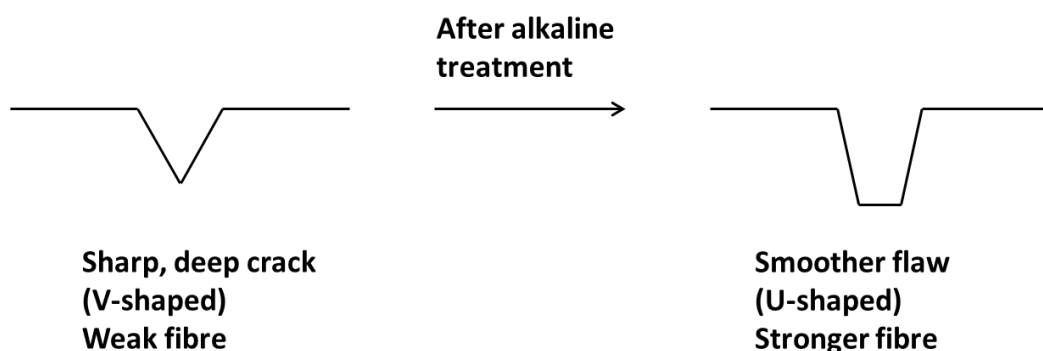


Figure 3.51 - Schematic showing strength regeneration mechanism of glass fibre by alkaline solution

To verify that the strength regeneration mechanism schematically represented in Figure 3.51 is followed, an examination of a surface flaw on a fibre before and after alkaline treatment would be required; however these flaws cannot be easily imaged even with a powerful SEM. When fibres fail as a result of a surface flaw, there are three distinct regions usually present on the fracture surface (cross-section)- mirror, mist and hackle. The branches which are referred to as hackle are easily imaged under the SEM as shown in Figure 3.50. If a cross-section of a fibre is treated in alkaline solution and the branches are smoothed out, then this suggests that the flaw modification theory schematically represented in Figure 3.51 could indeed be the process by which alkaline treatment regenerates fibre strength. Figure 3.52a shows an SEM image of the cross-section of a fibre that failed as a result of a surface flaw, possessing a mirror, mist and hackle region. Figure 3.52b shows another SEM image, where the cross-section of a fibre was treated in alkaline solution (5 M NaOH for 120 minutes).

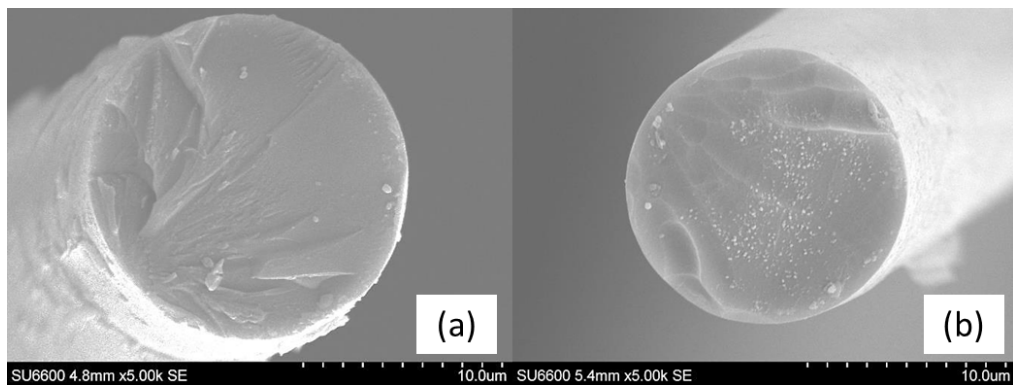


Figure 3.52 - SEM images of the cross-section of (a) untreated glass fibre, and (b) glass fibre treated in 5 M NaOH solution for 120 minutes

It is evident that branches on the fibre cross-section (the hackle region) are smoothed out following alkaline treatment. This suggests that alkaline solution regenerates strength in HT glass fibres through a flaw blunting mechanism. In addition, previous mass loss data demonstrate that alkaline solutions can etch glass fibres; although this is thought to be the mechanism by which HT fibre strength is restored, it can be seen from FTIR data that excessive treatment can lead to bulk glass network damage.

This chapter has so far looked into the properties of HT glass fibres after treatment in alkaline solutions. Though work has been done with examining the performance of virgin glass fibres in alkaline solution [18, 21, 22] it has not, to the author's knowledge, been conducted in conjunction with HT fibres. The purpose of the next section is to examine the durability of both virgin and HT OC glass fibres after treatment in alkaline solutions. The tensile strength and mass loss of these fibres are reported along with chemical structure analysis.

3.4.7 Effect of alkaline treatments on virgin and thermally treated glass fibres

It has been reported previously in the literature that alkaline treatments have a detrimental effect on the properties of virgin glass fibres [18, 21, 22]. To the best of the author's knowledge, an investigation has not been carried out to date on the effects of alkaline treatments on both virgin and HT fibres. In this section, bare, APS-sized and HT (initially APS-sized) OC glass fibres were treated in hot NaOH solution at different concentrations and times, and their strength and mass loss measured. In addition, aesthetic and compositional analyses of the fibres were performed using SEM and EDS respectively. An examination of the chemical structure of the glass fibres was also carried out using FTIR with DR interface.

Figure 3.53 displays the strength of bare, APS-sized and HT glass fibres after treatment in 3 M NaOH solution at different times. The HT data has been reported earlier in this chapter.

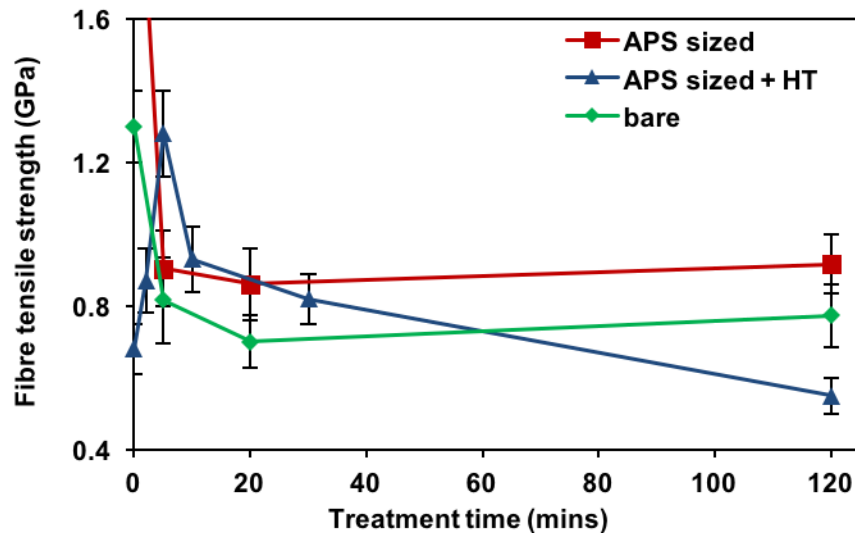


Figure 3.53 – Average strength of APS-sized, HT and bare glass fibres after treatment in 3 M NaOH solution at various times

The initial strength of the virgin APS-sized glass fibres is the highest out of all the fibre types (2.3 GPa) due to the protective capability of the silane coating; the y-axis is cut off below this value to allow easier discrimination of other data points. The absence of this coating (bare fibres) results in a drop in strength to around 1.3 GPa. The weakest of all are the APS-sized fibres that were HT, as the coating was removed exposing the fibre surface to physical and chemical damage.

Application of alkaline solution to the virgin APS-sized and bare glass fibres leads to a dramatic loss in strength, even at a short treatment time of 5 minutes; although the APS-sized glass fibres possess an initially higher strength than the bare fibres, the

strength falls to a similar value of around 0.9 GPa showing that APS offered little protection from NaOH damage. At this treatment duration the strongest fibres are in fact those that were HT (1.3 GPa), since the alkaline solution regenerated the strength by smoothing out severe surface defects. Beyond this optimal treatment time the HT fibre strength begins to decrease, converging with the strength of the virgin APS-sized and bare fibres. After the precipitous drop in strength of the APS-sized and bare fibres after 5 minutes of alkaline treatment, the strength is fairly unaffected by treatment duration. On the other hand, the HT fibre strength appears to decline continuously with treatment time, even below values measured without any alkaline treatment. It was suggested earlier in this chapter from FTIR data that the eventual decrease in strength of HT fibres could have been due to severe glass network degradation by the alkaline solution. Given that this network dissolution should occur in virgin fibres, we would expect the strength to decrease further for APS-sized and bare glass fibres; Figure 3.53 shows a dramatic reduction in strength of these virgin fibres at just 5 minutes of NaOH treatment, and then remains constant with time. An FTIR analysis of alkali treated virgin fibres was conducted and the results reported later in this section.

The strength of APS-sized fibres after 120 minutes alkaline treatment is the highest, followed by bare then HT; this correlates with the baseline strength of the fibres. Despite the difference in strength of these fibre types at the longest alkaline treatment duration, it is apparent that convergence in strength occurs at an early stage. The dramatic loss in strength of virgin fibres after alkaline treatment agrees with previous studies [18, 21, 22]. The fact that this abrupt decrease in strength occurs for APS-sized fibres indicates that the APS was removed by the alkaline solution and thus offered little protection to the glass from dissolution.

As well as testing the strength of the fibres after alkaline treatment, the mass loss of some of the bundles was also measured and plotted in Figure 3.54.

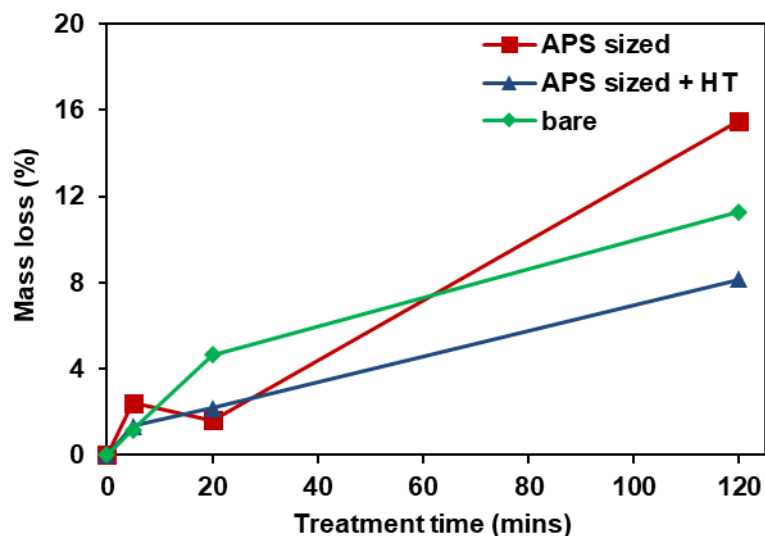


Figure 3.54 – Mass loss (%) of APS-sized, HT and bare glass fibres after treatment in 3 M NaOH solution at various times

Because the mass loss of only one bundle was measured after each treatment, it is not clear how the fibre type and treatment time affects the rate of dissolution of the glass. What is particularly unusual is that the APS-sized fibres show a higher mass loss after 120 minutes in NaOH solution, despite the fact that the APS would have retarded the dissolution rate of the glass to some extent at the beginning of the treatment. An attempt at relating the mass loss (and hence diameter reduction) of the fibres with the strength is made in Figure 3.55.

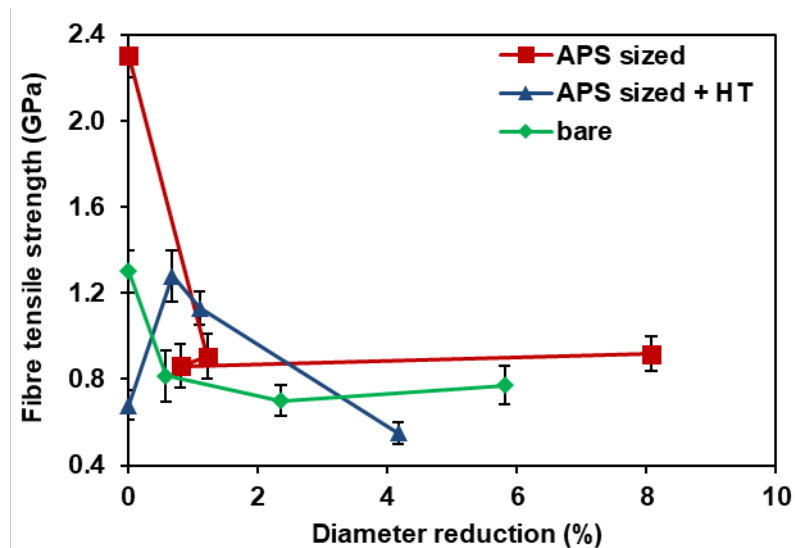


Figure 3.55 – Average strength of APS-sized, HT and bare glass fibres after treatment in 3 M NaOH solution as a function of diameter reduction (%)

The trend of diameter reduction (%) with strength is similar for the APS-sized and bare glass fibres. At 1% diameter reduction there is a sudden decline in strength of the fibres without heat treatment; beyond this point the strength is fairly constant as the diameter of the fibre continues to decrease. As for the HT fibres, the strength increases significantly at around 1% diameter reduction, and then gradually decreases.

Later in this chapter, virgin and HT fibres were treated in a relatively lower NaOH concentration of 1.5 M to see whether the strength would change more steadily with time. Additionally, a systematic investigation into the mass loss of the fibres after alkaline treatment was performed. FTIR and SEM-EDS analysis of the fibres was also carried out to further understand their interaction with the alkaline solution.

Figure 3.56 displays the average tensile strength of APS-sized, HT and bare glass fibres after treatment in hot 1.5 M NaOH solution for various times.

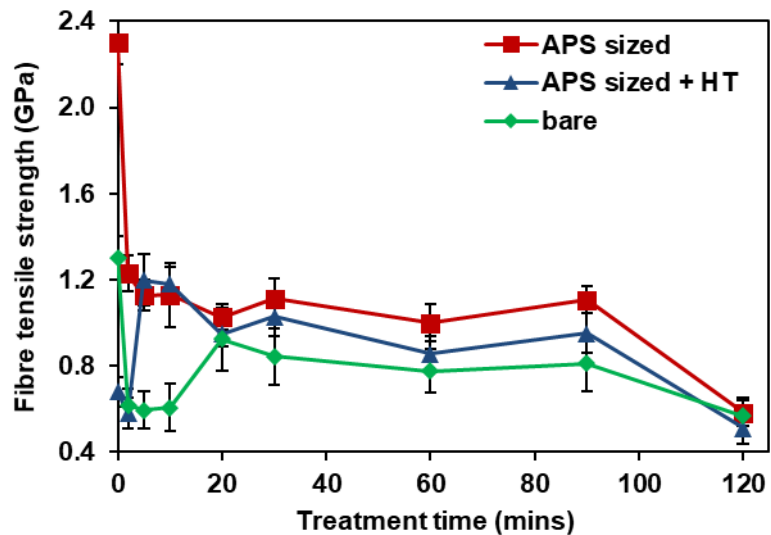


Figure 3.56 – Average strength of APS-sized, HT and bare glass fibres after treatment in 1.5 M NaOH solution for various times

The strength of the virgin fibres decreases significantly after a short alkaline treatment. A short period of NaOH treatment (2 minutes) had little effect on the strength of HT fibres, though a positive impact can be seen from 5 minutes onwards. Both the bare and APS-sized glass fibres lose approximately half their strength after 2 minutes of NaOH treatment; the fact that the strength reduction is severe even for APS-sized fibres indicates that the protective coating was readily removed by the alkaline solution, resulting in considerable damage of the glass surface underneath. The strength of the APS-sized fibres does not appear to decrease further with extended treatment, remaining at around 1.2 GPa up to 90 minutes. Interestingly, the bare fibre strength declines at the early stages of the treatment, and then increases up to around 1 GPa from 20 minutes; this suggests that the alkaline treatment might have damaged the fibre surface then subsequently healed the flaws. However, such an effect does not appear to occur for the case of APS-sized and HT fibres. Unlike previously with the more corrosive 3 M NaOH treatments, the strength of all three fibre types converges at various stages in Figure 3.56, even at

120 minutes where there is finally irreversible bulk glass network damage (as supported by FTIR and other studies). The fact that the strength at convergence is typically around 1 to 1.2 GPa is interesting, particularly as this is close to the strength of bare fibres without alkaline treatment. These results imply that regardless of the potential benefit of alkaline treatment for HT fibres, the strength cannot surpass that of virgin bare fibre; in other words, the strength can never reach that of virgin fibre coated with APS. At 120 minutes, the strength of all three fibre types decreases significantly to around the same value as the initial HT fibre strength; as discussed previously through FTIR, this strength decrease could be due to glass network degradation. In addition, the measured strength of these fibres at 120 minutes could be higher than the true strength from possible bias towards stronger fibres in the dataset.

As well as measuring the tensile strength of the fibres, the mass loss was also determined. Similar to a previous study, the mass of three bundles was measured before and after treatment in the alkaline solution at a particular time. The bundles were thoroughly rinsed in acid and water after the treatment to remove as much residue as possible. The mass of the bundles before and after rinsing was also obtained to investigate the extent of residual build-up on the fibres. Figure 3.57 gives the mass loss (%) of the fibre bundles after treatment in hot 1.5 M NaOH solutions at various times, after rinsing. The error bars represent the standard deviation.

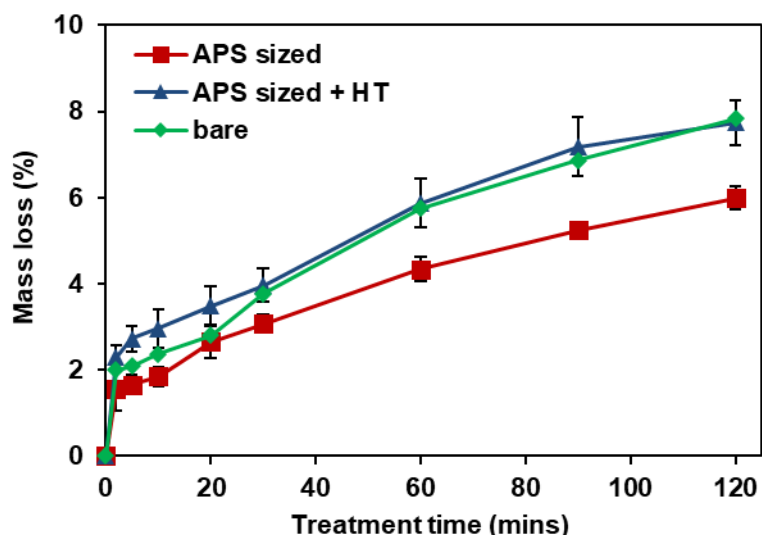


Figure 3.57 – Mass loss (%) of fibre bundles after treatment in 1.5 M NaOH solution at various times

A mass loss of around 2% is observed after just 2 minutes of alkaline treatment of the HT and bare fibres; the mass loss of APS-sized fibres appears to be lower. As the treatment progresses the dissolution of the fibres appears to continue, following a logarithmic curve. This gradual reduction in the dissolution rate of the fibres can be attributed to the build-up of product layers on the glass surface over the course of the treatment, and/or the ineffective removal of residue from the rinsing procedure. The latter seems unlikely given the rigorous acid rinsing process adopted in this experiment. The extent of dissolution of HT and bare fibres is similar, being slightly higher than APS-sized fibres throughout the course of the treatment. Although the APS coating might have been removed eventually by the alkaline solution, it would have offered some initial protection to the glass surface resulting in a slight retardation in the rate of dissolution. The results contradict those presented in Figure 3.54, which show APS-sized fibres dissolving more readily in 3 M NaOH solution; it is worth bearing in mind, however, that in the previous study the mass loss of only one bundle was measured at each treatment time. After 120 minutes of 1.5 M NaOH

treatment, the mass loss of bare and HT fibres was almost 8%; when considering this in absolute terms, it was equivalent to a fibre bundle with an initial mass of 305 mg, which lost 23 mg after alkaline treatment resulting in a final mass of 282 mg.

Figure 3.58 provides the mass gain (%) of the fibre bundles after treatment in 1.5 M NaOH solutions at various times, before acid rinsing was carried out to remove residue.

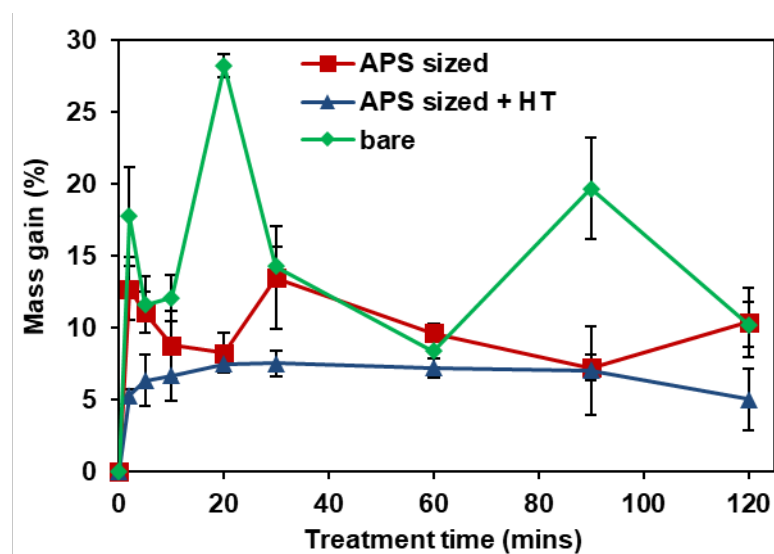


Figure 3.58 – Mass gain (%) of fibre bundles after treatment in 1.5 M NaOH solution at various times, without rinsing

The mass gain seems to be consistent (around 7%) at various stages of the treatment of HT fibres. As for the virgin bare and APS-sized fibres, the mass gain fluctuates regularly, and was likely due to fibres being handled more gently at certain treatment times than others. There appears to be no trend in mass gain against treatment time of the fibres, however the constant mass loss shown in Figure 3.57 indicates that no matter how variable the residue amount can be on the

fibres after alkaline treatment, the rinsing procedure is capable of removing the deposits effectively.

Because the fibre strength after alkaline treatment is mainly controlled by the etching of the glass surface, a plot was constructed (Figure 3.59) showing the tensile strength of the fibres as a function of diameter reduction, which was determined from the mass loss.

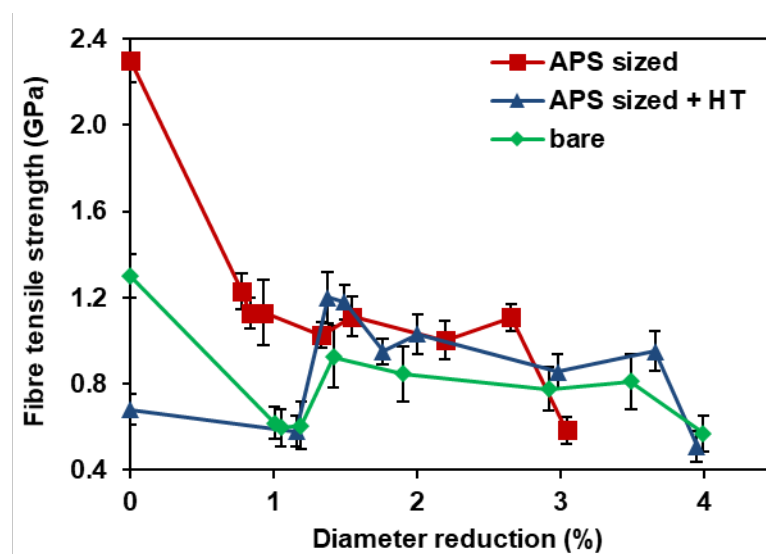


Figure 3.59 – Average strength of APS-sized, HT and bare glass fibres against their diameter reduction after treatment in 1.5 M NaOH solution at various times

At the initial stage of the treatment (where there is up to 1% diameter reduction), the alkaline treatment already has a detrimental effect on the strength of the virgin fibres; the strength of the HT fibres is relatively unchanged. Once diameter reduction exceeds 1%, the strength of the bare and HT fibres begins to increase, converging with the strength of APS-sized fibres, which remains at approximately 1.2 GPa. After 3% diameter reduction for APS-sized fibres, and unusually at 4% for bare and HT

fibres, the strength finally drops possibly due to the excessive glass network degradation.

The fibre surface after alkaline treatment (before and after rinsing) was examined with an SEM to investigate the residual build-up and to see more clearly how effective the rinsing procedure was to remove the deposits. Figure 3.60, Figure 3.61 and Figure 3.62 show SEM images of APS-sized, HT and bare fibres respectively after treatment in 1.5 M NaOH solution for 30 and 120 minutes, with and without acid rinsing.

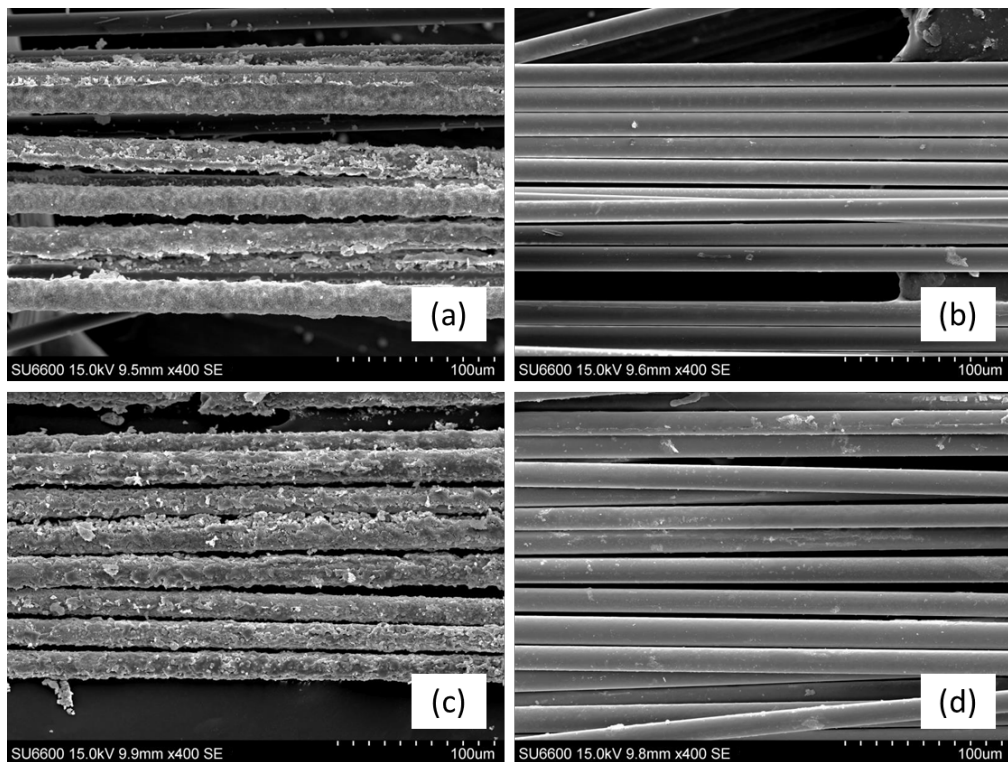


Figure 3.60 – SEM images of APS-sized glass fibres after 1.5 M NaOH treatment for (a) 30 minutes (without rinsing), (b) 30 minutes (with rinsing), (c) 120 minutes (without rinsing), and (d) 120 minutes (with rinsing)

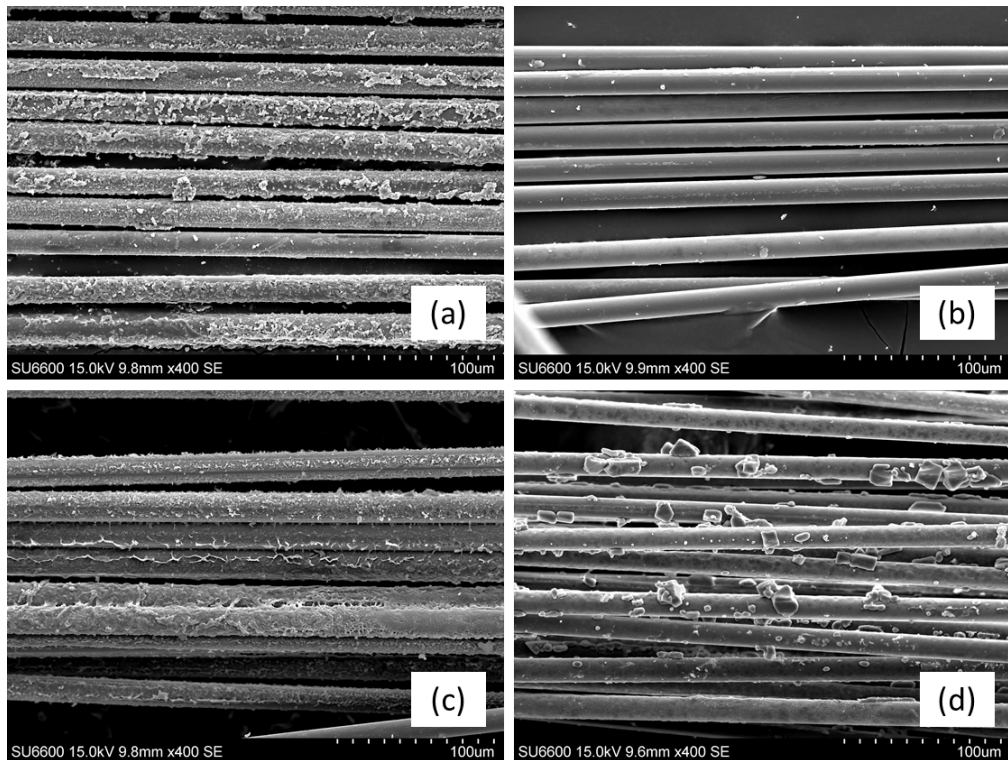


Figure 3.61 - SEM images of HT glass fibres after 1.5 M NaOH treatment for (a) 30 minutes (without rinsing), (b) 30 minutes (with rinsing), (c) 120 minutes (without rinsing), and (d) 120 minutes (with rinsing)

From SEM investigation it is evident that a significant amount of residue builds up on the fibre surface after alkaline treatment, irrespective of treatment time; this is consistent with results in Figure 3.58 which show little trend in mass gain of fibres treated in alkaline solution at various times, without rinsing. What is also apparent is that for fibres treated in alkaline solution at 30 and 120 minutes, the acid rinse managed to remove most of the residue, leaving a reasonably clean fibre surface. From SEM imaging it can be seen that the fibre surface after 30 minutes of alkaline treatment is marginally cleaner than the fibres treated for 120 minutes, which could account for the slight retardation in mass loss of the fibres shown in Figure 3.57.

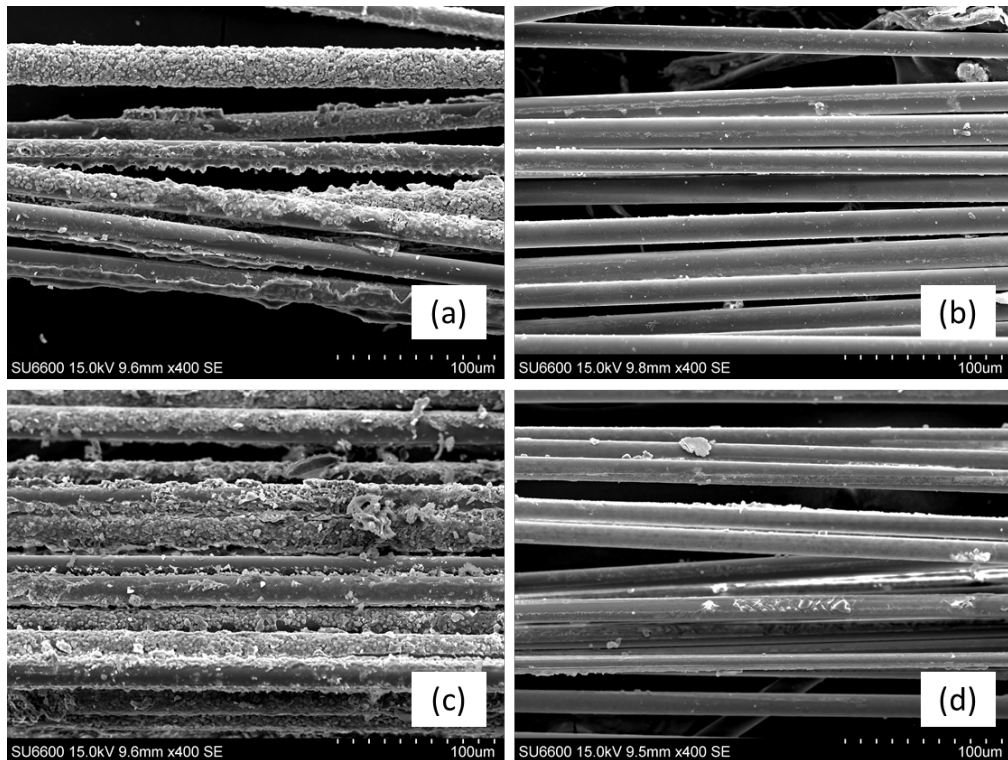


Figure 3.62 - SEM images of bare glass fibres after 1.5 M NaOH treatment for (a) 30 minutes (without rinsing), (b) 30 minutes (with rinsing), (c) 120 minutes (without rinsing), and (d) 120 minutes (with rinsing)

As well as imaging the fibres under SEM, EDS was also used for compositional analysis of the surface and residue. Figure 3.63 shows the elemental composition of APS-sized fibres before and after alkaline treatment. For the alkali treated and rinsed fibres, EDS analysis was conducted both of the fibre surface and the remaining residue. Because the alkali treated and unrinsed fibres had a significant build-up of residue, analysis was not possible of the fibre surface so measurement was made only of the residue. The elements listed in Figure 3.63 are those that are generally present in E-glass fibre formulations. Chlorine (Cl) was also included in the element list because the fibres were rinsed in HCl after alkaline treatment. Although untreated APS-sized fibres would contain other elements such as nitrogen (N) and carbon (C) from the APS coating, these were removed for simplicity and to allow

comparison with fibres where the APS coating was not present or removed by the alkaline solution.

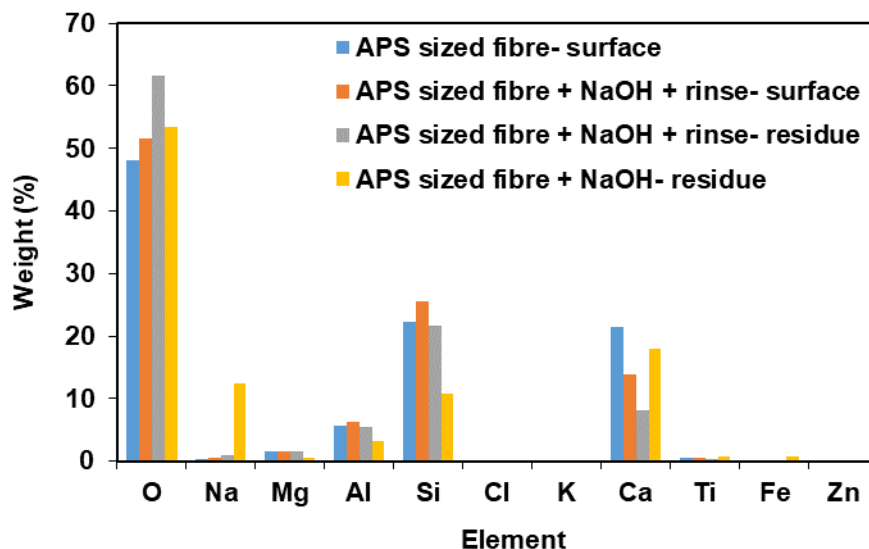


Figure 3.63 – Weight (%) of elements present on APS-sized glass fibres before and after alkaline treatment

There is little change in the elemental compositional of the fibre surface itself after alkaline treatment, other than the slight decrease in concentration of Ca, which could have been due to CaO dissolving into the alkaline solution to form Ca(OH)₂. The composition of the residue following acid rinsing appears to be similar to the fibre surface, suggesting that the surface composition was mainly contributing to the EDS measurement instead. Because the unrinsed alkali treated fibres possessed a considerable amount of residue on the surface the EDS measurement was more straightforward, registering a high concentration of Na. This could have resulted from residual NaOH precipitating on the fibre surface or it could have originated from Na-based products between the glass and alkali. The fact that the Ca level

increases implies that dissolved $\text{Ca}(\text{OH})_2$ might have precipitated back onto the fibre.

Figure 3.64 shows the EDS compositional analysis of the HT fibres before and after alkaline treatment.

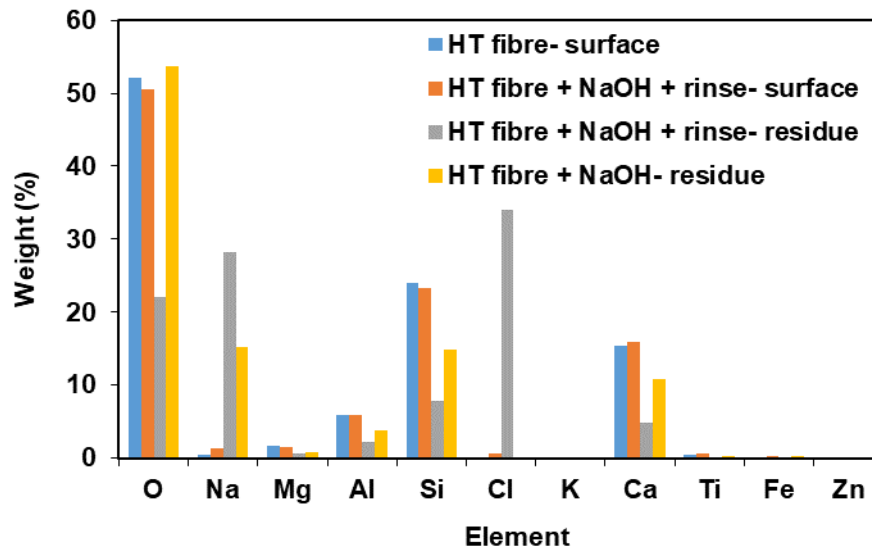


Figure 3.64 - Weight (%) of elements present on HT glass fibres before and after alkaline treatment

Once again, the elemental composition of the fibre surface is relatively unchanged following alkaline treatment. Interestingly, the residue left on the fibres after acid rinsing registered an overwhelming concentration of Na and Cl. NaCl is a product of the reaction of NaOH with HCl, so it can be said that the residue remaining on the fibre surface after acid rinsing was likely to have been composed of NaCl. Given that a significant weight (%) of O is still shown in Figure 3.64 for the residue of the rinsed fibres indicates that some NaOH was also present. Unsurprisingly, no Cl was

detected on the residue of the unrinsed fibres, and was possibly a mixture of leftover NaOH, Na-based products, and precipitated $\text{Ca}(\text{OH})_2$.

Figure 3.65 shows that the elemental composition of the surface of bare glass fibres does not change significantly after alkaline treatment.

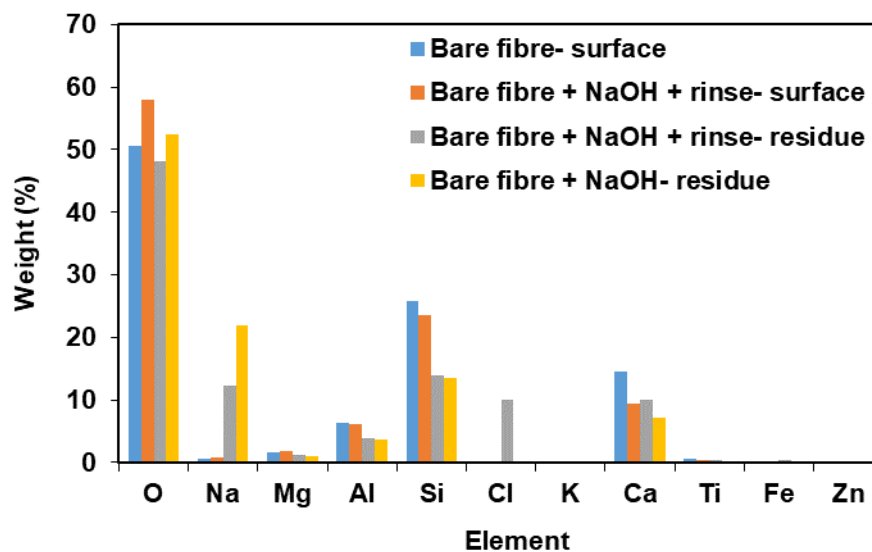


Figure 3.65 – Weight (%) of elements present on bare glass fibres before and after alkaline treatment

When the bare fibres were treated in alkaline solution and rinsed in acid, the remaining deposits showed a considerable amount of Cl and Na according to EDS; again, this could have been attributed to the production of NaCl from the reaction of residual NaOH and HCl during the rinsing procedure. The residue of the unrinsed fibres shows high levels of Na and O, which was likely to have been due to the presence of residual NaOH from the alkaline treatment. The EDS results also indicate that some other materials like precipitated $\text{Ca}(\text{OH})_2$ and Na-based products

like sodium silicate and sodium aluminate could have been present in the residual deposits.

Figure 3.66 shows the FTIR diffuse reflectance spectra of the APS-sized glass fibres before and after NaOH treatment for 30 and 120 minutes (with and without rinsing).

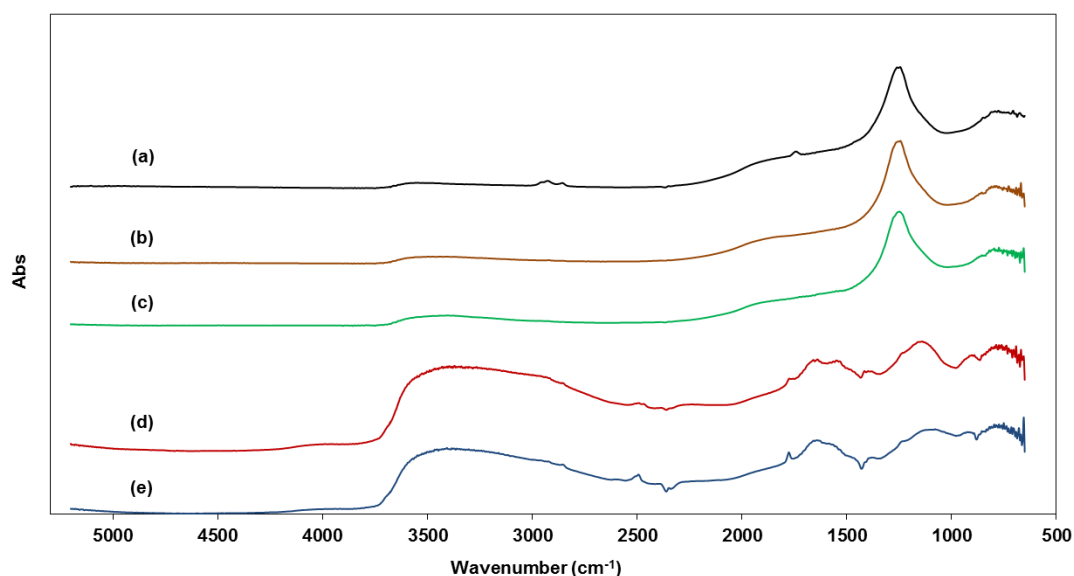


Figure 3.66 - Stacked view of FTIR diffuse reflectance spectra of glass fibres (a) APS-sized only, then after 1.5 M NaOH treatment for (b) 30 minutes (with rinsing), (c) 120 minutes (with rinsing), (d) 30 minutes (without rinsing), and (e) 120 minutes (without rinsing)

The spectrum for APS-sized fibres shows a weak absorbance band around 3500 cm⁻¹ which is likely from Si-OH in the glass [101]. Peaks at just below 3000 cm⁻¹ are indicative of hydrocarbon absorbance from the APS coating [101]. The weak IR absorption at 2300 cm⁻¹ and 1750 cm⁻¹ is present due to carbon dioxide or other carboxylate species, which can be commonly found in IR spectra [103-105]. The band at 1000 cm⁻¹ (which points downwards due to the reststrahlen effect) is from absorbance by Si-O-Si in the glass fibre [101]. When APS-sized glass fibres were treated in alkaline solution and rinsed, most if not all the IR absorption from APS

appear to be removed, indicating that the APS coating was removed from the fibres. There seems to be no difference in the SiOH and Si-O-Si absorbance of fibres before and after treatment with rinsing. When the unrinsed fibres were analysed, it was found that the IR absorbance was predominantly of the residue (mostly NaOH), as shown by the strong OH absorbance band at 2500 to 3700 cm^{-1} and the dampening of the Si-O-Si absorbance. Other peaks seem to have emerged for the alkali treated and unrinsed fibres; though not well-resolved and easily assignable it can be supposed that some of them are as a result of IR bending vibrations of the OH, and of contaminants. Such a trend is also observed with the case of APS-sized and HT fibres (Figure 3.67).

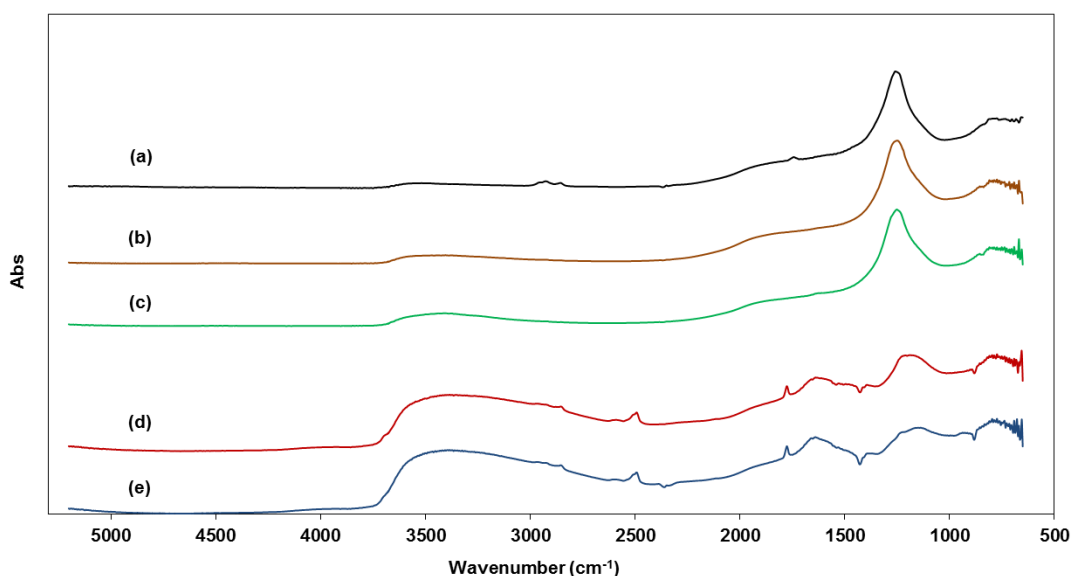


Figure 3.67 - Stacked view of FTIR diffuse reflectance spectra of glass fibres (a) APS-sized + HT only, then after 1.5 M NaOH treatment for (b) 30 minutes (with rinsing), (c) 120 minutes (with rinsing), (d) 30 minutes (without rinsing), and (e) 120 minutes (without rinsing)

The Si-OH band appears to increase slightly in absorbance when the fibres were treated for 120 minutes in alkaline solution and rinsed, as opposed to the shorter time of 30 minutes; this proves that a prolonged alkaline treatment leads to an

increase in the rate of hydroxide attack of the silicate network, and hence a greater concentration of Si-OH groups. With the unrinsed fibres, there is again an overwhelming absorbance possibly of residual NaOH. In addition, there is a peak that develops at around 2500 cm^{-1} , which was only slightly visible in Figure 3.66; this absorbance could have been from carbonate groups present on the fibres as a result of contamination [104]. These absorption peaks appear for alkali treated and unrinsed bare fibres as well, according to Figure 3.68.

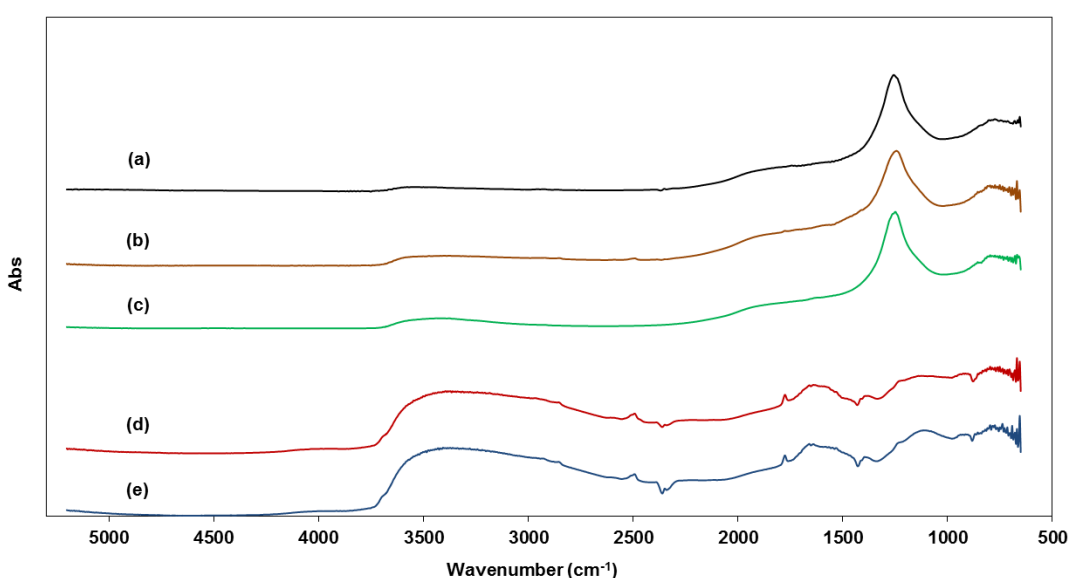


Figure 3.68 - Stacked view of FTIR diffuse reflectance spectra of glass fibres (a) bare only, then after 1.5 M NaOH treatment for (b) 30 minutes (with rinsing), (c) 120 minutes (with rinsing), (d) 30 minutes (without rinsing), and (e) 120 minutes (without rinsing)

It can be presumed that any hydrocarbon absorbance from alkali treated and unrinsed glass fibres could be due to contamination on the surface. There is also the possibility that some residual APS was on the fibres, however this is unlikely the case particularly for bare fibres as they do not possess an organic coating in the first place. Overall, it can be deduced that alkaline treatment of the fibres, regardless of

whether they were APS-sized, HT or bare, leads to the degradation of the silicate network and the increase in silanol groups. In addition, it can be said that the absorbance of the alkali treated and unrinsed fibres is mainly of the residual NaOH.

3.5 Conclusions

Glass fibres exhibit up to 70% tensile strength loss after conditioning at a thermal recycling temperature of 450 °C. It has been demonstrated from this research study that a short treatment of HT glass filaments in hot NaOH or KOH can almost double their strength, allowing their potential reuse as reinforcement in GRP materials. LiOH, however, was unable to restore strength in HT fibres. KOH, shown to be a milder glass fibre etchant from mass loss and diameter reduction experiments, improved fibre strength at higher molarity and longer treatment times. Conversely NaOH was a highly corrosive alkaline reagent towards glass fibre, and proved to be a much more efficient strength regenerator. For a given etchant, the maximum strength regeneration was affected by molarity and treatment time. Interaction of alkaline solution with the glass surface resulted in the formation of residual deposits, which were more prominent for fibres treated in NaOH than KOH as shown by SEM and AFM investigations. The degradation of the glass network, as indicated by FTIR spectra, correlated with the decrease in fibre strength when treatment in NaOH and KOH was excessive. On a positive note, the fact that NaOH was highly corrosive meant only low molarity of solution and short treatment time was required to regenerate HT fibre strength; when conditions became severe there was a drop in strength of HT fibres. It is thought the reduction in severity of surface flaws on HT fibre explained why strength initially improved with alkaline treatment. Despite the degradation of the glass fibre network as a whole after excessive treatment,

examination of fibre fracture surfaces indicated that the origin of failure could still have been at the surface.

The effect of alkaline treatment (NaOH) on the strength of virgin APS-sized and bare glass fibres was also investigated. This treatment decreased the strength of the virgin fibres, consistent with previous studies in the literature. Interestingly, the strength of APS-sized, HT and bare fibres after alkaline treatment eventually converged at around 1 GPa, close to the strength of untreated virgin bare fibre. This was close to the limit at which the alkaline treatment could improve the strength of HT fibres; the strength of these fibres so far has never shown to surpass that of virgin bare fibres, in other words they could never reach the strength of glass fibres commercially sized with APS. Although it was assumed that the APS coating was mainly removed from the fibres during alkaline treatments, results showed that the virgin APS-sized fibres were overall more resistant to dissolution by the alkaline solution than the HT and bare fibres.

4 Kinetics of dissolution of glass fibre in hot alkaline solution

4.1 Introduction

The strength loss of glass fibres after being thermally recycled from GRP waste is a major barrier to their reuse in second-life composite applications [8-10]. Recent work has shown that the strength of these damaged filaments can be restored by means of chemical treatment with HF or hot alkaline solution [11, 13, 14]. An in-depth study into the effects of alkaline treatments on the properties of thermally conditioned glass fibres is presented in Chapter 3. Both HF and alkaline solutions are thought to strengthen the fibres by blunting cracks through chemical etching; in fact, Yang et al. [11] shows that the reduction in fibre diameter after HF treatment can be related to strength increase.

The dissolution of silicate glass in alkali is well documented in literature [15-17], however the use of these corrosive substances for strengthening thermally treated glass fibres is a novel concept; it is believed the reaction of silica (SiO_2) with hydroxide ions (OH^-) from the alkaline solution [20] leads to a modification of the damaged fibre surface and improves tensile strength. The strength increase of thermally conditioned glass fibres from a short term of hot alkaline treatment can be achieved at little expense of removing surface materials, according to results presented in Chapter 3 and in [2]. This contrasts with the behaviour of HF, which significantly etches the glass fibre at its optimum treatment duration of 2.5 minutes [11]. Understanding and controlling the strength regeneration mechanism of thermally conditioned glass fibres through alkaline treatments require the

investigation of the kinetics of the reaction between the glass and the alkaline solution. To obtain accurate and reliable kinetic data, the conversion of glass fibres after alkaline treatment needs to be measurable. Although an excessive alkaline treatment can eventually lead to strength decrease of thermally conditioned fibres as shown in Chapter 3, a measurable fibre diameter reduction can be obtained, particularly when fibres are immersed individually in the alkaline solution.

Dissolution experiments are mainly conducted with bulk silicate glasses in the literature, and glasses which include a significant amount of various metal oxides in their formulation, such as E-glass, are not explored very often. In addition, little study on the dissolution kinetics of glass fibres immersed individually in alkaline solution has been conducted. This chapter presents the results of an investigation into the reaction kinetics of E-glass fibre dissolution in alkaline solution. Firstly, a literature review on the dissolution of bulk and fibrous glass in alkaline solution is given in the chapter.

To measure the dissolution rate in this study, individual E-glass fibres were immersed in the alkaline solution for prolonged periods of time, rinsed to remove residue and measured for obtaining fibre diameter with a scanning electron microscope (SEM). Measurement was taken of the corresponding untreated fibre in order to calculate the fibre diameter reduction. It is thought the effect of etching of the glass surface by alkaline treatment is strongly dependent on various reaction conditions including nature of alkaline solution, temperature, concentration and treatment duration. Both KOH and NaOH were investigated as a corrosive medium in this work. The temperature and concentration of these alkaline solutions and treatment duration were varied to determine the activation energy and reaction order, respectively. In addition, the fibre diameter reduction data was plotted with the strength results from Chapter 3 to determine whether an optimum etching rate for

strength regeneration exists. The key results given in this chapter were recently published in a conference paper [68] and journal article [107].

4.2 Literature review

The literature review in Chapter 3 focuses on the effects of chemical treatments on the properties of glass fibres. The review in this chapter concentrates more on the kinetics of dissolution of bulk and fibrous glass in alkaline solutions.

4.2.1 Dissolution studies of glass in alkaline solution

Bulk glass is used in a variety of applications, such as in the manufacture of laboratory apparatus. It is therefore important to look into the durability of these glasses in various corrosive environments, such as in hot alkaline solution. Molchanov and Prikhidko [16, 93, 108-110] published some of the earliest work on the dissolution behaviour of bulk silicate glasses in alkaline solutions. The first communication [16] presents the results of an investigation into the corrosion of quartz and laboratory glasses in NaOH and sodium carbonate solutions. The extent of dissolution was determined by measuring the thickness of the glass plates before and after aggressive alkaline treatment (standard molarity and temperature of NaOH solution being 0.5 mol/L and 90 °C respectively) using an interference microscope. The authors found that the dissolution rate of the glasses was overall higher when using NaOH as the alkali. In addition, the corrosion rate of glass increased with alkali concentration and temperature. Crystalline quartz was found to be the most stable out of all the glasses.

The composition of the glass can also have an effect on corrosion resistance; it was shown that replacing some of the silica in binary sodium and potassium glass with metal oxides can decrease its stability to alkaline attack [108]. On the contrary, introducing metal oxides such as Al_2O_3 into silicate glasses can retard their corrosion in alkaline solution [109]. Molchanov and Prikhidko also examined the influence of alkaline solutions based on different alkali metals (NaOH, KOH, LiOH, and so on) on the dissolution rate of bulk silicate glasses [93]. Results indicated that NaOH was the most corrosive solution towards glass, followed by KOH, LiOH and others. The increase in dissolution rate with certain alkaline solutions was attributed to their higher dissociation constants, meaning more hydroxide ions would be available to react with the glass. The fact that NaOH has a slightly lower dissociation constant than KOH and was found to be the most corrosive towards glass led the authors to believe that the reaction of NaOH and glass proceeded more readily and more exothermally [93]. As well as these alkalis the authors also studied the effect of hot water on the corrosion behaviour of glass; they believed that hot water not only leached the glass but also dissolved it to some degree. The dissolution of the glass in hot water was observed through a decrease in thickness of the glass plates; in some cases, the dissolution rate was comparable to that of glasses treated in alkaline solutions. The authors believed this dissolution was mainly due to the secondary reaction of the glass with alkaline components that were leached out by the hot water [93]. Taking into account this etching effect of hot water, one might consider it to be a safer and more cost-effective alternative to alkaline solution for regenerating the strength of thermally recycled glass fibres. The ability of this treatment to recover fibre strength has been investigated previously in [66] and will be explored to some extent in this chapter. A more thorough investigation into the effect of NaOH solution concentration on the dissolution rate of silicate glasses was also carried out by Molchanov and Prikhidko in [110]; they found that silica-rich

glasses dissolved proportionally to the alkali concentration, and the dissolution rate of glasses rich in elements such as magnesium eventually retarded by the build-up of certain metal oxide inhibitors and the formation of a magnesium hydroxide protective layer on the glass surface.

Many authors along with Molchanov and Prikhidko studied the dissolution behaviour of glass in alkaline solution [15, 17, 96, 111, 112]. Greenberg [111] found that amorphous silica dissolved more readily in alkaline solution than quartz, and the rate of dissolution was related to the silica surface area and structure. Hooley [96] published a study into the effects of various alkaline solutions on the dissolution rate of vitreous silica glass, and found that NaOH was the most corrosive solution (see Figure 4.1). This was consistent with results presented by Kouassi et al. [17] who looked into the dissolution behaviour of waste glass. Jendoubi et al. [112] observed a rapid dissolution of silica sand in NaOH solution in a pressure vessel at 220 °C.

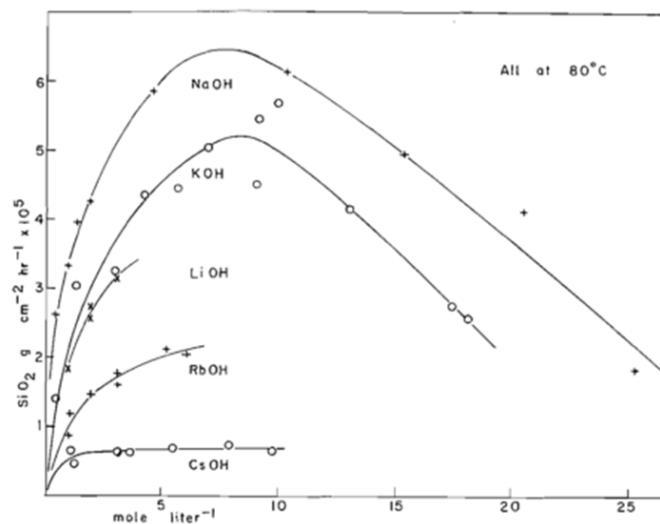


Figure 4.1 – Initial dissolution rate of vitreous silica glass in various alkaline solutions and concentrations at 80 °C. Reproduced from [96]

Investigating the dissolution behaviour of glasses has not only been for the purpose of examining their durability in corrosive environments. For example, Hawkins [98] and Kawano and Tomita [100] analysed the kinetics of dissolution of volcanic glass in terms of the rate of formation of zeolites, which are a class of aluminosilicate minerals used commercially in water purification among other applications. Tanaka and Takahashi [113] also looked into silica dissolution with regards to the formation of silicate products, and examined their chemical structures using FAB-MS (fast atom bombardment mass spectrometry). Fernandez et al. [114] looked into the kinetics of the reaction of fly ash (a by-product from coal plants, rich in silica) with calcium hydroxide solution ($\text{Ca}(\text{OH})_2$) as this process leads to the formation of sorbents that are widely used in flue gas desulfurization. Du et al. [115] investigated the dissolution kinetics of diatomite (a sedimentary rock rich in silica) in NaOH solution to look into how the formation of the sodium silicate product can be optimised. Sodium silicate is used commercially in a wide range of applications, for example as an adhesive and also as an ingredient for making skincare products. Gin et al. [116] examined the corrosion mechanism of international simple glass in KOH solution to help develop a unified model for glass dissolution.

Although there are comprehensive studies published on the dissolution behaviour of bulk glass in alkaline solution, fibrous glass has received little attention, despite its prevalent use in composites manufacturing. Some work has been reported on the corrosion of glass fibres in alkaline solutions [18-22, 78, 117] (see the literature review in Chapter 3), but these studies focus more on the mechanical properties of the fibres and do not go deep into the fundamental process of dissolution and its kinetics. Al Cheikh and Murat [118] analysed the dissolution behaviour of E-glass fibres in saturated $\text{Ca}(\text{OH})_2$ solution at room temperature over several months. They discovered that the mass loss of the fibres (after rinsing) was not constant with time

(see Figure 4.2), and believed it was due to the formation and removal of product layers on the glass surface during the treatment, which impeded and then resumed the dissolution of the fibres. Kinetic parameters such as the activation energy of the dissolution reaction were not reported.

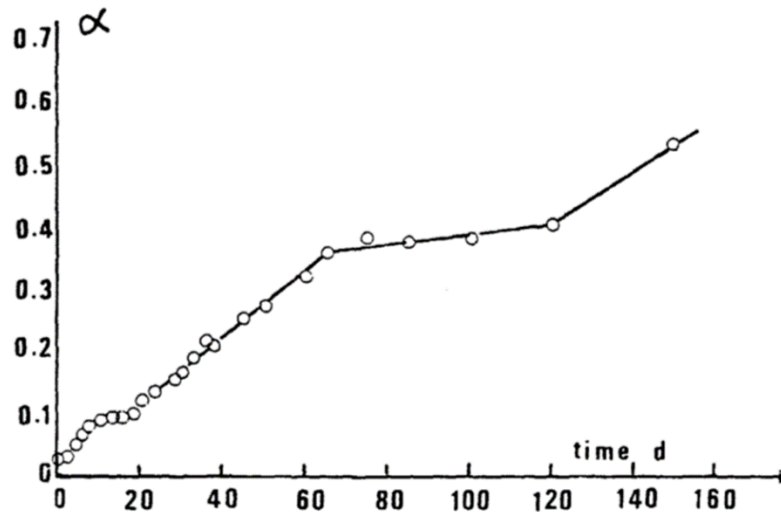
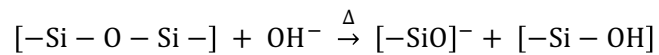


Figure 4.2 – Mass loss fraction (α) of glass fibres after treatment in saturated Ca(OH)_2 solution at 25 °C for several days. Reproduced from [118]

It is evident from the literature that the dissolution kinetics of bulk glass in alkaline solution has been carried out extensively. There is, however, very little investigation on the kinetics of dissolution of fibrous glass. The next section looks into the various solid-state kinetic models developed and which ones best describe the glass dissolution studies reported in the literature.

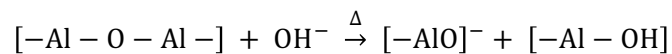
4.2.2 Solid-state kinetic models for glass dissolution in alkaline solution

SiO₂ is the major component in virtually all types of bulk and fibrous glass. For simplicity silica is commonly referred to as SiO₂, but in reality the SiO₂ exists as a complex network. When glass, regardless of its form, is in contact with hot, concentrated alkaline solution, the hydroxyl ions attack the SiO₂ framework according to Equation 4.1. These processes contribute to the dissolution of the glass.



Equation 4.1

In some cases Al₂O₃ can also form part of the silica network structure, and can react with OH⁻ from alkaline solution in a similar fashion to SiO₂ as shown in Equation 4.2.



Equation 4.2

Various models have been developed and are used extensively to describe solid-state reactions [119-129]. These models require the input of the conversion (α), which is a measurement of the change in mass of the solid before and after the reaction according to Equation 4.3.

$$\alpha = \frac{M_o - M_t}{M_o}$$

Equation 4.3

M_o is the initial mass of the solid (at $t = 0$) and M_t is the mass of the remaining solid at time t of the reaction.

Usually the conversion values are extracted directly from mass change but because this study involved the dissolution of individual glass fibres, it was more appropriate to measure the fibre diameter reduction using SEM, and then calculating the conversion using Equation 4.4.

$$\alpha = 1 - (1 - \Delta D)^2$$

Equation 4.4

where ΔD is the fibre diameter reduction as a fraction. This equation is developed from the volume of a cylinder, and how it is related to the square of its radius; the mathematical derivation is shown elsewhere [127].

When looking into the dissolution process of bulk or fibrous glass in alkaline solution, there are usually three possible rate determining steps which need to be considered. One of them is the diffusion of OH^- ions through the solution, and can be described by the zero order model (Equation 4.5) [115, 121, 124, 127, 129]. This model relates the conversion rate of the glass to the diffusion rate of the ions. The

reaction is zero order with respect to the glass thus Equation 4.5 is essentially the expression for zero order kinetics.

$$\alpha = rt$$

Equation 4.5

The reaction rate (or conversion rate) (r) can be extracted from the slope of the conversion of the glass fibres (α) against reaction time (t). The conversion rate is dependent on factors such as the glass surface area, concentration of the solution, and the diffusion rate of the OH^- ions [115].

Another potential rate limiting step is the hydroxide attack of the glass, which results in a contraction of the geometry of the solid. For the case of a glass fibre, this would mean a reduction in diameter. The shrinking cylinder model (Equation 4.6) [121, 124, 127, 129] can therefore be used to describe this rate limiting step of the dissolution process.

$$1 - (1 - \alpha)^{1/2} = rt$$

Equation 4.6

Here Equation 4.3 is modified to relate the conversion of a cylinder with the change in radius over time, eventually leading to Equation 4.6; the full mathematical derivation is given elsewhere [127]. Notice how rearranging Equation 4.6 to find α

leads to an expression of a similar form to Equation 4.4 where $rt = \Delta D$, proving that the shrinking cylinder model, in effect, gives the fibre diameter reduction. The reaction rate r can therefore be considered as the rate of fibre diameter reduction, and its value is related to the hydroxide concentration on the glass surface and the glass surface area [115].

Because most dissolution studies involve the use of bulk glass, the shrinking sphere/cube model is normally applied (Equation 4.7) [115, 121, 124, 127, 129], which takes a similar form to Equation 4.6.

$$1 - (1 - \alpha)^{1/3} = rt$$

Equation 4.7

Finally, when the glass reacts with the alkaline solution a product layer may form around the surface, meaning the hydroxide ions need to subsequently diffuse through this layer before reacting with the silicate network. The product layer thickness can increase with time, meaning the hydroxide ions take longer to diffuse through and consequently the rate of glass dissolution will decrease. For this scenario the 2-D diffusion model can be employed (Equation 4.8) [121, 124, 127] with glass fibre as the substrate, whereas for bulk glass the well-known shrinking core model (Equation 4.9) [115, 120, 123, 125, 129] is typically applied.

$$((1 - \alpha) \ln(1 - \alpha)) + \alpha = rt$$

Equation 4.8

$$1 - 3(1 - \alpha)^{2/3} + 2(1 - \alpha) = rt$$

Equation 4.9

Equation 4.8 describes the radial diffusion of species through a product layer of a long cylinder, and the thickness of this layer increases with time (unlike in previous cases where the product layer thickness is constant). This is a similar description for Equation 4.9, except this model usually applies to spherical particles. A schematic of the shrinking core model is shown in Figure 4.3.

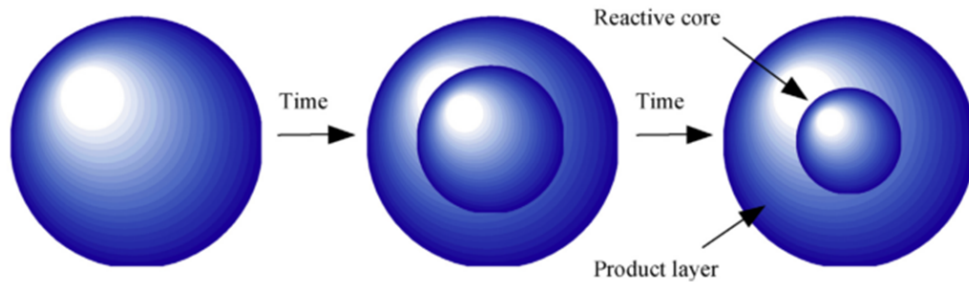


Figure 4.3 – Schematic diagram of the shrinking core model. Reproduced from [129]

The derivations of Equation 4.8 and Equation 4.9 can be found in [127] and [123] respectively. The reaction rate for both of these models depends on factors such as the concentration of hydroxide ions, and the rate of their diffusion through the product layer [115]. All the models described in this section, or similar, have been applied previously for the dissolution of glass in alkaline solution [114, 115, 123]. The model describes the reaction well if there is a linear fit of the data against time. The next section summarises which models were the best fit for the kinetic data

presented in the literature, and also the values of kinetic parameters such as activation energy.

4.2.3 Kinetic parameters determined from dissolution studies of glass in alkaline solution

As mentioned previously, numerous studies have been conducted on the dissolution of glass in alkaline solution. Many of these investigations involved fitting the kinetic data in various solid-state models to find which one gave the best fit and hence what was the rate determining step of the dissolution reaction. As well as model fitting, researchers have calculated other kinetic parameters, for example the activation energy (which is the minimum energy required to initiate a reaction). Reaction order, with respect to the alkaline solution, is another kinetic parameter that is commonly determined; this essentially means by what factor the reaction rate is increased as the concentration of one of the reactants (in this case alkali) is increased.

Table 4.1 summarises the kinetic factors calculated in various dissolution experiments reported in the literature.

Table 4.1 – Summary of kinetic parameters obtained from various glass dissolution studies in the literature

Reference	Reactants used	Kinetic model that gave best fit	Reaction order (with respect to alkali)	Activation energy (kJ/mol)
Greenberg [111]	Silica and NaOH	-	-	90.0
Molchanov and Prikhidko [16]	Quartz and NaOH	-	-	158.2
Hooley [96]	Vitreous silica and NaOH	-	-	92.0
	Vitreous silica and KOH	-	-	83.7
Jendoubi et al. [112]	Sand and NaOH	-	0.47	-
Fernandez et al. [114]	Fly ash and Ca(OH) ₂	Shrinking core model	-	100.4
Du et al. [115]	Diatomite and NaOH	Shrinking core model	2	28.1

Although kinetic modelling has not been carried out extensively for the case of complex glass dissolution, it is clear that the shrinking core model seems to show the best fit, suggesting that the diffusion of hydroxide ions through the product layer of the glass substrate is the rate limiting step of the dissolution reaction. The reaction order with respect to the alkaline solution appears to vary, with Jendoubi et al. [112] reporting a value of 0.47 and Du et al. [115] a value of 2. The activation energy is calculated in the majority of the articles referenced in Table 4.1, with values differing depending on the nature of the glass reactant. The lowest activation energy is 28.1 kJ/mol for the reaction of diatomite with NaOH solution [115], and the highest value is reported to be 158.2 kJ/mol for the dissolution of quartz [16]; this is not unexpected given that quartz is the most stable form of glass. There is only a slight increase in activation energy for the dissolution of vitreous silica in NaOH compared to when KOH is used as the alkali [96].

In this study, the dissolution behaviour of glass fibres in both NaOH and KOH solution is reported. The data was fit into the solid-state kinetic models and the reaction order and activation energy of the dissolution process was determined. These results are compared with those given in the literature, as shown later in this chapter.

4.2.4 Conclusions of literature review

From reviewing the literature it is apparent that the dissolution reaction of bulk glass in alkaline solution (particularly NaOH) has been studied in depth, unlike fibrous glass. The reaction of glass fibres with alkaline solution has mainly been investigated with regards to how their mechanical properties are affected. From the bulk glass studies, it is proven that the dissolution rate increases as a function of alkaline solution temperature, concentration and treatment time. It is also widely accepted that NaOH is the most corrosive alkaline solution towards glass. The nature of the silica can also have an effect on the dissolution rate, as the crystalline form (known as quartz) is more resistant to alkaline attack. In some experiments, the kinetic data was fit into various solid-state models to determine the rate limiting step of the dissolution reaction. The shrinking core model seems to be the best fit for some of the data in the literature, indicating that the diffusion of hydroxide ions through the product layer on the glass surface is likely to be the rate limiting step of the reaction. Other kinetic factors such as reaction order and activation energy have been reported widely in the literature. The values can differ greatly in each study because of the variation in the form of silica used and the nature of the alkaline solution, as well as other parameters such as the temperature of the reaction system.

4.3 Experimental

This section details the experimental procedure followed to measure the dissolution rate of the glass fibres in alkaline solutions. The process was mentioned briefly in Chapter 3 but is described in more depth here.

4.3.1 Materials

Boron-free E-glass fibres supplied by Owens Corning (OC) were used in this study. These OC fibre rovings were manufactured on a pilot scale bushing and received as 20 kg continuous single end square edge packages. Each roving had a nominal tex of 1200 and a nominal fibre diameter of 17 μm . The fibres were sprayed with water after production; these fibres are therefore commonly referred to as 'water-sized' or 'bare'. Mechanical properties of these fibres at room temperature are reported elsewhere [47]. The chemicals used in this project were purchased from Sigma Aldrich and included NaOH pellets, KOH flakes (both at commercial grade), and standard 37% concentrated hydrochloric acid (HCl).

4.3.2 Single fibre treatment in alkaline solution

Glass fibres were treated individually in alkaline solution whilst varying particular reaction parameters such as temperature and concentration of solution and treatment time. Figure 4.4 shows a schematic of the fibre sample preparation for alkaline treatment.

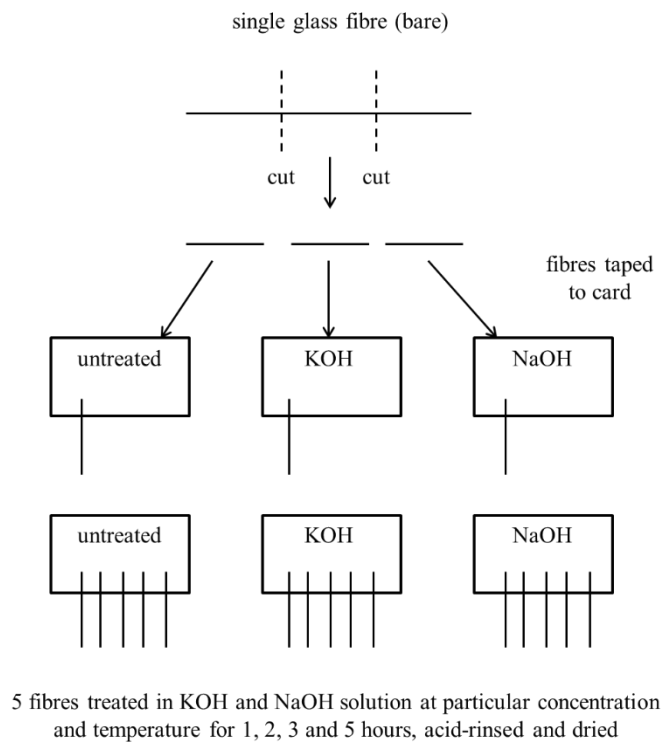


Figure 4.4 – Schematic showing the fibre sample preparation for alkaline treatment

Each fibre was cut into three portions; the first portions were the control (untreated) fibres and the other two portions were the fibres to be treated in KOH and NaOH solution at a particular set of reaction conditions which involved varying the conditions of alkaline solution as indicated in Table 4.2. Five fibre samples were prepared for treatment at each time. The fibres were mounted on labelled cards with tape, and the length of fibre immersed in alkaline solution was around 3 cm.

Table 4.2 - Alkaline treatment conditions employed for kinetic study of glass fibre dissolution

Condition	Concentration of alkaline solution (mol/L)	Temperature of alkaline solution (°C)	Treatment time in alkaline solution (hours)
1	0.5	95	1, 2, 3, 5
2	1.0	95	1, 2, 3, 5
3	1.5	95	1, 2, 3, 5
4	2.0	95	1, 2, 3, 5
5	3.0	95	1, 2, 3, 5
6	3.0	75	1, 2, 3, 5
7	3.0	80	1, 2, 3, 5
8	3.0	85	1, 2, 3, 5
9	3.0	90	1, 2, 3, 5

NaOH and KOH solutions were prepared in polypropylene containers according to the following concentrations: 0.5, 1.0, 1.5, 2.0, and 3.0 mol/L (concentration will be referred to as mol/L instead of M in this chapter as this is the notation normally used in kinetic analysis). 500 ml of solution was prepared for each treatment to fully immerse the fibres. Containers were sealed and heated to 95 °C before treating the fibre samples. The fibres were immersed in solution by mounting the cards on the inside of the container. After each treatment time, the designated fibre samples were removed from the solution, rinsed in diluted HCl (10% v/v) for 10 minutes, followed by rinsing with deionised water for one minute. The purpose of this rinsing procedure, particularly with acid, was to ensure the effective removal of any residual deposits which could have remained on the fibre surface at the end of the alkaline treatment [21]. In addition, previous experimentation did not show any significant change in glass fibre diameter after this acid rinsing procedure alone. Once the fibres were rinsed after alkaline treatment, they were left to dry in an oven at 110 °C for 15 minutes. By varying the concentration of solution (0.5 - 3.0 mol/L) at a constant temperature of 95 °C, the kinetic data can allow the determination of the reaction order with respect to KOH and NaOH. Furthermore, the variation of solution

temperature (75, 80, 85, 90 and 95 °C) at a constant concentration of 3 mol/L means the activation energy of the reaction of glass fibre with alkaline solution can be calculated.

4.3.3 Scanning electron microscopy (SEM)

After alkaline treatment, fibres were mounted on an SEM plate. A HITACHI SU-6600 field emission scanning electron microscope (FE-SEM) was used for measuring the diameters of the fibres. Samples were coated in gold using an Edwards S150 sputter coater in order to prevent charge build-up as glass fibres are non-conductive. The gold coating is normally a few nanometres thick and is negligible with respect to the fibre diameter change observed in this work. The electron beam was rotated so that the fibre was as horizontal as possible in order to measure fibre diameter through automatic scaling of the SEM. SEM images were captured at an accelerating voltage of 15 kV and extraction voltage of 1.8 kV. An example of how a fibre was measured for its diameter is shown in Figure 4.5.

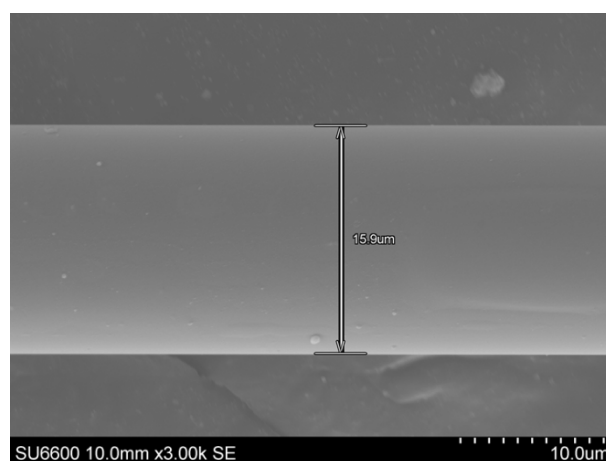


Figure 4.5 – SEM image of a fibre being measured for its diameter

Once the diameter measurements were made under SEM, the fibre diameter reduction was determined (as a fraction) for each reaction condition using Equation 4.10.

$$\Delta D = \frac{D_o - D_t}{D_o}$$

Equation 4.10

D_0 is the initial fibre diameter (untreated) and D_t is the diameter after treatment of the fibre in alkaline solution for time t . The diameters of around five different fibres were measured, and for each fibre, measurements of diameter were made at three different points (although it was found that the diameter was consistent throughout the length of the fibre). The diameters of each fibre were then averaged to give the average fibre diameter reduction for a particular reaction condition (for example 3 mol/L NaOH, 95 °C, 1 hour).

4.4 Results and discussion

4.4.1 Effect of alkaline solution concentration on diameter reduction of glass fibres

Figure 4.6 shows the fibre diameter reduction of the glass fibres following treatment in KOH solution at 0.5, 1.0, 1.5, 2.0 and 3.0 mol/L for 1, 2, 3 and 5 hours, with a constant KOH solution temperature of 95 °C. The error bars used for measurements of diameter reduction show 95% confidence limits.

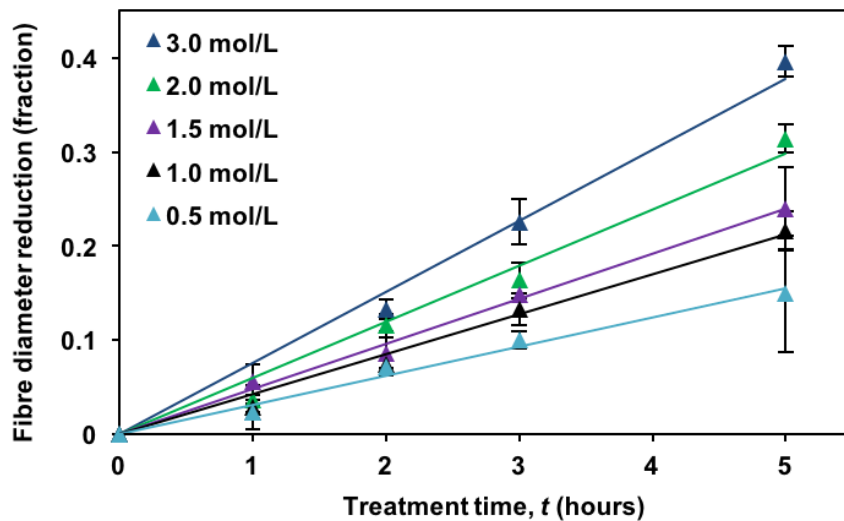


Figure 4.6 - Diameter reduction in glass fibres after treatment in KOH solution at various concentrations and times

From Figure 4.6 it is clear that for each KOH solution concentration the fibre diameter reduction increases at a constant rate with time, though in some cases there seems to be an induction period before this linear increase. In addition, the diameter reduction for each treatment time appears to increase with KOH solution concentration. The fact that the diameter reduction increases at a constant rate with time means the slope of the line can be used to denote the rate of fibre diameter reduction.

Figure 4.7 shows the fibre diameter reduction with time for fibres treated in NaOH at various concentrations.

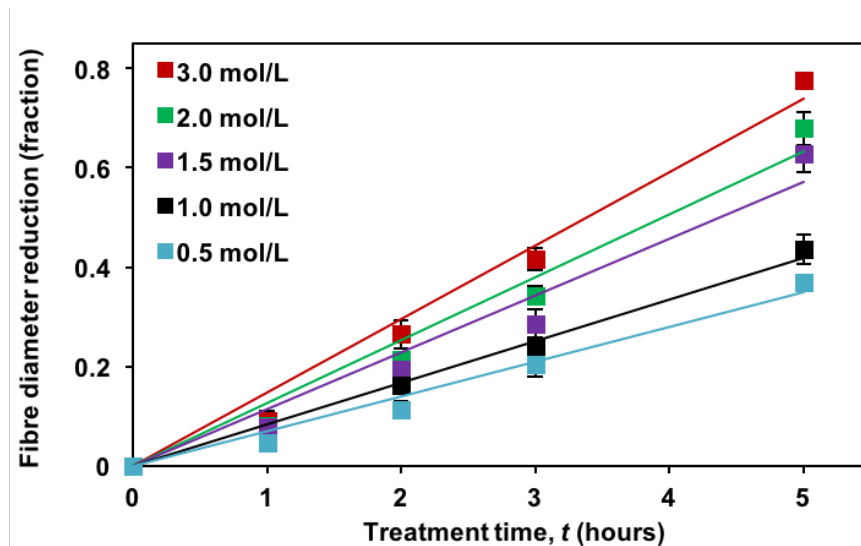


Figure 4.7 - Diameter reduction in glass fibres after treatment in NaOH solution at various concentrations and times

Figure 4.7 presents overall a similar trend to that for KOH in Figure 4.6 as the diameter reduction increases linearly with time, and the rate increases as a function of concentration.

The glass dissolution process in hot KOH and NaOH solutions involves many elementary steps; the hydroxide ions initially have to diffuse through the bulk solution phase, and eventually some of these ions would come into contact with the localised glass surface and potentially react. It is therefore the interaction of the hydroxide ions with the glass surface which results in glass fibre dissolution/diameter reduction. From these experimental results it is clear that the rate of dissolution of the glass fibres increases with solution concentration. This could be due to more hydroxyl ions being able to collide with the glass fibre surface with enough energy to result in a reaction, as there was an increased concentration in the bulk phase originally.

Figure 4.8 summarises the effect of solution concentration of KOH and NaOH on the rate of fibre diameter reduction.

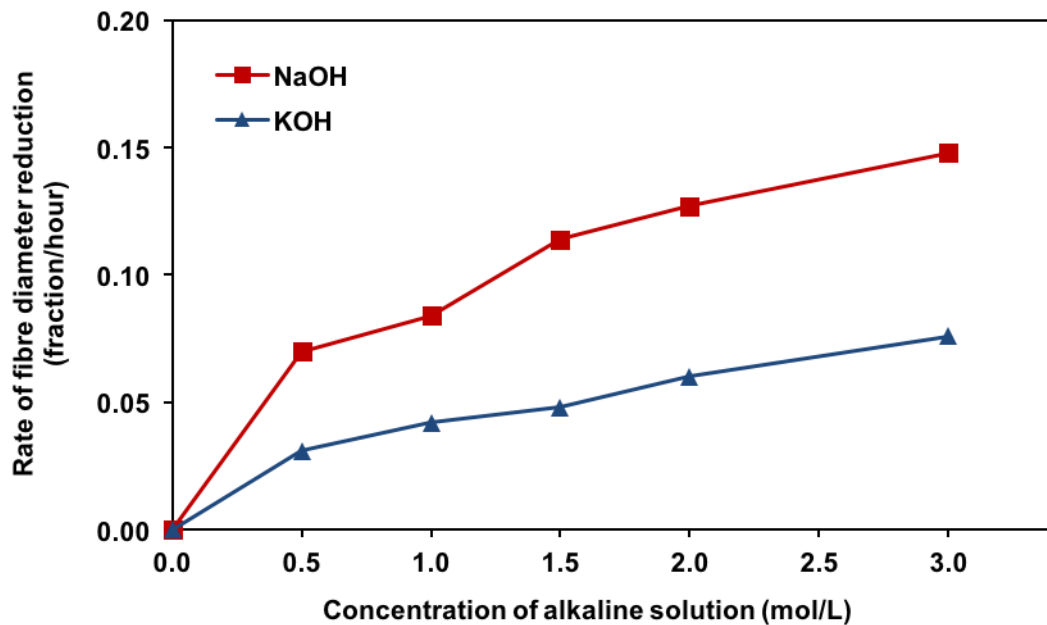


Figure 4.8 - Rate of diameter reduction in glass fibres after treatment in KOH and NaOH solution at various concentrations

It can be observed from Figure 4.8 that the rate of diameter reduction increases with the concentration of KOH and NaOH solution. In addition, it appears that the diameter reduction rate in NaOH solution is approximately double that in KOH solution at a given concentration. This suggests that NaOH is a more corrosive E-glass fibre etchant than KOH and this is consistent with previous investigations concerning bulk glass [17, 93, 96]. The disparity in behaviour of KOH and NaOH with E-glass fibre is clear in Figure 4.9, which shows SEM images of a fibre untreated and after treatment in 3 mol/L KOH and NaOH for 5 hours at 95 °C.

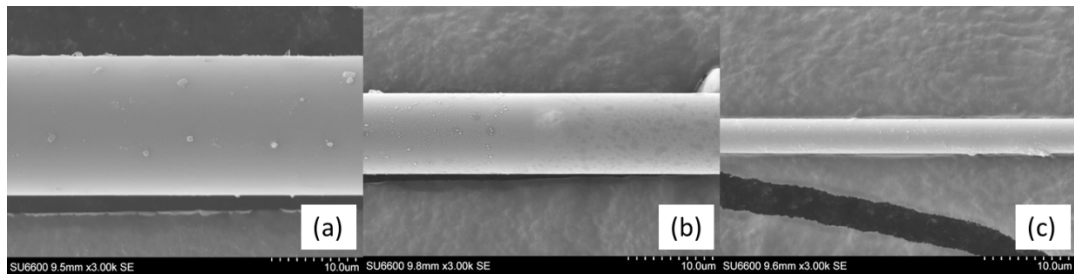


Figure 4.9 - SEM images of glass fibre (a) untreated (16.5 µm), (b) treated in 3 mol/L KOH at 95 °C for 5 hours (9.7 µm) and (c) treated in 3 mol/L NaOH at 95 °C for 5 hours (3.5 µm)

NaOH and KOH are considered to be strong bases as they completely dissociate into the metal cations and hydroxide anions in water. Some early studies suggest, however, that NaOH does not completely dissociate [93-95]. Observations here with E-glass fibre and previous studies with bulk glass [17, 93, 96] show NaOH is the most corrosive alkali towards glass, not KOH. The reason for this is seldom explained, though it is suggested it could be due to the reaction products from NaOH and glass being formed more readily and more exothermally [93]. Another possible theory is that the smaller Na^+ ions have a stronger attraction to OH^- ions in solution, which reduces the likelihood of OH^- ions to interact with neighbouring water molecules and as a result they are more likely to come into contact with the glass [97].

4.4.2 Effect of alkaline solution temperature on diameter reduction of glass fibres

Figure 4.10 displays a plot of the fibre diameter reduction of glass fibres after treatment in KOH solution for 1, 2, 3 and 5 hours at a constant concentration of 3 mol/L, whilst varying the solution temperature (75, 80, 85, 90 and 95 °C).

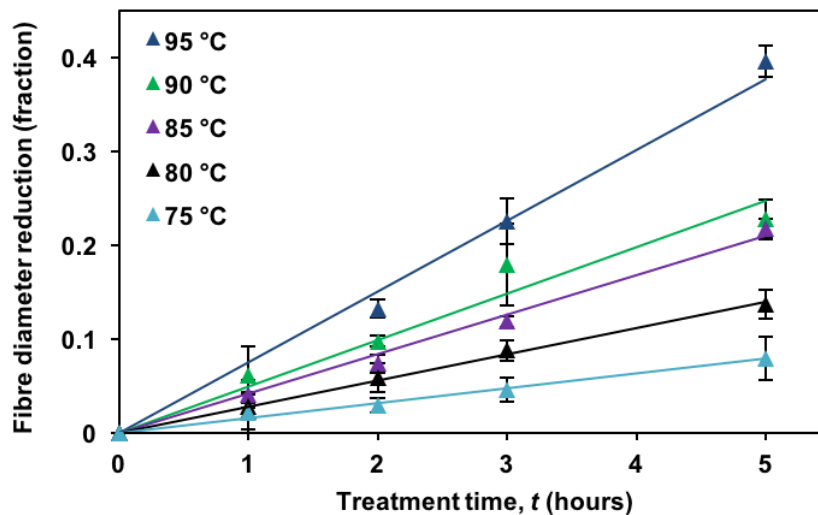


Figure 4.10 - Diameter reduction in glass fibres after treatment in KOH solution at various temperatures and times

For each temperature it is evident the diameter reduction increases at a constant rate with time. As a result, the gradient from plotting the diameter reduction against time at each temperature can be used as an indication of the rate at which the glass fibre has reacted with the solution. It is clear from the results in Figure 4.10 that the reaction rate is increased by raising temperatures.

Figure 4.11 shows the diameter reduction of glass fibres after treatment in NaOH solution at 75 - 95 °C for 1, 2, 3 and 5 hours.

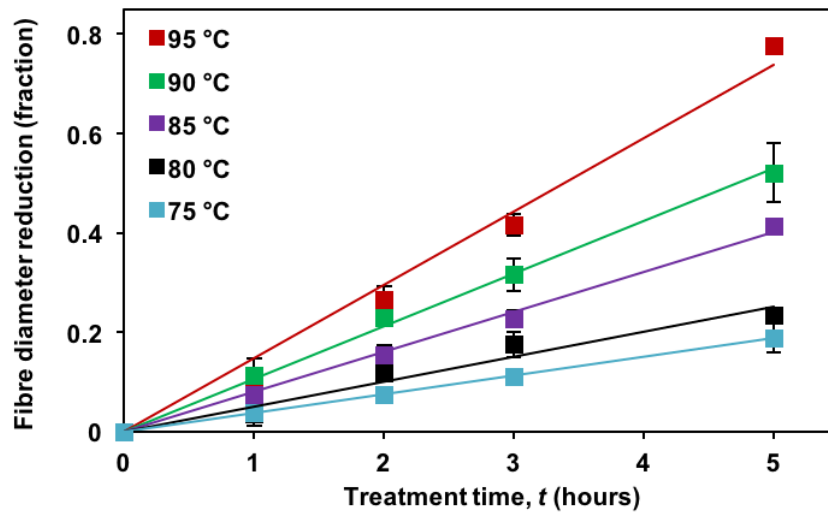


Figure 4.11 - Diameter reduction in glass fibres after treatment in NaOH solution at various temperatures and times

Similar to the case of KOH in Figure 4.10, there is a constant increase in the fibre diameter reduction with time at a given solution temperature and reaction rate increases as temperature increases. Figure 4.12 gives the rate of fibre diameter reduction against the temperature of KOH and NaOH solution.

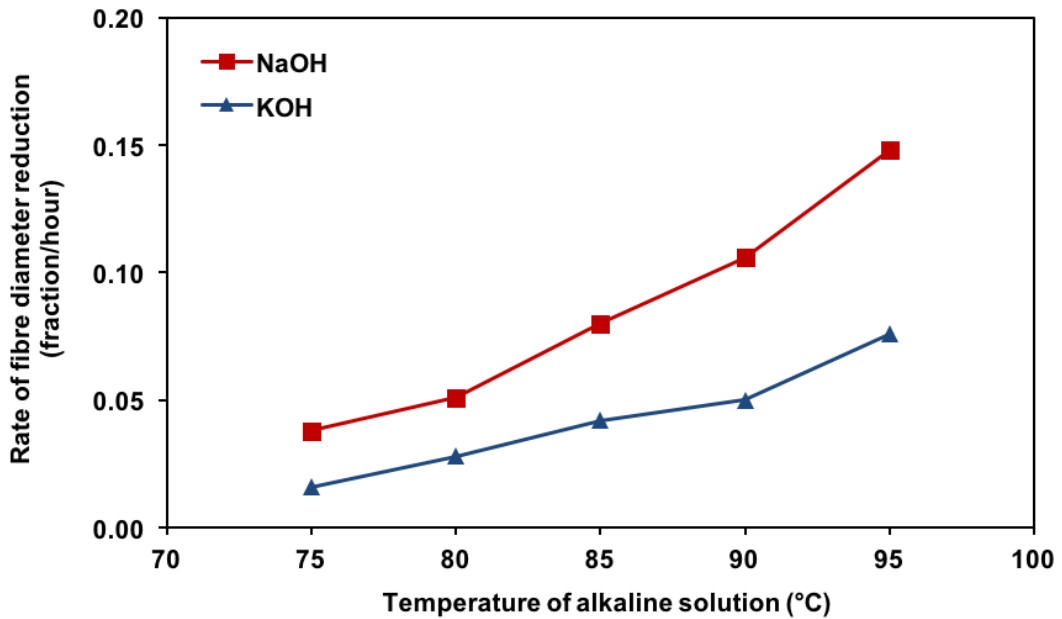


Figure 4.12 - Rate of diameter reduction in glass fibres after treatment in KOH and NaOH solution at various temperatures

It is shown both for KOH and NaOH treated glass fibres that increasing the solution temperature results in an increase in the rate of diameter reduction. Again, it appears that NaOH overall reduces the glass fibre diameter up to twice the magnitude of KOH for each solution temperature.

In order for a reaction to occur, reactants must not only collide with each other, but the collision needs to possess enough energy to overcome the activation barrier of the reaction; this is referred to as the activation energy (E_a), and can be determined from the Arrhenius equation. As the temperature increases, the hydroxide anions gain more kinetic energy and therefore there will be statistically more collisions with enough energy to result in a reaction. On the other hand, the level of temperature variation in the present work would have little influence on the kinetic energy of the glass network as it is in the solid-state.

4.4.3 Modelling of glass fibre dissolution in alkaline solution

E-glass fibre is composed mainly of silica, which forms a complex network. Al_2O_3 can also form part of this network structure. When the E-glass fibre is immersed in the hot concentrated alkaline solution, the hydroxide ions break down the silicate and aluminate network. Due to their basic nature, CaO (which is the second largest E-glass component) and MgO may not react directly with KOH or NaOH but they are soluble in the alkaline solution, resulting in further disruption of the glass network structure. It is thought that the breakdown of the silicate network is a key process of the reaction of E-glass fibre with alkaline solution, and the dispersion of network modifiers such as CaO into solution can also contribute to the fibre dissolution and diameter reduction. Gin et al. [116] proposed that ion-exchange was the dominant process in the reaction of bulk glass with alkaline solution prepared at pH 9 at 90 °C, and at higher concentrations (pH 11.5) there was a rapid dissolution of the glass due to hydroxide attack. The solutions in this work were prepared at a pH above 14, in which case the hydrolysis of the glass network is believed to be a more dominating process of the reaction than ion-exchange.

As discussed previously, various kinetic models have been developed to describe solid-liquid reactions. The models that are relevant for this work are the zero order, shrinking cylinder, and 2-D (cylindrical) diffusion models. The zero order model refers to the diffusion of hydroxide ions through the solution, the shrinking cylinder model describes the hydroxide attack at the glass surface leading to diameter reduction, and the 2-D diffusion model represents the diffusion of hydroxide ions through the product layer on the glass surface, which impedes the dissolution process. The model with a more linear fit for the experimental data in this work will indicate what was most likely to have been the rate controlling factor of the glass fibre dissolution reaction. Figure 4.13 gives an example of model-fitting for the case

of glass fibre treatment in 3 mol/L KOH and NaOH at 75 °C for 1, 2, 3 and 5 hours. The value of α was calculated from the fibre diameter reduction at each treatment time using Equation 4.4, and these values were inserted into the models (Equation 4.5, Equation 4.6 and Equation 4.8) and plotted against treatment time t . A linear fit indicates that particular model best describes the glass fibre dissolution process.

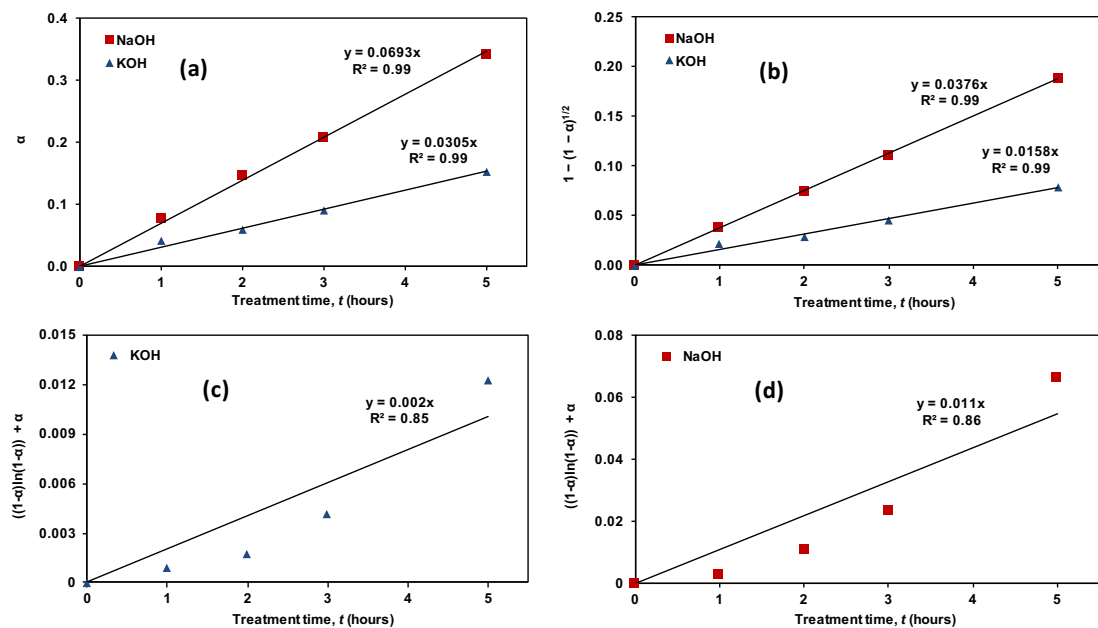


Figure 4.13 - Fitting of kinetic data for 3 mol/L KOH and NaOH treatment of glass fibres at 75 °C in (a) zero order model, (b) shrinking cylinder model, (c) 2-D diffusion model (KOH), (d) 2-D diffusion model (NaOH)

From Figure 4.13 it is clear both the zero order and shrinking cylinder models show an excellent fit, suggesting either the diffusion of OH^- ions through the solution or the glass fibre etching itself (fibre diameter reduction) could have been rate controlling factors. The fact that the data fit well in both the zero order and shrinking cylinder models indicates the diffusion of hydroxide ions through the solution and the etching process could both have occurred at a similar rate.

Conversely the non-linearity of the plots in Figure 4.13c and Figure 4.13d implies the 2-D diffusion model does not describe the reaction well, and suggests the product layer present on the fibre surface was very thin or small amounts of product was built up on the surface since individual fibres were treated in alkaline solution. As a result, the diffusion of OH^- ions through the thin product layer on the glass fibre was likely to have occurred at a rapid rate (in other words, not a rate determining step). This trend with model-fitting was observed for all other alkaline treatment conditions. When the glass fibres reacted with the alkaline solution, a product layer was formed on the surface. This product layer was likely to have been comprised of sodium or potassium silicates, depending on whether NaOH or KOH was employed. Due to the extremely corrosive solution and the solubility of these silicates, it was likely that the product layer was constantly removed during the treatment duration; it was unlikely that the product layer increased in thickness to impede the glass dissolution reaction. During the acid rinsing procedure, any remnants of residue and product layer were effectively removed to allow an accurate measurement of the fibre diameter with SEM.

The data obtained from a mass loss study of fibre bundles, treated in 3 M KOH and NaOH solution at 95 °C for various times, was also fit into the solid-state kinetic models (see Chapter 3 for more information on the experimental). In contrast with the data in this chapter on individual fibres, the kinetic data from treating fibre bundles in alkaline solution seem to fit best in the 2-D diffusion model, particularly for KOH treated samples (see Figure 4.14). This suggests that the diffusion of hydroxide ions through the product layer was likely to have been the rate limiting step when fibres were treated in alkaline solution in the form of bundles as opposed to individual fibres. The fact that the 2-D diffusion model shows the best fit for glass fibre bundle treatment in alkaline solution also indicates that the product layer on the

glass fibre surface in the bundle increased in thickness with time. The build-up of the product layer was probably because the fibres were close together in a bundle and therefore it was not peeled off easily in the solution. As a result, the hydroxide ions had to diffuse through a product layer that was building up with time, leading to a reduced rate of dissolution of the glass. The significant build-up of residue on fibre bundles after alkaline treatment was shown through SEM imaging in Chapter 3; in particular, the bundles treated for several hours showed the residual deposits merge into a film that completely covered the fibres.

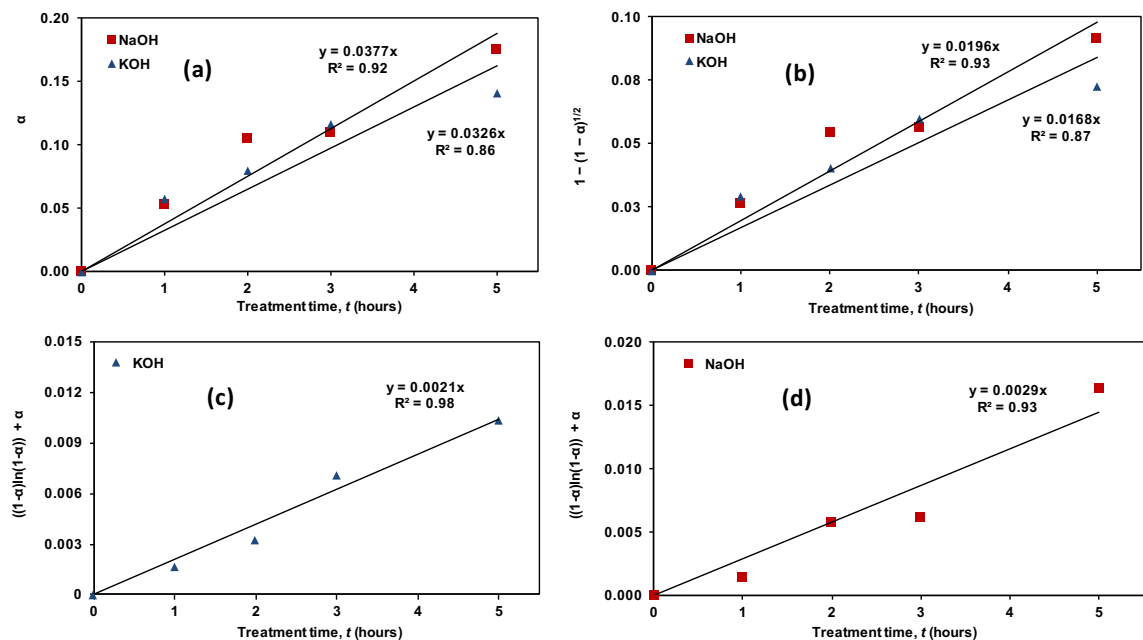


Figure 4.14 - Fitting of kinetic data for 3 mol/L KOH and NaOH treatment of glass fibre bundles at 95 °C in (a) zero order model, (b) shrinking cylinder model, (c) 2-D diffusion model (KOH), (d) 2-D diffusion model (NaOH)

The next section shows how the dissolution data of the individual glass fibres in alkaline solution can be used to determine the reaction order (with respect to the alkali) and the activation energy of the reaction.

4.4.4 Determination of reaction order and activation energy

By conducting glass fibre treatments in various concentrations of alkaline solution, the reaction order with respect to KOH and NaOH and their associated rate constants can be determined. These parameters are related according to Equation 4.11.

$$r = k S [OH^-]^n$$

Equation 4.11

$[OH^-]$ is the initial concentration of alkaline solution in mol/L and the superscript, n , is the reaction order with respect to OH^- . S is the initial glass surface area, and k is the rate constant. The linear fit of the experimental data in this work in the zero order and shrinking cylinder model means the reaction rate r (also denoted as initial reaction rate) from both models can be used. Note the zero order model refers to the reaction being zero order with respect to the glass. To determine the rate constant k and the reaction order with respect to KOH and NaOH (n), the natural logarithm is taken of both sides of Equation 4.12.

$$\ln(r) = n \ln[OH^-] + \ln(kS)$$

Equation 4.12

Figure 4.15 shows how to obtain the reaction order through the use of Equation 4.12; $-\ln(r)$ is plotted against $\ln[\text{OH}^-]$, where $[\text{OH}^-]$ refers to the concentration of the KOH solution. The r values for each KOH concentration are presented numerically in Table 4.3.

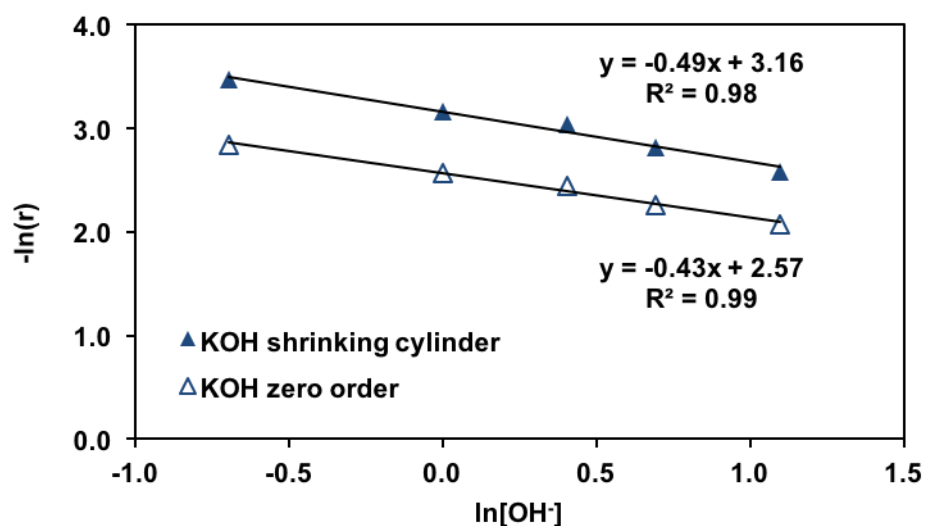


Figure 4.15 - Plot to determine reaction order with respect to KOH through curve fitting

Table 4.3 - Rate of reaction (r) of glass fibre with KOH and NaOH solution at various concentrations and constant temperature (95 °C)

Concentration of alkaline solution (mol/L)	Reaction rate, r (%/hour)			
	KOH		NaOH	
	zero order	shrinking cylinder	zero order	shrinking cylinder
0.5	5.8	3.1	11.9	7.0
1.0	7.7	4.2	13.8	8.4
1.5	8.6	4.8	17.0	11.4
2.0	10.4	6.0	18.2	12.6
3.0	12.6	7.5	20.1	14.7

Clearly the reaction rate increases as a function of KOH solution concentration, and the data shows a linear fit; the slope of the line gives the reaction order with respect to KOH (n), which are 0.43 and 0.49 for the zero order and shrinking cylinder plots respectively. The intercepts of the linear regression give the values of the product of rate constant and initial surface area of the fibre. Using the specific surface area of the glass fibre ($0.092 \text{ m}^2/\text{g}$) in place of S , the value of the rate constant k equals to $1.3 \times 10^{-4} \text{ g}/(\text{m}^2.\text{s})$ using the shrinking cylinder model and $2.4 \times 10^{-4} \text{ g}/(\text{m}^2.\text{s})$ using the zero order model.

Figure 4.16 shows the use of Equation 4.12 to find the reaction order, this time, for NaOH (numerical data presented in Table 4.3).

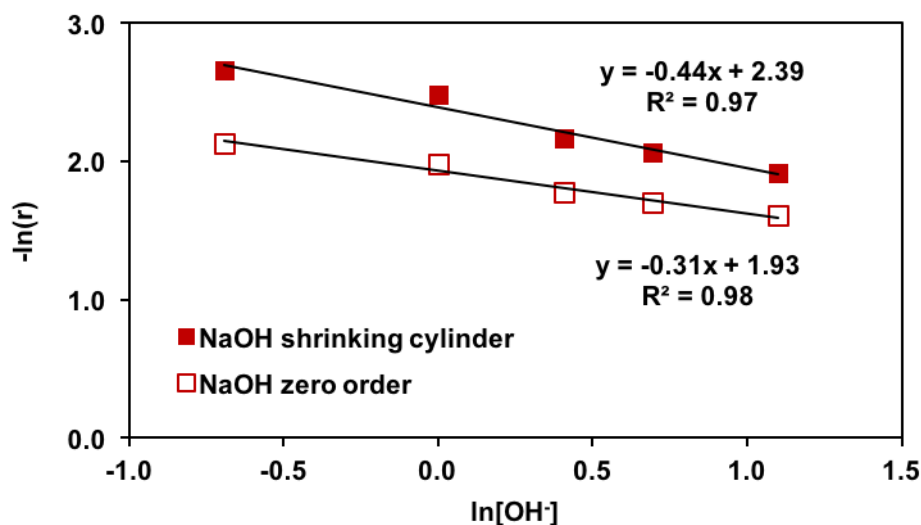


Figure 4.16 - Plot to determine reaction order with respect to NaOH through curve fitting

It can be seen from the gradients of the lines that the reaction order is 0.31 with the zero order model and 0.44 for the shrinking cylinder model. The reaction order from the shrinking cylinder equation is slightly lower than what is observed for KOH. The

zero order model for the reaction of NaOH with glass gives a significantly lower reaction order of 0.31 compared to KOH, which suggests that increasing the concentration of NaOH did not increase the rate of diffusion of hydroxide ions to as much an extent as for KOH. Because the hydroxide ions are strongly attracted to Na cations (due to their smaller atomic radius than K), there could have been less interaction between the hydroxide ions and neighbouring water molecules [97]. This could explain why the diffusion of hydroxide ions from NaOH through the solution might already have been quite high, which consequently resulted in a greater dissolution rate of the glass compared to when KOH was used. Reaction orders of 0.43 – 0.49 for KOH and 0.31 – 0.44 for NaOH are fairly consistent with the value reported by Jendoubi et al. [112] of 0.47 when reacting silica sand and aqueous NaOH. From these calculated reaction orders it can be said that doubling the concentration of alkaline solution leads to an increase in reaction rate by around 1.38 for KOH, and 1.30 for NaOH. Furthermore, the rate constant for glass fibre treatment in NaOH at 95 °C is found to be $2.7 \times 10^{-4} \text{ g}/(\text{m}^2 \cdot \text{s})$ from the shrinking cylinder model and $4.3 \times 10^{-4} \text{ g}/(\text{m}^2 \cdot \text{s})$ from the zero order model. Note the prediction of the reaction rate at any alkaline solution concentration can be achieved using the correlating equations given in Figure 4.15 and Figure 4.16, or alternatively the non-logarithm form in Equation 4.11 with using k_S .

As well as determining the reaction order for KOH and NaOH in the glass fibre dissolution process, the activation energy (E_a) may be calculated through the application of the Arrhenius equation (Equation 4.13).

$$k = A e^{\frac{-E_a}{RT}}$$

Equation 4.13

A is the pre-exponential factor, R is the gas constant (8.314 J/(mol. K)) and T is the absolute temperature. The E_a value can be calculated through graphing similar to what is shown in Figure 4.15 and Figure 4.16. Firstly, the natural logarithm is taken of both sides of Equation 4.13 to convert it to Equation 4.14.

$$\ln(k) = \left(\frac{-E_a}{R}\right) \frac{1}{T} + \ln(A)$$

Equation 4.14

The rate constant, k, can be calculated for each temperature change using Equation 4.11. The value of k after treatment of glass fibres in 3 mol/L KOH and NaOH solutions at different temperatures is presented in Table 4.4.

Table 4.4 - Rate constant (k) of glass fibre reaction with KOH and NaOH solutions at various temperatures and constant concentration (3 mol/L)

Temperature of alkaline solution (°C)	Rate constant, k ($\times 10^{-4}$ g/(m ² .s))			
	KOH		NaOH	
	zero order	shrinking cylinder	zero order	shrinking cylinder
75	0.6	0.3	1.5	0.7
80	1.0	0.5	2.0	0.9
85	1.4	0.7	2.9	1.5
90	1.7	0.9	3.6	2.0
95	2.4	1.3	4.3	2.7

To obtain the activation energy, $\ln(k)$ is plotted against the reciprocal of T ($\times 10^3$), as shown in Figure 4.17 with the case of glass fibre treatment in KOH.

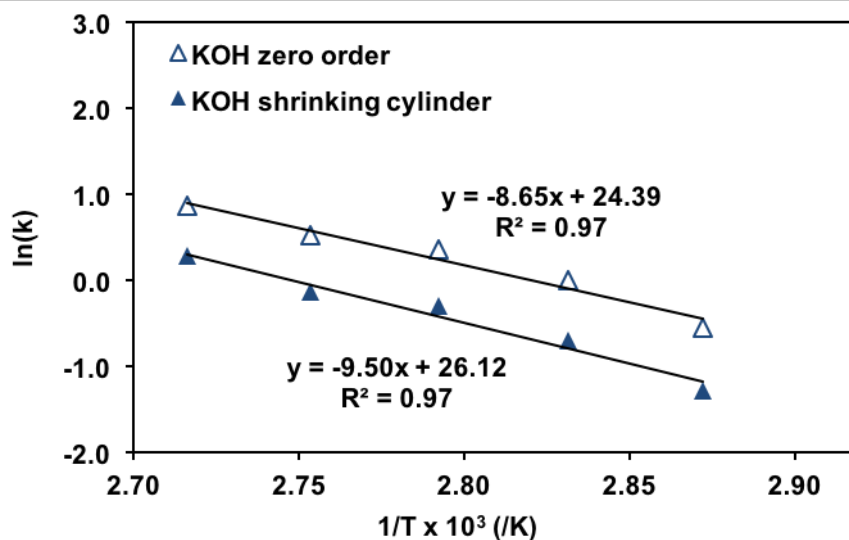


Figure 4.17 - Plot to determine activation energy for glass fibre reaction with KOH through curve fitting

It was observed previously in Figure 4.12 that as the temperature of the alkaline solution increases, so does the rate of fibre diameter reduction. Taking the natural

logarithm of the rate constant and plotting against the reciprocal of solution temperature (in Kelvin) results in a straight line, as shown in Figure 4.17 when using k values from both the zero order and shrinking cylinder models. Because $1/T$ is already multiplied by 10^3 , the slope of the line ($-E_a/R$) is simply multiplied by the gas constant R to obtain E_a directly in kJ/mol. The activation energy for the reaction of glass fibre with KOH solution is therefore calculated as 72 kJ/mol (using k values from the zero order model) and 79 kJ/mol (using k values from the shrinking cylinder model). It is apparent that the activation energies are similar when rate constants are used from both models. The values are comparable with some of those in the literature concerning the reaction of bulk silicate glass with alkaline solution [96, 111].

The plots of $\ln(k)$ against $1/T$ ($\times 10^3$) for glass fibres treated in 3 mol/L NaOH and the raw numerical data are displayed in Figure 4.18 and Table 4.4 respectively.

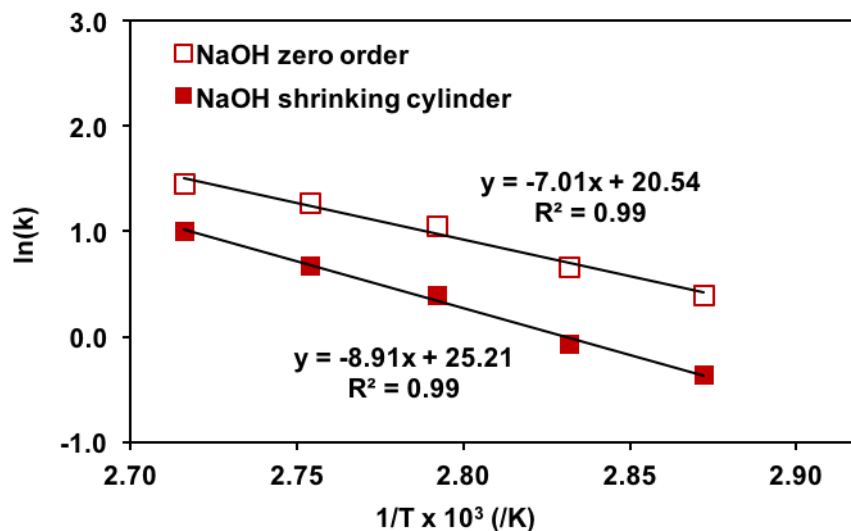


Figure 4.18 - Plot to determine activation energy for glass fibre reaction with NaOH through curve fitting

Similar to KOH, the plots are linear in nature and the gradients are multiplied by the gas constant to give activation energies of 58 kJ/mol (using k values from the zero order model) and 74 kJ/mol (using k values from the shrinking cylinder model). On this occasion there is a disparity in the calculated activation energy when using rate constants from the two models. The activation energy of the glass fibre reaction with NaOH from the shrinking cylinder model is similar to the value given for KOH from the same model, suggesting the initiation of the glass fibre etching process required similar energy regardless whether KOH or NaOH was employed as the alkaline solution. Because the shrinking cylinder model defines the glass fibre etching mechanism, which results in fibre diameter reduction, it makes sense to use the activation energy obtained from this model as the activation energy of the reaction of glass fibre with alkaline solution. The activation energy given from the zero order model for glass fibre treatment in NaOH is significantly lower than for KOH; this suggests less energy was required for the diffusion of hydroxide ions through the solution if they originated from NaOH. This is unusual considering both KOH and NaOH should effectively have dissociated into metal cations and hydroxide anions in solution; in fact the dissociation constant for NaOH was expected to have been slightly lower. This shows how the nature of the metal cation could have played a significant role in the diffusion of the hydroxide ions through the solution, which consequently had an effect on the dissolution rate of the glass fibres. Overall, the activation energies obtained from the reaction of glass fibre with KOH and NaOH solutions are similar to those reported in previous studies, although the value of 28 kJ/mol for the reaction of diatomite with NaOH is lower [115], and 159 kJ/mol, given by Molchanov and Prikhidko [16] for the dissolution of quartz in NaOH solution is significantly high; this comes as no surprise given that quartz is a crystalline form of silica and is therefore more stable towards hydroxide attack.

4.4.5 Correlating fibre diameter reduction with strength

Strength recovery treatments conducted in previous works [11, 13, 14] and in this thesis (Chapter 3) were of fibre bundles coated with an APS sizing and then heat treated (HT) to temperatures between 450 and 600 °C to simulate thermal recycling procedures for GRP waste. The etching rate predicted for individual bare fibres at short treatment times from this study can be correlated to strength increase of HT glass fibre bundles after KOH and NaOH treatment at various times and solution concentrations (reported in Chapter 3), with the following assumptions: 1) heat treatment resulted in the removal of the APS sizing from the bundles, leaving a fairly clean glass surface similar to bare fibre (with the exception that silicate groups from the APS would remain on HT fibres, however E-glass fibre is mainly silicate-based anyway), and, 2) although the etching rate of individual fibres is not directly comparable to that of fibre bundles, it was expected that the increase in severity of alkaline treatment conditions (by increasing the molarity for example) would have resulted in an increase in fibre diameter reduction of fibre bundles, like what was observed with individual fibres but on a different scale. It is worth bearing in mind the glass fibre bundles used for comparison with the etching rate data in this study were treated in KOH and NaOH at a constant temperature of 95 °C but with varying the molarity and treatment duration. The effect of solution temperature and other reaction parameters on the strength recovery of fibres has not been carried out, but could be the subject of future work. In this section, the fibre diameter reduction (conversion according to the shrinking cylinder model) is predicted of individual fibres after short treatment times and compared to the strength recovery of the bundles under the same alkaline treatment conditions (shown earlier in Chapter 3). For KOH, the reaction conditions for bundle treatments were 5, 10, 20, 30 and 120 minutes at molarities of 1.5, 3.0 and 5.0 mol/L. Due to the narrower operational

window of NaOH, a treatment time of 2 minutes was investigated, along with 5, 10, 30 and 120 minutes at the same solution concentrations as for KOH. Note one of the molarities used for treatment of bundles was 5 mol/L, which was too corrosive for the kinetic experiment with single fibres; almost 100% conversion of the individual fibres was observed after immersion in 3 mol/L NaOH solution for 5 hours. Despite the absence of kinetic data for 5 mol/L alkaline solution, the equations given in Figure 4.15 and Figure 4.16 allow the prediction of the etching rate at any molarity.

Figure 4.19 shows the strength recovery (%) of HT glass fibre bundles treated in KOH at various solution molarities and treatment durations, plotted against the predicted conversion from the shrinking cylinder model of single fibres at the associated conditions.

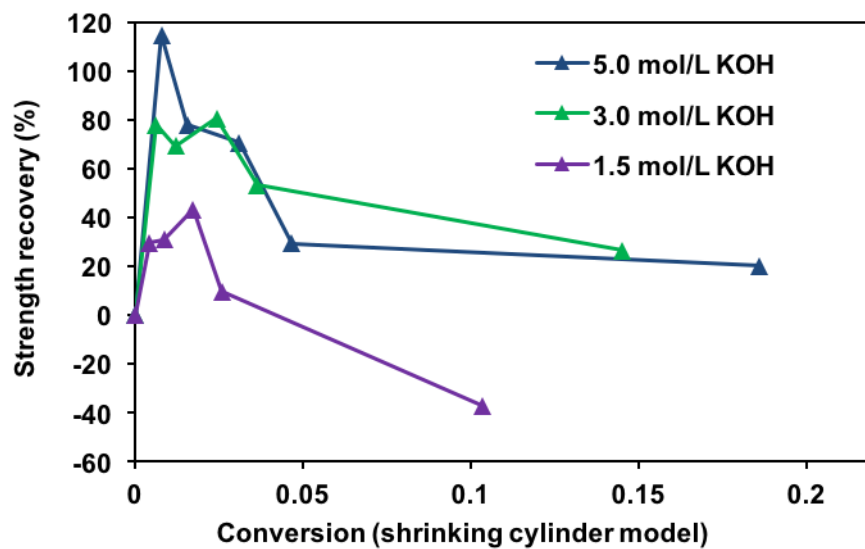


Figure 4.19 - Plot of strength recovery (%) of HT fibre bundles against conversion (shrinking cylinder model) of single fibres after KOH treatment at various conditions

Strength recovery is almost at 120% for fibres treated in 5 mol/L KOH for 5 minutes, and the corresponding etching rate appears to be fairly low (nearly 0.01 conversion). With the exception of this value, the strength increase seems to be around 80% for both 3.0 and 5.0 mol/L treatment up to a conversion of nearly 0.03. Beyond this point, the strength of the bundles begins to decrease abruptly. For 1.5 mol/L KOH treatment the optimum strength recovery is not as high, being just above 40% at a conversion of approximately 0.02 before decreasing in a similar fashion to 3.0 and 5.0 mol/L KOH.

Figure 4.20 displays the strength increase of HT fibre bundles after treatment in NaOH at different molarities and treatment times, plotted against the corresponding etching rate of single fibres.

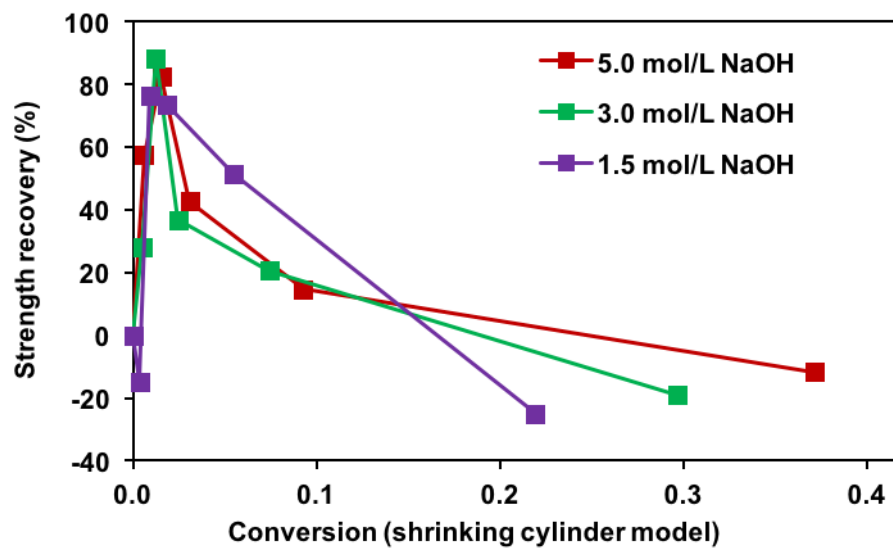


Figure 4.20 - Plot of strength recovery (%) of HT fibre bundles against conversion (shrinking cylinder model) of single fibres after NaOH treatment at various conditions

Similar to 5 mol/L KOH, the most corrosive molarity for that particular alkali, the strength recovery of fibre bundles treated in NaOH at 1.5, 3.0 and 5.0 mol/L is optimal at a short treatment time of 5 minutes (conversion of approximately 0.01 for individual fibres), being around 80 to 90%. As conversion exceeds 0.01 the treatment proves detrimental to fibre strength, as is also the case for KOH at a high molarity of 5 mol/L; at milder KOH solution concentrations the strength begins to decline after a greater conversion. Despite the fact the etching rate of bare single fibres is plotted with the strength recovery of HT fibre bundles originally coated with APS, it is evident the degree to which the fibres are etched has an effect on the resulting strength; there is an optimum range, wider for KOH given it is a milder glass etchant, where strength recovery is high. With excessive etching a decrease in fibre strength is observed, possibly due to the alkaline solution beginning to damage the bulk glass network structure. The decrease in strength is more rapid for fibres treated in NaOH, consistent with the kinetic experiments which show it to be more corrosive towards E-glass fibre than KOH.

4.5 Conclusions

The dissolution behaviour of individual E-glass fibres in high-temperature and corrosive alkaline environments was studied. The kinetic data show the diameter reduction of fibres after KOH or NaOH treatment increases fairly linearly with time. NaOH was more reactive than KOH with E-glass fibres; at times it was found that NaOH etched glass fibres up to twice the magnitude of KOH. Increasing the concentration and temperature of the alkaline solution resulted in an increase in the reaction rate. Given the alkaline solutions were highly concentrated and prepared at elevated temperatures, it is believed the hydrolysis of the glass network by OH⁻ ions

was a key mechanism in the glass fibre dissolution process. The fact that the data in this work fit best in the shrinking cylinder and zero order models indicates the etching of the glass fibre and/or the diffusion of the hydroxide ions through the solution could have been rate controlling factors. The generally poor agreement with the 2-D diffusion model implies the diffusion of the OH⁻ ions through the product layer on the glass surface was unlikely to have been a rate determining step. The reaction rates and rate constants obtained from the zero order and shrinking cylinder models were used in the determination of the reaction order with respect to the alkaline solution, and the activation energy. The reaction order was found to be 0.43 – 0.49 for KOH and 0.31 – 0.44 for NaOH. It was evident, particularly with using the rate constants from the zero order equation, that the activation energy for the reaction of E-glass fibre with NaOH (58 kJ/mol) was significantly lower than for KOH (72 kJ/mol); this suggests that the diffusion of the hydroxide ions through the solution required less energy if NaOH was employed as the corrosive medium. The fact that hydroxide ions from NaOH diffused more easily through the solution could have explained the greater dissolution of the glass fibres. In addition, the similar values of activation energy from the shrinking cylinder model for glass fibre dissolution in KOH (79 kJ/mol) and NaOH (74 kJ/mol) implies that once the hydroxide ions were at the glass surface, the energy needed to initiate the etching procedure was the same regardless of the nature of alkaline solution used. In addition, the rate constant for the reaction of glass fibre with alkaline solution at 95 °C was found to be between 1.3×10^{-4} and 4.3×10^{-4} g/(m².s). Despite the fact that strength regeneration treatments of glass fibres (results reported in Chapter 3) were done in the form of bundles, there can be a correlation between this strength recovery and the etching rate of fibres measured in the kinetic study.

5 Regenerating the performance of thermally recycled glass fibres

5.1 Introduction

Earlier in the thesis, it was discussed how the landfilling of a large volume of composite waste each year is becoming socially and economically unacceptable [11, 14]. Glass fibre is the most commonly used reinforcement material in composites; currently, it is used in over 90% of all fibre-reinforced composites produced worldwide. Much of these composites are glass fibre reinforced thermosetting polymers (GRP), which possess high specific properties and chemical resistance. These attributes result in excellent performance of the composite, but also poor recyclability. As a result, GRP materials are very often deposited in landfill sites when they are no longer fit for use. Stringent legislation in addition to rising costs associated with landfill means this method of disposal of composite waste is becoming more undesirable. Clearly there is a need for an alternative approach to deal with composite waste [3], especially given the accelerating growth in use of GRP materials particularly in the production of wind turbine blades [4].

In order to address the environmental and economic issues associated with the disposal of end-of-life composite materials, various recycling technologies have been developed [5, 6]. One of the common techniques exploited commercially is thermal treatment, where the composite is heated to elevated temperatures to degrade the polymeric matrix and allow the extraction of fibrous reinforcement. Due to the severity of the procedure, the glass fibres lose a significant amount of strength and therefore cannot be reused in various composite applications [8-10]. It was

found that dilute hydrofluoric acid (HF) solution can regenerate the strength of glass fibres thermally treated at 450 to 600 °C [11]. It is thought that HF strengthens glass by smoothing out sharp, severe surface flaws [12]. More recently, it was discovered that a similar degree of strength recovery can be achieved through treating the fibres in relatively safer alkaline solutions [13, 14]. An in-depth investigation into the effects of alkaline treatments on the strength of thermally treated glass fibres is reported in Chapter 3. From this work, a hypothesis has been developed that alkaline treatments regenerate fibre strength by etching away the damaged surfaces, similar to HF [11, 12]. It is well established in the literature that hot and concentrated alkaline solutions can dissolve bulk and pristine fibrous glass (see the literature review sections in Chapters 3 and 4). Although alkaline treatments were shown to be effective in improving strength in Chapter 3, the fibres were not thermally recycled but heated in a furnace to simulate recycling conditions. Because an in-house fluidised bed is now operational in the lab, glass fibres are able to be thermally recycled out of composite waste rather than simply being heated in a furnace.

This chapter reports on recent investigations into the effect of chemical treatments on the performance of thermally recycled glass fibres. To begin with, a literature review of recycling processes for end-of-life composite materials is presented. The properties of thermally recycled glass fibres are also discussed, as well as the work carried out previously to regenerate the performance of such fibres. In this study, glass fibres were thermally recycled out of an end-of-life wind turbine blade at approximately 500 °C, using the in-house fluidised bed. An investigation into the effects of concentrated alkaline treatments on the strength of these fibres is reported. In addition, fibres were treated in milder (pH-scale) alkaline solutions for a prolonged treatment time to determine whether strength regeneration of thermally

recycled fibres can be achieved with less chemicals. It is established that some silane coupling agents like APS are slightly alkaline [45, 46, 103, 104, 130, 131], and coupling agents are designed to improve the adhesion of the glass fibres to the polymer matrix in the composite. Because of these two characteristics of APS, coupled with the fact that hot alkaline treatments are shown to improve fibre strength, it was thought that hot APS treatments of thermally recycled glass fibres might improve both the strength and interface. Hence in this chapter the effect of hot APS treatments on the strength and interface of thermally recycled glass fibres was also carried out. For the milder alkaline treatments, the pH of the solution was adjusted with sodium hydroxide (NaOH), and measured accurately using a pH meter. Some of the recycled fibres also showed possible craters under a scanning electron microscope (SEM), and so were analysed further with atomic force microscopy (AFM). In addition, a case study into the commercial feasibility of treating recycled glass fibres in alkaline solution was conducted and reported in this chapter.

5.2 Literature review

A review of the literature concerning the properties of glass fibres thermally treated to mimic thermal recycling conditions is given in Chapter 3. This literature review focuses more on the various recycling technologies used commercially to recover glass fibres from composite waste, particularly thermal recycling processes. The properties of thermally recycled glass fibres are also discussed and work done so far in recovering the performance of such fibres is presented.

5.2.1 Methods of recycling glass fibres from end-of-life composites

A range of recycling techniques have been developed to address the environmental and economic issues associated with the disposal of composite waste, and reviews on the advantages and limitations of each recycling procedure are available in the literature [3, 5, 6, 132]. The difficulty in recycling certain composite materials often lies in the nature of the polymer matrix; thermosetting polymers (which are used to manufacture GRP composites) are cross-linked and cannot be remoulded or re-melted easily like thermoplastics [5]. Because of this, composite materials based on thermosetting polymers can be more challenging to recycle. Figure 5.1 displays the various recycling technologies available for composite waste.

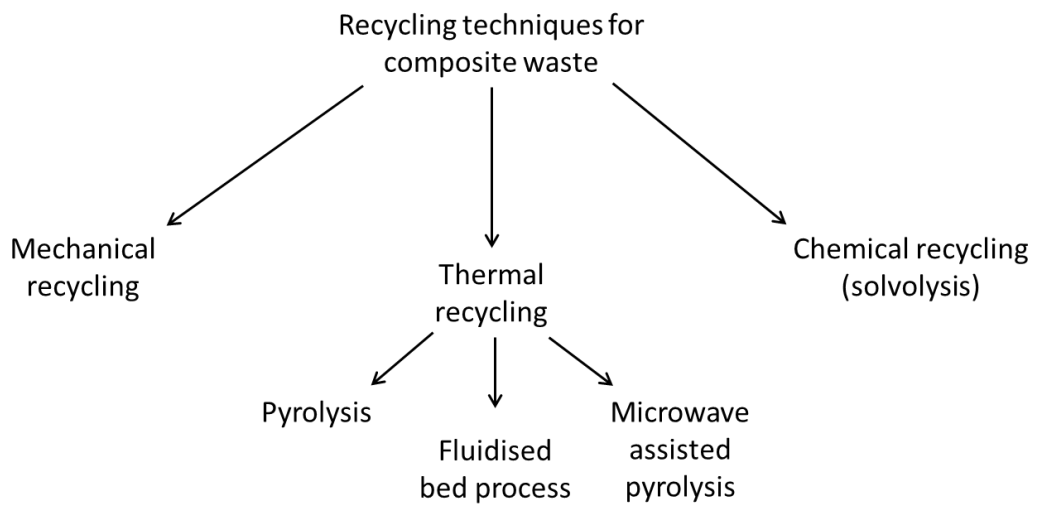


Figure 5.1 – Recycling techniques developed for composite waste

The recycling processes can be split into three main categories: mechanical, thermal, and chemical. Mechanical recycling involves crushing or shredding the composite material into smaller fragments before being ground more finely; the

recyclate can then be used as a filler or reinforcement [3, 5, 6, 132-136]. Separating the fibrous components from the matrix is difficult and is usually achievable with thermal recycling or solvolysis; however, it is argued that because of the low production cost of virgin glass fibres, mechanical recycling is a more viable option for GRPs [6]. It is worth bearing in mind that glass fibres are the most widely-used reinforcement materials in composites manufacturing, and more often glass fibre reinforced composite waste is not even mechanically recycled but goes straight to landfill. There is also a disadvantage with mechanical recycling itself, as it leads to a fine material that is limited to being used as a low grade filler or reinforcement.

Thermal recycling involves subjecting the composite waste to elevated temperatures (usually between 450 and 600 °C, at times even 700 °C) to degrade the polymeric matrix and extract the fibrous reinforcements [3-6, 132, 135-142]. In some cases, the polymeric fraction can also be reclaimed and used as a filler or energy source [5, 6, 132, 135-140, 142]. Pyrolysis, a thermal recycling process, typically involves heating the composite material in the absence of oxygen [5, 6, 132, 137, 142]. Another thermal recycling procedure, involving the use of a fluidised bed, has been developed to recover glass and carbon fibres from composite waste; research in this field has been carried out extensively by the University of Nottingham [5, 138-141]. A schematic diagram of the fluidised bed recycling process is shown in Figure 5.2.

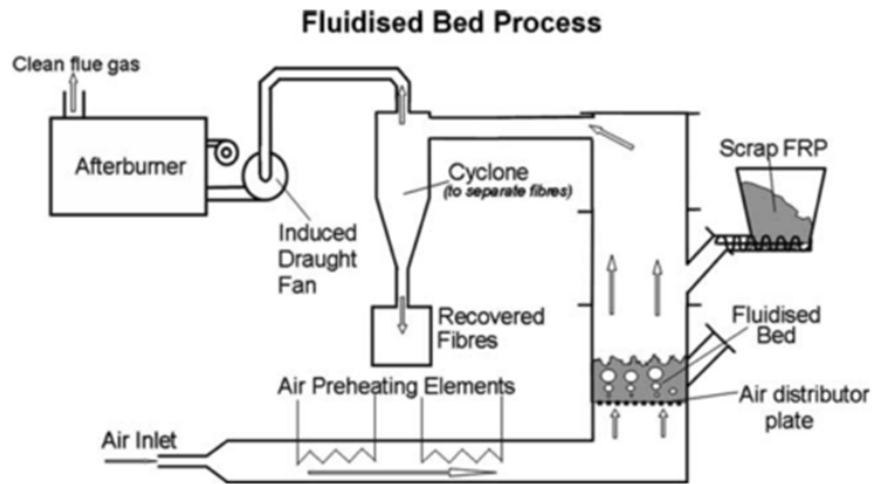


Figure 5.2 – Schematic showing the fluidised bed recycling process. Reproduced from [5]

Firstly, the composite is broken into smaller fragments before being fed into the bed, which is filled with silica sand. Hot air fluidises the sand and the polymeric component of the composite material volatilises, allowing the release and retrieval of the fibres and fillers. The hot combustion products of the polymer can then be used as an energy source [5]. The fibres recycled from this procedure are fluffy in nature with lengths ranging from 6 to above 10 mm [5]. In addition, provided the optimum fluidised bed recycling conditions are adopted, the recycled fibres tend to be cleaner compared to fibres recycled via pyrolysis. The typical temperature range used for fluidised bed recycling is 450 to 550 °C, the upper limit generally applicable to certain thermoset resins like epoxy. One of the major issues associated with this recycling technique is the strength loss of the fibres as a result of exposure to elevated temperatures and mechanical damage. More of this is discussed in the next section.

Another possible route to recovering fibres from composite waste is by degrading the polymer with chemical treatment using a solvent at a certain temperature and

pressure, with or without the aid of a catalyst [3, 6, 132, 133, 135, 136, 143]. This technique, known as solvolysis, can deliver clean fibres and usually the temperatures required are lower than those used in thermal recycling [6]. Examples of solvents that have been employed for solvolysis of composite waste include subcritical and supercritical water [6, 132]. A drawback of this recycling process can be the cost, particularly when supercritical conditions are required.

It can be said that thermal recycling is one of the most suitable recycling techniques when trying to recover fibres from composite waste. Due to the high production cost of virgin carbon fibres, more effort has been made in trying to employ these recycling technologies to retrieve carbon fibres from composite waste materials. Whilst glass fibres are relatively cheap to produce, there is a need to develop economically viable recycling methods given that glass fibre reinforced composites make up the majority of composite waste. As mentioned earlier, fibres, particularly glass fibres, can lose a significant amount of strength from thermal recycling. The next section discusses the properties of thermally recycled glass fibres in more detail, and work that has been carried out to recover their performance to allow their reuse in composite applications.

5.2.2 Properties of thermally recycled glass fibres

Significant research into the properties of glass fibres recycled from composite materials via a fluidised bed has been carried out by Kennerley et al. [138-140]. In one article, the tensile strength of individual glass fibres was measured after being recycled from scrap thermoset composites in a fluidised bed [138]. They found that fibres suffered a severe loss in strength after thermal recycling and it was concluded that a low fluidised bed temperature and short residence time of the fibres was

needed to improve their strength retention. In another publication, Kennerley et al. again reported that glass fibres lose a considerable amount of strength from fluidised bed recycling, even at 450 °C where strength is roughly half that of virgin fibres [140]. In addition, the authors found that up to 50% of the virgin glass fibres in a dough moulding compound (DMC) can be substituted with the recycled fibres without compromising the physical properties of the material [140]. Pickering et al. [141] examined the properties of glass fibres thermally recycled from a sheet moulding compound (SMC) using the fluidised bed (image of recovered fibres given in Figure 5.3).



**Figure 5.3 – Image of glass fibres recovered from SMC feed using the fluidised bed.
Reproduced from [141]**

The tensile test results of the glass fibres (results shown in Figure 5.4) indicate a decrease in strength with fluidised bed temperature. At a temperature of 450 °C, the strength is approximately half that of the virgin glass fibres, with around 90% strength reduction reported at 650 °C [141]. The strength values given by the authors agree fairly well with previous studies where glass fibres were simply heated rather than thermally recycled out of a composite.

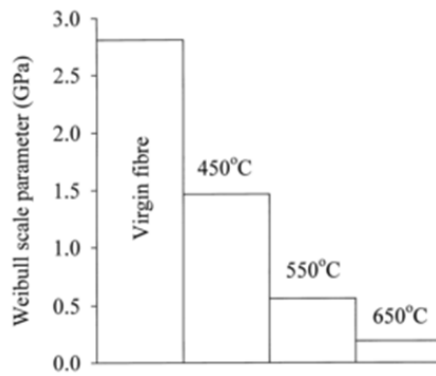


Figure 5.4 – Strength of glass fibres recycled from SMC feed at different fluidised bed recycling temperatures. Reproduced from [141]

More recently, the feasibility of reprocessing thermally recycled glass fibres in second-life composite materials was assessed [10, 67]. In order to have glass fibres representative to those thermally recycled from a composite, chopped fibres were heat treated in a furnace at 500 °C [67]. This procedure was also followed by Saez who investigated the effects of chemical treatments on the strength regeneration of thermally treated glass fibre bundles [13]. Thomason et al. [14] conducted research on the influence of hot NaOH treatment on the strength of thermally treated and thermally ‘recycled’ glass fibres. APS-sized glass fibre bundles were unidirectionally aligned in a casting mould and infused with polyester resin, which was then cured. This model composite was then placed in a furnace at 600 °C for an hour under air to thermally ‘recycle’ out the glass fibres. The strength of these filaments was reasonably similar to fibres that were simply heat treated in a furnace at the same temperature. Pender and Yang [144, 145] adopted a similar approach to recover glass fibres from model epoxy composites, whilst also trying to improve the fibre strength retention by accelerating the thermal degradation of the epoxy using metal oxides.

In recent years, the University of Strathclyde carried out extensive research into glass fibres recycled from an in-house fluidised bed (see Figure 5.5); Pender [66] investigated the properties of glass fibres thermally recycled out of model epoxy composites. Fibres were recycled from the composites at various temperatures, fluidisation velocities and residence times in the fluidised bed. Figure 5.6 shows the appearance of the fibres after being recycled at various fluidised bed temperatures. Some of the fibres were also thermally cleaned, in which case they were placed in a furnace at 550 °C for 1 hour after recycling to remove any remaining residue.



Figure 5.5 – Images of the in-house developed fluidised bed. Reproduced from [66]



Figure 5.6 - Glass fibres recycled in the fluidised bed at a temperature of a) 400 °C, b) 450 °C, c) 500 °C, d) 550 °C and e) 500 °C + thermal cleaning. Reproduced from [66]

From Figure 5.6 it is clear that the temperature of the fluidised bed has a significant impact on the cleanliness of the fibres. At lower temperatures, fibres are visibly darker and when recycled at higher temperatures coupled with thermal cleaning, fibres appear very clean. The darkening of the fibres is said to be due to non-decomposed epoxy residue or char [66]. As well as examining the surface of recycled fibres for residue, the tensile strength was also measured at each fluidised bed temperature (see Figure 5.7).

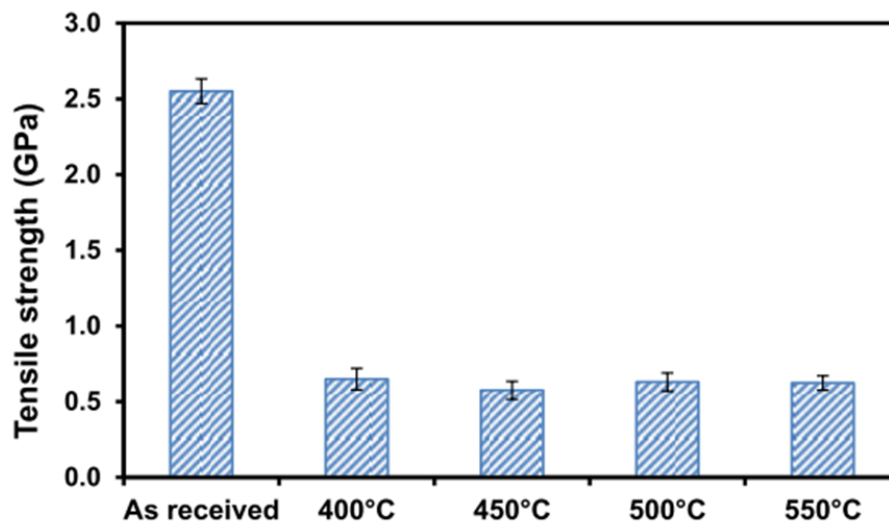


Figure 5.7 - Tensile strength of glass fibres recycled at various fluidised bed temperatures. Reproduced from [66]

In contrast with the results reported by Pickering et al. [141] (see Figure 5.4), the strength of the fibres seems to decrease to a similar extent at each recycling temperature (around 75% strength loss). Because higher fluidised bed temperatures did not further damage the fibres and led to a cleaner surface, a temperature of 500 °C was chosen for later studies.

More recently, glass fibres were recycled from an end-of-life wind turbine blade using the fluidised bed. These fibres underwent various chemical treatments in an attempt to regenerate their strength and interface, the results of which are reported in this thesis. Pender carried out initial studies into the properties of these fibres before and after treatment in chemical solutions [66]. A review of some of these treatments and their effect on the performance of the recycled fibres is given in the following section. SEM examinations of these recycled glass fibres without any post treatment indicate possible scratches on the surface (see Figure 5.8).

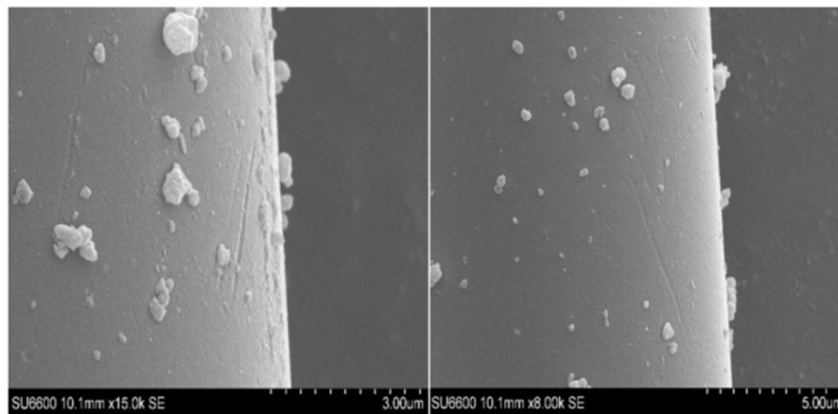


Figure 5.8 - SEM images showing scratches on the surface of glass fibres recycled in the fluidised bed at 500 °C. Reproduced from [66]

It was thought that the presence of these scratches was likely due to abrasion of the fibres by the silica sand in the fluidised bed [66]. Because these features were never observed for fibres thermally treated in a furnace, it was suggested that they were created as a result of the recycling process in the fluidised bed. Feih et al. [51] created an artificial flaw on the surface of glass fibres using focused ion beam (FIB) milling. To the best of the author's knowledge, no naturally-occurring flaws have been observed on the surface of glass fibres up to now. Further analysis of the fibre

features with an AFM would confirm whether these are indeed surface flaws and if, or to what degree, these flaws contributed to the strength loss of the fibre. An AFM investigation of recycled fibres that showed possible craters under the SEM is reported in this thesis.

It is evident from the literature that thermally recycled glass fibres lose a significant amount of strength. Regenerating the strength of these fibres is required to allow their reuse in second-life composite applications. It is also well established that at the thermal recycling temperatures usually applied, degradation of the fibre sizing occurs; hence fibres also need to be resized to promote their adhesion to the polymer matrix in the new composite. The next section describes some of the work carried out so far in improving the strength and interface of thermally recycled glass fibres.

5.2.3 Regenerating strength and interface of thermally recycled glass fibres

As mentioned earlier, Thomason et al. investigated the feasibility of hot alkaline treatments to recover the strength of glass fibres that were thermally 'recycled' out of a model polyester composite in a furnace at 600 °C [14]. Such alkaline treatments, mainly based on NaOH, were performed initially by Saez on glass fibres that were heated in a furnace to simulate thermal recycling conditions [13]. An in-depth study into the effects of alkaline treatments on the strength of thermally treated glass fibres was carried out and reported in Chapter 3 of this thesis. Figure 5.9 displays the tensile strength of thermally treated and 'recycled' glass fibres before and after treatment in 3 M NaOH solution for 10 minutes at 90 °C [14]. NaOH-treated fibres were also treated in APS solution to improve the interface.

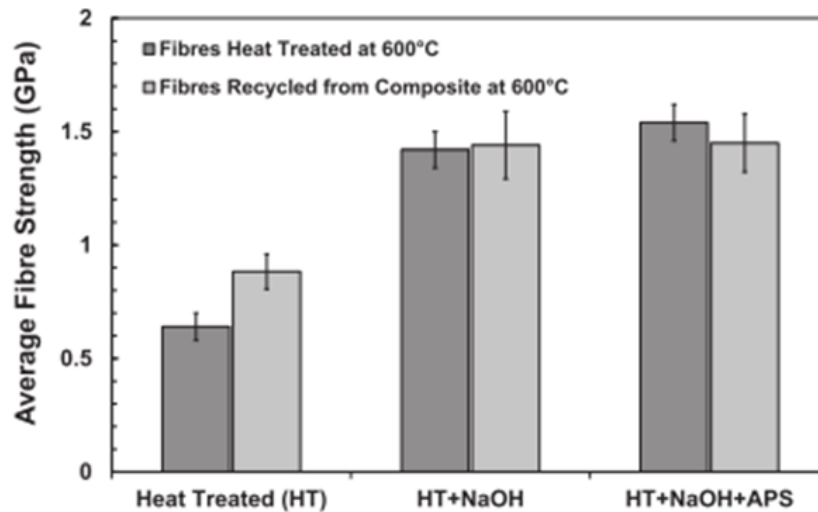


Figure 5.9 – Tensile strength of glass fibres thermally treated and thermally ‘recycled’ out of a composite at 600 °C, before and after treatment in NaOH and APS solution. Reproduced from [14]

It is unclear why the strength of the thermally ‘recycled’ glass fibres is marginally higher than fibres thermally treated in a furnace at the same temperature; this could be due to the fact that the fibres recycled from the composite were better dispersed and hence easier to separate for preparing tensile test samples (recall the effect of pre-washing fibre bundles described in Chapter 3). Applying a hot NaOH treatment to both these fibre types leads to a similar degree of strength recovery, approaching 1.5 GPa. A value of 1.5 GPa is an important target strength for recycled glass fibres to reach, as this would allow them to compete with chopped glass fibre products in terms of performance [14]. Figure 5.9 also indicates that the strength of thermally treated and ‘recycled’ glass fibres treated in NaOH solution is increased slightly further with application of a silane coating (APS). It is argued that APS treatment itself does not regenerate fibre strength but rather protects the surface from damage due to handling and sample preparation [14, 47].

As well as measuring the tensile strength of the glass fibres before and after chemical treatment, the interfacial shear strength (IFSS) was also determined by Thomason et al. using polypropylene (PP) as the polymer matrix [14]. IFSS is essentially a measure of the apparent adhesion of the fibres with the polymer matrix; the level of this adhesion would have a major impact on the properties of the final composite. Figure 5.10 displays the IFSS values of glass fibres following various treatments, with PP as the polymer matrix.

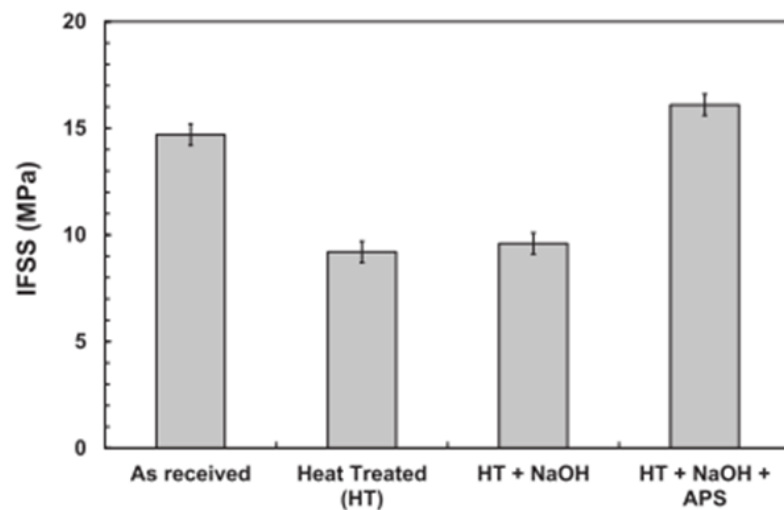


Figure 5.10 – Effect of treatments on IFSS of glass fibre with PP matrix. Reproduced from [14]

There is a significant drop in IFSS following heat treatment of the glass fibre; this can be attributed to the removal of the APS coating (sizing), the function of which is to promote the adhesion of glass fibres to the polymeric matrix. Although NaOH treatment is shown to improve the strength of the thermally treated fibres, there is no major improvement in IFSS; this increase is only demonstrated with application of APS to the NaOH-treated fibres. Figure 5.10 indicates that applying APS treatment

to the fibres can lead to an IFSS value that is similar to, if not better than, the IFSS of as-received fibres. The recovery of tensile strength of the heat treated fibres by NaOH solution coupled with interface regeneration by APS leads to an enhanced strength of the final composite material (glass mat thermoplastic or GMT) with PP as the matrix, according to Figure 5.11.

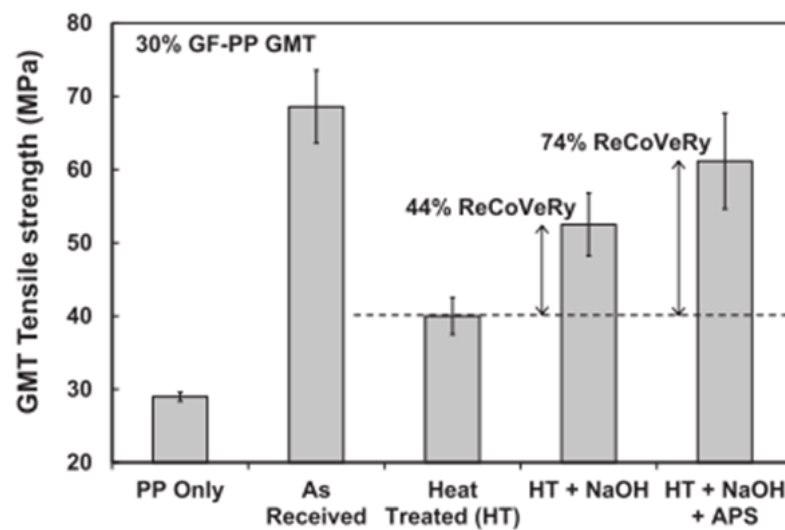


Figure 5.11 – Tensile strength of GMT with the glass fibres receiving different treatments. Reproduced from [14]

Pender investigated a range of chemical treatments and their effect on the strength and interface of both thermally treated and recycled glass fibres [66]. Glass fibres were recycled from a model epoxy composite using a furnace and also the in-house fluidised bed. In addition, glass fibres were heat treated alone in the furnace (thermally treated). It was discovered that in the NaOH molarity range investigated (1.5 to 5 M), a short alkaline treatment had no positive impact on the strength of glass fibres recycled either in the furnace or fluidised bed; there was however an increase in strength of thermally treated fibres as a function of alkaline solution

concentration [66]. Interestingly, the fluidised bed recycled fibres which were treated in alkaline solution showed potential surface pitting under the SEM (see Figure 5.12).

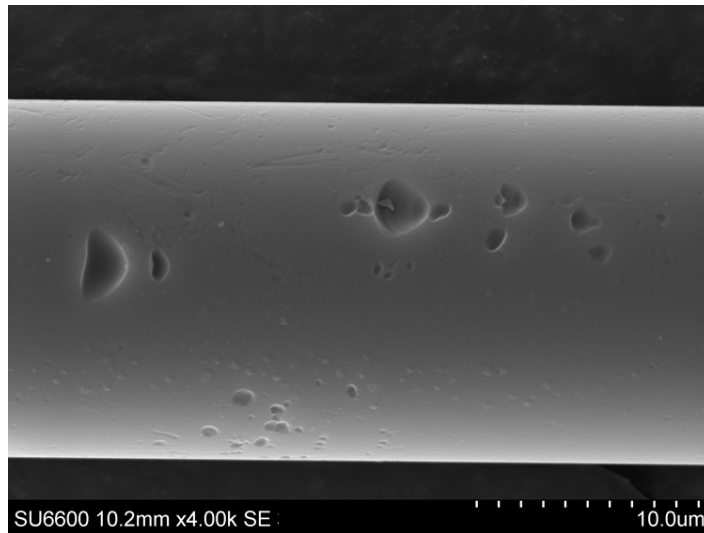


Figure 5.12 - SEM image of fluidised bed recycled glass fibre treated in 5 M NaOH solution for 20 minutes, showing possible surface pitting.

Such features were also discovered on recycled glass fibres without any post treatment, though they appeared more like scratches (see Figure 5.8). Unlike the scratches on the recycled only fibres, the craters shown in Figure 5.12 appear uneven and could have resulted from the glass surface being etched by the alkaline solution; this agrees with the AFM study reported in Chapter 3.

When the fluidised bed recycled fibres were treated in alkaline solutions under more aggressive conditions (higher concentration and longer treatment time) the strength did manage to improve, as shown in Figure 5.13.

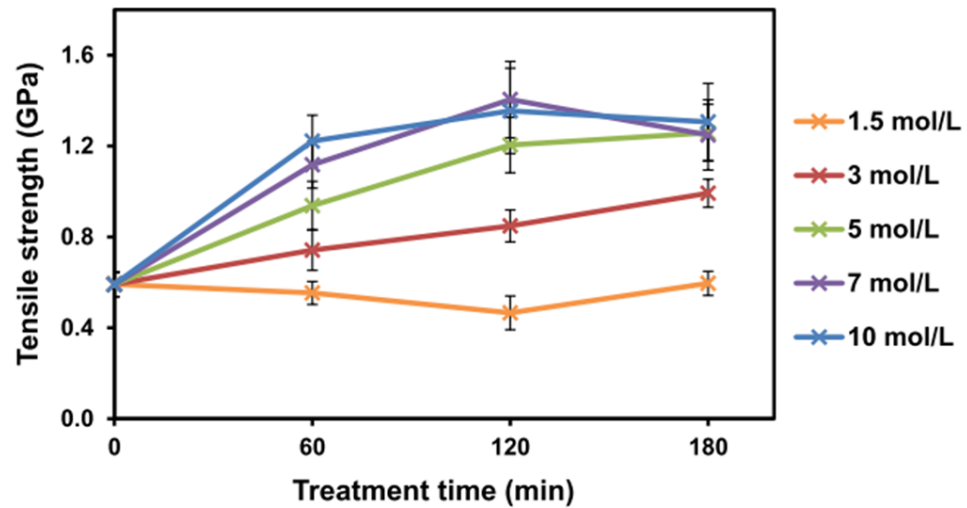


Figure 5.13 – Tensile strength of glass fibres recycled from model epoxy composite in fluidised bed and treated in hot NaOH solution at various concentrations and times. Reproduced from [66]

With the exception of 1.5 M, the alkaline treatment appears to improve the strength of the fibres with increasing concentration and treatment time; for the 7 and 10 M treatments, the strength begins to level off with time. The reason why a more aggressive treatment is effective for recycled glass fibres is not fully understood, though it is suggested it could be due to the fibres being initially weaker and possessing residue on the surface. Given the extended treatment times and high concentration of alkaline solution, the recycled glass fibres underwent significant diameter reduction [66].

In addition to concentrated alkaline treatments, Pender also investigated the effects of hot water on the strength of the fluidised bed recycled fibres. Figure 5.14 displays the tensile strength of glass fibres recycled from model epoxy composites using the fluidised bed, after treatment in hot water over several hours.

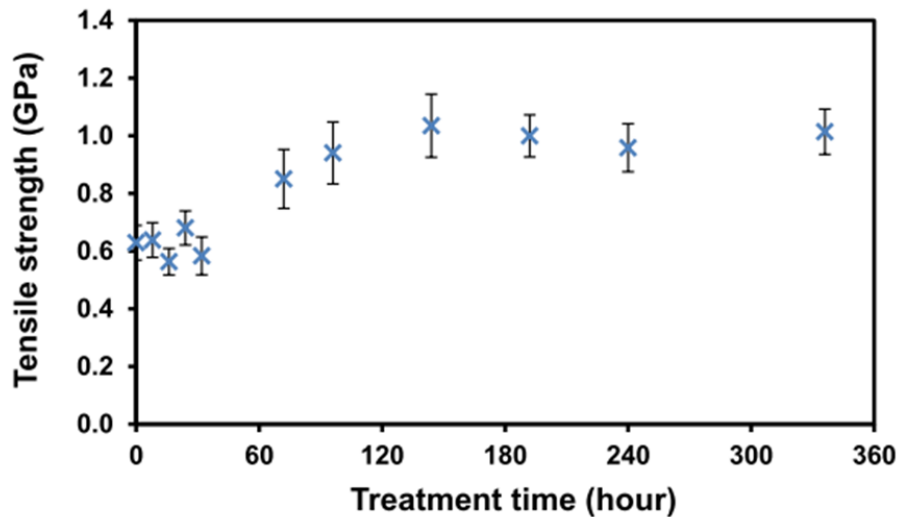


Figure 5.14 - Tensile strength of glass fibres recycled from model epoxy composite in fluidised bed and treated in hot water at various times. Reproduced from [66]

Results show that treatment of recycled fibres in hot water for a number of days can almost double their strength. The mechanism behind this strength increase is not yet established, though it is suggested to involve the formation of compressive stress around the crack tip on the glass surface, hence ‘shielding’ the crack [63, 66]. The lack of diameter reduction of the fibres and the absence of surface pitting under the SEM suggests etching does not contribute to the strength increase [66]. The fact that no visible diameter reduction was observed contradicts previous studies which show that hot water can significantly etch glass [93].

Saez [13] saw an improvement in the strength of thermally treated glass fibres after treatment in hot APS solution, and proposed that the mechanism of this strength increase involved the coverage of the damaged glass surface with long chain APS molecules. Although the effect of hot APS treatment on thermally recycled glass fibres has not been investigated in depth, it is well established that application of

APS coating, whether hot or ambient, improves the adhesion of the fibres to the polymer matrix.

Pender applied hot alkaline and water treatments from his study on glass fibres thermally recycled from model epoxy composites in the fluidised bed, to fibres recycled from the end-of-life wind turbine blade. Figure 5.15 shows the strength of the glass fibres after thermal recycling in the fluidised bed, and after treatment in hot alkaline solution (7 M NaOH for 2 hours) and hot water (4 days).

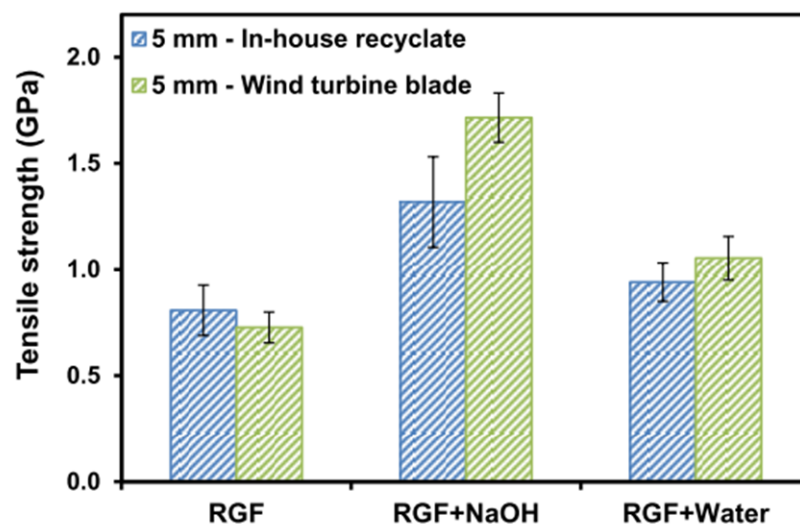


Figure 5.15 – Tensile strength of glass fibres recycled from model epoxy composite (in-house recycle) and end-of-life wind turbine blade, before and after treatment in hot alkaline solution (7 M NaOH for 2 hours) and hot water (4 days). Reproduced from [66]

It is evident that hot alkaline and water treatments lead to a similar degree of strength recovery of glass fibres recycled from the wind turbine blade waste. Pender has shown that the combined strength regeneration of thermally recycled glass fibres by alkaline solution and interface improvement by APS can result in an overall increase in tensile strength of the final composite [66]. The strength increase of

recycled fibres from hot water treatment was not as significant, and this translated to little or no improvement in tensile strength of the composite material [66].

5.2.4 Conclusions of literature review

A range of recycling techniques has been developed in recent years to tackle the issue of large volumes of composite waste. Thermal recycling, such as that involving a fluidised bed, is advantageous since the fibrous reinforcement can be reclaimed. Unfortunately, because of the elevated temperatures required to degrade the polymer matrix component, the fibres (particularly glass fibres) lose a significant amount of strength. Furthermore, thermally recycled fibres are fluffy in nature and can be contaminated with residual char. Studies into the effects of chemical treatments to regenerate the performance of such fibres have been conducted. It was discovered that thermally recycled glass fibres require a more aggressive alkaline treatment in order to regenerate strength compared to fibres thermally treated in a furnace. There is also the possibility of a prolonged treatment of fibres in hot water to recover their strength, though so far it did not translate to an improved strength of the final composite. Recoating thermally recycled and treated fibres in a silane such as APS was shown to improve their adhesion to the polymer matrix, which in turn resulted in improved composite properties. It was also discovered from SEM that some thermally recycled glass fibres had possible scratches on the surface from the recycling process, and after alkaline treatment, fibre surfaces often showed possible pitting; an AFM analysis would confirm whether these are indeed surface flaws and to what degree they would have contributed to the strength of the fibre.

5.3 Experimental

5.3.1 Materials

Glass fibres thermally recycled out of a large on-shore wind turbine blade were used in this research study; more information on the recycling procedure is given in the following section. A 25 kg section of the blade was provided by Off-shore Renewable Energy, and was comprised of continuous glass fibre reinforced epoxy sandwiching balsa wood [66]. By carrying out a degradation study of a small section of the blade in the furnace, it was found that the fibre weight fraction of the part was 68%; the rest was composed of a mixture of wood and epoxy. Before feeding the blade into the fluidised bed, it had to be cut into smaller pieces with a water jet cutter. Figure 5.16 shows the blade section before and after downsizing for thermal recycling in the fluidised bed.

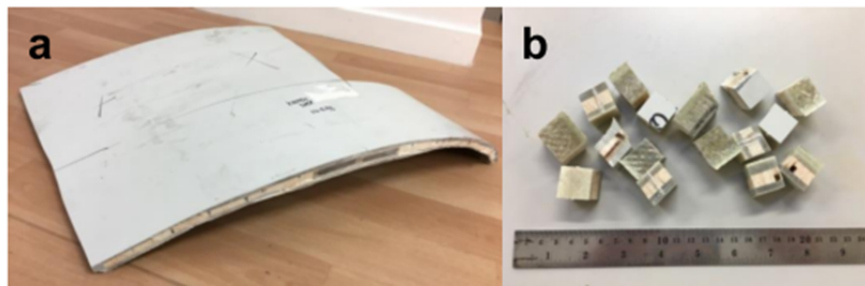


Figure 5.16 – Image of wind turbine blade aerofoil (a) before downsizing, and (b) after downsizing for thermal recycling. Reproduced from [66]

The glass fibres recycled from the blade (shown in Figure 5.17) had a nominal diameter of 15 μm , however the glass composition and the nature of the coatings applied to the fibres during manufacturing were unknown.



Figure 5.17 – Image of glass fibres thermally recycled from wind turbine blade in the fluidised bed

The chemicals used in this study included NaOH pellets, 37% concentrated HCl, and APS, which were purchased from VWR and Sigma Aldrich. PP and PP combined with different concentrations of maleic anhydride grafted polypropylene (MAPP, at 1.5 and 12 wt%) were used as the polymer matrices in the measurement of the interfacial adhesion (IFSS) of the fibres.

5.3.2 Thermal recycling of end-of-life composite

As mentioned in the previous section, the wind turbine blade had to be downsized to small squares (15 x 15 mm) for thermal recycling in the fluidised bed. Glass fibres were recovered from the blade at a fluidised bed temperature of approximately 500 °C within 15 to 25 minutes. Once the fibres were recycled out of the blade they were treated in various chemical solutions. More information on the fluidised bed recycling procedure can be found in [66].

5.3.3 Concentrated alkaline treatment

100 ml of NaOH solution was prepared at a specific concentration (7, 8, 10 and 12 M) in a volumetric flask and poured into a small PP container. The container was sealed and left in a preheated Carbolite oven for two hours to allow the solution to heat up to 95 °C. 0.3 g of the recycled glass fibres was then immersed in the hot solution and the closed container kept in the oven for 2 hours. Once the fibres were treated for the set duration, they were drained out of the solution. Since more aggressive alkaline treatment conditions were employed in this experiment compared to the one detailed in Chapter 3, a more rigorous rinsing procedure had to be adopted to ensure the effective removal of residue from the fibres. This method involved rinsing the fibres for 1 minute in a fresh 10% HCl solution four times, before immersing once in hot deionised water for 1 minute and twice in cold deionised water for 1 minute. The rinsed fibres were then placed in the oven at 110 °C for 15 minutes to dry.

5.3.4 Mild alkaline treatment (pH-scale)

As well as treating recycled fibres in concentrated NaOH solution for a few hours, they were also treated in milder, pH-scale alkaline solution for a prolonged period of time to see whether strength regeneration can still be achieved. In this experiment, 0.3 g of recycled fibre was placed in a small PP container along with 100 ml of the treating solution at a particular pH value. The sealed container was placed in an oven at 95 °C for a specific time (on a scale of days). Because of the extended amount of time the solution and fibres were kept for in the oven, an initial heating period for the solution alone was not deemed necessary.

NaOH and deionised water were used to prepare the solution in a volumetric flask at a theoretical pH value of 14 according to Equation 5.1.

$$pH = 14 + \log[M]$$

Equation 5.1

where M is the concentration of NaOH solution in mol/L. In this case, a 1 M NaOH solution would have a theoretical pH of 14. pH 14 solution was also used to prepare pH 10 solution by diluting it with water at a factor of 10,000. This was thought to be a more accurate method of preparing the solution at pH 10 rather than making a fresh solution using a very small mass of NaOH, which would be difficult to weigh correctly even with a microbalance. Note the above equation assumes complete dissociation of NaOH into metal and hydroxide ions in water; although early studies suggest NaOH does not completely dissociate, it is still considered to be a strong base meaning its concentration can be easily converted to pH [95].

A treating solution with no NaOH (deionised water only) was given a theoretical pH of 7. The true pH of all the solutions prepared in this experiment was measured accurately with a pH meter before and after fibre treatments. To remove alkaline residue from the treatment, the fibres were rinsed in 3.7% HCl for 10 minutes followed by 1 minute in deionised water. Following the rinsing procedure, the fibres were dried in an oven at 110 °C for 15 minutes.

5.3.5 Silane treatment

In an attempt to regenerate both the strength and interfacial properties of thermally recycled glass fibres, they were treated in hot APS solution (which is known to be slightly alkaline) for various periods of time. 100 ml of APS solution was prepared at 1 vol% in a volumetric flask, and poured into a small PP container. The container was sealed to allow the APS to hydrolyse either at room temperature for 24 hours, or at 95 °C for 5 hours. For the hot hydrolysis, the lid was removed from the container for a few seconds every hour to let the ethanol vapour escape; this was done as the rapid build-up of ethanol gas from the hot hydrolysis could have led to rupture of the lid and container. Once the APS solution was hydrolysed (either hot or ambient temperature), 0.3 g of recycled glass fibre was immersed in the solution and the sealed container left in the oven at 95 °C for a certain time. As a control, fibres were also treated in room temperature hydrolysed APS solution for 15 minutes at room temperature.

It is well established that a 1 wt% APS solution (which is fairly close to 1 vol%) has a pH value of around 10.6 [45, 46, 103, 104, 130, 131]. Hence fibre treatments were conducted at a timescale similar to the mild alkaline treatments described in the previous section. Once the treatment was finished, the fibres were drained out of the APS solution and dried in an oven at 110 °C for 15 minutes. The true pH of the APS solution before and after fibre treatment was measured with a pH meter. According to the literature, the pH of silane solutions have been typically measured with a standard glass electrode pH meter [103, 130], and researchers never reported on the silane damaging the glass probe. Hence in this research study a standard glass electrode pH meter was used to measure pH of the APS solution, though the probe was still rinsed thoroughly in acetone between measurements. The pH of a buffer

solution (pH 7) was also measured in between to make sure the glass probe was still functional. Although the majority of the APS solutions used to treat the fibres were at 1 vol%, the concentration was varied in another experiment (to 0.5 and 5 vol%) to examine its effect on the strength and interface of the fibres.

5.3.6 Single fibre tensile testing

To measure the tensile strength of the recycled fibres, individual filaments were carefully separated and mounted on tensile test card. Because of the short length of the fibres, they were tested at 5 mm gauge length. Figure 5.18 shows a schematic of a tensile test card with a mounted fibre.

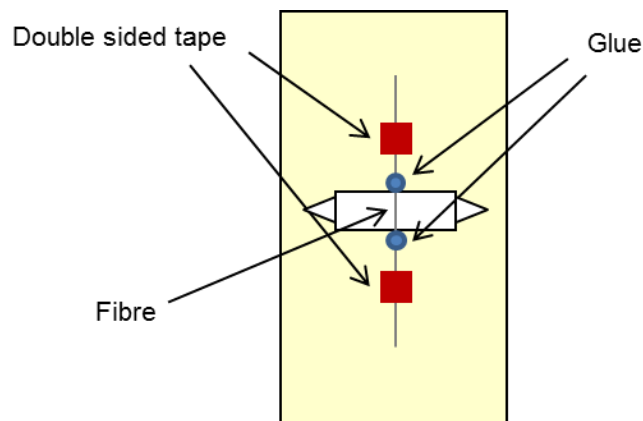


Figure 5.18 – Schematic of fibre tensile test card at 5 mm gauge length

Unlike previously with the case of thermally treated glass fibres, thermally recycled fibres were mounted on tensile test cards with a 5 mm length window. Due to the short length of the fibres the tape was mounted close to the window to help align the sample. Once the fibre was placed as vertical and straight as possible, it was

mounted with superglue as shown in Figure 5.18. Because of the nature and length of the fibres they were susceptible to premature breakage, particularly when the sides of the window were cut for testing. Because of this, triangles were cut to the sides of the window to reduce the volume of card that had to be cut when loading the sample onto the tensile testing instrument.

As before, 30 fibre tensile test samples were prepared at each treatment condition. Once the superglue was cured overnight, the fibres were imaged under an optical microscope and their diameters measured with ImageJ. The fibres were then tested for tensile strength using a Testometric tensile testing machine at ambient environment. The load cell was 5 N with a strain rate of 1.5%/min applied to the samples. The fibre strength was calculated for each treatment condition by averaging from the 30 samples, and the error bars associated with the strength measurements represent 95% confidence limits. More information about the single fibre tensile testing procedure can be found in Chapter 3 of this thesis.

5.3.7 Microbond testing

The microbond test was performed to measure the IFSS of the fibres. The polymer matrix was chosen to be PP, and PP combined with different concentrations of MAPP (1.5 and 12 wt%). The polymer (which was either in the form of pellets or fibres) was melted on a hotplate. Tweezers were used to draw out the molten polymer to form a PP fibre, which was tied into a knot around a glass fibre as indicated in Figure 5.19.

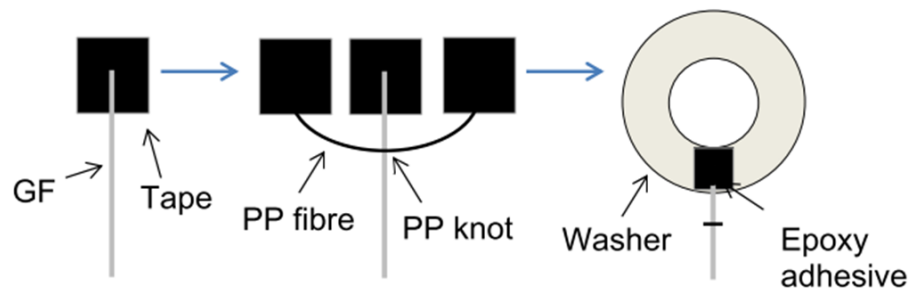


Figure 5.19 – Schematic showing sample preparation for microbond test. Reproduced from [66]

The glass fibre was mounted onto a piece of double-sided tape with tweezers. The PP or PP/MAPP fibre was knotted round the glass fibre. The ends of the polymer fibre were stuck to tape on either side of the sample to minimise their movement, and allow the polymer fibre to be trimmed off close to the knot with micro-scissors. The glass fibre sample with the polymer knot was then mounted onto a washer with epoxy adhesive and left to set for a minimum of 8 hours at room temperature. The microbond test samples were suspended on metal wire frames and placed in an OV-11 vacuum oven to allow the polymer knots to form droplets on the glass fibres. The oven was purged with nitrogen (to prevent PP from thermal oxidative degradation) and heated to 220 °C before slowly cooling to room temperature. The oven temperature profile is shown graphically in Figure 5.20.

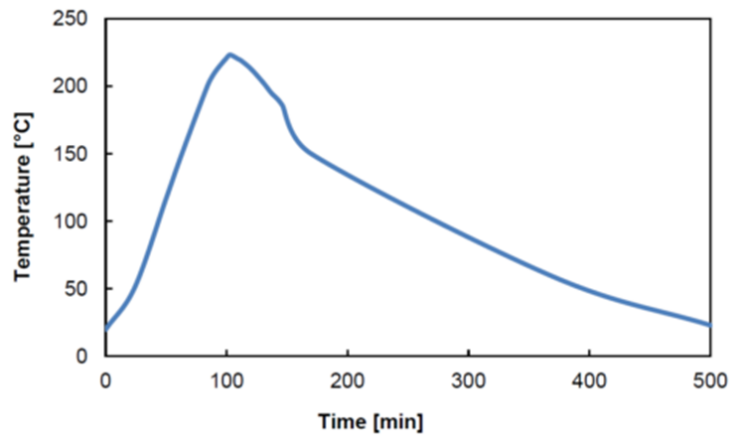


Figure 5.20 – Vacuum oven temperature profile for preparing microbond samples. Reproduced from [66]

The glass fibre diameter, polymer droplet diameter and the embedded length of the samples were measured with an optical microscope and ImageJ software. Only microbond samples with symmetric droplets were tested. The range of embedded lengths and droplet diameters used in the microbond test typically range from 120 – 200 μm and 80 – 180 μm respectively [66]. Figure 5.21 gives an example of a droplet formed on a glass fibre, being measured using ImageJ.

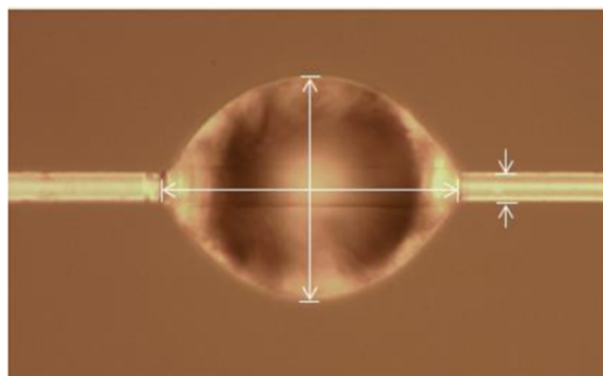


Figure 5.21 – Image of a polymer droplet formed on a glass fibre, being measured using ImageJ. Reproduced from [66]

To measure the IFSS of the samples, an Instron 3342 universal testing machine equipped with a 10 N load cell was used. The washer with the attached fibre hanging vertically downward was placed on a hook as shown in Figure 5.22.

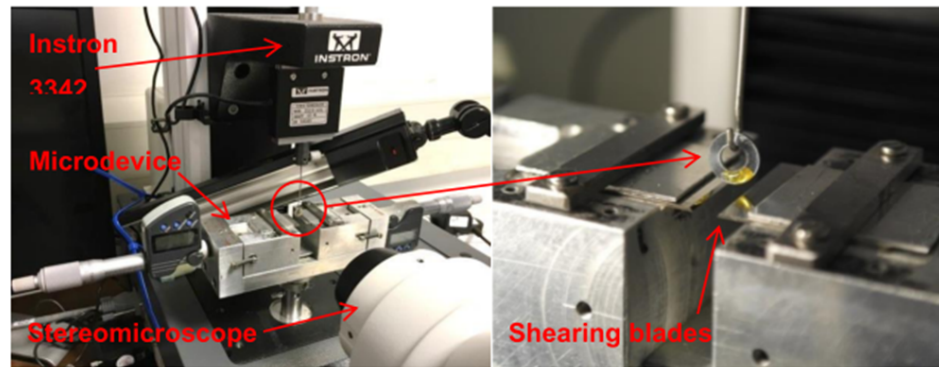


Figure 5.22 – Image of the microbond test setup on the Instron. Reproduced from [66]

The shear blades were moved closer to the glass fibre and then the polymer droplet height was adjusted so that it was below the blades. To image the samples and blades closely, a microscope with 45x magnification equipped with a video camera was used. Once the sample was positioned correctly, a load was applied at a speed of 0.1 mm/min (all tests were performed at ambient environment). Figure 5.23 shows a schematic of a droplet during the microbond test.

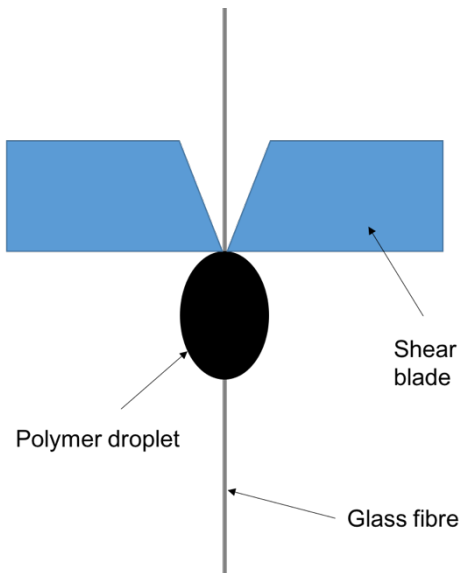


Figure 5.23 – Schematic of droplet during microbond test

The load applied on the microbond sample was displayed by the software as a function of displacement. Once the load reached a peak and then dropped to a plateau like what is shown in Figure 5.24, the test was stopped.

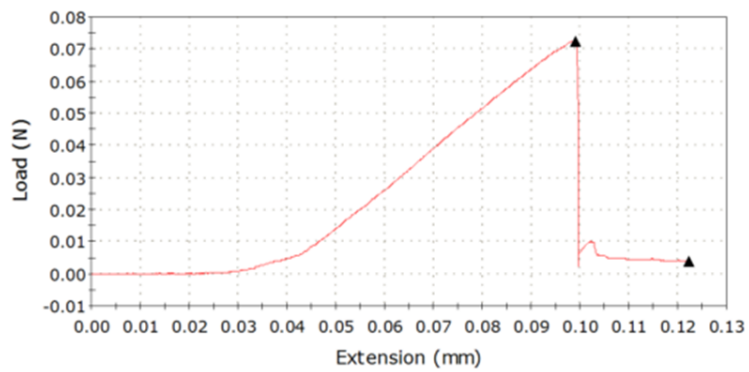


Figure 5.24 - Example of a typical load-extension plot output from Instron Bluehill 2 software. Reproduced from [66]

To calculate the IFSS of a sample, the peak load at droplet de-bond was divided by the fibre-matrix contact area according to Equation 5.2.

$$IFSS = \frac{F_{db}}{\pi D l_d}$$

Equation 5.2

where F_{db} , D and l_d denote the load at droplet de-bond, diameter of the glass fibre and embedded length respectively. The average IFSS was calculated from around 20 fibre samples for each treatment condition. More information on the microbond test procedure can be found elsewhere [66, 146, 147].

5.3.8 Atomic force microscopy (AFM)

The majority of the thermally recycled glass fibres before and after alkaline treatment showed possible surface scratches or pitting under the SEM; to determine whether these were surface flaws, an AFM analysis of the fibre samples was conducted using a Bruker Innova AFM (tapping mode). Individual fibres were mounted on an AFM plate and different regions of the fibres were scanned in a 3 x 3 μm area. Height and phase images were flattened with NanoScope Analysis software at 2nd order to remove the fibre curvature, thus only revealing features of the surface. Where potential craters or flaws were detected in the height image, NanoScope Analysis was also used to investigate their depth and geometry. Using a fracture mechanics model, the depth of these features can potentially allow the back-calculation of the strength of the fibre. If this strength value is similar to the

measured strength by tensile testing, then it can be said that the flaw studied under AFM contributed to the strength of the fibre (is a critical flaw). Chapter 3 gives more details on the AFM analysis procedure, and the theory of AFM can be found in the Appendix.

5.4 Results and discussion

5.4.1 Effect of alkaline treatments on recycled glass fibre strength

Figure 5.25 shows the average tensile strength of recycled glass fibres after treatment in hot and concentrated NaOH solution for 2 hours at various molarities (7, 8, 10 and 12 M).

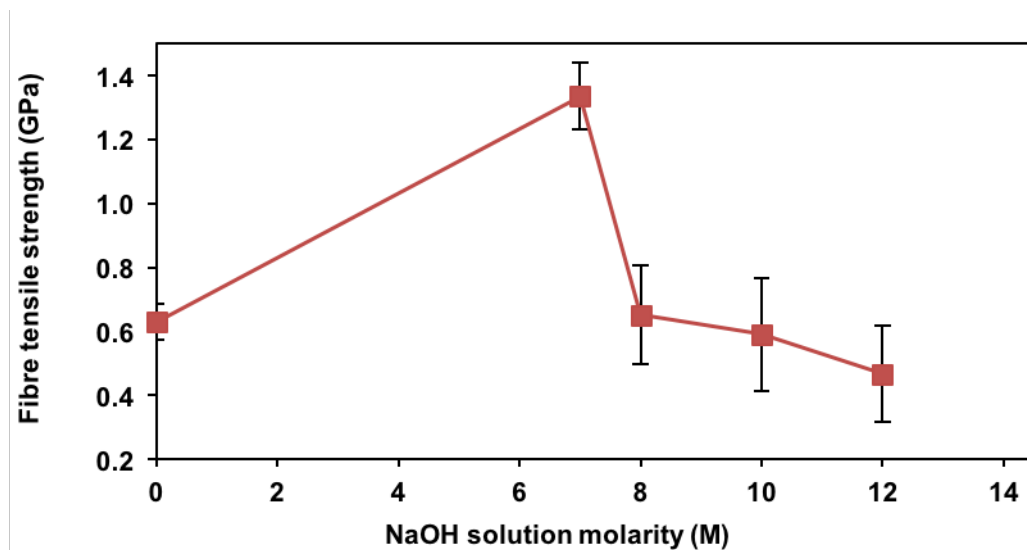


Figure 5.25 – Tensile strength of thermally recycled glass fibres after treatment in hot NaOH solution for 2 hours at various concentrations

The strength of the thermally recycled glass fibres appears to be very low, around 0.63 GPa. At this strength the fibres would be deemed unfeasible for reuse in second-life composite applications. Results in Figure 5.25 indicate that treating these fibres in hot 7 M NaOH solution for 2 hours can significantly improve their strength, approaching the 1.5 GPa target [14]. As the concentration of the alkaline solution increases, it begins to have a detrimental effect on fibre strength; from 8 to 12 M, the strength is fairly similar to fibres that were thermally recycled without any post-treatment. It was likely that at this point the bulk network structure of the glass was compromised with the severe alkaline treatment conditions, hence negating the positive effect from removing surface flaws. It was found that the mass loss of the glass fibres after alkaline treatment was significantly high, being around 36.2% for 7 M and peaking at 45.5% for 12 M.

The strength results in Figure 5.25 show that a concentrated NaOH treatment at 7 M can have a positive impact on recycled fibre strength. Reducing the treatment time and molarity of the solution to below 7 M might result in greater strength improvement of the fibres, however this will require a more in-depth investigation which can be carried out in future. The next section veers away from aggressive alkaline treatment conditions and instead focuses on milder, more cost-effective means to regenerate the strength of thermally recycled glass fibres.

5.4.2 Effect of pH-scale alkaline treatments on recycled glass fibre strength

This section looks into the effects of very mild NaOH solutions (pH above 7, up to 14), heated to 95 °C, on the tensile strength of recycled fibres. Treatment of fibres was also performed in hot water without any added alkali, which was given a

theoretical pH of 7. The true pH of these solutions was measured before and after fibre treatments and reported.

Figure 5.26 displays the strength of the recycled glass fibres following treatment in pH 7, 10 and 14 solutions at various times.

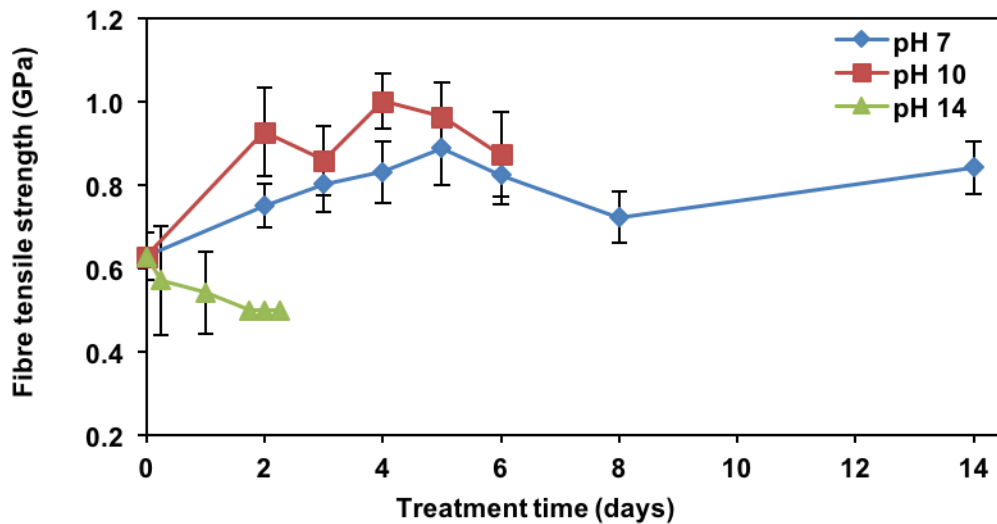


Figure 5.26 – Tensile strength of thermally recycled glass fibres after treatment in pH 7, 10 and 14 solutions at various times

The strength of the glass fibres is too low for reprocessing after thermal recycling alone (0.63 GPa). Fortunately, a significant amount of strength can be recovered through chemical treatment of the fibres. Figure 5.26 shows an improvement in fibre strength after a simple hot water treatment, reaching approximately 0.9 GPa after 5 days. There appears to be a trend where increasing the pH value leads to a decrease in the time required for strength recovery of the fibres to be at its optimum; for pH 10 solution the optimal treatment duration is 4 days as the strength of the fibres reaches 1 GPa. For pH 14 no strength measurements were made after 2 days

due to significant dissolution of the glass fibres. Overall, the pH 14 treatments appear to have a detrimental effect on fibre strength at the prolonged treatment times investigated. In fact, no values were obtained at 1.75, 2 and 2.25 days as fibre samples failed prematurely; these samples were assigned strength values of 0.5 GPa. It can be deduced, from the results in Chapter 3 and the previous section of this chapter involving concentrated alkaline treatments, that a shorter treatment time of fibres in pH 14 solution (which is essentially 1 M NaOH) would lead to a strength increase. This would maintain the notion that increasing the pH value of the solution decreases the time necessary to regenerate strength of the fibres. Eventually the fibre strength declines once it reaches its optimum as shown in Figure 5.26, particularly in the case of pH 10 and 14 treatments. As discussed earlier, the decrease in fibre strength with prolonged treatment could have been due to substantial leaching of metal ions from the glass and breakdown of the bulk network structure.

It has been postulated that the strength regeneration of thermally treated or recycled glass fibres by concentrated alkaline solution involves the etching of the damaged surface layer. This theory might also hold true for fibres treated in high pH value solutions, especially if they show a clear reduction in diameter after treatment. Figure 5.27 gives the average diameters of fibres (from tensile testing) after treatment in solutions at different pH values and treatment times.

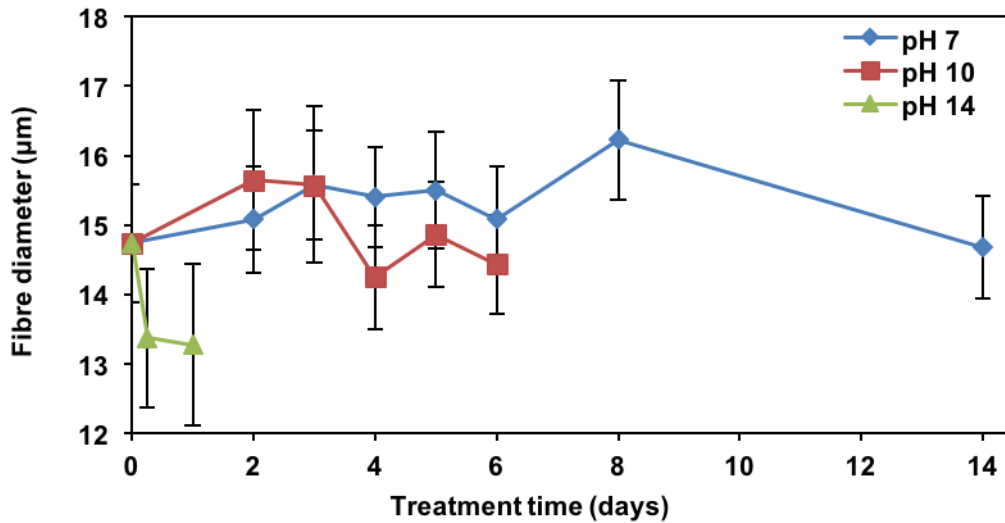


Figure 5.27 – Average diameters of thermally recycled glass fibres after treatment in pH 7, 10 and 14 solutions at various times

There is little change in the diameter of fibres after treatment in hot water over several days, suggesting that a mechanism other than flaw etching could have been responsible for strength increase as discussed previously in the literature review. A slight reduction in fibre diameter is observed after treatment in pH 10 solution at 4 days and beyond, which is where a significant increase in tensile strength occurs according to Figure 5.26. The diameter of fibres decreases considerably even after 0.25 days treatment in pH 14 solution as shown in Figure 5.27; this is not unexpected given the much higher concentration of hydroxide ions now available to react with the glass surface. These results suggest that pH 10 and 14 solutions exhibit an etching effect on glass fibres. For the case of pH 10 treatments, this could be the mechanism by which fibre strength is increased.

Irrespective of the nature of the treatment applied to the fibres, they appeared cleaner compared to when they were thermally recycled only (see Figure 5.28). The cleanliness of chemically treated fibres can be attributed to the removal of residual

char. Furthermore, the pH 14 treated fibres appear gummed together, which suggests that the prolonged treatment of fibres in concentrated alkaline solution could have led to other products being formed that are not readily removed by acid.

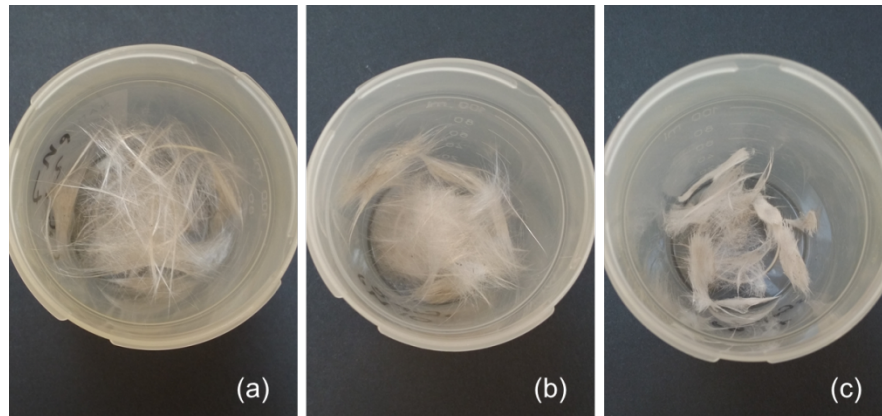


Figure 5.28 – Images of thermally recycled glass fibres after treatment in solution for 2 days at (a) pH 7, (b) pH 10, and (c) pH 14

The appearance of the solutions before and after fibre treatments was also examined; although in all cases the fibres were cleaner after chemical treatment, the pH 14 solution, particularly at 2 days, was browner in colour compared to other solutions (see Figure 5.29).

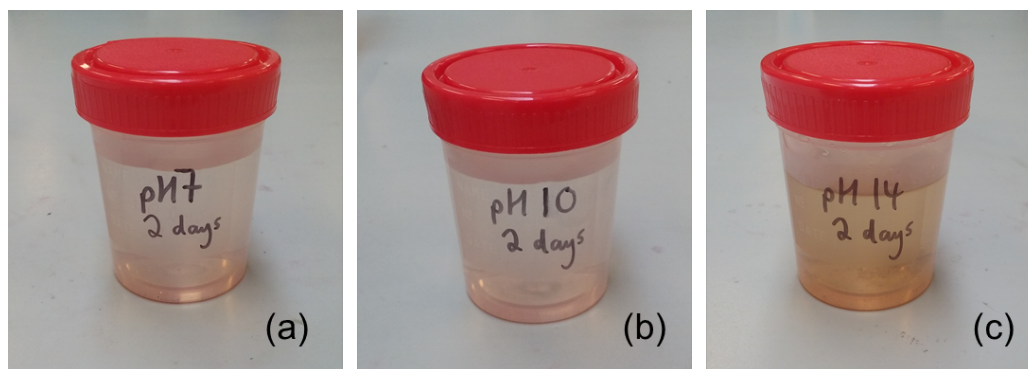


Figure 5.29 - Images of solutions after treating thermally recycled glass fibres for 2 days at (a) pH 7, (b) pH 10, and (c) pH 14

The discolouration of the pH 14 solution suggests more of the char was removed from the fibres, and perhaps other reactions might have occurred between the alkali and glass resulting in products that gave the solution its off-brown appearance. The true pH of all these solutions before and after immersion of fibres was measured accurately with a pH meter to provide further insight into processes that might have ensued over the course of the treatment. Figure 5.30 displays the measured pH of the solutions at different theoretical pH values, before and after they were used to treat the recycled fibres at various times.

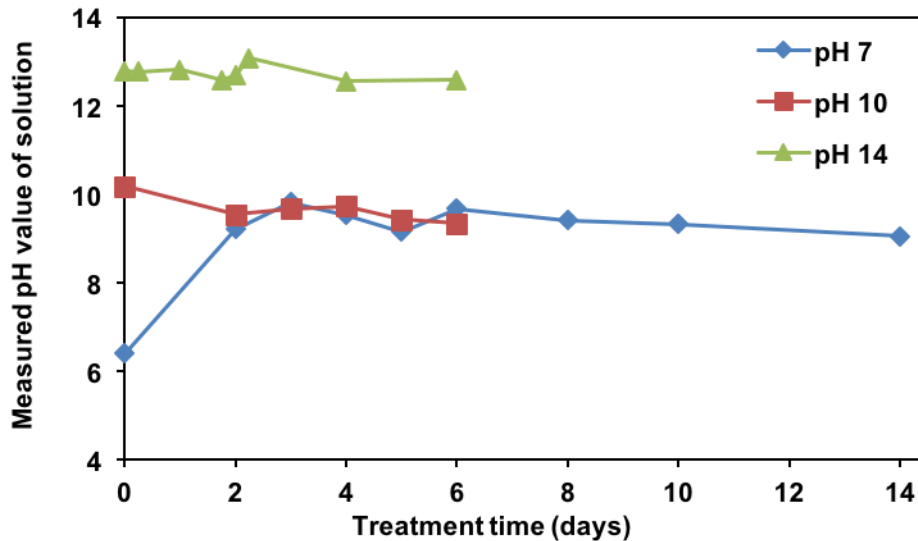


Figure 5.30 – Measured pH of solutions (25 °C) prepared at different theoretical pH values, before and after treatment of thermally recycled glass fibres at various times

The measured pH of the solutions before fibre treatments (0 days) agree reasonably well with theoretical values, particularly for pH 10. The absorption of atmospheric carbon dioxide can result in solutions becoming more acidic; for pH 7 solution the measured value is clearly lower (more acidic), possibly because the absolute number of hydroxide ions was so low meaning even little absorption of carbon dioxide would have led to a significant decrease in pH. The pH 14 solution has a measured pH of just below 13; however, it is worth bearing in mind that the pH 10 solution was prepared by dilution of the pH 14 solution. The fact that the pH 10 solution had an accurate measured pH suggests the pH 14 solution was prepared correctly. The inaccurate measured value could be due to the pH meter approaching the upper limit of its measurable pH range.

With the exception of the pH 10 and 14 solutions, the pH 7 solutions appear to increase in pH value to around 10 when they are used to treat the fibres. This indicates that the fibres themselves could have been self-treating; the leaching of

metal oxides such as CaO and MgO from the glass might have increased the alkalinity of the solution resulting in strength regeneration of the fibres in some cases. The measured pH of these solutions remains around 10, regardless of treatment time of the fibres. On the other hand, because of the very low absolute number of hydroxide ions initially in the pH 7 solutions, there could have been an abrupt increase as a result of particular contaminants on the glass fibre dissolving into the solution. It can be argued that such contaminants would also dissolve in the pH 10 and 14 solutions, but because the total hydroxide count in these solutions would already be significantly higher at the beginning, any pH change from dissolved glass fibre contaminants would be irrelevant.

The results reported in this section clearly show that mild alkaline treatments and even water, prepared at elevated temperature, can regenerate the strength of thermally recycled glass fibres. Although these treatments are for an extended period of time and not as effective at improving fibre strength as a short concentrated alkaline treatment, less corrosive chemicals are used making the process easier to implement and safer. The next section focuses on developing treatments based on a silane (APS) to try and improve both the strength and interface of thermally recycled glass fibres.

5.4.3 Effect of hot APS treatment on strength and surface functionality of recycled glass fibres

So far it has been proven that concentrated and mild alkaline treatment, for short and prolonged treatment times respectively, can recover the tensile strength of glass fibres thermally recycled out of an end-of-life wind turbine blade. Although these regenerated fibres can potentially compete with virgin fibres in terms of strength,

they still require a sizing to aid their adhesion with the polymer matrix in the new composite, and to protect the surface from damage. As discussed earlier in Chapter 2, one of the most vital components of commercial glass fibre sizings is the silane coupling agent; not only does it improve the bonding of the fibres to the composite matrix, but it also protects the surface from damage due to handling and the environment. One of the most commonly-used silane coupling agents is APS, and it naturally has an alkaline pH (around pH 10.6 at 1 wt% in water). It was therefore expected that the 1 vol% APS solutions used in this study would have a similar pH. Treatment of the thermally recycled glass fibres was performed in APS solution at 95 °C at treatment times similar to those employed previously for pH 10 alkaline treatments. The tensile strength and IFSS of these fibres (using PP or PP/MAPP as the matrix) was measured through single fibre tensile testing and microbond testing respectively.

Figure 5.31 shows the tensile strength of the fibres after treatment in hot APS solution at 1 vol% for various times, where the hydrolysis step was carried out at ambient temperature. Treatment of fibres was performed in hot APS solutions that were hydrolysed at elevated temperature as well, and the previous results on pH 10 NaOH treatments is also plotted here for comparison.

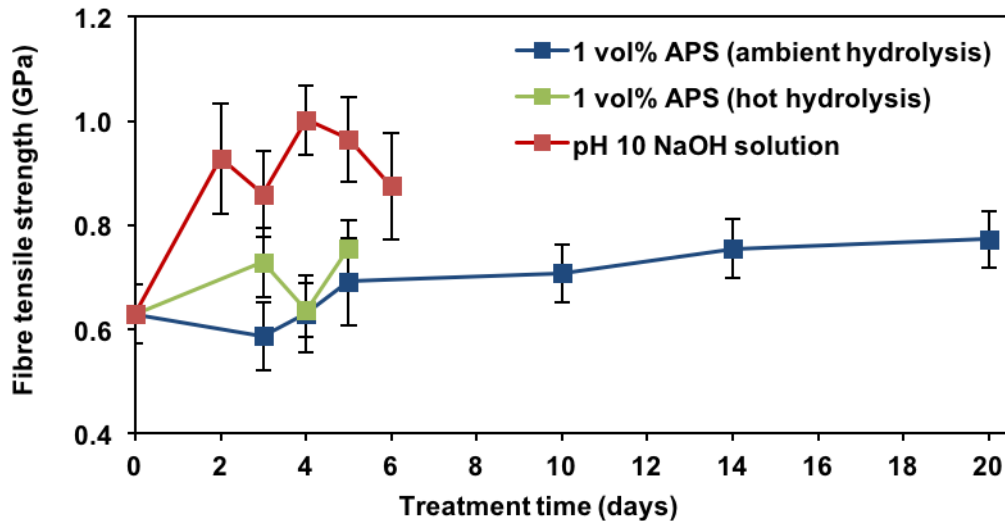


Figure 5.31 – Tensile strength of thermally recycled glass fibres after treatment in hot 1 vol% APS solution (hydrolysed hot or ambient) or pH 10 NaOH solution for various times

It appears that the strength of the fibres increases steadily with treatment time in hot APS solution (ambient hydrolysis), from around 0.6 to 0.8 GPa at 20 days. This contrasts with the pH 10 NaOH treatment, which leads to a more significant increase in tensile strength (to 1 GPa) of the fibres and at a shorter time of 4 days. Heating the APS solution during the hydrolysis seemed to have had no considerable impact on the strength of the thermally recycled glass fibres; this contradicts with the results in [13] which show that APS solution, when hydrolysed at elevated temperature, can recover a substantial amount of strength in thermally treated fibres. The data presented in Figure 5.31 seem to suggest that APS solution, whether hydrolysed at ambient or elevated temperature, does not significantly regenerate the strength of thermally recycled glass fibres when treatment is carried out at 95 °C and for a prolonged period of time. Moreover, treatment of the recycled fibres in 1 vol% APS solution under standard conditions (room temperature hydrolysis and treatment, and treatment time of 15 minutes) resulted in no improvement in tensile strength.

Figure 5.32 shows the strength of thermally recycled fibres after treatment in hot APS solution for 5 days (hot hydrolysis) at different concentrations.

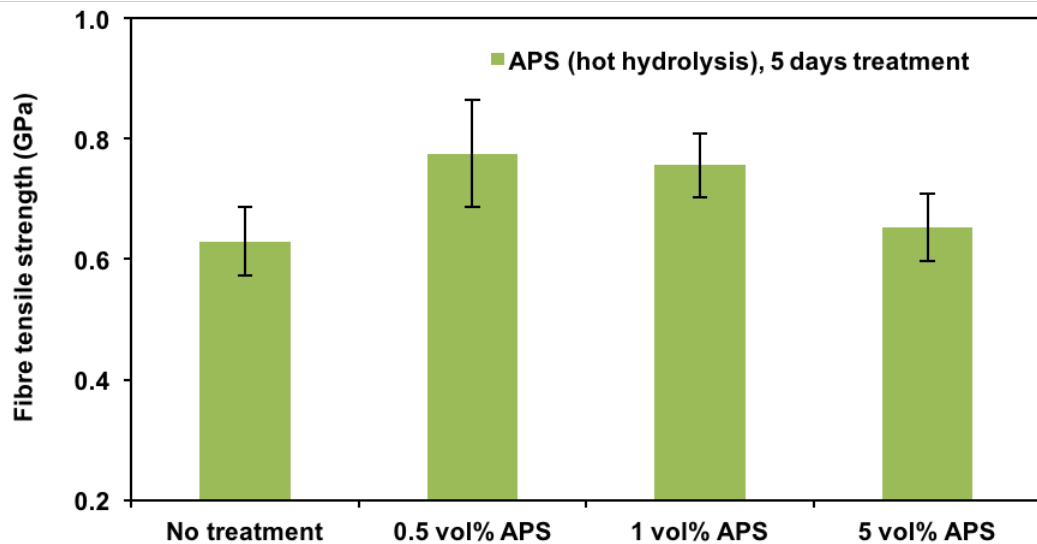


Figure 5.32 – Tensile strength of thermally recycled glass fibres after treatment in hot APS solution (hot hydrolysis) for 5 days at various concentrations

The results in Figure 5.32 indicate that varying the concentration of APS solution does not have any benefit on fibre strength. In fact, increasing the concentration to 5 vol% seems to start reducing the effect of the treatment on fibre strength; this could be due to a thicker layer of APS forming on the fibres resulting in filaments bonding together making them difficult to separate and thus leading to lower measured strength.

The pH of the APS solutions in this study was measured with a pH meter before and after they were used to treat the fibres. Figure 5.33 displays the measured pH of the APS solutions at different concentrations after treatment of fibres at various times.

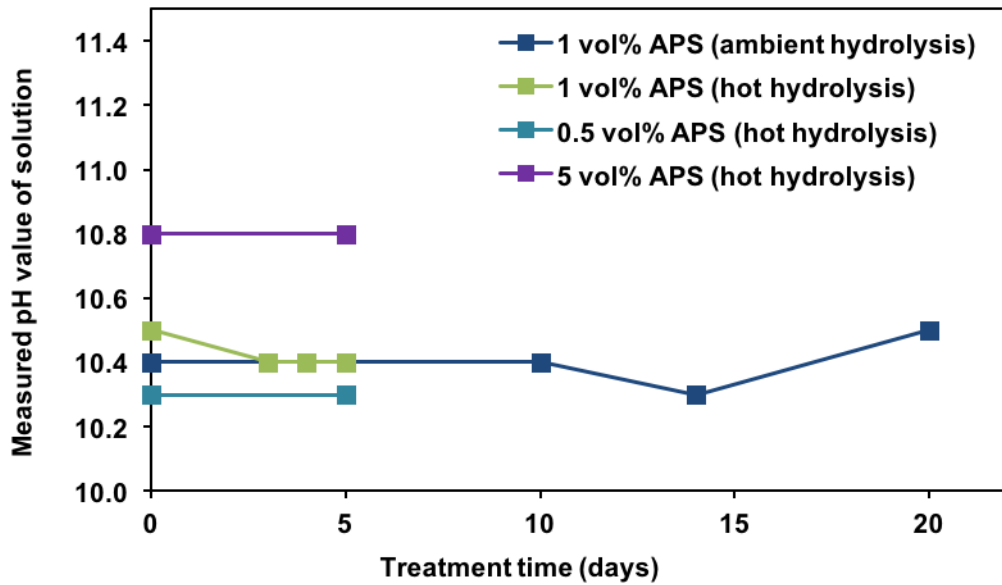


Figure 5.33 - Measured pH of APS solutions (25 °C) prepared at different concentrations, before and after treatment of thermally recycled glass fibres at various times

The pH of the 1 vol% APS solutions is around 10.4 to 10.5, similar to the literature value of pH 10.6 [45, 46, 103, 104, 130, 131]. Overall, there is very little change in the pH of the solutions before and after fibre treatments, though there is a slight increase for the case of 1 vol% APS (ambient temperature hydrolysis) at 20 days. The pH of the solution marginally increases with APS concentration, from pH 10.3 at 0.5 vol% APS to pH 10.8 at 5 vol%. The fact that APS solutions are alkaline indicates that hydroxide ions or hydroxide ion containing species are present, meaning they can potentially react with the glass to modify surface cracks. However, results in Figure 5.31 and Figure 5.32 suggest that APS solutions have no positive effect on the strength of thermally recycled glass fibres. Furthermore, no apparent diameter reduction was observed of the fibres after any of the APS treatments conducted in this investigation. This suggests that hydrolysed APS solution, though alkaline in nature, does not react with glass in a similar manner to NaOH; the interaction is likely to primarily involve the bonding of the glass surface to the APS

molecules, forming a protective barrier and improving the adhesion of the fibres to the polymer matrix. The interfacial properties of the thermally recycled glass fibres, and the extent to which they can improve after treatment in APS solution, were examined and reported in this thesis.

Figure 5.34 shows the IFSS of the fibres after treatment in hot 1 vol% APS solution (ambient temperature hydrolysis) for various times, with PP as the polymer matrix.

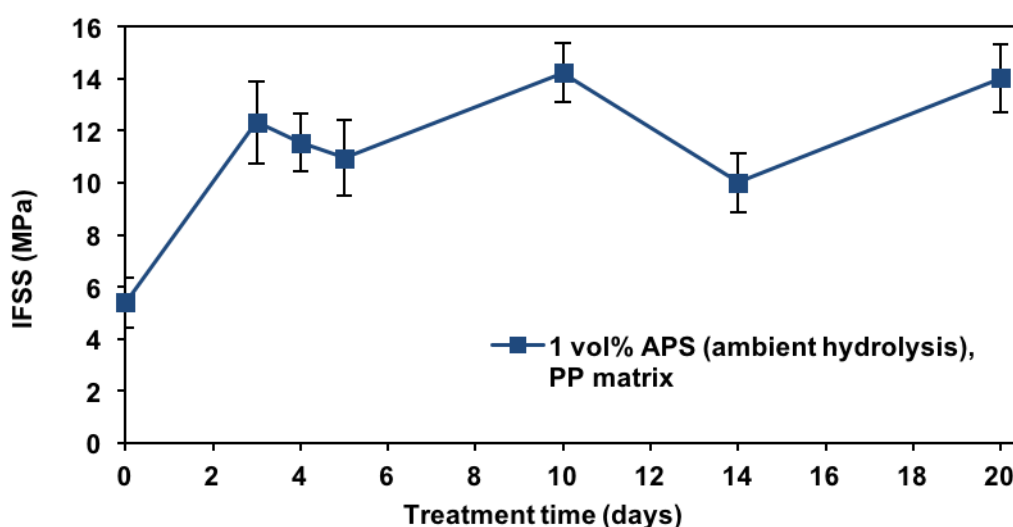


Figure 5.34 – IFSS of thermally recycled glass fibres after treatment in hot 1 vol% APS solution (ambient hydrolysis) for various times, with PP as matrix

The IFSS of the thermally recycled glass fibres with PP matrix is very poor without APS treatment (below 6 MPa); this is attributed to the fact that the bare glass surface is polar in nature due to the presence of silanol groups, which do not interact with the non-polar PP matrix. So, it can be concluded that thermally recycled glass fibres not only possess low tensile strength, but also poor adhesion to the PP

polymer matrix. Some polarity can be introduced to the PP via MAPP, and the IFSS of fibres with these PP/MAPP polymer matrices is explored later in this chapter.

Results in Figure 5.34 show that hot APS treatment of the thermally recycled glass fibres, where the hydrolysis step was carried out at room temperature, significantly improves the IFSS with PP. There appears to be no trend of IFSS with APS treatment time, as it mainly fluctuates from 10 to 14 MPa.

Figure 5.35 displays the IFSS of the fibres with PP when hot APS treatment was applied up to 5 days, and the hydrolysis step was carried out either hot or ambient.

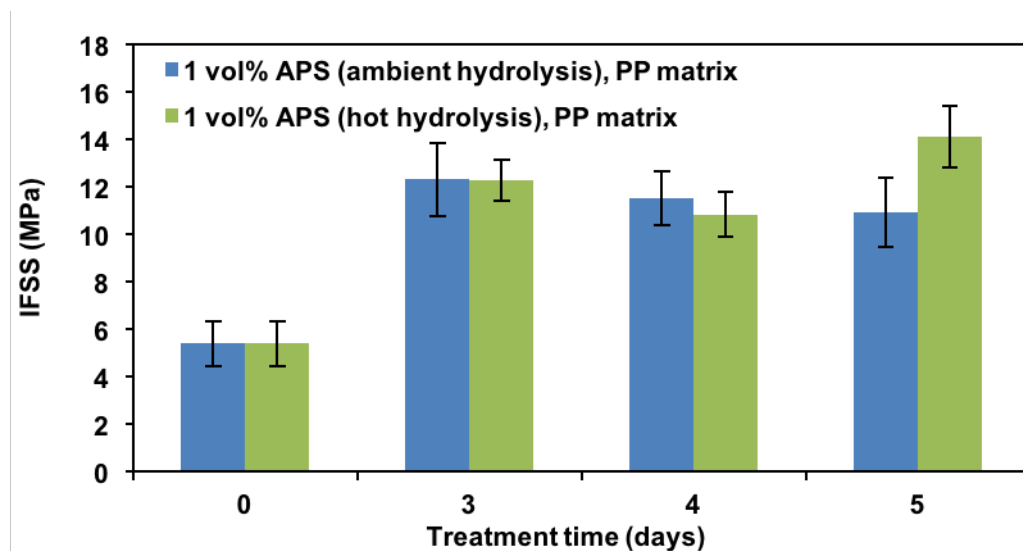


Figure 5.35 – IFSS of thermally recycled glass fibres after treatment in hot 1 vol% APS solution (ambient and hot hydrolysis) for various times, with PP as matrix

Overall, heating the APS solution during the hydrolysis process does not have a considerable impact on the extent of the increase in IFSS, though at 5 days there appears to be further improvement. Although the data presented in Figure 5.35 suggest that hot APS treatments can significantly improve the adhesion of thermally

recycled glass fibres to a PP matrix, in practice PP is usually combined with a small concentration of MAPP as it typically improves the adhesion further. To determine whether this is the case for fibres treated in hot APS solution, the IFSS was measured using PP blended with MAPP at 1.5 and 12 wt%. Figure 5.36 shows the IFSS of thermally recycled glass fibres with these various polymer matrices, before and after treatment in APS solution under different conditions.

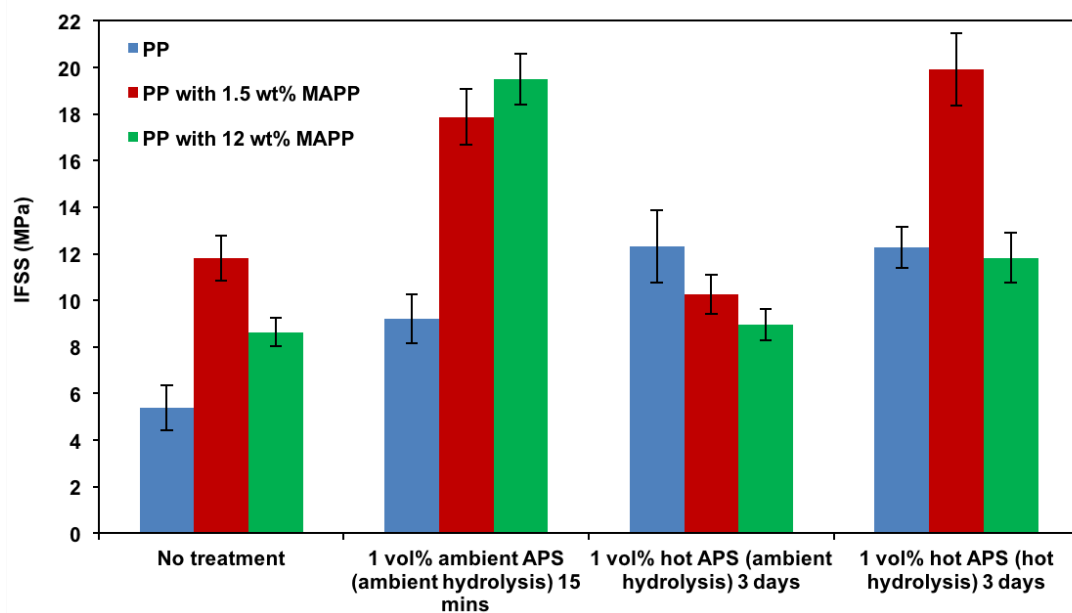


Figure 5.36 – IFSS of thermally recycled glass fibres after treatment in various APS solutions, with PP and PP/MAPP as matrices

The lowest measured IFSS is found in untreated recycled fibres with PP as the matrix (below 6 MPa). Because MAPP is slightly polar, using PP/MAPP does improve the IFSS (to around 12 MPa), though it appears to drop when the MAPP content is high (12 wt%). It has been discussed previously that including too much MAPP in the PP can have a detrimental effect on the IFSS of glass fibres; this could be due to an increased number of MA monomers reacting with the fibre surface,

meaning MAPP could not react [66, 67]. When APS solution is applied to the thermally recycled glass fibres under ambient conditions (ambient temperature hydrolysis and treatment, and a treatment time of 15 minutes), the IFSS increases only slightly when employing PP as the matrix. On the other hand, using a combination of PP and MAPP drastically enhances the IFSS of the fibres, peaking at around 20 MPa for PP blended with 12 wt% MAPP. When hot APS treatment (ambient hydrolysis) is applied to the fibres for 3 days, the IFSS with PP matrix is better than when ambient temperature APS or no APS treatment is used, reaching approximately 12 MPa. Conversely, the IFSS diminishes with MAPP content in the matrix, dropping to around 9 MPa for the case of PP combined with 12 wt% MAPP. As discussed earlier in Chapter 2, APS hydrolyses in water and then molecules condense to form short APS polymer chains (oligomers). The condensation process involves the removal of hydroxide groups from the hydrolysed APS molecules as they combine together to form a condensed oligomer. Heating the APS promotes the condensation of the APS molecules, resulting in longer and hence more non-polar chains. Because of this, increasing the concentration of MAPP (which is slightly polar) in the PP matrix can lead to poorer interaction with the APS and a reduction in IFSS, as indicated in Figure 5.36. When fibres are treated in hot APS solution with hot hydrolysis, the IFSS again increases slightly with the PP matrix. On the contrary, the IFSS improves considerably with PP and 1.5 wt% MAPP, reaching a similar value to fibres that were treated in APS under ambient conditions (ambient temperature hydrolysis and treatment). Like with the case of non-APS treated fibres, the IFSS of these fibres then begins to decrease with more MAPP in the PP matrix. The disparity in IFSS of fibres treated in hot APS solution with ambient and hot hydrolysis is not fully understood, though it is likely to be due to the structure of APS and how it is affected by temperature during the hydrolysis and condensation stage.

The results presented in this chapter indicate that hot APS treatment has no additional benefit on the strength or interface of thermally recycled glass fibres. Ambient APS treatment can deliver improved IFSS of the fibres with PP/MAPP at a shorter time and without the need for elevated temperatures either during the hydrolysis or fibre treatment step. With regards to fibre strength, none of the APS treatments performed in this research resulted in a significant improvement, despite the fact APS is shown to be alkaline in nature. The next sub-chapter looks more deeply into the surface state of thermally recycled glass fibres using the AFM, and whether the supposed flaws detected with this technique were critical to their failure.

5.4.4 Examination of surface flaws of recycled glass fibre by AFM

It was discussed in the literature review that potential scratches or craters were recently observed of thermally recycled glass fibres under an SEM. Given the fact that these features were not detected previously for thermally treated glass fibres suggested that they were present as a result of the recycling procedure in the fluidised bed, probably by abrasion with the bed sand. This section details an AFM investigation into thermally recycled glass fibres, with or without concentrated NaOH treatment, which showed possible surface pitting under the SEM. The height images from the AFM would confirm whether these were indeed flaws on the fibre surface, and by measuring their depths and inputting the values into a fracture mechanics model, the strength of the fibre can be back-calculated and compared to the measured strength obtained by tensile testing.

The fracture mechanics model used in this study is shown in Equation 5.3 [51].

$$\sigma_{f,av} = \frac{K_{Ic}}{(\pi c)^{1/2}}/Y$$

Equation 5.3

Equation 5.3 relates the strength of the glass fibre ($\sigma_{f,av}$, in MPa) to the fracture toughness (K_{Ic}), which was measured to be 0.91 MPa m^{0.5} by Feih et al. [51]. c denotes the critical flaw depth (m). The geometry factor, Y , varies depending on the geometry of the critical flaw (0.73 for half-penny, and 1.12 for straight). This equation allows the calculation of the strength of the glass fibre from the critical surface flaw depth, and does not take the gauge length effect into consideration. It has been reported previously that as the gauge length of the glass fibre test sample is decreased, the measured tensile strength increases [47]; this could be because as the length of the fibre sample is reduced, there are statistically fewer severe surface flaws that would be critical to failure of the fibre. An ideal experiment would be to scan the entire area of a fibre at the gauge length used for tensile testing, however given the nature of AFM and the fact that half the fibre is mounted on carbon tape, this approach would prove to be too challenging. In this study, AFM analysis of the recycled fibre surfaces was therefore conducted in a similar manner to that described in Chapter 3. Figure 5.37 shows a representative 3-D AFM height image (and corresponding phase image) of the surface of a glass fibre thermally recycled from the wind turbine blade waste using the fluidised bed.

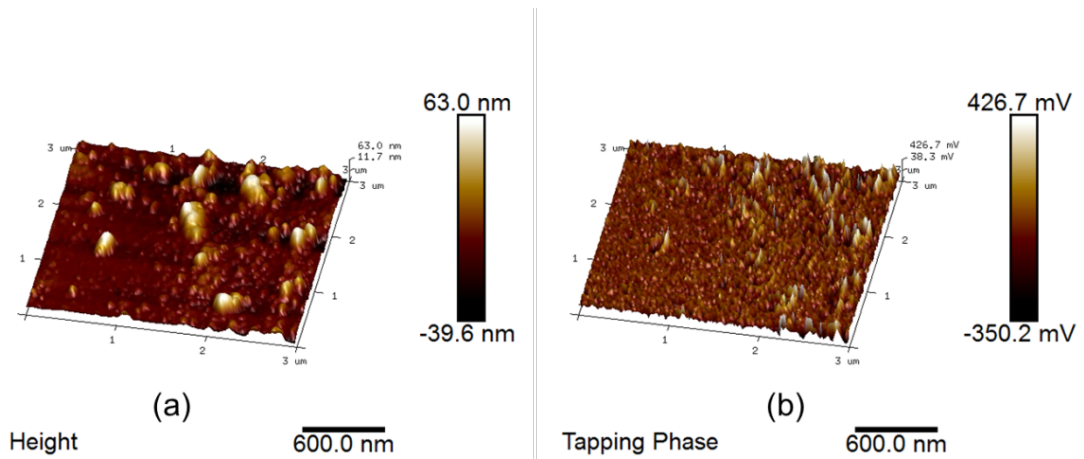


Figure 5.37 – 3-D AFM (a) height image, and (b) phase image of the surface of a glass fibre thermally recycled from an end-of-life wind turbine blade using the fluidised bed

Despite the fact the fibres were not treated in alkaline solution, there appears to be some residue on the fibre surface according to the height and phase image; this could be residual char from the recycling process. Some of the heightened regions however do not translate to phase shifts, implying that the topography of the glass surface was affected by the thermal recycling procedure. Because these fibres were not treated in alkaline solution, the roughness of the glass surface could not have resulted from etching, but probably from deposits of the silica sand dusts of the fluidised bed. The fact that some areas of the height image are darker than the bulk further suggests that craters were present on the glass surface, which was suspected earlier from SEM studies. NanoScope Analysis software was used to measure the depth of some of these potential craters or surface flaws, as shown in Figure 5.38.

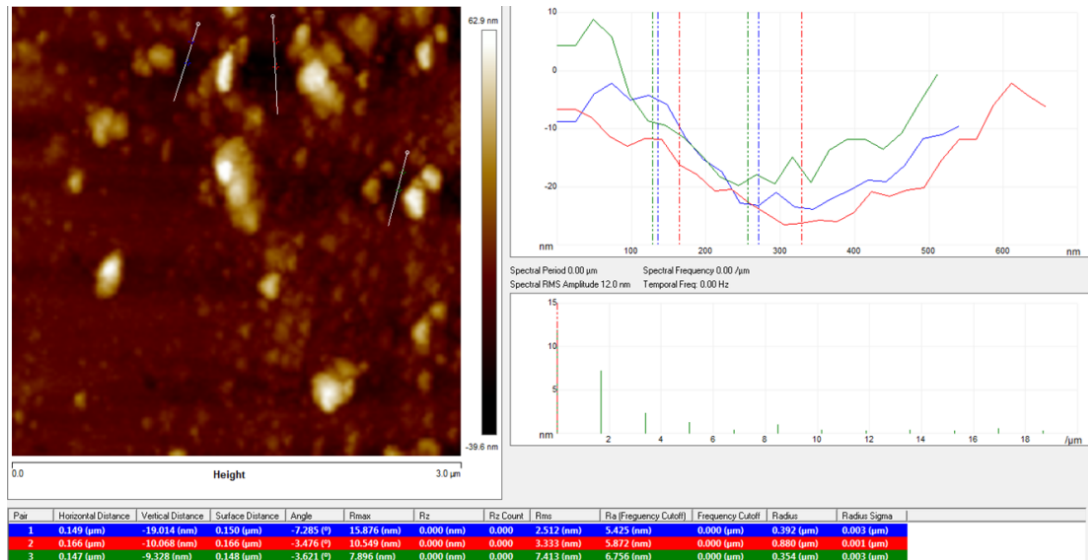


Figure 5.38 – Screenshot of NanoScope Analysis software being used to measure the depth of potential surface flaws on a glass fibre thermally recycled from an end-of-life wind turbine blade in the fluidised bed

Figure 5.38 also gives a line drawing (distance around 600 nm) showing both the depth and geometry of the surface craters. The graph suggests these possible flaws are more U-shaped. The c values given in the bottom table indicate the exact depths of the three craters selected. These depths were entered into the fracture mechanics model (Equation 5.3) to back-calculate the strength of the fibre; values are presented in Table 5.1.

Table 5.1 - Predicted strength of glass fibre thermally recycled from an end-of-life wind turbine blade using the fluidised bed, based on crater depths from the AFM

	c (nm)	$\sigma_{f,av}$ (GPa)	
		Y min (straight)	Y max (half-penny)
Crater 1	15.88	3.64	5.58
Crater 2	10.55	4.46	6.85
Crater 3	7.90	5.16	7.91

The measured depths of the craters are very low resulting in much higher predicted tensile strength of the fibre than expected (measured strength from tensile testing was 0.63 GPa). Even the lowest of the predicted strengths, from crater 1 and assuming the flaw was straight, appears to be 3.64 GPa, which is even above the strength measured of typical pristine glass fibre. This implies that neither of the craters detected under the AFM were critical to the failure of the fibre. Given the small area of fibre that was scanned ($3 \times 3 \mu\text{m}$) it was going to be challenging, even after numerous scans, to identify the critical fibre flaw. Fortunately, after scanning just a few regions of a fibre thermally recycled from a model epoxy composite and treated in alkali, a surface with very deep and potentially critical surface craters was observed. This scan area was then expanded to $10 \times 10 \mu\text{m}$ to see whether other neighbouring craters were present on the fibre surface (though scanning in a large area is usually not recommended since it could lead to damage of the AFM tip if it ends up travelling away from the fibre and onto the carbon tape). Figure 5.39 presents 3-D AFM height and phase images of the fibre that showed possible surface pitting.

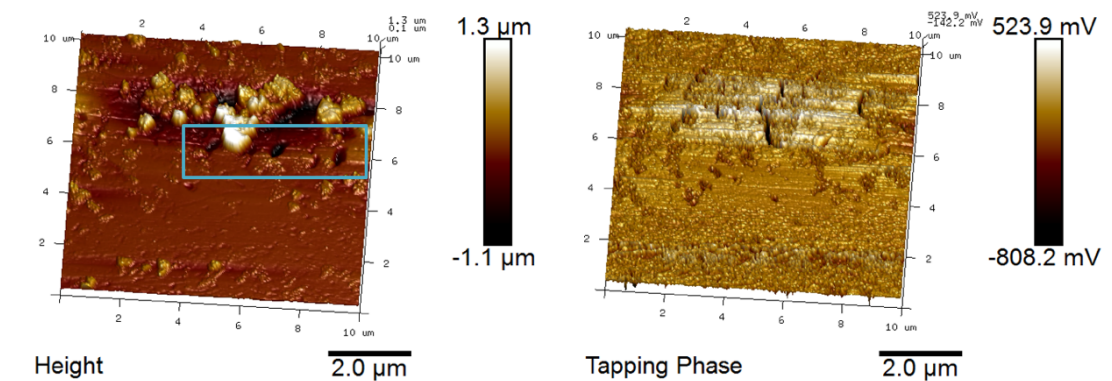


Figure 5.39 - 3-D AFM (a) height image, and (b) phase image of the surface of a glass fibre thermally recycled from a model epoxy composite using the fluidised bed, and treated in 90 °C 5 M NaOH solution for 20 minutes

As before, some changes in height correspond to phase shifts, indicating that residue (most likely from alkaline treatment) was present on the surface of the fibre. The craters observed in the height image do not appear to result in a change in phase, suggesting that these features are indeed of the glass itself. What is unusual is how the craters seem to be in a line on the fibre surface. This could potentially have been the contact point with another fibre, so separating them during single fibre sample preparation might have resulted in damage as indicated by the surface flaws. Furthermore, treating the fibre in alkaline solution could have increased the prominence of the craters through the etching effect. Figure 5.40 shows how the depth of the craters was measured using NanoScope Analysis.

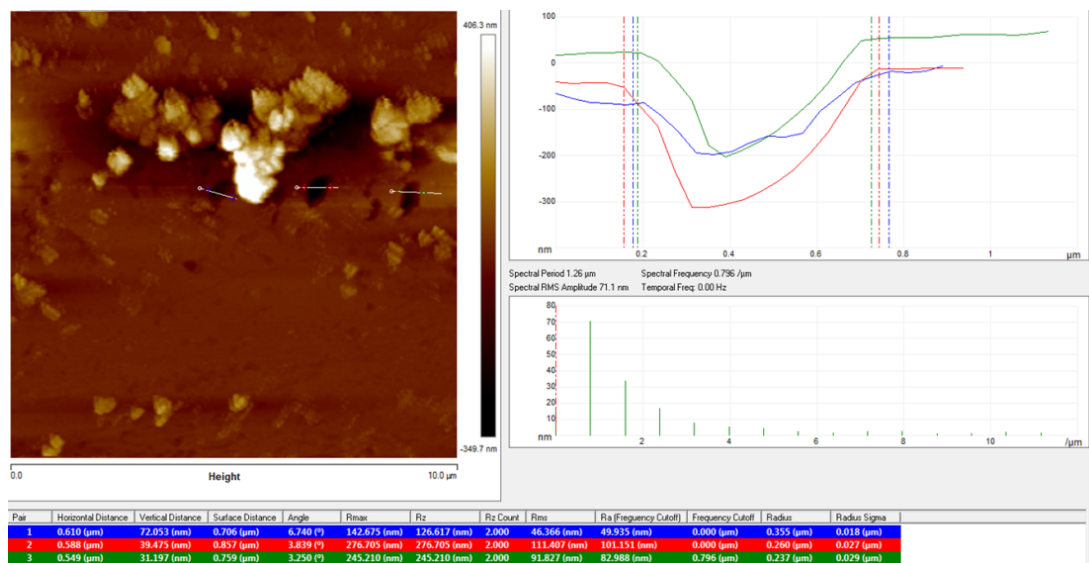


Figure 5.40 - Screenshot of NanoScope Analysis software being used to measure the depth of potential surface flaws on a glass fibre thermally recycled from a model epoxy composite using the fluidised bed, and treated in 90 °C 5 M NaOH solution for 20 minutes

According to Figure 5.40, the craters appear to have a smaller radius. The depths of the craters along with the predicted tensile strength are displayed in Table 5.2.

Table 5.2 – Predicted strength of glass fibre thermally recycled from a model epoxy composite using the fluidised bed, and treated in 90 °C 5 M NaOH solution for 20 minutes, based on crater depths from the AFM

	c (nm)	$\sigma_{f,av}$ (GPa)	
		Y min (straight)	Y max (half-penny)
Crater 1	142.68	1.21	1.86
Crater 2	276.71	0.87	1.34
Crater 3	245.21	0.93	1.42

All three craters possess a measured depth of a few hundred nm, which leads to calculated strengths that are more comparable to the measured strength by tensile testing. Specifically crater 2, which is almost 300 nm in depth, results in a predicted strength (assuming a straight surface flaw) of 0.87 GPa, which is not too far from the measured strength of 0.67 GPa from the tensile test. These results indicate that severe surface flaws on a fibre can be detected by AFM, and the depths can be measured and inputted into a fracture mechanics model to predict the strength of the fibre. Because of the nature of the technique, discovering the flaw that would lead to the failure of the fibre (the critical flaw) would be challenging. The current method of determining the strength of the fibres, which involves single fibre tensile testing, seems to be more straightforward.

5.4.5 Case study into the costs of industrial-scale alkaline treatment of recycled glass fibres

The results reported in this chapter show the positive effect of chemical treatments on the strength of thermally recycled glass fibres, particularly hot alkaline treatment (7 M NaOH for 2 hours). If this treatment were to be scaled up, the commercial feasibility would have to be examined; this would include an evaluation into the cost

of using chemicals to prepare the solution, and also implementing heat. There are other factors which would have to be considered, such as the cost of downsizing the composite waste material into smaller fragments for fluidised bed recycling, and running the fluidised bed itself to recycle fibres out of the composite. As this case study focuses more on the expenses associated with the alkaline treatment, parameters such as the operation of the fluidised bed are not assessed.

There are ways in which the alkaline treatment cost can be offset; one is by charging companies for collection of composite waste. Currently, the cost of depositing composite waste in landfill (landfill tax and transportation) is around £140 per tonne. We can charge this amount for collection of composite waste, difference being that instead of going to landfill we would recycle the material, making it a more environmentally-friendly disposal option for businesses. Another method of offsetting the costs of the treatment would be to sell the recycled glass fibre once it has been regenerated. The current price of commercial chopped glass fibre is £0.8 per kg, so assuming that these regenerated fibres can compete on performance with commercial chopped fibres, we can charge at a similar price.

Before investigating the costs of the treatment, an estimate on the volume of solution required needs to be given. Usually the composite waste would have 70 wt% of glass fibre, so if 1 tonne (1000 kg) of composite waste was collected, that would mean around 700 kg glass fibre recycled. From conducting large laboratory-scale treatments, it was found that 5 L of alkaline solution was needed to fully immerse 100 g of glass fibre (when using a cubic container). When applying this ratio, it is calculated that 35,000 L of 7 M NaOH solution (9800 kg NaOH) would be required to fully submerge 700 kg of fibre; in practice, the solution volume can be reduced if the fibres are treated in smaller batches but this case study looks into crude estimates. The cost of heating the solution to 95 °C also needs to be

considered. According to Process Heating Services Ltd, 2872.22 kW power is required to heat 35,000 L water by 70 °C (25 to 95 °C) for 1 hour (h). The price charged by Scottish Power (excluding VAT) is around 12.376 p per kWh, so this would add to £355.47 (assuming that the vessel is self-insulating after the 1 hour of heating). For simplicity, the cost of tap water (which is £0.001 per L) is considered in this case study with the assumption that it will not adversely affect the treatment.

As well as treating the fibres in alkaline solution, they also have to be rinsed in diluted HCl and water to remove residue. It was found that rinsing fibres in 10 vol% HCl solution (3.7% concentration) for a prolonged time was effective in removing alkaline residue. To make 10 vol% HCl solution at 35,000 L, 3500 L HCl (37% concentration) would be required. Taking into account the density of HCl being around 1.2 g/ml for that concentration, 4200 kg of 37% concentrated HCl would be needed. 31,500 L of water would also be required to dilute the HCl to 10 vol%. In this case study, the assumption is that rinsing the fibres repeatedly in this HCl solution and rinsing in water thereafter is sufficient to remove residue from the alkaline treatment.

Table 5.3 below gives the quantities and cost of chemicals for alkaline treatment of 700 kg recycled glass fibre. The cost of the NaOH and HCl are based on bulk orders from Alibaba.

Table 5.3 – Estimate of quantities and costs of chemicals for large-scale alkaline treatment of recycled glass fibres

Chemical	Quantity required	Cost per unit	Total cost
NaOH	9.8 tonnes	£227.10 per tonne	£2225.58
HCl	4.2 tonnes	£68.13 per tonne	£286.15
Tap water	101,500 L	£0.001 per L	£101.50
Heat	2872.22 kW power	£0.12 per kWh	£355.47
Total cost of treatment			£2968.70

When glass fibres are treated in alkaline solution on a large-scale in the laboratory, around 10 wt% mass loss occurs; although this is lower than the values reported earlier in this chapter from small-scale treatments, there is still considerable strength recovery. The benefit of a reduced mass loss from scaling up the treatment would be that more glass fibre is recovered for selling as regenerated chopped fibre. A 10 wt% loss of 700 kg fibre from an industrial-scale treatment means 630 kg can be recovered, and selling these fibres (at £0.8 per kg) would result in a revenue of £504. This, combined with the composite waste collection fee of £140, amounts to a total income of £644, which partially covers the expenses related to the treatment (which is almost £3000). Even without considering other processes like fluidised bed operation and sizing application to the fibres, the expenditure from carrying out an industrial-scale alkaline treatment of the fibres still far outweighs the revenue. There is, however, potential for profit to be made; provided the alkaline solution remains effective, it can be used multiple times for treating recycled fibres. This means more revenue can be earned from collecting a greater volume of composite waste, and selling greater volumes of regenerated chopped fibre. In addition, the leftover chemical solutions might find uses in other industrial applications.

5.5 Conclusions

Recycling glass fibres from wind turbine blade waste (using the fluidised bed) leads to a severe reduction in their strength. The work carried out in this research study indicates that chemical treatment can be an effective method to regenerate strength and interfacial properties of such fibres. Treating the fibres in hot NaOH solution at a high concentration of 7 M resulted in a significant improvement in tensile strength. A further increase in solution molarity led to reduced strength and very high dissolution rate of the fibres.

In this work, the recycled glass fibres were also treated in milder, pH-scale NaOH solutions for a prolonged time. Results showed that treating the fibres in pH 7 (water only) and pH 10 solution at elevated temperature over several days almost doubled their strength. There was a slight reduction in fibre diameter after pH 10 treatment (within error) suggesting that flaw geometry modification through etching has probably been responsible for strength increase.

Because of the slight alkalinity of APS and the fact that it is a widely used silane coupling agent for glass fibres, it made sense to treat recycled glass fibres in hot APS solution for an extended period of time to try and regenerate both their strength and fibre surface functionality. It was found that although hot APS treatment had no significant effect on the strength, the IFSS of the fibres was improved particularly with PP as the matrix. Despite this observation, it was clear that treating the fibres with APS under room temperature conditions led to the highest increase in IFSS, especially with PP/MAPP.

It was discovered from SEM imaging that some thermally recycled glass fibres, before and after alkaline treatment, possessed craters on the surface. These were examined in more detail using an AFM. Using the measured depth of the craters or

flaws from the AFM, the strength of the fibre was back-calculated using a fracture mechanics model. The unusually high predicted strengths from the model implied that although surface flaws were detected under the AFM, the ones examined were unlikely to have been of critical size. Finding the critical surface flaw of a fibre might be possible with the AFM but given that only small areas can be scanned each time, this approach might not be feasible enough in practice. In spite of this, it can be said that surface flaws of glass fibres can be detected using SEM and AFM, and to the author's knowledge, this was the first instance of natural surface flaws being detected and profiled on glass fibres. In fact, some of the flaws identified on the fibres had depths which resulted in a calculated tensile strength that was quite close to values obtained through tensile testing.

Finally, a case study into the costs of treating recycled fibres in alkaline solution on a commercial scale was carried out and reported in this chapter. The cost of conducting alkaline treatments of recycled fibres on a large scale would far outweigh the revenue (from composite waste collection and selling regenerated fibre). Profit can potentially be made if the treatment solution is used repeatedly for multiple batches of fibres, provided its strength regeneration effect does not diminish.

6 Conclusions

It is widely accepted that subjecting glass fibres to elevated temperatures leads to a severe reduction in their mechanical properties, hence rendering them unfeasible for reuse in composite applications. The work reported in this thesis generally involved treating glass fibres, damaged by thermal treatment or thermal recycling, in a chemical solution to regenerate their strength. The majority of these treatments were based on hot concentrated alkaline solutions, such as sodium hydroxide (NaOH) and potassium hydroxide (KOH). This chapter summarises the conclusions of Chapters 3 to 5, which reported on the experimental investigations conducted to achieve the project objectives. The key aim of this research study was to develop a post-recycling treatment to regenerate enough strength in thermally treated and recycled glass fibres to allow their reuse in second-life composite applications.

6.1 Regenerating the strength of thermally conditioned glass fibres through hot alkaline treatments (Chapter 3)

APS-sized E-glass fibre bundles were heat treated (HT) in a furnace at elevated temperature (typically 450 °C) to simulate recycling conditions, before being treated in concentrated alkaline solution (heated to 95 °C) to regenerate strength. It was found that lithium hydroxide (LiOH) solution had no positive impact on HT fibre strength. However, both NaOH and KOH solutions were able to significantly improve the strength of the fibres at concentrations of 1.5 M and above, and when the treatment duration was at the scale of minutes. After investigating the dissolution rate of the fibres in both alkaline solutions, it was discovered that NaOH solution was the most corrosive; this could have explained why a relatively milder

concentration and treatment time than KOH solution was required to recover HT fibre strength. By analysing the fibres through Fourier transform infrared spectroscopy (FTIR), it was suggested that the eventual decline in HT fibre strength with prolonged alkaline treatment could have been due to significant bulk glass network degradation. Fracture surface analysis indicated that the failure of such fibres was still likely to have initiated at the surface; so despite the breakdown of the bulk glass network, the surface would have had to react first with the alkaline solution and hence remain the weakest region. Analytical techniques such as atomic force microscopy (AFM) showed that alkali treated fibres possessed a rougher surface due to the etching of the glass and the presence of residue that failed to remove after the acid rinsing procedure. It was hypothesised (and supported by fractography) that the mechanism of strength increase of HT glass fibres by alkaline solution involved the smoothing of the sharp, severe cracks on the surface.

In this work, the effect of alkaline treatment on the properties of virgin APS-sized and bare glass fibres was also examined. Overall these treatments had a detrimental effect on the strength of virgin fibres, an observation that agreed well with the literature. The strength of APS-sized, HT and bare fibres after alkaline treatment eventually converged at around 1 GPa. It was interesting to note that the strength of alkali treated HT fibres never surpassed that of virgin bare fibres; even when optimal alkaline treatment conditions were applied to the HT fibres, their strength never matched that of virgin APS-sized fibres. The precipitous drop in strength of virgin APS-sized fibres led to the assumption that most of the protective APS coating was removed from the fibres by the alkaline solution. A mass loss study of the fibres before and after alkaline treatment indicated that despite the removal of the majority of the APS coating, the virgin APS-sized fibres were overall more resistant to dissolution by the alkaline solution than the HT and bare fibres.

6.2 Kinetics of dissolution of glass fibre in hot alkaline solution (Chapter 4)

Given that the strength regeneration mechanism of HT glass fibres by hot alkaline solution was thought to involve the etching of the damaged surface layer, it made sense to investigate the kinetics of glass dissolution. In this study, glass fibres were individually treated in hot KOH and NaOH solution at different molarities and times before being measured for diameter reduction using a scanning electron microscope (SEM). Results showed that NaOH solution etched fibres up to twice the magnitude of KOH. Furthermore, the rate of dissolution of the fibres increased fairly linearly with time, and also as a function of solution temperature and concentration. The kinetic data from this work fit well in the shrinking cylinder and zero order models, suggesting that the etching of the glass fibres and/or the diffusion of hydroxide ions through the solution could have been rate controlling factors. The poor agreement with the 2-D diffusion model indicated that the diffusion of the hydroxide ions through the product layer on the glass fibre surface was unlikely to have been a rate determining step. Using the reaction rates and rate constants from the shrinking cylinder and zero order model, the reaction order was determined to be 0.43 – 0.49 for KOH and 0.31 – 0.44 for NaOH. The activation energy of the reaction from employing the zero order model was 58 kJ/mol for NaOH and 72 kJ/mol for KOH; this disparity suggested that diffusion of hydroxide ions through the solution required less energy if NaOH was used as the alkali, hence resulting in greater fibre dissolution. The activation energy calculated from the shrinking cylinder model was similar for both alkaline solutions (79 kJ/mol for KOH and 74 kJ/mol for NaOH), implying that once the hydroxide ions were at the glass surface, the energy needed to initiate the etching procedure was the same regardless of the nature of alkaline solution used.

6.3 Regenerating the performance of thermally recycled glass fibres (Chapter 5)

Glass fibres experience severe loss in strength and interfacial properties during thermal recycling/treatment. In this work, glass fibres were thermally recycled out of an end-of-life wind turbine blade using an in-house fluidised bed. Various chemical treatments were then applied to these fibres in an attempt to regenerate their strength. It was found that treating the fibres in hot and concentrated alkaline solution (NaOH) for a few hours led to a significant increase in tensile strength, approaching the 1.5 GPa target required to allow their reuse in second-life composite applications. When the treatment was too aggressive, however, a reduction in fibre strength was observed because of the degradation of the bulk internal glass network structure. The fact that almost half of the mass of the recycled fibres was lost as a result of the treatment highlighted the extremely corrosive behaviour of the alkaline solution. A case study into the costs of treating recycled fibres in hot alkaline solution on an industrial scale was reported in this thesis. It was found that the cost of chemicals and heat can be partially covered by charging businesses for collecting their composite waste and selling the regenerated fibres.

The recycled glass fibres were also treated in milder, pH-scale NaOH solution to see whether strength can be regenerated in a safer manner. Results showed that treating the fibres in pH 7 (simply water) and pH 10 solutions for several days and at elevated temperature can almost double their strength. Whilst the strength increase was not as considerable as that from concentrated alkaline treatment, this procedure was safer and more economical. APS, a widely used silane coupling agent, is slightly alkaline in nature, meaning there was the potential to regenerate both the strength and interface of the recycled fibres in one chemical treatment.

Unfortunately, it was found that treating the fibres in hot APS solution for several days led to little or no improvement in strength, however there was an observed increase in IFSS when using PP as the polymer matrix. A standard room temperature treatment of the fibres in APS solution showed a better improvement in adhesion, particularly when using PP combined with MAPP.

Potential surface pitting was found on thermally recycled glass fibres (before and after alkaline treatment) with SEM imaging. These features were probed under the AFM to find their depth and geometry. In addition, the measured depths of the craters or flaws were used in a fracture mechanics model to back-calculate the strength of the fibre. Because of the high strengths predicted from the model it was concluded that the flaws observed under the AFM were unlikely to be critical to the fibre failure. Nevertheless, this was the first instance, to the author's knowledge, of natural surface flaws being detected on a glass fibre.

7 Future work

In this research, a significant amount of experimental work was carried out to address the project objectives. Although it was found that certain chemical treatments managed to regenerate the mechanical properties of thermally treated and recycled glass fibres, there are areas where further research can be advantageous. In this section, potential experiments that can be conducted in future are discussed. The areas for future work are described here under the relevant chapter headings of the thesis.

7.1 Regenerating the strength of thermally conditioned glass fibres through hot alkaline treatments (Chapter 3)

In this chapter, it was discovered that treating thermally conditioned glass fibre bundles in hot NaOH and KOH solution at a specific concentration and time significantly regenerated their strength. Although promising results were obtained with alkaline treatments of the fibres, they were only heat treated at the lower end of the thermal recycling temperature range (450 °C). Above this temperature, the alkaline treatments had little or no effect on the fibre strength, unless a prewashing step was introduced before the thermal conditioning procedure. Because thermal recycling processes typically operate above 450 °C, it would be beneficial to do a more detailed and systematic investigation into the effects of alkaline treatments on fibres thermally conditioned at higher temperatures. Such a study might provide further insight into why thermally recycled glass fibres (recycled at around 500 °C) require at times more aggressive alkaline treatment conditions in order to improve in strength.

AFM examination of the alkali treated fibre surfaces indicate a build-up of residual deposits and etching of the glass itself, resulting in an overall increase in roughness. There was found to be a relationship between the roughness (R_q) of the fibre surface and the measured tensile strength at that particular alkaline treatment condition. FTIR spectroscopy also proved to be a useful technique in examining the chemical structure of the glass fibres before and after alkaline treatment. There is therefore the potential of both AFM and FTIR being effective tools in pre-validating that optimum alkaline treatment conditions had been applied to the thermally conditioned fibres at 450°C. Further research could involve a systematic study into the effects of alkaline treatment conditions on the roughness of the fibre surface measured by AFM, and also the degree of absorbance of silicate and silanol groups from FTIR analysis. It was shown from the diffuse reflectance FTIR data that the reststrahlen effect [102] resulted in the inversion of the silicate absorbance bands, often making it challenging to see clearly the trends with the different alkaline treatments applied to the fibres. These derivative-shaped bands can be removed by Kubelka-Munk transformation [148] to make it easier to observe the change in silicate absorbance, and can allow quantitative data to be extracted from FTIR. By carrying out this investigation along with AFM studies, we will be able to deduce whether the alkaline treatment condition (and hence tensile strength of the fibres) directly affects the FTIR absorbance and fibre surface roughness.

To the author's knowledge, the work carried out in this project was the first to involve examining the strength of both thermally treated and virgin glass fibres before and after alkaline treatment in conjunction. Results proved that the strength increase of thermally treated fibres and decrease of the virgin fibres eventually led to a convergence at around 1 GPa. Further research into the processes that result in the strength increase and decrease of thermally conditioned and virgin fibres

respectively would be of benefit, as it could help with understanding the convergence.

7.2 Kinetics of dissolution of glass fibre in hot alkaline solution (Chapter 4)

The research presented in Chapter 4 involved treating individual bare glass fibres in hot alkaline solution and measuring their diameter reduction accurately with an SEM. Results suggested this was an effective method of analysing reaction kinetics of glass fibre dissolution in alkaline solution. The reason why bare glass fibres instead of thermally conditioned fibres were used in this study was because they were stronger and therefore easier to handle. Carrying out a similar experiment using thermally treated fibres would be beneficial though, given that in practice, the hot alkaline treatments would be applied to thermally treated fibres to regenerate their strength. It might also be useful to analyse the reaction kinetics of thermally recycled glass fibre dissolution in hot alkaline solution, to see whether there is a disparity in behaviour.

Although measuring the diameter reduction of the glass fibres after alkaline treatment can be an effective way of determining the dissolution rate, it can only be speculated how the dissolution reaction proceeds chemically. Given that E-glass fibres contain various metal oxides as well as the principal component of silica, the overall dissolution reaction is thought to involve multiple processes that occur simultaneously or at different stages. Krauklis [149] recently published work on the long-term dissolution of glass fibres in hot water. As well as measuring the diameter change of the fibres after the water treatment, the concentration of ions that

dissolved from the glass into the water was also measured using inductively coupled plasma mass spectrometry (ICP MS). The employment of such an analytical technique could be useful in this research, as it would provide further information into how the various constituents of E-glass fibres react with alkaline solution, and whether these processes are dependent on each other.

7.3 Regenerating the performance of thermally recycled glass fibres (Chapter 5)

In this research, a range of chemical treatments were applied to glass fibres that were thermally recycled out of an end-of-life wind turbine blade using the in-house fluidised bed. It was found that a hot concentrated NaOH treatment (at 7 M) of the fibres for a couple of hours was able to significantly regenerate their tensile strength to allow their reuse in a second-life composite application. A systematic investigation into the effect of treatment time and alkaline solution molarity would help in determining the optimum conditions required to recover recycled fibre strength. To offset the environmental and economic concerns with using concentrated alkaline solutions, they can be subsequently employed in another application such as geopolymer synthesis [150-159]. To produce a good quality geopolymer, a combination of very concentrated NaOH solution and sodium silicate would be necessary as the alkaline activator. Hence it is important that not only the NaOH treatment is effective at improving fibre strength, but is also within the molarity range required for use as feedstock in geopolymer production. Sodium silicate happens to be a by-product from the reaction of the silica component in glass fibres with the NaOH solution; thus the fibre treatment process can be tuned so that a sufficient amount of sodium silicate is produced in the NaOH solution, and the NaOH solution

concentration is also high enough to use as an alkaline activator in geopolymer synthesis. Another approach could be to by-pass the fibre strength regeneration process altogether and essentially dissolve all the recycled fibres into the NaOH solution to produce sodium silicate for geopolymer manufacturing.

Finally, it was discovered that the strength of recycled glass fibres can be improved by treatment in a milder pH-scale alkaline solution (or simply water) at elevated temperature for several days. Whilst this treatment is not as effective as concentrated alkali and requires a very long treatment time, the advantage is that the procedure is more environmentally-friendly and less expensive. More research still needs to be carried out into the effects of pH, treatment time and temperature in order to find optimum conditions to regenerate fibre strength. If the strength of recycled fibres can be increased more significantly through milder alkaline conditions, then this could prove to be a more commercially-feasible treatment option.

8 References

- [1] S Job, G Leeke, P Mativenga, G Oliveux, SJ Pickering, N Shuaib (2016), Report for Composites UK Ltd. Available at https://compositesuk.co.uk/system/files/documents/Recycling_Report_2016.pdf.
- [2] ST Bashir, L Yang, R Anderson, PL Tang, JJ Liggat, JL Thomason (2017) Composites Part A: Applied Science and Manufacturing 102: 76. Doi:<http://dx.doi.org/10.1016/j.compositesa.2017.07.023>
- [3] S Job (2013) Reinforced Plastics 57: 19. Doi:[http://dx.doi.org/10.1016/S0034-3617\(13\)70151-6](http://dx.doi.org/10.1016/S0034-3617(13)70151-6)
- [4] H Albers, S Greiner, H Seifert, U Kühne (2009), DEWI Magazin
- [5] SJ Pickering (2006) Composites Part A: Applied Science and Manufacturing 37: 1206.
- [6] G Oliveux, LO Dandy, GA Leeke (2015) Progress in Materials Science 72: 61. Doi:10.1016/j.pmatsci.2015.01.004
- [7] S Feih, E Boiocchi, G Mathys, Z Mathys, AG Gibson, AP Mouritz (2011) Composites Part B: Engineering 42: 350. Doi:10.1016/j.compositesb.2010.12.020
- [8] PG Jenkins, L Yang, JJ Liggat, JL Thomason (2014) Journal of Materials Science 50: 1050. Doi:10.1007/s10853-014-8661-x
- [9] JL Thomason, L Yang, R Meier (2014) Composites Part A: Applied Science and Manufacturing 61: 201. Doi:10.1016/j.compositesa.2014.03.001
- [10] U Nagel, L Yang, CC Kao, JL Thomason (2016) Polymer Composites. Doi:10.1002/pc.24029
- [11] L Yang, ER Sáez, U Nagel, JL Thomason (2015) Composites Part A: Applied Science and Manufacturing 72: 167. Doi:10.1016/j.compositesa.2015.01.030
- [12] GACM Spierings (1993) Journal of Materials Science 28: 6261. Doi:10.1007/bf01352182
- [13] E Sáez (2016) University of Strathclyde, PhD Thesis
- [14] JL Thomason, U Nagel, L Yang, E Sáez (2016) Composites Part A: Applied Science and Manufacturing 87: 220. Doi:10.1016/j.compositesa.2016.05.003
- [15] RD Smith, PE Corbin (1949) Journal of the American Ceramic Society 32: 195. Doi:10.1111/j.1151-2916.1949.tb19767.x
- [16] VS Molchanov, NE Prikhidko (1957) Bulletin of the Academy of Sciences of the USSR, Division of chemical science 6: 1179. Doi:10.1007/bf01167384

- [17] SS Kouassi, J Andji, J-P Bonnet, S Rossignol (2010) *Ceramics-Silikáty* 54: 235.
- [18] M Friedrich, A Schulze, G Prösch, et al. (2000) *Microchimica Acta* 133: 171.
- [19] H Gu (2008) *Materials & Design* 29: 1893.
- [20] C Scheffler, T Förster, E Mäder, G Heinrich, S Hempel, V Mechtcherine (2009) *Journal of Non-Crystalline Solids* 355: 2588. Doi:10.1016/j.jnoncrysol.2009.09.018
- [21] B Wei, H Cao, S Song (2010) *Materials & Design* 31: 4244. Doi:10.1016/j.matdes.2010.04.009
- [22] J Liu, M Jiang, Y Wang, G Wu, Z Wu (2013) *Ceramics International* 39: 9173. Doi:10.1016/j.ceramint.2013.05.018
- [23] PG Jenkins (2016) *Materials Science and Technology*: 1. Doi:10.1080/02670836.2016.1180743
- [24] S Feih, K Manatpon, Z Mathys, AG Gibson, AP Mouritz (2008) *Journal of Materials Science* 44: 392. Doi:10.1007/s10853-008-3140-x
- [25] PG Jenkins (2016) University of Strathclyde, PhD Thesis
- [26] S Games (1941) US Patent 2,230,272,
- [27] S Games (1944) US Patent 2,339,431,
- [28] S Games (1947) US Patent 2,431,205,
- [29] S Games, E Fletcher (1949) US Patent 2,489,242,
- [30] J Emsley (1983) *New Scientist* 100: 728.
- [31] FT Wallenberger (2000) *Advanced Inorganic Fibers* Springer,
- [32] AA Griffith, M Eng (1921) *Phil. Trans. R. Soc. Lond. A* 221: 163.
- [33] N Kivi, A Moore, K Dyar, S Haaf (2016) University of Tennessee Knoxville.
- [34] L Zhuravlev (1987) *Langmuir* 3: 316.
- [35] L Zhuravlev (2000) *Colloids and Surfaces A: Physicochemical and Engineering Aspects* 173: 1.
- [36] AA Christy, PK Egeberg (2005) *Analyst* 130: 738.
- [37] X Liu, J Thomason, F Jones (2009) *Silanes and other coupling agents* 5: 25.
- [38] R Fry, K Mueller, C Pantano (2003) *Physics and Chemistry of Glasses* 44: 64.

- [39] FT Wallenberger, JC Watson, H Li (2000) Inc., ASM International, Ohio, USA.
- [40] J Thomason, L Adzima (2001) Composites Part A: Applied Science and Manufacturing 32: 313.
- [41] P Zinck, M Pay, R Rezakhanlou, J Gerard (1999) Journal of materials science 34: 2121.
- [42] P Zinck, E Mäder, J Gerard (2001) Journal of materials science 36: 5245.
- [43] EP Plueddemann (1991) Silane Coupling Agents. Springer US
- [44] PG Pape (2011) Applied Plastics Engineering Handbook Elsevier, US
- [45] D Wang, FR Jones, P Denison (1992) Journal of Adhesion Science and Technology 6: 79. Doi:10.1163/156856192x00070
- [46] X Liu, JL Thomason, FR Jones (2008) The Journal of Adhesion 84: 322. Doi:10.1080/00218460802004386
- [47] L Yang, JL Thomason (2012) Journal of Materials Science 48: 1947. Doi:10.1007/s10853-012-6960-7
- [48] JL Thomason, DW Dwight (2000) Journal of Adhesion Science and Technology 14: 745. Doi:10.1163/156856100742852
- [49] PK Gupta (2002) Fiber fracture, Elsevier
- [50] PK Gupta, D Inniss, CR Kurkjian, Q Zhong (2000) Journal of non-crystalline solids 262: 200.
- [51] S Feih, AP Mouritz, SW Case (2015) Composites Part A: Applied Science and Manufacturing 76: 255. Doi:<http://dx.doi.org/10.1016/j.compositesa.2015.06.006>
- [52] WH Otto (1961) Journal of the American Ceramic Society 44: 68.
- [53] N Cameron (1965) Journal of the American Ceramic Society 48: 385.
- [54] PJ Lezzi, QR Xiao, M Tomozawa, TA Blanchet, CR Kurkjian (2013) Journal of Non-Crystalline Solids 379: 95. Doi:10.1016/j.jnoncrysol.2013.07.033
- [55] S Ito, M Tomozawa (1982) Journal of the American Ceramic Society 65: 368.
- [56] S Gao, E Mäder, R Plonka (2007) Acta Materialia 55: 1043.
- [57] S-L Gao, E Mäder, R Plonka (2008) Composites Science and Technology 68: 2892.
- [58] FT Wallenberger (2010): 3. Doi:10.1007/978-1-4419-0736-3_1
- [59] ML Korwin-Edson, DA Hofmann, PB McGinnis (2012) International Journal of Applied Glass Science 3: 107.

- [60] FR Jones, NT Huff (2018) in Bunsell AR (ed) Handbook of Properties of Textile and Technical Fibres (Second Edition) Woodhead Publishing,
- [61] R Charles (1958) Journal of Applied Physics 29: 1549.
- [62] FFY WANG, F Tooley (1958) Journal of the American Ceramic Society 41: 521.
- [63] S Wiederhorn, ER Fuller, R Thomson (1980) Metal science 14: 450.
- [64] B Ramachandran, B Pai, N Balasubramanian (1980) Journal of the American Ceramic Society 63: 1.
- [65] H Li, P Gu, J Watson, J Meng (2013) Journal of Materials Science 48: 3075. Doi:10.1007/s10853-012-7082-y
- [66] K Pender (2018) University of Strathclyde, PhD Thesis
- [67] U Nagel (2016) University of Strathclyde, PhD Thesis
- [68] S Bashir, L Yang, J Liggat, J Thomason (2018) 18th European Conference on Composite Materials, Athens, Greece
- [69] S Bashir, L Yang, R Anderson, et al. (2016) 17th European Conference on Composite Materials, Munich, Germany
- [70] J Schultz, C Lhymn (1984) Polymer composites 5: 208.
- [71] AB Sun, BY Li (2011) 18th International Conference on Composite Materials,
- [72] B Wei, H Cao, S Song (2011) Corrosion Science 53: 426. Doi:<https://doi.org/10.1016/j.corsci.2010.09.053>
- [73] H Li, M Yan, D Qi, et al. (2011) Journal of Petroleum Science and Engineering 78: 371.
- [74] P Hogg, D Hull (1980) Metal Science 14: 441.
- [75] SJ Harris, B Nobel, MJ Owen (1984) Journal of Materials Science 19: 1596. Doi:10.1007/bf00563057
- [76] W Mingchao, Z Zuoguang, L Yubin, L Min, S Zhijie (2008) Journal of Reinforced Plastics and Composites 27: 393.
- [77] B Ramachandran, V Velpari, N Balasubramanian (1981) Journal of Materials Science 16: 3393.
- [78] V Velpari, B Ramachandran, T Bhaskaran, B Pai, N Balasubramanian (1980) Journal of Materials Science 15: 1579.
- [79] M Aslanova (1960) Glass and Ceramics 17: 563.
- [80] M Piggott, J Yokom (1968) Glass technology 9: 172.

- [81] B Ramachandran, G Basavarajappa, B Pai, N Balasubramanian (1984) *Journal of materials science letters* 3: 685.
- [82] S Sakka (1956) *Bulletin of the Institute for Chemical Research* 34(6): 316.
- [83] M Aslanova, V Rudnev, A Filonenko (1969) *Glass and Ceramics* 26: 404.
- [84] W Thomas (1960) *Glass and Ceramics* 17: 549.
- [85] N Cameron (1968) *Glass technology* 9: 121.
- [86] ST Tso, JA PASK (1982) *Journal of the American Ceramic Society* 65: 360.
- [87] G Trucks, K Raghavachari, G Higashi, Y Chabal (1990) *Physical Review Letters* 65: 504.
- [88] G Spierings (1991) *Journal of materials science* 26: 3329.
- [89] J Bühler, F Steiner, H Baltes (1997) *Journal of Micromechanics and Microengineering* 7: R1.
- [90] DM Knotter (2000) *Journal of the American Chemical Society* 122: 4345. Doi:10.1021/ja993803z
- [91] C Iliescu, J Jing, FEH Tay, J Miao, T Sun (2005) *Surface and Coatings Technology* 198: 314. Doi:<http://dx.doi.org/10.1016/j.surfcoat.2004.10.094>
- [92] E Saez Rodriguez, L Yang, J Thomason (2013) 19th International Conference on Composite Materials, Montreal, Canada
- [93] VS Molchanov, NE Prikhid'ko (1958) *Bulletin of the Academy of Sciences of the USSR, Division of chemical science* 7: 893. Doi:10.1007/bf00911336
- [94] R Bell, J Prue (1949) *Journal of the Chemical Society (Resumed)*: 362.
- [95] F Gimblett, C Monk (1954) *Transactions of the Faraday Society* 50: 965.
- [96] JG Hooley (1961) *Canadian Journal of Chemistry* 39: 1221. Doi:10.1139/v61-155
- [97] B Chen, I Ivanov, JM Park, M Parrinello, ML Klein (2002) *The Journal of Physical Chemistry B* 106: 12006. Doi:10.1021/jp026504w
- [98] DB Hawkins (1981) *Clays and Clay Minerals* 29: 331.
- [99] K Beneke, G Lagaly (1989) *American Mineralogist* 74: 224.
- [100] M Kawano, K Tomita (1997) *Clays and Clay Minerals* 45: 365.
- [101] H Ishida, JL Koenig (1978) *Journal of colloid and interface science* 64: 555.
- [102] C Ricci, C Miliani, BG Brunetti, A Sgamellotti (2006) *Talanta* 69: 1221. Doi:10.1016/j.talanta.2005.12.054

- [103] S Culler, S Naviroj, H Ishida, J Koenig (1983) Journal of colloid and interface science 96: 69.
- [104] S Culler, H Ishida, J Koenig (1986) Polymer composites 7: 231.
- [105] H Ishida, JL Koenig (1978) Journal of colloid and interface science 64: 565.
- [106] HJ Gulley-Stahl, SB Bledsoe, AP Evan, AJ Sommer (2010) Applied spectroscopy 64: 15.
- [107] ST Bashir, L Yang, JJ Liggat, JL Thomason (2018) Journal of Materials Science 53: 1710. Doi:10.1007/s10853-017-1627-z
- [108] V Molchanov, N Prikhid'ko (1958) Russian Chemical Bulletin 7: 1.
- [109] V Molchanov, N Prikhid'ko (1958) Russian Chemical Bulletin 7: 783.
- [110] V Molchanov, N Prikhid'ko (1959) Russian Chemical Bulletin 8: 1.
- [111] S Greenberg (1957) The Journal of Physical Chemistry 61: 960.
- [112] F Jendoubi, A Mgaidi, M El Maaoui (1997) The Canadian Journal of Chemical Engineering 75: 721. Doi:10.1002/cjce.5450750409
- [113] M Tanaka, K Takahashi (1999) Analytical sciences 15: 1241.
- [114] J Fernandez, MJ Renedo, A Pesquera, JA Irabien (2002) Chemical Engineering Communications 189: 310. Doi:10.1080/00986440212083
- [115] G Du, G LÜ, X He (2013) Chinese Journal of Chemical Engineering 21: 736. Doi:10.1016/s1004-9541(13)60533-9
- [116] S Gin, P Jollivet, M Fournier, et al. (2015) Geochimica et Cosmochimica Acta 151: 68. Doi:10.1016/j.gca.2014.12.009
- [117] A Norström, H Watson, B Engström, J Rosenholm (2001) Colloids and Surfaces A: Physicochemical and Engineering Aspects 194: 143. Doi:[https://doi.org/10.1016/S0927-7757\(01\)00783-X](https://doi.org/10.1016/S0927-7757(01)00783-X)
- [118] A Al Cheikh, M Murat (1988) Cement and Concrete Research 18: 943.
- [119] J Crank (1975) The Mathematics of Diffusion. Clarendon Press,
- [120] M Dudukovic (1984) Industrial & Engineering Chemistry Process Design and Development 23: 330.
- [121] C Dickinson, G Heal (1999) Thermochemica Acta 340: 89.
- [122] J Moon, V Sahajwalla (2001) ISIJ international 41: 1.
- [123] H Brouwers, R Eijk (2002) Concrete Science and Engineering 4: 106.
- [124] J Orfao, F Martins (2002) Thermochemica Acta 390: 195.

- [125] PK Gbor, CQ Jia (2004) *Chemical Engineering Science* 59: 1979. Doi:10.1016/j.ces.2004.01.047
- [126] V Buscaglia, C Milanese (2005) *The Journal of Physical Chemistry B* 109: 18475.
- [127] A Khawam, DR Flanagan (2006) *The Journal of Physical Chemistry B* 110: 17315. Doi:10.1021/jp062746a
- [128] P Michèle, F Loïc, S Michel (2011) *Thermochimica Acta* 525: 93. Doi:10.1016/j.tca.2011.07.026
- [129] T Salmi, H Grénman, J Wärnå, DY Murzin (2013) *Chemical Engineering Research and Design* 91: 1876. Doi:10.1016/j.cherd.2013.08.004
- [130] S Naviroj, S Culler, J Koenig, H Ishida (1984) *Journal of colloid and interface science* 97: 308.
- [131] C Heitz, G Laurent, R Briard, E Barthel (2006) *Journal of colloid and interface science* 298: 192. Doi:10.1016/j.jcis.2005.12.011
- [132] Y Yang, R Boom, B Irion, D-J van Heerden, P Kuiper, H de Wit (2012) *Chemical Engineering and Processing: Process Intensification* 51: 53. Doi:10.1016/j.cep.2011.09.007
- [133] J Palmer, OR Ghita, L Savage, KE Evans (2009) *Composites Part A: Applied Science and Manufacturing* 40: 490. Doi:10.1016/j.compositesa.2009.02.002
- [134] A Jacob (2011) *Reinforced Plastics* 55: 45.
- [135] N Perry, A Bernard, F Laroche, S Pompidou (2012) *CIRP Annals - Manufacturing Technology* 61: 151. Doi:10.1016/j.cirp.2012.03.081
- [136] AC Meira Castro, MCS Ribeiro, J Santos, et al. (2013) *Construction and Building Materials* 45: 87. Doi:<http://dx.doi.org/10.1016/j.conbuildmat.2013.03.092>
- [137] I de Marco, JA Legarreta, MF Laresgoiti, et al. (1997) *Journal of Chemical Technology & Biotechnology* 69: 187. Doi:10.1002/(sici)1097-4660(199706)69:2<187::aid-jctb710>3.0.co;2-t
- [138] J Kennerley, N Fenwick, S Pickering, C Rudd (1997) *Journal of Vinyl and Additive Technology* 3: 58.
- [139] J Kennerley (1998) University of Nottingham,
- [140] JR Kennerley, RM Kelly, NJ Fenwick, SJ Pickering, CD Rudd (1998) *Composites Part A: Applied Science and Manufacturing* 29: 839. Doi:[http://dx.doi.org/10.1016/S1359-835X\(98\)00008-6](http://dx.doi.org/10.1016/S1359-835X(98)00008-6)
- [141] S Pickering, R Kelly, J Kennerley, C Rudd, N Fenwick (2000) *Composites Science and Technology* 60: 509.

- [142] AM Cunliffe, N Jones, PT Williams (2003) *Journal of Analytical and Applied Pyrolysis* 70: 315. Doi:10.1016/s0165-2370(02)00161-4
- [143] F Ahmad, D Mujah, H Hazarika, A Safari (2012) *Journal of Cleaner Production*. Doi:10.1016/j.jclepro.2012.05.047
- [144] K Pender, L Yang (2017) *Composites Part A: Applied Science and Manufacturing* 100: 285.
- [145] K Pender, L Yang *Polymer Composites* 0. Doi:doi:10.1002/pc.25213
- [146] JL Thomason, L Yang (2014) *Composites Science and Technology* 96: 7. Doi:10.1016/j.compscitech.2014.03.009
- [147] L Yang, JL Thomason (2012) *Polymer Testing* 31: 895. Doi:10.1016/j.polymertesting.2012.07.001
- [148] SN Thennadil (2008) *J. Opt. Soc. Am. A* 25: 1480. Doi:10.1364/JOSAA.25.001480
- [149] AE Krauklis, AT Echtermeyer (2018) *Open Chemistry* 16: 1189.
- [150] J Davidovits (1991) *Journal of Thermal Analysis and calorimetry* 37: 1633.
- [151] SEWDMJS Djwantoro Hardjito, BV Rangan (2004) *Materials Journal* 101. Doi:10.14359/13485
- [152] D Hardjito, SE Wallah, DM Sumajouw, B Rangan (2004) *civil engineering dimension* 6: 88.
- [153] JL Provis, JSJ van Deventer (2007) *Chemical Engineering Science* 62: 2318. Doi:<https://doi.org/10.1016/j.ces.2007.01.028>
- [154] BA Latella, DS Perera, D Durce, EG Mehrtens, J Davis (2008) *Journal of Materials Science* 43: 2693. Doi:10.1007/s10853-007-2412-1
- [155] F Hamzah, P Didik, Z Zezhi, Z Dongke (2012) *Asia-Pacific Journal of Chemical Engineering* 7: 73. Doi:doi:10.1002/apj.493
- [156] M Torres-Carrasco, F Puertas (2015) *Journal of Cleaner Production* 90: 397. Doi:<https://doi.org/10.1016/j.jclepro.2014.11.074>
- [157] MN Hadi, M Al-Azzawi, T Yu (2018) *Construction and Building Materials* 175: 41.
- [158] Na Jaya, L Ming, MMAB Abdullah, H Cheng-Yong, H Kamarudin (2018) *Effect of Sodium Hydroxide Molarity on Physical, Mechanical and Thermal Conductivity of Metakaolin Geopolymers*.
- [159] T Tho-In, V Sata, K Boonserm, P Chindaprasirt (2018) *Journal of Cleaner Production* 172: 2892.

A Appendix

A.1 AFM theory

A.1.1 Introduction

Atomic force microscopy (AFM) is a technique used widely to analyse the surface topography of a sample. As well as generating high resolution topographical images, AFM can also be used to measure mechanical properties like the Young's modulus, and the sample composition. AFM image dimensions can range from a few micrometres to hundreds of micrometres in the x-y direction and usually a few micrometres in the z direction. This chapter explains briefly how the AFM probe interacts with the surface of the specimen to produce a topographical image, and the principle setup of intermittent contact AFM.

A.1.2 Interaction of AFM probe with sample surface

To produce an image, the AFM probe needs to interact with the surface of the sample. AFM probes are typically made of silicon or silicon nitride, and comprise of a tip attached to a cantilever and its base according to the schematic diagram in Figure A.1.

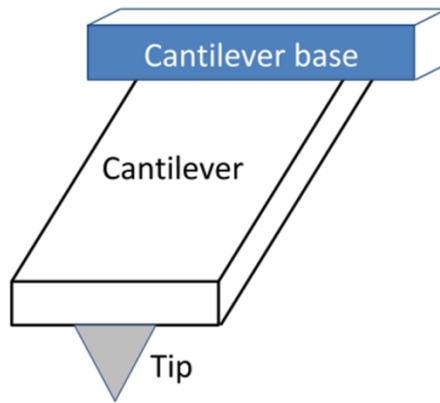


Figure A.1 – Schematic diagram of an AFM probe showing the cantilever and tip. Reproduced from [25]

The probe is usually moved using a piezoelectric tube. The AFM probe is positioned as close to the sample surface as possible and is then engaged, analysing the topography of the surface in the x-y plane. When the tip arrives at a heightened region of the sample it moves up, and the cantilever bends upwards; conversely, any recession in height causes the cantilever to bend downwards. A laser shines onto the back of the cantilever as it makes these subtle movements, and is reflected onto a photodiode based detector. The next section looks more into the principles of intermittent contact (tapping mode) AFM, which was the mode implemented in this research study when examining glass fibres.

A.1.3 Principles of intermittent contact AFM

The more basic contact mode AFM involves the tip touching the sample surface to measure its topography. Due to the nature of the technique there is often damage inflicted on the sample and AFM tip. To overcome this issue, an intermittent contact

mode (or tapping mode as trademarked by Bruker) of AFM was developed; a schematic of the setup is shown in Figure A.2.

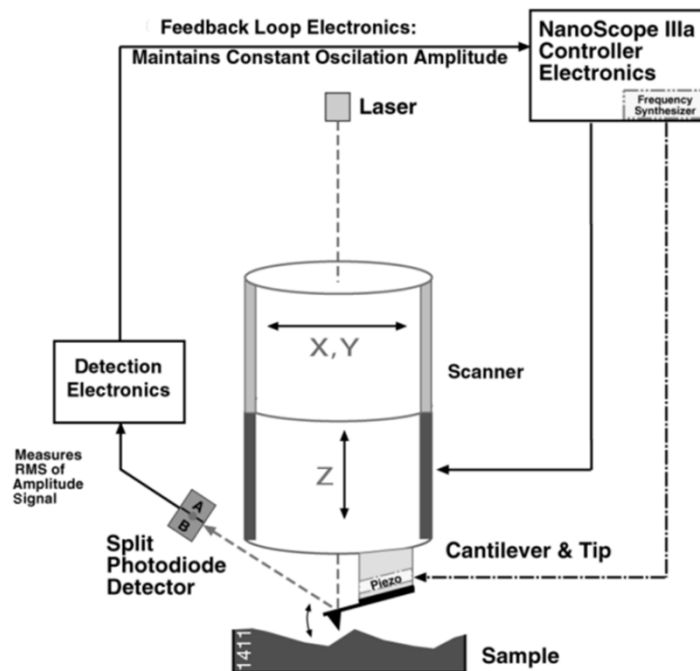


Figure A.2 – Schematic diagram showing the feedback loop electronics for AFM in intermittent contact mode. Reproduced from [25]

In this mode, the cantilever is oscillated at constant amplitude. As the tip is moved towards the sample, it experiences atomic forces that results in a similar force being directed on the cantilever. This force leads to a reduction in oscillation amplitude, which becomes more severe the closer the tip is to the sample surface. The piezoelectric tube then alters the cantilever position in the z direction in order to keep the oscillation amplitude constant; it is these changes that give information on the topography of the sample surface. Because adhesion force and viscoelastic property can vary with the material, tapping mode AFM can also be used to distinguish between different phases in a specimen.

A.2 FTIR theory

A.2.1 Introduction

Infra-red (IR) spectroscopy involves passing IR radiation through a sample. The sample can absorb some of the radiation, or the radiation will pass through (be transmitted). The IR spectrum gives the molecular absorption or transmission of the sample. An IR spectrum will not be the same for samples with different molecular structures, and so this spectroscopic technique is very useful in qualitative analysis.

A.2.2 Parameters in IR spectroscopic analysis

The electromagnetic radiation in IR spectroscopy can be split into far-IR, mid-IR and near-IR regions; far-IR ranges from around $400 - 0 \text{ cm}^{-1}$, mid-IR is usually in the range $4000 - 400 \text{ cm}^{-1}$, and near-IR is around $14000 - 4000 \text{ cm}^{-1}$. The wavenumber ($\tilde{\nu}$, cm^{-1}) is the number of electromagnetic waves in a one centimetre length, and is derived from the wavelength (λ , m) according to Equation A.1.

$$\tilde{\nu} = \frac{1}{(\lambda \times 100)} = \frac{\nu}{(c \times 100)}$$

Equation A.1

where c is the velocity of light ($2.997925 \times 10^8 \text{ m sec}^{-1}$), λ is the wavelength (in m) and ν is the frequency (number of vibrations [sec^{-1} or Hz]).

An IR spectrum typically presents the absorbance (A) of the sample against the wavenumber. The absorbance is directly proportional to the sample thickness and concentration, and coupled with the extreme accuracy and sensitivity of FTIR detectors and numerous software algorithms, can allow quantitative analysis to be performed. The absorbance and transmittance (T) are related according to Equation A.2.

$$A = \log\left(\frac{1}{T}\right) = -\log(T)$$

Equation A.2

The transmittance for each wavelength is obtained from I (intensity of IR radiation passed through the sample) divided by I_0 (intensity of IR radiation entering the sample), as shown in Equation A.3.

$$T = \frac{I}{I_0}$$

Equation A.3

Different functional groups present in the sample (for example O-H and C=O) will absorb IR radiation at different wavenumbers, which explains the complexity of the IR spectrum. In order for a particular molecule to be IR active, the molecular vibration that occurs from absorbing the IR radiation must cause a change in the dipole moment (μ); μ is a measurement of the polarity of the molecule. This explains

why homonuclear diatomic molecules such as H₂ and O₂ are IR inactive as they have no dipole moment, or there might be a very small change in dipole moment from their molecular vibrations, leading to very weak IR absorption bands.

A.2.3 General setup of an FTIR

There are numerous advantages of FTIR compared to classical dispersive IR instruments, such as better spectral quality, increased speed of data collection, and the fact it is a generally non-destructive IR spectroscopy technique. The typical components of an FTIR spectrometer are shown in Figure A.3.

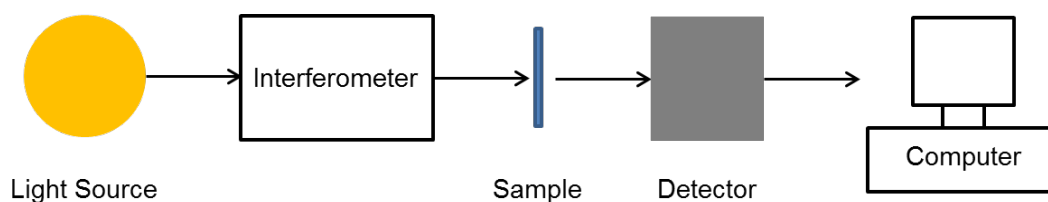


Figure A.3 - Basic components of an FTIR spectrometer

The **Light Source** is where the IR radiation is emitted. The IR beam then passes through the **Interferometer** where the spectral information is converted to the interferogram signal. The beam then approaches the **Sample**; the radiation is either passed through the sample or is reflected from its surface, depending on the type of FTIR analysis being employed. The sample absorbs the IR radiation at particular wavenumbers, depending on the nature of molecules present. The IR beam then travels to the **Detector** for final measurement of the interferogram signal. Finally, this signal is digitised and sent to the **Computer**. Fourier transformation then takes

place, which converts the digitised signal into a spectrum that can easily be interpreted by the user. Modern FTIR instruments are equipped with various interfaces, and the one selected for analysis would depend on the nature of the sample being investigated and the type of spectral information required.

Examples of FTIR interfaces include diffuse reflectance (DR), specular reflectance (SR) and attenuated total internal reflectance (ATR). The key difference between these techniques is the way in which the IR beam interacts with the sample, as shown schematically in Figure A.4.

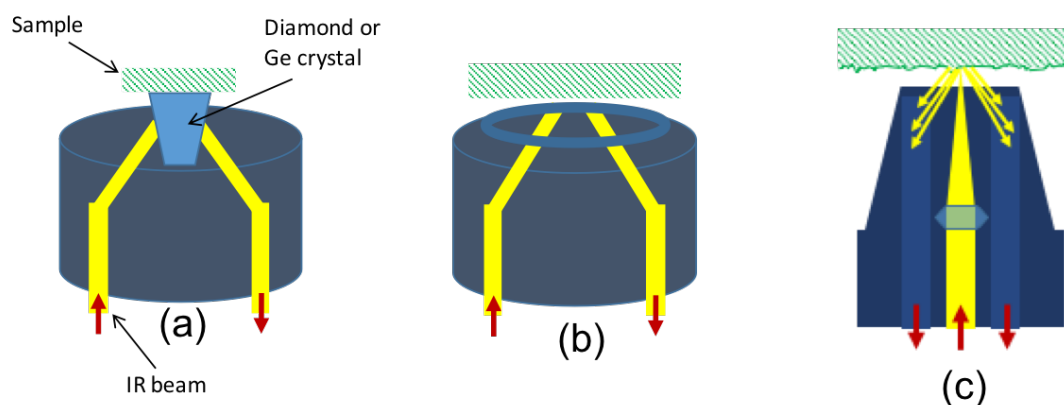


Figure A.4 – Schematic showing the IR beam paths in (a) ATR, (b) SR, and (c) DR

In ATR, an internal reflection element (IRE) is present, which is usually a diamond or germanium (Ge) crystal. The IR beam hits the edge of the crystal then interacts with the sample surface. The beam then leaves the crystal and is directed to the FTIR detector. The penetration depth of the sample depends on the refractive index of both the sample and crystal, and the angle and wavelength of the entering IR beam; usually, the sampling depth would be a few micrometres. Due to the absence of an

IRE in SR and DR interfaces, the IR beam can penetrate further into the sample (few hundred micrometres). With the SR interface, the IR beam enters at an angle and reflects off the sample surface. DR is better suited to rough sample surfaces; in this technique, the IR beam approaches the sample orthogonal to the surface, and if the sample surface is textured, the IR radiation reflects off in different directions and fed to the FTIR detector. Because of the high penetration depth of DR it is ideal for analysing inhomogeneous materials such as glass fibres. Due to the IR beam path for SR interface, it is more suitable for smooth samples and is used commonly in the analysis of coatings and contamination of metals. The low penetration depth of ATR means it is better suited for analysis of thin, homogeneous materials such as polymer films.